AD 600160

IITRI

HARD COPY	$ 6.38
MICROFICHE	$ 1.25

218p

CLEARINGHOUSE FOR FEDERAL SCIENTIFIC AND TECHNICAL INFORMATION CFSTI
DOCUMENT MANAGEMENT BRANCH 410.11

LIMITATIONS IN REPRODUCTION QUALITY

ACCESSION # AD 608168

☑ 1. WE REGRET THAT LEGIBILITY OF THIS DOCUMENT IS IN PART UNSATISFACTORY. REPRODUCTION HAS BEEN MADE FROM BEST AVAILABLE COPY.

☐ 2. A PORTION OF THE ORIGINAL DOCUMENT CONTAINS FINE DETAIL WHICH MAY MAKE READING OF PHOTOCOPY DIFFICULT.

☐ 3. THE ORIGINAL DOCUMENT CONTAINS COLOR, BUT DISTRIBUTION COPIES ARE AVAILABLE IN BLACK-AND-WHITE REPRODUCTION ONLY.

☐ 4. THE INITIAL DISTRIBUTION COPIES CONTAIN COLOR WHICH WILL BE SHOWN IN BLACK-AND-WHITE WHEN IT IS NECESSARY TO REPRINT.

☐ 5. LIMITED SUPPLY ON HAND: WHEN EXHAUSTED, DOCUMENT WILL BE AVAILABLE IN MICROFICHE ONLY.

☐ 6. LIMITED SUPPLY ON HAND: WHEN EXHAUSTED DOCUMENT WILL NOT BE AVAILABLE.

☐ 7. DOCUMENT IS AVAILABLE IN MICROFICHE ONLY.

☐ 8. DOCUMENT AVAILABLE ON LOAN FROM CFSTI (TT DOCUMENTS ONLY).

☐ 9.

PROCESSOR: Bernan

TSL-107-10/64

Final Report IITRI Project No. K6056

DYNAMICS OF FLEXIBLE ROTORS

Bureau of Ships
Department of the Navy
Washington 25, D. C.

IIT RESEARCH INSTITUTE
Technology Center
Chicago, Illinois 60616

Final Report IITRI Project No. K6056

DYNAMICS OF FLEXIBLE ROTORS

Contract No. NObs-88607
June 11, 1963 to June 11, 1964

by

R. A. Eubanks

and

R. L. Eshleman

Bureau of Ships
Department of the Navy
Washington 25, D. C.

October 1964

FOREWORD

This is the final report of IIT Research Institute Project No. K6056, entitled "Dynamics of Flexible Rotors." This project was conducted for the Department of the Navy, Bureau of Ships, Washington 25, D. C. under Contract No. NObs–88607, during the period June 11, 1963 to June 11, 1964.

The project was monitored by Mr. F. F. Vane, Code 345, Bureau of Ships. Contributing IITRI personnel include Dr. R. A. Eubanks, Mr. L. Bujalski, Mr. T. L. Bush, Mr. R. L. Eshleman, Mr. C. E. Gebhart, Dr. E. E. Hahn, Mr. A. P. Meyers, Mr. W. F. Ridenour, and Mr. T. M. Scopelite.

Respectfully submitted,

IIT RESEARCH INSTITUTE

R. A. Eubanks
Project Engineer

APPROVED:

V. F. Volpe

V. F. Volpe, Assistant Director
Mechanical Engineering

TABLE OF CONTENTS

LIST OF ILLUSTRATIONS

LIST OF ILLUSTRATIONS (Cont'd)

DYNAMICS OF FLEXIBLE ROTORS

I. INTRODUCTION-SUMMARY

The present program had several, somewhat disparate, goals in the general subject area of Rotor Dynamics. Primary among these was an inquiry into the effect of gyroscopic and rotatory inertial effects on the whirling of rotating shafts. The secondary goals included the development of a computer program for the prediction of whirling of stepped shafts, the completion of an inquiry into an approximate method of analysis which is used widely in Naval predictions of shaft whirling phenomena, and the development of a very versatile and dependable test rig for the experimental investigation of primary and secondary effects in Rotor Dynamics.

An appendix contains a complete derivation of equations of motion for shafts which rotate at constant speed. The equations of motion reflect a quite general characterization of such shafts. Hence, while it is assumed that the cross sections of the shafts have equal inertial moment, e.g., circular or square cross section, this cross section as assumed to vary arbitrarily as a function of axial position. The assumption of equal inertial moment is not considered to be unduly restrictive inasmuch as previous investigations have clearly pointed out the disruptive whirling effects which can be experienced if this is not the case. The rotor is supported in lubricated massive bearings on flexible damped supports. Material damping in the shaft, and external damping such as that provided by air, are assumed small in comparison with the support damping. Although the effects of deformation due to transverse shear forces were neglected in this analysis attention was paid to the effects of gyroscopic moment and rotatory inertia of the shaft (and incidentally of any disk or disks which are carried by this shaft).

Sections II and III of this report contain analyses of specific shaft systems which were performed with the use of the basic differential equations. The critical speeds and mode shapes were found for a uniform undamped rigidly supported cylindrical rotor with gyroscopic and rotatory inertia effects included. The cylindrical rotor was analyzed in fixed short bearings as well as in fixed long bearings.

A second analysis inquired into the critical speeds of a system consisting of a single disk loaded at an arbitrary location on a uniform continuous shaft which was mounted on short fixed bearings. Critical speeds were found for various disk sizes and locations.

In general, it was found that there are two critical speeds for each order of flexible mode shape. Furthermore, the rotor does not deform in a plane curve as is normally assumed in classical analysis.

The frequency equation for the uniform cylindrical rotor in either mounting can be uncoupled, yielding two equations which represent the two sets of critical speeds associated with backward and forward whirl of the rotor. The critical speeds for each mode order were found as a function of r (the ratio of the rotor or shaft radius to its length). The effects of rotatory inertia and gyroscopic forces effectively broaden the apparent resonance at lower order modes. However, as the rotational speed of the rotor increases, the resonance peaks separate and become distinct. The equations predict that, at larger values of r, it is possible to encounter a backward whirl of higher order before one encounters a forward whirl of lower order. Hence, for example, a mode shape with five nodes may occur at a lower speed than will a mode shape with four nodes. This produces a unusual situation at values of r where the curves for different order critical speeds intersect. The mode shape at these critical speeds appear to be indeterminant when using linear, undamped, analysis.

At this point, it should be emphasized that the analysis under discussion concerns itself with the rotatory inertia and gyroscopic moments which are distributed in a uniform shaft. The effects of these perturbing influences become increasingly pronounced as the rotational speed increases and similarly, as the ratio of rotor diameter to rotor length increases. On the other hand, at higher values of these parameters the effect of shear deformation in the shaft becomes significant. Hence, the quantitative predictions of this theory must be held in question. There is, of course, every reason to believe that the predictions are qualitatively correct, inasmuch as an elementary analysis will show that the primary effect of shear deformations is that of increasing the apparent value of r which appears in the results.

The gyroscopic effects of the rotor tend to alternately advance and retard its whirling motion as the rotational speed is increased. The rotor mounted on short bearings has quite simple mode shapes. These mode shapes are more complicated when the rotor is mounted on long bearings. In operation the critical speeds of backward whirl should be avoided, since a fatigue problem is encountered when the rotor assumes this whirl configuration. For example, a point on the periphery of the shaft undergoes two complete reversed stress cycles per revolution while operating at the first critical speed in the backward whirl configuration.

The results which were obtained for the rotor when mounted on long bearings were, in general, similar to those which were obtained for short bearings. The solution of the frequency equation is more complicated. Both the critical speeds associated with backward and forward whirl are, again uncoupled. Therefore, the shaft exhibits the same general behavior namely, a critical speed at which forward whirl occurs and a critical speed at which backward whirl occurs at each order mode.

The critical speeds of the system consisting of a single disk mounted on a continuous shaft depend upon the disk size and location. The gyroscopic and rotatory inertia effects of the shaft were neglected since they are small compared to the gyroscopic and rotatory effects of the disk. The two major influences on the critical speeds are the "mass effect," which is the ratio of the mass disk to the mass of the shaft, and the "disk effect," which is the ratio of the radius of the disk to twice the length of the shaft. The mass effect tends to lower the critical speeds of the system, when not located at a nodal point, as the mass of the disk is increased and the disk effect may increase or decrease the critical speed of the system. The disk effect tends to effectively stiffen or soften the spring constant of the shaft, when the shaft is thought of as a single spring, giving double criticals at each order mode shape except when the disk is mounted at an antinode.

In the classical approach of finding the critical speeds of the disk-shaft system, only as many critical speeds as the number of disks on the shaft can be found. This does not mean other critical speeds of the system do not exist but only that the classical mathematical model does not fit the physical model accurately. The present representation does fit the physical model and these higher order criticals were found.

The critical speeds of the system were found with the disk at three different locations and the size of the disk used at each location was varied.

The critical speeds of a system with the disk located at the bearing show no "mass effect" because this is a nodal point. The "disk effect" tends to spread the critical speeds as the size of the disk increases and the critical speeds become asymptotic to $p = \frac{n\pi}{4}$, where n = 5, 9, 13, etc.

When the disk is mounted at the quarter point on the shaft, the critical speeds corresponding to the first and second order modes are in general decreased by the "mass effect" and two critical are obtained due to the "disk effect." The third order critical speeds show only slight "mass effect" and a large "disk effect" because in the fourth order mode shape the disk is located near an antinode.

For the disk mounted at the center of the shaft, only one critical speed is obtained for the odd order modes which indicates only "mass effects" are important, while for the even order modes two critical speeds are obtained indicating the presence of both "mass and disk" effects. Finally as the rotational speed and the size of the disk is increased the critical speeds approach: the value $n\pi/2$, where n = 5, 9, 13, etc.

Experimental runs were made to check on the predictions of the analysis. No conclusions could be reached in the case of the bare rotor since the ratio of rotor radius to length (approximately 0.015) was too small to permit separation of the forward and reverse whirl speeds. However, the first critical speed, forward whirl, showed good agreement with the analytical results considering the fact that transverse shear effects were omitted. Good agreement was obtained in the case of the rotor-disk system with both forward and backward whirling modes being identified. In each case the backward whirling modes were difficult to detect and had relatively small amplitudes of displacement, while the forward whirling modes were easy to identify and had relatively large amplitudes of displacement. A gravity critical speed was obtained when the disk was mounted at the mid point and at the quarter point. Again, here, an attempt was made to increase the operating speed to a point at which the forward and reverse whirls would theoretically coincide, in order that this phenomenon could be observed experimentally. The power capabilities of the drive system were not found to be equal to the task. An attempt should be made to study this phenomenon at a later date.

The secondary goals are completely reported upon in the appendices. Little not need be made of them here. It should, however, be pointed out that the computer program which is reported upon has been completely de-bugged and is operational. A complete program listing together with FORTRAN and operating decks for the IBM 7090-7094 computer systems have been completed and delivered to Code 345, Bureau of Ships. It will be observed that this program is very general and should find immediate applicability.

Several areas of continued work in this area of Rotor Dynamics are apparent. Included among these are the following:

1. Extension of the basic mathematical model and system of equations to include the effect of transverse shear forces on deformations. Not only should this information be of value in the analysis of relatively uniform heavy rotors; the prediction of higher critical speeds for rotors of small diameter which support rotating disks of large inertia should also be improved.

2. Further experimental work should be performed with a view towards actually attaining the speed at which forward and reverse whirl modes theoretically coincide. Information in this area can be obtained analytically only with great difficulty. Since it appears possible that operation

in the neighborhood of such a phenomenon may be quite disruptive it is certainly germane to study such operation in detail.

3. Most studies of Rotor Dynamics have concerned themselves with rotors which operate under constant speed and have completely neglected the kinetics of such operation. Since useful rotating shafts transmit torque the effect of such torque on the whirling of shafts should be studied. It is apparent that not only is the transmission of torque of constant magnitude of importance, load fluctuations can have important effect on the operation of power transmission systems. Hence, it is recommended that both theoretical and experimental studies be made on the effects of fluctuating and steady state torque on rotating systems.

II. CYLINDRICAL ROTORS WITH GYROSCOPIC EFFECTS

Previous investigations have resulted in the determination of critical speeds of simplified models of continuous shafts. Prominent among the simplifications utilized is one which assumes that the rotor dynamics of uniform shafts are little affected by rotatory inertia and gyroscopic effects. In the present section of this report we inquire into this assumption, its basis, and the range of its validity.

The model for this study is the shaft of Appendix A, which, for the immediate study, will be assumed to be uniform and circular. Thus, we conclude the following specializations.

$$
\begin{aligned}
I\,(x) &= \text{constant} \\
A\,(x) &= \text{constant} \\
r\,(x) &= \text{constant} \\
\rho\,(x) &= \text{constant} \\
S\,(x) &= \text{constant}
\end{aligned}
\tag{2.1}
$$

The equations of motion now assume a form which appears tractable. For convenience, we introduce the following notation.

$$
\begin{aligned}
p^2 &= \frac{A \rho\, \Omega^2 L^4}{S} \\
h &= \frac{g}{L\Omega^2}
\end{aligned}
\tag{2.2}
$$

The equations of motion have the following form in space-fixed coordinates.

$$
\frac{1}{p^2} \frac{\partial^4 u_1}{\partial x^4} + \frac{\partial^2 u_1}{\partial \tau^2} - \frac{r^2}{4} \frac{\partial^3}{\partial x^2 \partial \tau} \left(\frac{\partial u_1}{\partial \tau} + 2\, u_2 \right) = a_1 \cos \; - a_2 \sin \tag{2.3}
$$

$$
\frac{1}{p^2} \frac{\partial^4 u_2}{\partial x^4} + \frac{\partial^2 u_2}{\partial \tau^2} - \frac{r^2}{4} \frac{\partial^3}{\partial x^2 \partial \tau} \left(\frac{\partial u_2}{\partial \tau} - 2\, u_1 \right) = a_1 \sin \tau + a_2 \cos \tau - h \tag{2.4}
$$

The first task is the determination of natural rotor frequencies. We consider the homogeneous form of (2.3), (2.4), with $a_1 = a_2 = h = 0$ and following the procedure of Contract NObs – 86805, introduce trial solutions of the form

$$u_1 = A_e^{\alpha x + i \gamma \tau}$$
$$u_2 = B_e^{\alpha x + i \gamma \tau} \tag{2.5}$$

where A, B, α, and γ are, in general, complex constants to be determined by the end conditions. Equation (2.5) and similar expressions are interpreted as meaning that u_1 and u_2 are the real parts of the right hand sides. When equation (2.5) is substituted in (2.3) and (2.4), it is found that these constants are related by equations (2.6),

$$\left[\frac{\alpha^4}{p^2} - \gamma^2 + \frac{r^2}{4} \alpha^2 \gamma^2\right] A - \frac{i r^2 \alpha^2 \gamma}{2} B = 0$$
$$\left[\frac{\alpha^4}{p^2} - \gamma^2 + \frac{r^2}{4} \alpha^2 \gamma^2\right] B + i \frac{r^2 \alpha^2 \gamma}{2} A = 0 \tag{2.6}$$

The determinant of coefficients of A and B must vanish. This leads to the following relation between α and γ.

$$\left(\frac{\alpha^4}{p^2} - \gamma^2 + \frac{r^2 \alpha^2 \gamma^2}{4}\right)^2 - \left(\frac{r^2 \alpha^2 \gamma}{2}\right)^2 = 0 \tag{2.7}$$

Equation (2.7) permits α to be expressed explicity in terms of μ. Let ϵ_1, ϵ_2, and ϵ_3 be independent constants, all of which can assume values ± 1;

$$\epsilon_1^2 = 1, \quad \epsilon_2^2 = 1, \quad \epsilon_3^2 = 1 \tag{2.8}$$

Then

$$\alpha = \epsilon_3 \sqrt{\gamma p - \left[\frac{r^2 p(\gamma + 2 \epsilon_1)}{8} + \epsilon_2 \sqrt{1 + \frac{r^4 p^2 (\gamma + 2 \epsilon_1)^2}{64}}\right]} \tag{2.9}$$

For each possible value of γ. There are eight values of α and sixteen constants A_j, B_j. These constant values are not independent, by (2.6) they are related. Equations (2.6), (2.9) yield the following simple relationship.

$$B_j = i \epsilon_1 A_j, \quad (j = 1, 2, 3, \ldots 8) \tag{2.10}$$

The exponentials α_j and the relation (2.10) are made specific by means of Table 1. For each unknown value of γ the solution has the form

$$\begin{aligned} u_1 &= \sum_{j=1}^{8} A_j e^{\alpha_j(\gamma)x + i\gamma\tau} \\ u_2 &= i \sum_{j=1}^{8} (\epsilon_1) A_j e^{\alpha_j(\gamma)x + i\gamma\tau} \end{aligned} \tag{2.11}$$

In general, it is clear that the shaft does not deform in a plane curve, as is normally concluded.

The constants of inte :ation must be found from the boundary conditions. In cases where these conditions are homogeneous, compatibility leads to an eigenvalue equation for γ and p.

Table 1
Parameter Values Corresponding to Solution Indices

Index j	ϵ_1	ϵ_2	ϵ_3
1	1	1	1
2	1	1	-1
3	1	-1	1
4	1	-1	-1
5	-1	1	1
6	-1	1	-1
7	-1	-1	1
8	-1	-1	-1

We shall examine the shaft behavior for different sets of end conditions.

A. RIGID SUPPORTS, SHORT BEARINGS, NO LUBRICANT

This is the classical case of "pinned bearings." The end conditions of Appendix A reduce the following.

$$\left.\begin{aligned}
&\text{On } x = 0: \quad && u_1 = u_2 = 0 \\
& && \frac{\partial^2 u_1}{\partial x^2} = \frac{\partial^2 u_2}{\partial x^2} = 0 \\
&\text{On } x = 1: && u_1 = u_2 = 0 \\
& && \frac{\partial^2 u_1}{\partial x^2} = \frac{\partial^2 u_2}{\partial x^2} = 0
\end{aligned}\right\} \tag{2.12}$$

Substitution of (2.11) into (2.12) yields the following algebraic system.

$$\left.\begin{aligned}
&\sum_{j=1}^{4} A_j = 0 && \sum_{j=5}^{8} A_j = 0 \\
&\sum_{j=1}^{4} \alpha_j^2 A_j = 0 && \sum_{j=5}^{8} \alpha_j^2 A_j = 0 \\
&\sum_{j=1}^{4} A_j e^{\alpha_j} = 0 && \sum_{j=5}^{8} A_j e^{\alpha_j} = 0 \\
&\sum_{j=1}^{4} \alpha_j^2 A_j e^{\alpha_j} = 0 && \sum_{j=5}^{8} \alpha_j^2 A_j e^{\alpha_j} = 0
\end{aligned}\right. \tag{2.13}$$

Two independent sets of equations for the A_j are apparent. The frequency equations are obtained by setting the product of the determinants of these systems equal to zero, thus producing the environment for nontrivial determination of A_j. Thus, we have

$$\Delta_1 \Delta_2 = 0 \tag{2.14}$$

$$\Delta_1 = \begin{vmatrix} 1 & 1 & 1 & 1 \\ \alpha_1^2 & \alpha_2^2 & \alpha_3^2 & \alpha_4^2 \\ e^{\alpha 1} & e^{\alpha 2} & e^{\alpha 3} & e^{\alpha 4} \\ \alpha_1^2 e^{\alpha_1} & \alpha_2^2 e^{\alpha 2} & \alpha_3^2 e^{\alpha 3} & \alpha_4^2 e^{\alpha 4} \end{vmatrix} \tag{2.15}$$

$$\Delta_2 = \begin{vmatrix} 1 & 1 & 1 & 1 \\ \alpha_5^2 & \alpha_6^2 & \alpha_7^2 & \alpha_8^2 \\ e^{\alpha 5} & e^{\alpha 6} & e^{\alpha 7} & e^{\alpha 8} \\ \alpha_5^2 e^{\alpha 5} & \alpha_6^2 e^{\alpha 6} & \alpha_7^2 e^{\alpha 7} & \alpha_8^2 e^{\alpha 8} \end{vmatrix} \tag{2.16}$$

By Table 1, and (2.9) we see that $1 + \gamma \longrightarrow (-\gamma)$:

$$\begin{array}{ll} \alpha_1 \rightarrow \alpha_7, & \alpha_2 \rightarrow \alpha_8 \\ \alpha_3 \rightarrow \alpha_5, & \alpha_4 \rightarrow \alpha_6 \\ \alpha_5 \rightarrow \alpha_3, & \alpha_6 \rightarrow \alpha_4 \\ \alpha_7 \rightarrow \alpha_1, & \alpha_8 \rightarrow \alpha_2 \end{array} \tag{2.17}$$

and

$$\Delta_1 \rightarrow \Delta_2$$

$$\Delta_2 \rightarrow \Delta_1$$

If γ^* satisfies the frequency equation for specific values of r and p then $(-\gamma^*)$ also satisfies the equation. Thus, γ must be real if solution amplitudes remain bounded with time. Of primary interest are the cases $\gamma = 1$ and $\gamma = -1$ which, of course, give rise to the same frequency equation. Since

$$U_1 + i\,U_2 = (V_1 + i\,V_2)\,e^{\,i} \tag{2.18}$$

it is clear from (2.5) that $\gamma = 1$ can imply that there is no time variation of the displacements of the rotating system. For $\gamma = 1$, the solution is neatest when expressed in terms of the following parameters.

For $\gamma = 1$ define

$$\begin{aligned}
\beta_1 &= \alpha_1 \sqrt{p\left[-\frac{3r^2p}{8} + \sqrt{1 + \left(\frac{3r^2p}{8}\right)^2}\right]} \\
\beta_2 &= -i\,\alpha_3 = \sqrt{p\left[\frac{3r^2p}{8} + \sqrt{1 + \left(\frac{3r^2p}{8}\right)^2}\right]} \\
\beta_3 &= \alpha_5 = \sqrt{p\left[\frac{r^2p}{8} + \sqrt{1 + \left(\frac{r^2p}{8}\right)^2}\right]} \\
\beta_4 &= -i\,\alpha_7 = \sqrt{p\left[-\frac{r^2p}{8} + \sqrt{1 + \left(\frac{r^2p}{8}\right)^2}\right]}
\end{aligned} \tag{2.19}$$

The determinants Δ_1 and Δ_2 can be written in terms of the β_j:

$$\Delta_1 = \begin{vmatrix} 1 & 1 & 1 & 1 \\ \beta_1^2 & \beta_1^2 & -\beta_2^2 & -\beta_2^2 \\ e^{\beta_1} & e^{-\beta_1} & e^{-i\beta_2} & e^{-i\beta_2} \\ \beta_1^2 e^{\beta_1} & \beta_1^2 e^{-\beta_1} & -\beta_2^2 e^{i\beta_2} & -\beta_2^2 e^{-i\beta_2} \end{vmatrix} \tag{2.20}$$

$$\Delta_2 = \begin{vmatrix} 1 & 1 & 1 & 1 \\ \beta_3^2 & \beta_3^2 & -\beta_4^2 & -\beta_2^2 \\ e^{\beta_3} & e^{-\beta_3} & e^{i\beta_4} & e^{-i\beta_4} \\ \beta_3^2 e^{\beta_3} & \beta_3^2 e^{-\beta_3} & -\beta_4^2 e^{i\beta_4} & -\beta_4^2 e^{-i\beta_4} \end{vmatrix} \tag{2.21}$$

Reduction yields the frequency equation:

$$(\beta_1^2 + \beta_2^2)^2 (\beta_3^2 + \beta_4^2)^2 \sinh \beta_1 \sin \beta_2 \sinh \beta_3 \sin \beta_4 = 0 \tag{2.22}$$

Now

$$(\beta_1^2+\beta_2^2)^2(\beta_3^2+\beta_4^2)^2 = 16\,p^4\left[1+\left(\frac{3r^2p^2}{8}\right)^2\right]\left[1+\left(\frac{r^2p^2}{8}\right)^2\right] \tag{2.23}$$

which is only zero for $p = 0$. The remaining factors yield the following expressions

$$\beta_1 = in\pi,\quad \beta_2 = n\pi,\quad \beta_3 = in\pi,\quad \beta_4 = n\pi \tag{2.24}$$

$$(n = 0, 1, 2, \ldots)$$

The whirl frequencies are thus described by the following sequences

$$p_+ = \frac{n^2\pi^2}{\sqrt{1-\dfrac{r^2n^2\pi^2}{4}}} \quad \text{(a)}$$

$$p_- = \frac{n^2\pi^2}{\sqrt{1+\dfrac{3r^2n^2\pi^2}{4}}} \quad \text{(b)} \tag{2.25}$$

$$(n = 0, 1, 2, \ldots)$$

These roots are plotted in figure 1.

As $r \rightarrow 0$, both sequences assume the classical values

$$r \rightarrow 0: \qquad p_c = n^2\pi^2$$

$$(n = 0, 1, 2, \ldots) \tag{2.26}$$

In general r, which is the ratio of the shaft radius to the shaft length, is small. Should this not be the case, equations (2.25) are not valid, since deformation due to shear is important and should be included. For the lower modes the effect of rotatory inertia and gyroscopic forces on a uniform round shaft is therefore effectively one of broadening the apparent resonance. A different effect becomes apparent as the rotational speed of the shaft increases. The resonance peaks separate and become distinct.

An interesting conclusion can be drawn from figure 1. It is clear that one can encounter backward whirls of high order before one encounters forward whirls of lower order. For example, for $r = 0.1$ it is seen that the fifth and sixth order backward whirls occur at lower shaft speeds than does the fourth order forward whirl. This effect may cause confusion in the interpretation of experimental results.

An effect of gyroscopic moments can be observed if it is noted that the critical frequencies have the following form when only the rotatory inertia of the cross sections is considered:

$$p_r = \frac{n^2 \pi^2}{\sqrt{1 + \frac{n^2 \pi^2 r^2}{2}}} \qquad (n = 0, 1, 2, \ldots) \tag{2.27}$$

Comparison of (2.27) with (2.25) reveals that

$$p_+ > n^2 \pi^2 > p_r > p_- \tag{2.28}$$

The gyroscopic moments thus tend to alternately advance and retard the shaft as the rotational speed increases.

The displacements are best found with a redefinition of coefficients. Define

$$\begin{aligned} C_1 &= A_1 + A_2 & C_2 &= A_1 - A_2 \\ C_3 &= A_3 + A_4 & C_4 &= i\,(A_3 - A_4) \\ C_5 &= A_5 + A_6 & C_6 &= A_5 - A_6 \\ C_7 &= A_7 + A_8 & C_8 &= i\,(A_7 - A_8) \end{aligned} \tag{2.29}$$

The following two systems of equations then hold.

$$\begin{gathered} C_1 + C_3 = 0 \\ \beta_1^2 C_1 - \beta_2^2 C_3 = 0 \end{gathered} \tag{2.30}$$

$$C_1 \cosh \beta_1 + C_2 \sinh \beta_1 + C_3 \cos \beta_2 = -C_4 \sin \beta_2$$

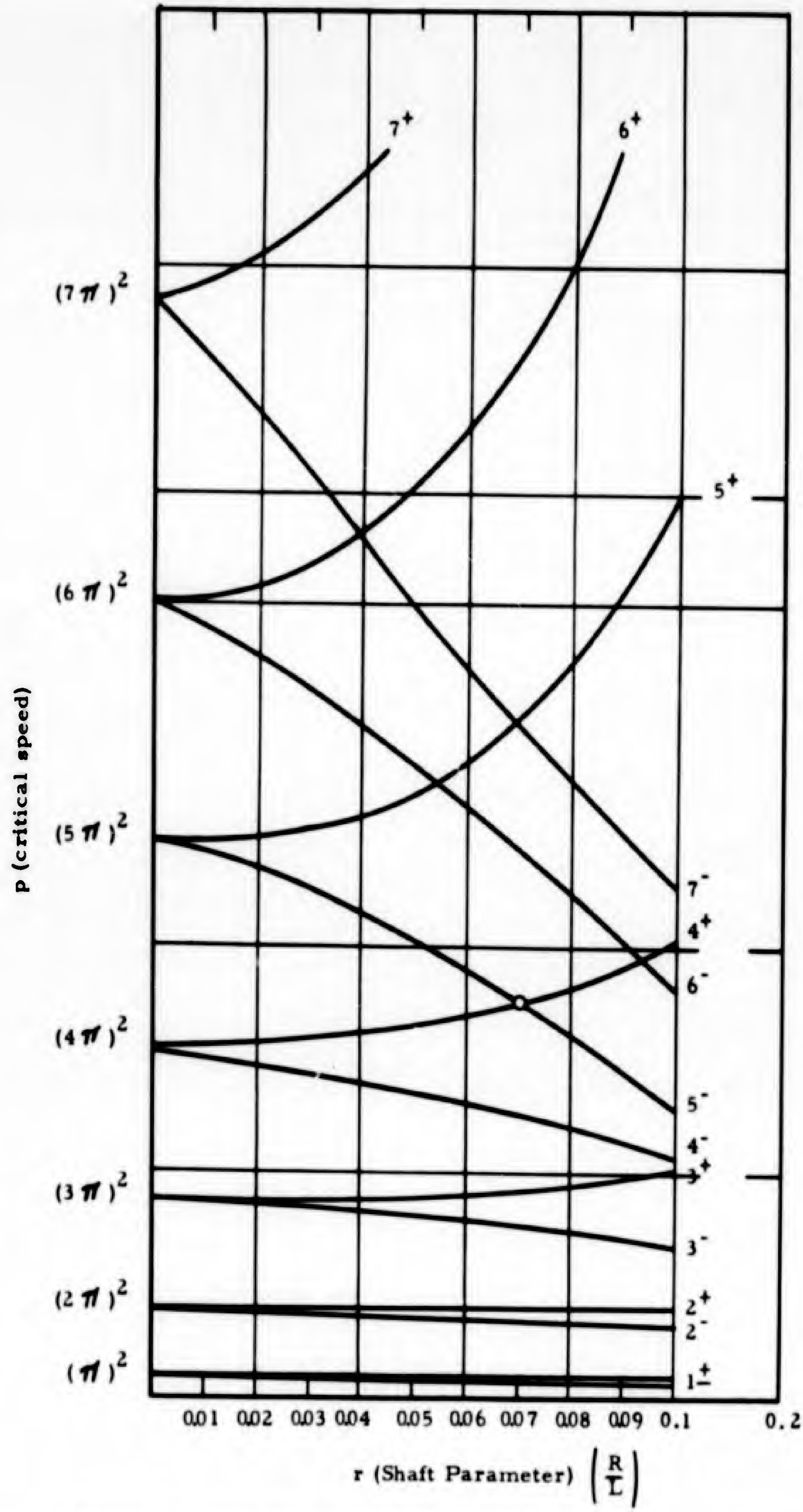

Figure 1 THE RELATIONSHIP BETWEEN CRITICAL SPEED AND GYROSCOPIC EFFECT FOR A PIN ENDED ROTATING SHAFT

$$C_5 + C_7 = 0$$

$$\beta_3^2 C_5 - \beta_4^2 C_7 = 0 \qquad (2.31)$$

$$C_5 \cosh \beta_3 + C_6 \sinh \beta_3 + C_7 \cos \beta_4 = -C_8 \sin \beta_4$$

At this point, some care is required. For $p = p_-$ equations (2.30) hold and C_5, C_6, C_7, C_8 must vanish. Similarly, for $p = p_+$ equations (2.31) hold and C_1, C_2, C_3, C_4 must vanish. Thus, the mode shapes are intrinsically different for advance and retardation.

Equations (2.30) for $p = p_-$ yield the following.

$$C_2 = -C_4 \frac{\sin \beta_2}{\sinh \beta_1}$$

$$C_1 = C_3 = C_5 = C_6 = C_7 = C_8 = 0 \qquad (2.32)$$

Similarly, equations (2.31) for $p = p_+$ yield

$$C_6 = -C_8 \frac{\sin \beta_4}{\sinh \beta_3}$$

$$C_1 = C_2 = C_3 = C_4 = C_5 = C_7 = 0 \qquad (2.33)$$

Both $\beta_1 = in\pi$ and $\beta_2 = n\pi$ yield the same value of p_-, while $\beta_3 = in\pi$ and $\beta_4 = n\pi$ yield the same value of p_+. Thus, to be specific we take

$$\beta_2 = n\pi \quad \text{for } p = p_-$$

$$\beta_4 = n\pi \quad \text{for } p = p_+$$

$$C_2 = 0 \text{ for } p = p_- \qquad (2.34)$$

$$C_6 = 0 \text{ for } p = p_+$$

This displacements u_1 and u_2 are real. Let C_8 and C_4 be real. Then for $p = p_-$

$$u_1 = C_4 \cos \tau \sin n\pi x$$

$$u_2 = -C_4 \sin \tau \sin n\pi x \qquad (2.35)$$

for p = p+

$$u_1 = C_8 \cos \tau \sin n\pi x$$
$$u_2 = C_8 \sin \tau \sin n\pi x \qquad (2.36)$$

The nondimensional coordinates which rotate with the shaft are ν_1 and ν_2 where

$$\gamma_1 = u_1 \cos \tau + u_2 \sin \tau$$
$$\gamma_2 = u_2 \cos \tau + u_1 \sin \tau \qquad (2.37)$$

The displacements u_1 and u_2 are shown below.

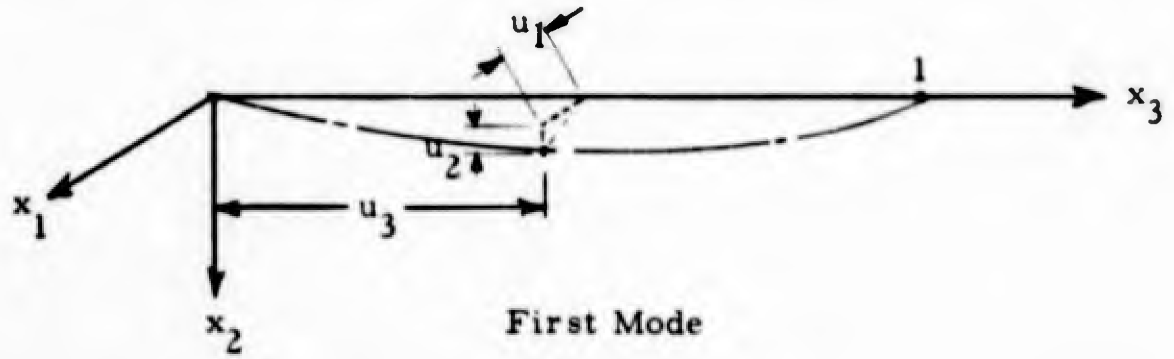

First Mode

Looking at an arbitrary cross section (u_3) while the shaft rotates with rotational speed Ω :

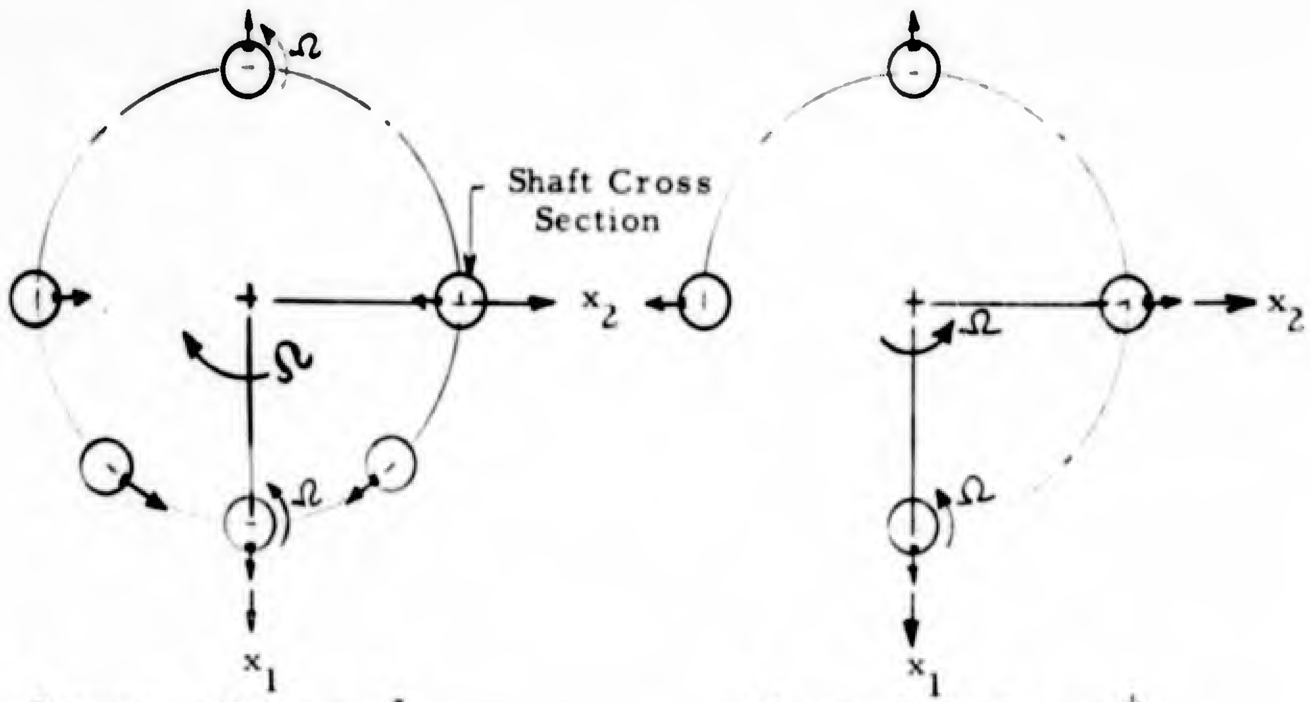

Reverse whirl $p = p^-$ Forward whirl $p = p^+$

The displacements in rotating coordinates have the following simple form for $p = p_-$

$$
\begin{aligned}
\gamma_1 &= C_4 \cos 2\tau \sin n\pi x \\
\gamma_2 &= -C_4 \sin 2\tau \sin n\pi x
\end{aligned}
\qquad (2.38)
$$

for $p = p_+$

$$
\begin{aligned}
\gamma_1 &= C_8 \sin n\pi x \\
\gamma_2 &= 0
\end{aligned}
\qquad (2.39)
$$

The frequency p_+ is a "frozen whirl" in which the shaft distorts in a single plane which then rotates at the applied speed. Conversely, $p = p_-$ is a "backward whirl."

The displacements as a function time in rotating coordinates are shown. Again, an arbitrary cross section of the shaft is shown in motion. (y_1, y_2) rotate with speed Ω.

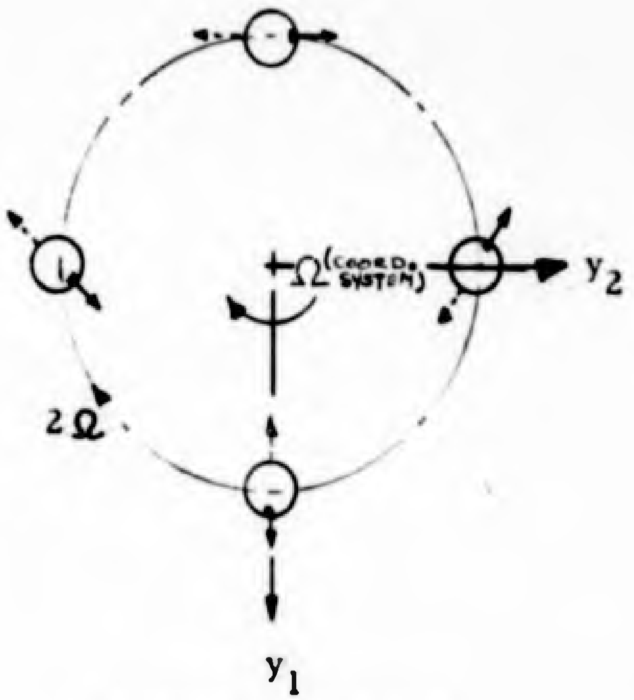

Reverse Whirl $p = p^-$

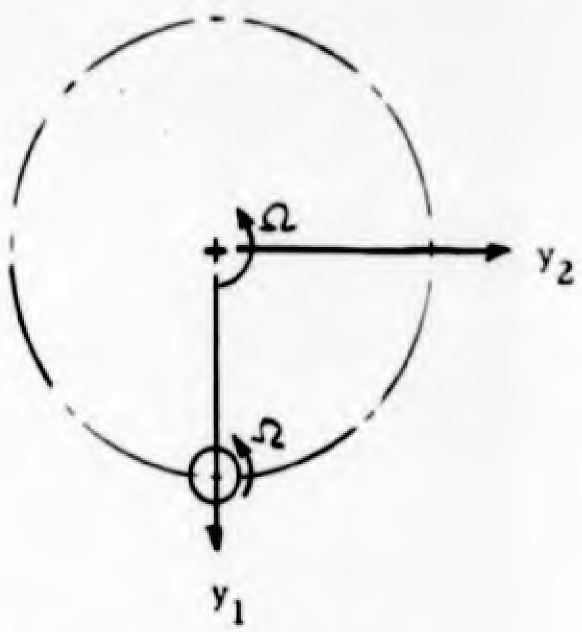

Forward Whirl $p = p^+$

B. RIGID SUPPORTS, LONG BEARINGS, NO LUBRICANT

Next, consider the case of "fixed bearings," whose boundary conditions are those of a fixed-fixed beam. Then the end conditions of Appendix A can be written as follows:

$$
\left.
\begin{aligned}
&\text{on } x = 0: && u_1 = u_2 = 0 \\
& && \frac{\partial u_1}{\partial x} = \frac{\partial u_2}{\partial x} = 0 \\
&\text{on } x = 1: && u_1 = u_2 = 0 \\
& && \frac{\partial u_1}{\partial x} = \frac{\partial u_2}{\partial x} = 0
\end{aligned}
\right\} \qquad (2.40)
$$

Again, substitution of (2.11) into (2.40) leads to equations to be satisfied.

$$
\left.
\begin{aligned}
&\sum_{j=1}^{4} A_j = 0 && \sum_{j=5}^{8} A_j = 0 \\
&\sum_{j=1}^{4} \alpha_j A_j = 0 && \sum_{j=5}^{8} \alpha_j A_j = 0
\end{aligned}
\right\} \qquad (2.41)
$$

$$\sum_{j=1}^{4} A_j e^{\alpha_j} = 0 \qquad \sum_{j=5}^{8} A_j e^{\alpha_j} = 0$$

$$\sum_{j=1}^{4} \alpha_j A_j e^{\alpha_j} = 0 \qquad \sum_{j=5}^{8} \alpha_j A_j e^{\alpha_j} = 0 \tag{2.41}$$

Two independent sets of equations for the A_j are obtained. The frequency equations are now found by setting the product of the determinants of these systems equal to zero.

$$\Delta_1 \cdot \Delta_2 = 0 \tag{2.42}$$

where

$$\Delta_1 = \begin{vmatrix} 1 & 1 & 1 & 1 \\ \alpha_1 & \alpha_2 & \alpha_3 & \alpha_4 \\ e^{\alpha_1} & e^{\alpha_2} & e^{\alpha_3} & e^{\alpha_4} \\ \alpha_1 e^{\alpha_1} & \alpha_2 e^{\alpha_2} & \alpha_3 e^{\alpha_3} & \alpha_4 e^{\alpha_4} \end{vmatrix} \tag{2.43}$$

$$\Delta_2 = \begin{vmatrix} 1 & 1 & 1 & 1 \\ \alpha_5 & \alpha_6 & \alpha_7 & \alpha_8 \\ e^{\alpha_5} & e^{\alpha_6} & e^{\alpha_7} & e^{\alpha_8} \\ \alpha_5 e^{\alpha_5} & \alpha_6 e^{\alpha_6} & \alpha_7 e^{\alpha_7} & \alpha_8 e^{\alpha_8} \end{vmatrix} \tag{2.43}$$

Now using (2. 17), (2. 18), and (2. 19)

$$\left.\begin{aligned} \Delta_1 &= \begin{vmatrix} 1 & 1 & 1 & 1 \\ \beta_1 & -\beta_1 & i\beta_2 & -i\beta_2 \\ e^{\beta_1} & e^{-\beta_1} & e^{i\beta_2} & e^{-i\beta_2} \\ \beta_1 e^{\beta_1} & -\beta_1 e^{-\beta_1} & i\beta_2 e^{i\beta_2} & -i\beta_2 e^{-i\beta_2} \end{vmatrix} \\ \Delta_2 &= \begin{vmatrix} 1 & 1 & 1 & 1 \\ \beta_3 & -\beta_3 & i\beta_4 & -i\beta_4 \\ e^{\beta_3} & e^{-\beta_3} & e^{i\beta_4} & e^{-i\beta_4} \\ \beta_3 e^{\beta_3} & -\beta_3 e^{-\beta_3} & i\beta_4 e^{i\beta_4} & -i\beta_4 e^{-\beta_4} \end{vmatrix} \end{aligned}\right\} \tag{2.44}$$

$$\left.\begin{aligned}
\Delta_1 &= 4i\left[\sin\beta_2 \sinh\beta_1 (\beta_1^2 - \beta_2^2) + 2\beta_1\beta_2(1-\cos\beta_2\cosh\beta_1)\right] \\
\Delta_2 &= 4i\left[\sin\beta_4 \sinh\beta_3 (\beta_3^2 - \beta_4^2) + 2\beta_3\beta_4(1-\cos\beta_4\cosh\beta_3)\right] \\
\Delta_1\Delta_2 &= 0
\end{aligned}\right\} \quad (2.45)$$

By using equations (2.19), find

$\beta_1^2 = \beta_2^2$, $\beta_3^2 - \beta_4^2$, $\beta_1\beta_2$, $\beta_3\beta_4$ in terms of r and p.

$$\left.\begin{aligned}
\beta_1^2 - \beta_2^2 &= -\frac{3}{4} r^2 p^2 \\
\beta_3^2 - \beta_4^2 &= \frac{p^2 r^2}{4} \\
\beta_1\beta_2 &= \pm p \\
\beta_3\beta_4 &= \pm p
\end{aligned}\right\} \quad (2.46)$$

and r and p in terms of β_1, β_2, β_3 and β_4 are shown below

$$\left.\begin{aligned}
p^- &= \beta_1\beta_2 && \text{(a)} \\
p^+ &= \beta_3\beta_4 && \text{(b)}
\end{aligned}\right\} \quad (2.47)$$

$$r^2 = \frac{4}{3} \frac{\beta_2^2 - \beta_1^2}{\beta_1^2 \beta_2^2} \quad \text{(c)}$$

$$r^2 = 4 \frac{\beta_3^2 - \beta_4^2}{\beta_3^2 \beta_4^2} \quad \text{(d)} \qquad (2.47)$$

From equations 2.45, the frequency equation is obtained.

$$-8\left[\sin \beta_2 \sinh \beta_1 (\beta_1^2 - \beta_2^2) + 2\beta_1 \beta_2 (1 - \cos \beta_2 \cosh \beta_1)\right]$$
$$\left[\sin \beta_4 \sinh \beta_3 (\beta_3^2 - \beta_4^2) + 2\beta_3 \beta_4 (1 - \cos \beta_4 \cosh \beta_3)\right] = 0 \qquad (2.48)$$

It is evident from equations 2.47 that if $\beta_1 = \beta_2$ or $\beta_3 = \beta_4$, then r must be zero and the frequency equation 2.48 reduces to cosh βcos β = 1. This is the case of a fixed-fixed nonrotating beam whose roots lie on a forty five degree line labeled r = 0 in figure 2. Therefore for the case of a rotating shaft where rotatory inertia and gyroscopic effects are considered, $r \neq o$ and thus $\beta_1 \neq \beta_2$ and $\beta_3 \neq \beta_4$.

The other extreme case in the range of values of r shown in figure 2- is $r \longrightarrow \infty$ which implies that either $\beta_1 = 0$ or $\beta_4 = 0$. $\beta_1 = \beta_2 = \beta_3 = \beta_4 \neq 0$ since this is the trivial case p = 0 by equations (2.47).

If $\beta_1 = \pm i \beta_2$ or $\beta_3 = \pm i \beta_4$, equation 2.48 is satisfied, but this solution has no physical meaning because by equations (2.46) p is imaginary.

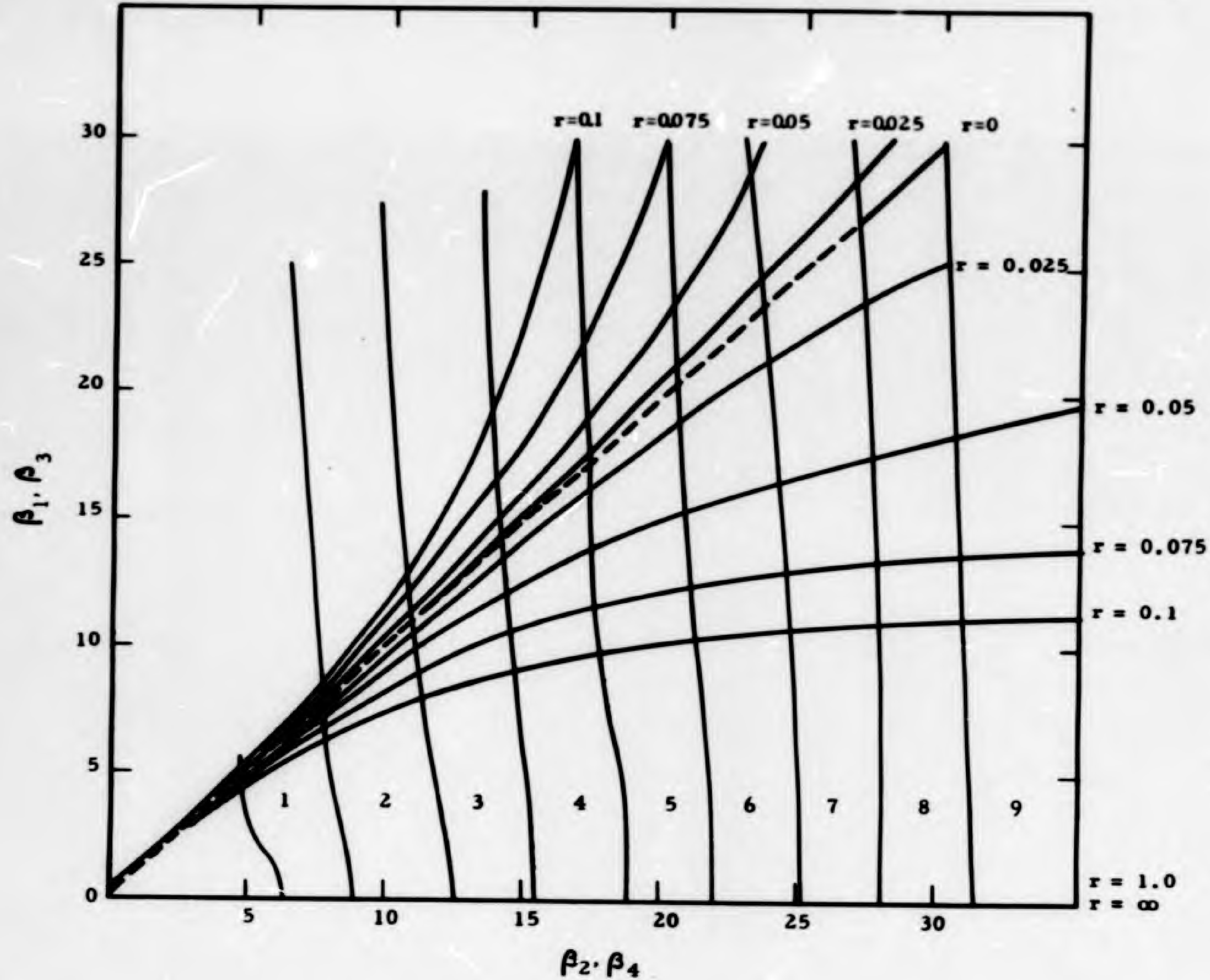

Figure 2 SOLUTION TO FREQUENCY EQUATIONS (2. 49) AS A FUNCTION OF THE SHAFT PARAMETER (r)

Then the frequency equation (2.48) is satisfied only if:

$$\left.\begin{aligned} &\sin\beta_2 \sinh\beta_1(\beta_1^2-\beta_2^2)+2\beta_1\beta_2(1-\cos\beta_2\cosh\beta_1)=0 \quad \text{(a)} \\ &\text{or} \\ &\sin\beta_4 \sinh\beta_3(\beta_3^2-\beta_4^2)+2\beta_3\beta_4(1-\cos\beta_4\cosh\beta_3)=0 \quad \text{(b)} \end{aligned}\right\} \quad (2.49)$$

where only real values of β_1, β_2, β_3, β_4 are admissible. Roots to equations 2.49 are shown in figure 2 for a range of values of r. There are two basic parts of this graph corresponding to the critical speeds p^+ and p^-. The roots of $\beta_1 \beta_2$ correspond to p^-, the critical speed of backward whirl. These roots all lie below the forty five degree line $r = 0$ and therefore $\beta_2 > \beta_1$. The roots of $\beta_3 \beta_4$ correspond to p^+, the critical speed of forward whirl. These roots lie above the forty five degree line $r = 0$ and therefore $\beta_3 > \beta_4$. In each case the roots are plotted for a range of values of r varying between $r = 0$ and $r \rightarrow \infty$.

According to equations (2.47), $p^- = \beta_1 \beta_2$ and $p^+ = \beta_3 \beta_4$ are the critical speeds. Therefore for a given shaft (r is known), n discrete values of β_1 and β_2 and n discrete values of β_3 and β_4 can be found. Therefore 2n critical speeds are obtained for each value of r.

Figure 3 shows the relationship between the critical speeds (p) and the shaft parameter r. This plot shows that as the ratio of the shaft radius to shaft length increases from the limiting case of $r = 0$ to $r = 0.1$, the critical speed progresses from one discrete critical to a wide critical and finally to two discrete critical speeds.

To find the displacements, the coefficients A_j will be redefined similar to (2.29).

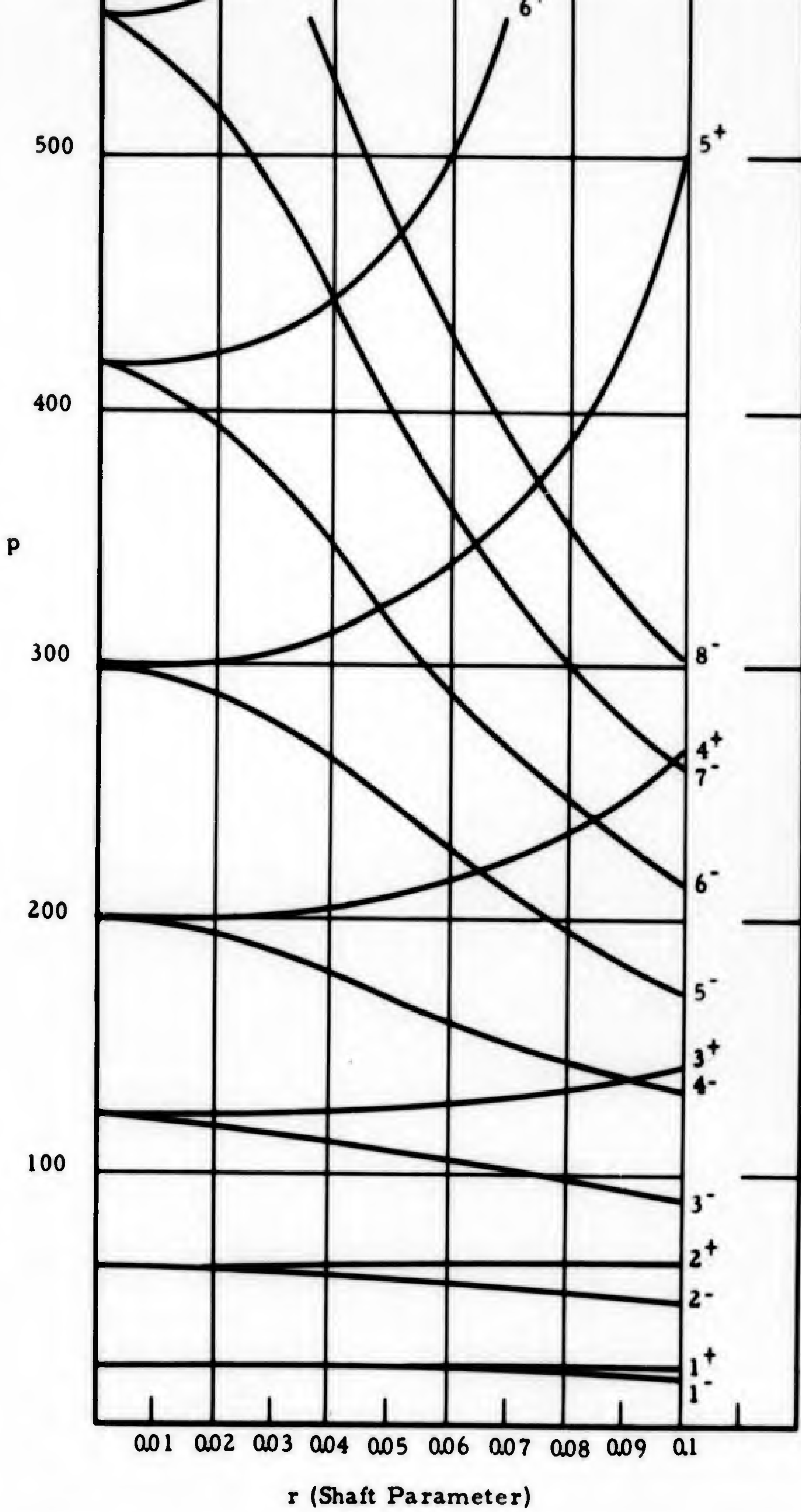

Figure 3 THE RELATIONSHIP BETWEEN CRITICAL SPEED AND GYROSCOPIC EFFECT FOR A FIXED ENDED SHAFT

$$\left.\begin{array}{ll} c_1 = A_1 + A_2 & c_2 = A_1 - A_2 \\ c_3 = A_3 + A_4 & c_4 = i\,(A_3 - A_4) \\ c_5 = A_5 + A_6 & c_6 = A_5 - A_6 \\ c_7 = A_7 + A_8 & c_8 = i\,(A_7 - A_8) \end{array}\right\} \quad (2.29)$$

Then by utilizing the set of equations (2.41), the following systems of equations hold.

$$\left.\begin{array}{l} c_1 + c_3 = 0 \\ \beta_1 c_2 + \beta_2 c_4 = 0 \\ c_1 \cosh \beta_1 + c_2 \sinh \beta_1 + c_3 \cos \beta_2 + c_4 \sin \beta_2 = 0 \\ \beta_1 c_1 \sinh \beta_1 + \beta_1 c_2 \cosh \beta_1 - \beta_2 c_3 \sin \beta_2 + \beta_2 c_4 \cos \beta_2 = 0 \end{array}\right\} \quad (2.50)$$

$$\left.\begin{array}{l} c_5 + c_7 = 0 \\ \beta_3 c_6 + \beta_4 c_8 = 0 \\ c_5 \cosh \beta_3 + c_6 \sinh \beta_3 + c_7 \cos \beta_4 + c_8 \sin \beta_4 = 0 \\ \beta_3 c_5 \sinh \beta_3 + \beta_3 c_6 \cosh \beta_3 - \beta_4 c_7 \sin \beta_4 + \beta_4 c_8 \cos \beta_4 = 0 \end{array}\right\} \quad (2.51)$$

Either equations (2.50) or equations (2.51) are admissible in describing the motion of the shaft at a critical speed p. If equation (2.49a) is satisfied and values of β_1 β_2 are obtained, then the motion corresponding to the critical speed of retardation (p^-) is obtained by allowing equations (2.50) to hold and letting $c_5 = c_6 = c_7 = c_8 = 0$.

Equations (2.50) yield:

$$\left.\begin{aligned} c_1 &= -c_3 \\ c_2 &= -\frac{\beta_2}{\beta_1} c_4 \\ c_1 \cosh \beta_1 + c_2 \sinh \beta_1 &+ c_3 \cos \beta_2 + c_4 \sin \beta_2 = 0 \\ c_1 \sinh \beta_1 + c_2 \cosh \beta_1 &- \frac{\beta_2}{\beta_1} c_3 \sin \beta_2 + \frac{\beta_2}{\beta_1} c_4 \cos \beta_2 = 0 \end{aligned}\right\} \quad (2.52)$$

where β_1 and β_2 are known for specific values of the shaft parameter r.

Rearranging (2.52)

$$\left.\begin{aligned} c_1 &= -c_4 \left[\frac{\frac{\beta_2}{\beta_1} \sinh \beta_1 - \sin \beta_2}{\cos \beta_2 - \cosh \beta_1} \right] \\ c_2 &= -\frac{\beta_2}{\beta_1} c_4 \\ c_3 &= c_4 \left[\frac{\beta_2}{\beta_1} \quad \frac{\sinh \beta_1 - \sin \beta_2}{\cos \beta_2 - \cosh \beta_1} \right] \end{aligned}\right\} \quad (2.53)$$

Now using equations (2.11) with $c_5 = c_6 = c_7 = c_8 = 0$ u_1 and u_2 are obtained:

$$\left.\begin{aligned} u_1 &= (A_1 e^{\alpha_1 x} + A_2 e^{\alpha_2 x} + A_3 e^{\alpha_3 x} + A_4 e^{\alpha_4 x})\, e^{i\tau} \\ u_2 &= i(A_1 e^{\alpha_1 x} + A_2 e^{\alpha_2 x} + A_3 e^{\alpha_3 x} + A_4 e^{\alpha_4 x})\, e^{i\tau} \end{aligned}\right\} \qquad (2.54)$$

and

$$e^{i\tau} = \cos\tau + i\sin\tau$$

Replace the constants A_j by C_j using equations (2.29) and express c_j in terms of c_4 using equations (2.53). Then the equations for the displacements u_1 and u_2 at a critical speed (p^-) become:

$$\left.\begin{aligned} u_1 &= c_4 \cos\tau \left[\sin\beta_2 x - \frac{\beta_2}{\beta_1}\sinh\beta_1 x + \left(\frac{\frac{\beta_1}{\beta_2}\sinh\beta_1 - \sin\beta_2}{\cos\beta_2 - \cosh\beta_1} \right) (\cos\beta_2 x - \cosh\beta_1 x) \right] \\ u_2 &= -c_4 \sin\tau \left[\sin\beta_2 x - \frac{\beta_2}{\beta_1}\sinh\beta_1 x + \left(\frac{\frac{\beta_1}{\beta_2}\sinh\beta_1 - \sin\beta_2}{\cos\beta_2 - \cosh\beta_1} \right) (\cos\beta_2 x - \cosh\beta_1 x) \right] \end{aligned}\right\} \qquad (2.55)$$

The motion corresponding to the critical speed of advance (p^+) is obtained next by allowing equation (2.49b) to be satisfied for values of β_3 and β_4, and further by allowing equations 2.51 to hold with $c_1 = c_2 = c_3 = c_4 = 0$. The descriptions of the motion (u_1, u_2) of advance have a form similar to the latter set of equations except that different values are obtained for β_3 and β_4.

Then for p^+ the motion is

$$u_1 = c_8 \cos \tau \left[\sin \beta_4 x - \frac{\beta_4}{\beta_3} \sinh \beta_3 x + \left(\frac{\frac{\beta_3}{\beta_4} \sinh \beta_3 - \sin \beta_4}{\cos \beta_4 - \cosh \beta_3} \right) (\cos \beta_4 x - \cosh \beta_3 x) \right] \tag{2.56}$$

$$u_2 = -c_8 \sin \tau \left[\sin \beta_4 x - \frac{\beta_4}{\beta_3} \sinh \beta_3 x + \left(\frac{\frac{\beta_3}{\beta_4} \sinh \beta_3 - \sin \beta_4}{\cos \beta_4 - \cosh \beta_3} \right) (\cos \beta_4 x - \cosh \beta_3 x) \right]$$

III. SINGLE DISK ON A CONTINUOUS SHAFT WITH GYROSCOPIC EFFECTS

The classical method of calculating the critical speed for a single disk mounted on a rotating shaft utilizes the assumption that the shaft is a massless spring and that the disk is the sole mass of the system.

Rotatory inertia, and gyroscopic forces of the disk are sometimes included in the calculation. In this section of the report, we will find the critical speeds of a system composed of a disk mounted on a rotating shaft mounted in short bearings. In this analysis, the shaft mass will be considered but the gyroscopic and rotatory inertia effects of the shaft will not be considered since they are negligible in comparison to the gyroscopic and rotatory inertia forces of the disk.

The equations of motion, continuity conditions, and boundary conditions for a straight circular shaft with a disk attached at an arbitrary location will be obtained. The expressions for the kinetic and potential energy for a round shaft were given in Appendix A. The expression given as equation (20), in Appendix A, will be modified to include the energies of the disk.

let

M_D = mass of the disk

I_D = mass moment of inertia of the disk about Y_2

$$I_D = \frac{1}{4} M_D R_D^2 \quad \text{- this implies that } \frac{h^2}{R_D^2} << 1$$

R_D = radius of disk

$r_D = L R_D$

The energies of the system are divided into three parts: the energy of the disk, the energy of the left hand portion of the shaft up to the disk, and the energy of the right hand portion of the shaft.

$$2\frac{(T-U)}{L^3 \Omega^2} = \int_0^{\xi} A\rho \left\{ \left(\frac{\partial u_1}{\partial \tau}\right)^2 + \left(\frac{\partial u_2}{\partial \tau}\right)^2 + a_1^2 + a_2^2 + 2\left[a_1\left(\cos\tau\frac{\partial u_2}{\partial \tau} - \sin\tau\frac{\partial u_1}{\partial \tau}\right)\right.\right.$$

$$\left. - a_2\left(\sin\tau\frac{\partial u_2}{\partial \tau} + \cos\tau\frac{\partial u_1}{\partial \tau}\right)\right] - \frac{S}{L^4 A\rho\,\Omega^2}\left[\left(\frac{\partial^2 u_1}{\partial x^2}\right)^2 + \left(\frac{\partial^2 u_2}{\partial x^2}\right)^2\right] - \frac{2g}{L\Omega^2} u_2$$

$$\left. + \frac{r^2}{4}\left[\left(\frac{\partial^2 u_1}{\partial x \partial \tau}\right)^2 + \left(\frac{\partial^2 u_2}{\partial x \partial \tau}\right)^2 + 2 + 2\frac{\partial^2 u_1}{\partial x \partial \tau}\frac{\partial u_2}{\partial x} - 2\frac{\partial^2 u_2}{\partial x \partial \tau}\frac{\partial u_1}{\partial x}\right]\right\}_{L^*} dx \tag{3.1}$$

$$+ \int_{\xi}^{1} A\rho \left\{ \left(\frac{\partial u_1}{\partial \tau}\right)^2 + \left(\frac{\partial u_2}{\partial \tau}\right)^2 + a_1^2 + a_2^2 + 2\left[a_1\left(\cos\tau\frac{\partial u_2}{\partial \tau} - \sin\tau\frac{\partial u_1}{\partial \tau}\right)\right.\right.$$

$$\left. - a_2\left(\sin\tau\frac{\partial u_2}{\partial \tau} + \cos\tau\frac{\partial u_1}{\partial \tau}\right)\right] - \frac{S}{L^4 A\rho\Omega^2}\left[\left(\frac{\partial^2 u_1}{\partial x^2}\right)^2 + \left(\frac{\partial^2 u_2}{\partial x^2}\right)^2\right] - \frac{2g}{L\Omega^2} u_2$$

$$\left. + \frac{r^2}{4}\left[\left(\frac{\partial^2 u_1}{\partial x \partial \tau}\right)^2 + \left(\frac{\partial^2 u_2}{\partial x \partial \tau}\right)^2 + 2 + 2\frac{\partial^2 u_1}{\partial x \partial \tau}\frac{\partial u_2}{\partial x} - 2\frac{\partial^2 u_2}{\partial x \partial \tau}\frac{\partial u_1}{\partial x}\right]\right\}_{R} dx$$

* Denotes left portion of the shaft

$$+ \int_o^1 \left(m_1 \left[\left(\frac{d\xi_1}{d\tau}\right)^2 + \left(\frac{d\xi_2}{d\tau}\right)^2 \right] + m_2 \left[\left(\frac{d\eta_1}{d\tau}\right)^2 + \left(\frac{d\eta_2}{d\tau}\right)^2 \right] dx \right.$$

$$+ \frac{M_D}{L} \left[\left(\frac{\partial u_1(\xi,\tau)}{\partial \tau} \right)^2 + \left(\frac{\partial u_2(\xi,\tau)}{\partial \tau} \right)^2 + a_1^2 + a_2^2 + 2 \left\{ a_1 \left(\cos\tau \frac{\partial u_2(\xi,\tau)}{\partial \tau} \right. \right. \right.$$

$$\left. \left. \left. - \sin\tau \frac{\partial u_1(\xi,\tau)}{\partial \tau} \right) - a_2 \left(\sin\tau \frac{\partial u_2(\xi,\tau)}{\partial \tau} + \cos\tau \frac{\partial u_1(\xi,\tau)}{\partial \tau} \right) \right\} \right]$$

$$+ \frac{I_D}{L^3} \left[2 + \left(\frac{\partial^2 u_1(\xi,\tau)}{\partial x \partial \tau} \right)^2 + \left(\frac{\partial^2 u_2}{\partial x \partial \tau} \right)^2 + 2 \frac{\partial^2 u_1}{\partial x \partial \tau} \frac{\partial u_2}{\partial x} - 2 \frac{\partial^2 u_2}{\partial x \partial \tau} \frac{\partial u_1}{\partial x} \right]_{\substack{x=\xi \\ t=\tau}}$$

$$- \frac{2M_D g u_2}{L^2 \Omega^2} - \int_o^4 (K_{11} \xi_1^2 + K_{12} \xi_2^2 + K_{21} \eta_1^2 + K_{22} \eta_2^2) \, dx$$

$$- \int_o^1 K A \rho \left[(u_1(o,\tau) - \xi_1)^2 + (u_2(o,\tau) - \xi_2)^2 + (u_1(1,\tau) - \eta_1)^2 + \right.$$

$$\left. (u_2(1,\tau) - \eta_2)^2 \right] dx$$

Using Hamilton's principle and taking the variation with respect to u_1,

$$- \frac{\partial^2 u_1}{\partial \tau 2} + a_1 \cos\tau - a_2 \sin\tau - \frac{1}{\rho A} \frac{\partial^2}{\partial x^2} \left(\frac{S}{L^4 \Omega^2} \frac{\partial^2 u_1}{\partial x^2} \right) + \frac{1}{4\rho A} \frac{\partial}{\partial x}$$

$$\left(r^2 A \rho \frac{\partial^3 u_1}{\partial x \partial \tau^2} \right) + \frac{2}{4\rho A} \frac{\partial}{\partial x} \left(r^2 A \rho \frac{\partial^2 u_2}{\partial x \partial \tau} \right) = 0$$

Equation of motion for left hand side.

The same equation of motion obtained for right hand side.

Boundary conditions at $x = 0$,

u_1 is prescribed or

$$- \frac{\partial}{\partial x} \left(\frac{S}{L^4 \Omega^2} \frac{\partial^2 u_1}{\partial x^2} \right) + \frac{r^2 A \rho}{4} \frac{\partial^3 u_1}{\partial x \partial \tau^2} + \frac{2 r^2 \rho A}{4} \frac{\partial^2 u_2}{\partial x \partial \tau}$$

$$- \int_0^1 K A \rho \, dx \, (u_1 - \xi_1) = 0$$

$\frac{\partial u_1}{\partial x}$ is prescribed or

$$\frac{\partial^2 u_1}{\partial x^2} = 0 \tag{3.2}$$

Boundary conditions at $x = 1$,

u_1 is prescribed or

$$\frac{\partial}{\partial x} \left(\frac{S}{L^4 \Omega^2} \frac{\partial^2 u_1}{\partial x^2} \right) - \frac{r^2 A \rho}{4} \frac{\partial^3 u_1}{\partial x \partial \tau^2} + \frac{2 r^2 \rho A}{4} \frac{\partial^2 u_2}{\partial x \partial \tau}$$

$$- \int_0^1 K A \rho \, dx \, (u_1 - \eta_1) = 0$$

$\frac{\partial u_1}{\partial x}$ is prescribed or

$$\frac{\partial^2 u_1}{\partial x^2} = 0$$

Continuity conditions at $x = \xi$,

u_1 must be prescribed or

$$\left[\frac{\partial}{\partial x}\left(\frac{S}{L^4\Omega^2}\ \frac{\partial^2 u_1}{\partial x^2}\right)\right]_L - \left[\frac{1}{4} r^2 A\rho \frac{\partial^3 u_1}{\partial x \partial \tau^2}\right]_L - \left[\frac{2r^2 \rho A}{4}\ \frac{\partial^2 u_2}{\partial x \partial \tau}\right]_L$$

$$+ \frac{M_D}{L}\left(- \frac{\partial^2 u_1}{\partial \tau^2} + a_1 \cos \tau - a_2 \sin \tau\right) - \left[\frac{\partial}{\partial x}\left(\frac{S}{L^4\Omega^2}\ \frac{\partial^2 u_1}{\partial x^2}\right)\right]_R$$

$$+ \frac{1}{4}\left[r^2 A\rho \frac{\partial^3 u_1}{\partial x \partial \tau^2}\right]_R + \left[\frac{2r^2 \rho A}{4}\ \frac{\partial^2 u_2}{\partial x \partial \tau}\right]_R = 0$$

Continuity condition at $x = \xi$

$\frac{\partial u_1}{\partial x}$ is prescribed or

$$- \left[\frac{S}{L^4\Omega^2}\ \frac{\partial^2 u_1}{\partial x^2}\right]_L + \left[\frac{S}{L^4\Omega^2}\ \frac{\partial^2 u_1}{\partial x^2}\right]_R - \frac{I_D}{L^3}\left[\frac{\partial^3 u_1}{\partial x \partial \tau^2} + 2\frac{\partial^2 u_2}{\partial x \partial \tau}\right] = 0$$

The variation with respect to u_2 yields

$$- \frac{\partial^2 u_2}{\partial \tau^2} + a_1 \sin \tau + a_2 \cos \tau - \frac{g}{L\Omega^2} - \frac{1}{\rho A L^4 \Omega^2}\ \frac{\partial^2}{\partial x^2}\left(S\ \frac{\partial^2 u_2}{\partial x^2}\right)$$

$$+ \frac{1}{4A\rho}\ \frac{\partial}{\partial x}\left[\rho A r^2 \left\{ \frac{\partial^3 u_2}{\partial x \partial \tau^2} - 2\ \frac{\partial^2 u_1}{\partial x \partial \tau}\right\}\right] = 0$$

Right
Left

Boundary conditions $x = 0$.

u_2 is prescribed or

$$-\frac{\partial}{\partial x}\left(\frac{S}{L^4\Omega^2}\frac{\partial^2 u_2}{\partial x}\right) + \frac{r^2 A\rho}{4}\frac{\partial^3 u_2}{\partial x \partial \tau^2} - 2\frac{r^2 A\rho}{4}\frac{\partial^2 u_1}{\partial x \partial \tau}$$

$$-K\int_o^1 \rho A dx\, (u_2(o, \tau) - \xi_2) = 0$$

$\frac{\partial u_2}{\partial x}$ is prescribed or (3.3)

$$\frac{\partial^2 u_2}{\partial x^2} = 0$$

Boundary conditions at $x = 1$,

u_2 is prescribed or

$$\frac{\partial}{\partial x}\left(\frac{S}{L^4\Omega^2}\frac{\partial^2 u_2}{\partial x^2}\right) - \frac{1}{4} r^2 A\rho\frac{\partial^3 u_2}{\partial x \partial \tau^2} + 2\frac{r^2 \rho A}{4}\frac{\partial^2 u_1}{\partial x \partial \tau}$$

$$-K\int_o^1 \rho A\, d x (u_2 - \eta_2) = 0$$

$\frac{\partial u_2}{\partial x}$ is prescribed or

$$\frac{\partial^2 u_2}{\partial x^2} = 0$$

Continuity at x = ξ

u_2 is prescribed or

$$\left[\frac{\partial}{\partial x}\left(\frac{S}{L^4\Omega^2}\frac{\partial^2 u_2}{\partial x^2}\right)\right]_L - \left[\frac{\partial}{\partial x}\left(\frac{S}{L^4\Omega^2}\frac{\partial^2 u_2}{\partial x^2}\right)\right]_R$$

$$-\left[\frac{r^2\rho A}{4}\frac{\partial^3 u_2}{\partial x\partial\tau^2}\right]_L + \left[\frac{r^2\rho A}{4}\frac{\partial^3 u_2}{\partial x\partial\tau^2}\right]_R + \left[\frac{2r^2\rho A}{4}\frac{\partial^2 u_1}{\partial x\partial\tau}\right]_L$$

$$-\left[2\frac{r^2\rho A}{4}\frac{\partial^2 u_1}{\partial x\partial\tau}\right]_R + \frac{M_D}{L}\left(-\frac{\partial^2 u_2}{\partial\tau^2} + a_1\sin\tau + a_2\sin\tau - \frac{g}{L\Omega^2}\right) = 0$$

$\frac{\partial u_2}{\partial x}$ is prescribed or

$$\left[\frac{S}{L^4\Omega^2}\frac{\partial^2 u_2}{\partial x^2}\right]_L + \left[\frac{S}{L^4\Omega^2}\frac{\partial^2 u_2}{\partial x^2}\right]_R + \frac{I_D}{L^3}\left[-\frac{\partial^3 u_2}{\partial x\partial\tau^2} + 2\frac{\partial^2 u_1}{\partial x\partial\tau}\right] = 0$$

A. RIGID SUPPORTS, SHORT BEARINGS, NO LUBRICANT

For this case, the gyroscopic and rotatory inertia terms of the shaft will now be neglected. The system is assumed to be placed in a vertical position and there is no unbalance in the disk. Therefore $r = 0$, $a_1(\xi) = 0$ $a_2(\xi) = 0$ and the gravity term in u_2 disappears leaving the new equations of motion from equations (3.2) and (3.3).

$$\frac{\partial^2 u_1}{\partial \tau^2} + \frac{S}{\rho A L^4 \Omega^2} \frac{\partial^4 u_1}{\partial x^4} = 0$$

$$\frac{\partial^2 u_2}{\partial \tau^2} + \frac{S}{\rho A L^4 \Omega^2} \frac{\partial^4 u_2}{\partial x^4} = 0 \tag{3.4}$$

The boundary conditions for short bearings,

$$x = 0 \qquad u_1 = 0 \qquad u_2 = 0$$

$$x = 1 \qquad \frac{\partial^2 u_1}{\partial x^2} = 0 \qquad \frac{\partial^4 u_2}{\partial x^4} = 0 \tag{3.5}$$

The continuity conditions are,

$$\left[\frac{\partial^3 u_1}{\partial x^3}\right]_L - \left[\frac{\partial^3 u_1}{\partial x^3}\right]_R - \frac{L^3 M_D \Omega^2}{S} \frac{\partial^2 u_1}{\partial \tau^2} = 0$$

$$\left[\frac{\partial^3 u_2}{\partial x^3}\right]_L - \left[\frac{\partial^3 u_2}{\partial x^3}\right]_R - \frac{L^3 M_D \Omega^2}{S} \frac{\partial^2 u_2}{\partial \tau^2} = 0 \tag{3.6}$$

$$-\left[\frac{\partial^2 u_1}{\partial x^2}\right]_L + \left[\frac{\partial^2 u_1}{\partial x^2}\right]_R - \frac{L\,\Omega^2 I_D}{S}\left[\frac{\partial^3 u_1}{\partial x \partial \tau^2} + 2\,\frac{\partial^2 u_2}{\partial x \partial \tau}\right] = 0$$

$$-\left[\frac{\partial^2 u_2}{\partial x^2}\right]_L + \left[\frac{\partial^2 u_2}{\partial x^2}\right]_R + \frac{L\,\Omega^2 I_D}{S}\left[-\frac{\partial^3 u_2}{\partial x \partial \tau^2} + 2\,\frac{\partial^2 u_1}{\partial x \partial \tau}\right] = 0 \tag{3.7}$$

$$\left[u_1\right]_R = \left[u_1\right]_L$$

$$\left[u_2\right]_R = \left[u_2\right]_L \tag{3.8}$$

$$\left[\frac{\partial u_1}{\partial x}\right]_R = \left[\frac{\partial u_1}{\partial x}\right]_L$$

$$\left[\frac{\partial u_2}{\partial x}\right]_R = \left[\frac{\partial u_2}{\partial x}\right]_L \tag{3.9}$$

The equations of motion are satisfied by the following assumed solution equations (3.10), if equations (3.11) hold.

Let

$$u_1 = X_1 \sin \tau$$

$$u_2 = X_2 \cos \tau \tag{3.10}$$

where

$$\tau = \Omega t$$

Substituting into equations of motion (3.4)

$$-X_1 + \frac{S}{\rho A L^4 \Omega^2} X_1^{IV} = 0$$

$$X_1^{IV} - p^4 X_1 = 0 \tag{3.11}$$

and

$$p^4 = \frac{\rho A L^4 \Omega^2}{S}$$

$$X_1 = C_1 \sin px + C_2 \cos px + C_3 \sinh px + C_4 \cosh px$$

Then to describe the motion completely we need (3.12)

$$X_2 = C_5 \sin px + C_6 \cos px + C_7 \sinh px + C_8 \cosh px$$

X_1^L = Left Hand Side

X_1^R = Right Hand Side

X_2^L = Left Hand Side (3.13)

X_2^R = Right Hand Side

and the constants are C_i^L

C_i^R $\quad i = 1, 8$

The boundary conditions are:

$$x = 0 \quad \left\{ \begin{array}{ll} \dfrac{\partial^2 X_1^L}{\partial x^2} = 0 & \dfrac{\partial^2 X_2^L}{\partial x^2} = 0 \\ X_1^L = 0 & X_2^L = 0 \end{array} \right\} \tag{3.14}$$

$$x = 1 \quad \left\{ \begin{array}{ll} \dfrac{\partial^2 X_1^R}{\partial x^2} = 0 & \dfrac{\partial^2 X_2^R}{\partial x^2} = 0 \\ X_1^R = 0 & X_2^R = 0 \end{array} \right\} \tag{3.15}$$

and continuity conditions at $x = \xi$ are,

Let

$$\mu_1 = \frac{M_D}{\rho A L} \qquad \mu_2 = \left(\frac{R_D}{2L}\right)^2$$

$$\frac{\partial^3 X_2^L}{\partial x^3} + \mu_1 p^4 X_1^L - \frac{\partial^3 X_1^R}{\partial x^3} = 0$$

$$\frac{\partial^3 X_2^L}{\partial x^3} + \mu_1 p^4 X_2^L - \frac{\partial^3 X_2^R}{\partial x^3} = 0$$

$$-\frac{\partial^2 X_1^L}{\partial x^2} + \frac{\partial^2 X_1^R}{\partial x^2} + \mu_1 \mu_2 p^4 \left[\frac{\partial X_1^L}{\partial x} + 2\,\frac{\partial X_2^L}{\partial x} \right] = 0$$

$$-\frac{\partial^2 X_2^L}{\partial x^2} + \frac{\partial^2 X_2^R}{\partial x^2} + \mu_1\mu_2 p^4 \left[\frac{\partial X_2^L}{\partial x} + 2\frac{\partial X_1^L}{\partial x}\right] = 0$$

$$\left.\begin{aligned}
X_1^L - X_1^R &= 0 \\
X_2^L - X_2^R &= 0 \\
\frac{\partial X_1^L}{\partial x} - \frac{\partial X_1^R}{\partial x} &= 0 \\
\frac{\partial X_2^L}{\partial x} - \frac{\partial X_2^R}{\partial x} &= 0
\end{aligned}\right\} \qquad (3.16)$$

The solution was given previously in terms of constants as equations

$$\begin{aligned}
X_1^L &= C_1^L \sin px + C_2^L \cos px + C_3^L \sinh px + C_4^L \cosh px \\
X_2^L &= C_5^L \sin px + C_6^L \cos px + C_7^L \sinh px + C_8^L \cosh px \\
X_1^R &= C_1^R \sin px + C_2^R \cos px + C_3^R \sinh px + C_4^R \cosh px \\
X_2^R &= C_5^R \sin px + C_6^R \cos px + C_7^R \sinh px + C_8^R \cosh px
\end{aligned} \qquad (3.13)$$

Inserting these values for X_i^j into the boundary and continuity conditions, the following set of homogeneous equations is obtained.

From equations (3.14)

$$\left.\begin{aligned}
&C_2^L + C_4^L = 0 \\
&-p^2 C_2^L + p^2 C_4^L = 0 \\
&C_6^L + C_8^L = 0 \\
&-p^2 C_6^L + p^2 C_8^L = 0
\end{aligned}\right\} \qquad (3.17)$$

$C_2^L = C_4^L = C_6^L = C_8^L = 0$ if the solution is to satisfy the boundary conditions at $x = 0$.

From equations (3.16),

$$\left.\begin{aligned}
&-p^3 \cos p\xi \, C_1^L + p^3 \cosh p\xi \, C_3^L + \mu_1 p^4 (C_1^L \sin p\xi + C_3^L \sinh p\xi) \\
&+ p^3 C_1^R \cos p\xi - p^3 C_2^R \sin p\xi - C_3^R p^3 \cosh p\xi - C_4^R p^3 \sinh p\xi = 0 \\
&-p^3 \cos p\xi \, C_5^L + p^3 C_7^L \cosh p\xi + \mu_1 p^4 (C_5^L \sin p\xi + C_7^L \sinh p\xi) \\
&+ C_5^R p^3 \cos p\xi - C_6^R p^3 \sin p\xi - p^3 C_7^R \cosh p\xi - p^3 C_8^R \sinh p\xi = 0
\end{aligned}\right\} \qquad (3.18)$$

$$C_1^L p^2 \sin p\xi - C_3^L p^2 \sinh p\xi - C_1^R p^2 \sin p\xi - C_2^R p^2 \cos p\xi + C_3^R p^2 \sinh p\xi$$

$$+ C_4^R p^2 \cosh p\xi + \mu_1 \mu_2 p^4 \Big[pC_1^L \cos p\xi + pC_3^L \cosh p\xi + 2C_5^L p \cos p\xi$$

$$+ 2C_7^L p \cosh p\xi \Big] = 0$$

$$C_5^L p^2 \sin p\xi - C_7^L p^2 \sinh p\xi - C_5^R p^2 \sin p\xi - C_6^R p^2 \cos p\xi + C_7^R p^2 \sinh p\xi$$

$$+ C_8^R p^2 \cosh p\xi + \mu_1 \mu_2 p^4 \Big[C_5^L p \cos p\xi + C_7^L p \cosh p\xi + 2C_1^L p \cos p\xi$$

$$+ 2C_3^L p \cosh p\xi \Big] = 0$$

$$C_1^L \sin p\xi + C_3^L \sinh p\xi - C_1^R \sin p\xi - C_2^R \cos p\xi - C_3^R \sinh p\xi - C_4^R \cosh p\xi = 0$$

$$C_5^L \sin p\xi + C_7^L \sinh p\xi - C_5^R \sin p\xi - C_6^R \cos p\xi - C_7^R \sinh p\xi - C_8^R \cosh p\xi = 0$$

$$C_1^L p \cos p\xi + pC_3 L \cosh p\xi - C_1^R p \cos p\xi + C_2^R p \sin p\xi - C_3^R p \cosh p\xi$$

$$- C_4^R p \sinh p\xi = 0$$

$$C_5^L p \cos p\xi + pC_7^L \cosh p\xi - C_5^R p \cos p\xi + C_6^R p \sin p\xi - C_7^R p \cosh p\xi$$

$$- C_8^R p \sinh p\xi = 0$$

and finally from equations (3.15)

$$C_1^R \sin p + C_2^R \cos p + C_3^R \sinh p + C_4^R \cosh p = 0$$

$$-p^2 C_1^R \sin p - p^2 C_2^R \cos p + p^2 C_3^R \sinh p + p^2 C_4^R \cosh p = 0$$

$$C_5^R \sin p + C_6^R \cos p + C_7^R \sin p + C_8^R \cosh p = 0$$

$$-C_5^R p^2 \sin p - C_6^R p^2 \cos p + p^2 C_7^R \sinh p + p^2 C_8^R \cosh p = 0$$

The determinant of these coefficients must vanish, to get nontrivial solutions. Now p, the critical speed, will be obtained for a range of values of M_1, μ_2, and ξ .

$$\begin{aligned}
&(-\cos p\xi + \mu_1 p \sin p\xi)\, C_1^L (\cosh p\xi + \mu_1 p \sinh p\xi)\, C_3^L \\
&+ \cos p\xi\, C_1^R - \sin p\xi\, C_2^R - \cosh p\xi\, C_3^R - \sinh p\xi\, C_4^R = 0 \\
&(-\cos p\xi + \mu_1 p \sin p\xi)\, C_5^L + (\cosh p\xi + \mu_1 p \sinh p\xi)\, C_7^L \\
&+ \cos p\xi\, C_5^R - \sin p\xi\, C_6^R - \cosh p\xi\, C_7^R - \sinh p\xi\, C_8^R = 0 \\
&(\sin p\xi + \mu_1\mu_2 p^3 \cos p\xi)\, C_1^L + (-\sin h\, p\xi + \mu_1\mu_2 p^3 \cosh p\xi)\, C_3^L \\
&+ 2u_1\mu_2 p^3 \cos p\xi\, C_5^L + 2\mu_1\mu_2 p^3 \cosh p\xi\, C_7^L - \sin p\xi\, C_1^R \\
&- \cos p\xi\, C_2^R + \sinh p\xi\, C_3^R + \cosh p\xi\, C_4^R = 0 \\
&2\mu_1\mu_2 p^3 \cos p\xi\, C_1^L + 2\mu_1\mu_2 p^3 \cosh p\xi\, C_3^L + (\sin p\xi + \mu_1\mu_2 p^3 \cos p\xi) \\
&C_5^L + (-\sinh p\xi + \mu_1\mu_2 p^3 \cosh p\xi)\, C_7^L - \sin p\xi\, C_5^R - \cos p\xi\, C_6^R \\
&+ \sinh p\xi\, C_7^R + \cosh p\xi\, C_8^R = 0 \\
&\sin p\xi\, C_1^L + \sinh p\xi\, C_3^L - \sin p\xi\, C_1^R - \cos p\xi\, C_2^R - \sinh p\xi\, C_3^R \\
&- \cosh p\xi\, C_4^R = 0
\end{aligned} \tag{3.20}$$

$$\sin p\xi\, C_5^L + \sinh p\xi\, C_7^L - \sin p\xi\, C_5^R - \cos p\xi\, C_6^R - \sinh p\xi\, C_7^R$$
$$- \cosh p\,\xi\, C_8^R = 0$$

$$\cos p\xi\, C_1^L + \cosh p\xi\, C_3^L - \cos p\xi\, C_1^R + \sin p\xi\, C_2^R - \cosh p\xi\, C_3^R$$
$$- \sinh p\xi\, C_4^R = 0$$

$$\cos p\xi\, C_5^L + \cosh p\xi\, C_7^L - \cos p\xi\, C_5^R + \sin p\xi\, C_6^R - \cosh p\xi\, C_7^R$$
$$- \sinh p\xi\, C_8^R = 0$$

$$(\sin p)\, C_1^R + \cos p\, C_2^R + \sinh p\, C_3^R + \cosh p\, C_4^R = 0$$
$$-\sin p\, C_1^R - \cos p\, C_2^R + \sinh p\, C_3^R + \cosh p\, C_4^R = 0$$
$$\sin p\, C_5^R + \cos p\, C_6^R + \sinh p\, C_7^R + \cosh p\, C_8^R = 0$$
$$-\sin p\, C_5^R - \cos p\, C_6^R + \sinh p\, C_7^R + \cosh p\, C_8^R = 0$$

The preceding set of homogeneous equations (3.20) is reduced to the following form.

$$(-\cos p\xi + \mu_1 p \sin p\xi)\, C_1^L + (\cosh p\xi + \mu_1 1 \sinh p\xi)\, C_3^L$$
$$+ (\cos p\xi + \sin p\xi \tan p)\, C_1^R + (-\cosh p\xi + \sinh p\xi \tan h\, p)\, C_3^R = 0$$

$$(\sin p\xi + \mu_1\mu_2 p^3 \cos p\xi)\, C_1^L + (-\sinh p\xi + \mu_1\mu_2 p^3 \cosh p\xi)\, C_3^L$$
$$+ 2\mu_1\mu_2 p^3 \cos p\xi\, C_5^L + 2\mu_1\mu_2 p^3 \cosh p\xi\, C_7^L + (-\sin p\xi + \cos p\xi \tan p)$$
$$C_1^R + (\sinh p\xi - \cosh p\xi \tanh p)\, C_3^R = 0$$

$$(-\cos p\xi + \mu_1 p \sin p\xi)\, C_5^L + (\cosh p\xi + \mu_1 p \sinh p\xi)\, C_7^L$$
$$+ (\cos p\xi + \sin p\xi \tan p)\, C_5^R + (-\cosh p\xi + \sinh p\xi \tanh p)\, C_7^R = 0$$

$$-2\mu_1\mu_2\, p^3 \cos p\xi\, C_1^L + 2\mu_1\mu_2\, p^3 \cosh p\xi\, C_3^L + (\sin p\xi + \mu_1\mu_2\, p^3 \cos p\xi)$$

$$C_5^L + (-\sinh p\xi + \mu_1\mu_2\, p^3 \cosh p\xi\, C_7^L + (-\sin p\xi + \cos p\xi \tan p)$$

$$C_5^R + (\sinh p\xi - \cosh p\xi \tanh p)\, C_7^R = 0$$

$$\sin p\xi\, C_1^L + \sinh p\xi\, C_3^L + (-\sin p\xi + \cos p\xi \tan p)\, C_1^R$$

$$+ (-\sinh p\xi + \cosh p\xi \tanh p)\, C_3^R = 0$$

$$\cos p\xi\, C_1^L + \cosh p\xi\, C_3^L + (-\cos p\xi - \sin p\xi \tan p)\, C_1^R$$

$$+ (-\cosh p\xi + \sinh p\xi \tanh p)\, C_3^R = 0$$

$$\sin p\xi\, C_5^L + \sinh p\xi\, C_7^L + (-\sin p\xi + \cos p\xi \tan p)\, C_5^R$$

$$+ (-\sinh p\xi + \cosh p\xi \tanh p)\, C_7^R = 0$$

$$\cos p\xi\, C_5^L + \cosh p\xi\, C_7^L + (-\cos p\xi - \sin p\xi \tan p)\, C_5^R$$

$$+ (-\cosh p\xi + \sinh p\xi \tanh p)\, C_7^R = 0$$

$$C_2^R = -\tan p\, C_1^R$$

$$C_4^R = -\tanh p\, C_3^R \qquad (3.21)$$

$$C_8^R = -\tanh p\, C_7^R$$

$$C_6^R = -\tan p\, C_5^R$$

The critical speeds of the system can now be found by finding the values of p which make the determinant of equations (3.21) equal zero. Equations (3.21) contain several dimensionless variables which must be specified in order to obtain values of p. These dimensionless variables specify the location of the disk on the shaft, ξ , the ratio of the mass of the disk to the mass of the shaft, μ_1, and the ratio of the radius of the disk to the length of the shaft, μ_2.

where

$$p = \sqrt[4]{\frac{\rho_s A\ L^4\ \Omega^2}{S}} \quad \text{-- critical speed}$$

$$\mu_1 = \frac{M_D}{\rho_s A\ L} \quad \text{-- mass effect}$$

$$\mu_2 = \left(\frac{R_D}{2L}\right)^2 \quad \text{-- disk effect} \tag{3.22}$$

$$\xi = \frac{a}{L} \quad \text{-- disk location}$$

The mass effect can be broken down into more fundamental dimensionless variables if more detailed specification of the system is desired.

$$M_D = \rho_D \pi\ R_D^2\ h$$

where

h = thickness of the disk.

Then

$$\mu_1 = \frac{\rho_D \pi\ R_D^2\ h}{\rho_s \pi\ R_s^2\ L}$$

$$\mu_1 = 4 \left(\frac{\rho_D}{\rho_s}\right) \left(\frac{R_D}{2L}\right)^2 \left(\frac{L}{R_s}\right)^2 \left(\frac{h}{L}\right) \tag{3.23}$$

where

$\frac{\rho_D}{\rho_S}$ = ratio of density of disk to density of shaft

$\frac{R_D}{2L}$ = disk effect

$$\frac{R_S}{L} = r \text{ - ratio of radius of shaft to shaft length}$$

$$\frac{h}{L} = \text{ratio of disk thickness to length of shaft}$$

In the following work, the following assumptions are made:

$$\frac{\rho_D}{\rho_S} = 1.0$$

$$\frac{R_S}{L} = \frac{1}{20}$$

$$\frac{h}{L} = \frac{1}{72}$$

The disk effect $\frac{R_D}{2L}$ is varied at specific locations of the disk in the calculation of the critical speeds p.

Thus for the following cases, the mass effect is a function of the disk effect.

$$\mu_1 = 22.22\,\mu_2 \tag{3.24}$$

Therefore, this is really a special case and the other parameters could be varied to get a more complete set of curves for the different physical variations of the basic system of the disk on the shaft. Caution must be observed in using h because the following assumption was made in the derivation $\left(\frac{h}{R_D}\right)^2 << 1$.

The frequency equation will now be obtained for some special cases. If $\xi = 0$, the disk is placid at the shaft support. This means that there will be no mass effect but only the effects of the gyroscopic forces and rotatory inertia. The following set of homogeneous equations is obtained from equations (3.21).

$$-C_1^L + C_3^L + C_1^R - C_3^R = 0$$

$$C_7 D_1^L + G\, C_3^L + 2G\, C_5^L + 2G\, C_7^L + C_1^R \tan p - C_3^R \tanh p = 0$$

$$-C_5^L + C_7^L + C_5^R - C_7^R = 0$$

$$2G\, C_1^L + 2G\, C_3^L + G\, C_5^L + G\, C_7^L + \tan p\, C_5^R - C_7^R \tanh p = 0$$

$$C_1^R \tan p + C_3^R \tanh p = 0 \qquad (3.25)$$

$$C_1^L + C_3^L - C_1^R - C_3^R = 0$$

$$C_5^R \tan p + C_7^R \tanh p = 0$$

$$C_5^L + C_7^L - C_5^R - C_7^R = 0$$

where

$$G = \mu_1 \mu_2 p^3$$

The frequency equation for the disk mounted at the edge of the shaft is obtained from equations (3.25) by making the determinant of the coefficients zero.

$$\left[G\left(1 - \frac{\tanh p}{\tan p}\right) - 2 \tanh p\right]^2 - \left[2G\left(1 - \frac{\tanh p}{\tan p}\right)\right]^2 = 0 \qquad (3.26)$$

$$\left.\begin{aligned} \cot_p &= \coth p + \frac{2}{\mu_1\mu_2 p^3} && \text{(a)} \\ \cot_p &= \coth p - \frac{2}{3\mu_1\mu_2 p^3} && \text{(b)} \end{aligned}\right\} \qquad (3.27)$$

Equation (3.27 a) is the governing frequency equation for critical speeds of forward whirl and equation (3.27 b) is the frequency equation for backward whirl. The variation of critical speeds with disk size is shown as figure 7 on page 69. A plot of equations (3.27 a) and (b) is given on page 53 for specific values of μ_1 and μ_2 and is valid for $p > \pi$.

Equation (3.21) are specialized for $\xi = \frac{1}{2}$ and the following set of homogeneous simultaneous equations is obtained.

$$\mu_1 p \sin p/2 \; C_1^L + (2 \cosh p/2 + \mu_1 p \sinh p/2)\, C_3^L - 2 \frac{\cosh p/2}{\cosh p} C_3^R = 0$$

$$(2 \sin p/2 + \mu_1\mu_2 p^3 \cos p/2)\, C_1^L + \mu_1\mu_2 p^3 \cosh p/2 \; C_3^L \qquad (3.28)$$

$$+ 2\mu_1\mu_2 p^3 \cos p/2 \; C_5^L + 2\mu_1\mu_2 p^3 \cosh p/2 \; C_7^L + 2 \frac{\sin p/2}{\cos p} C_1^R = 0$$

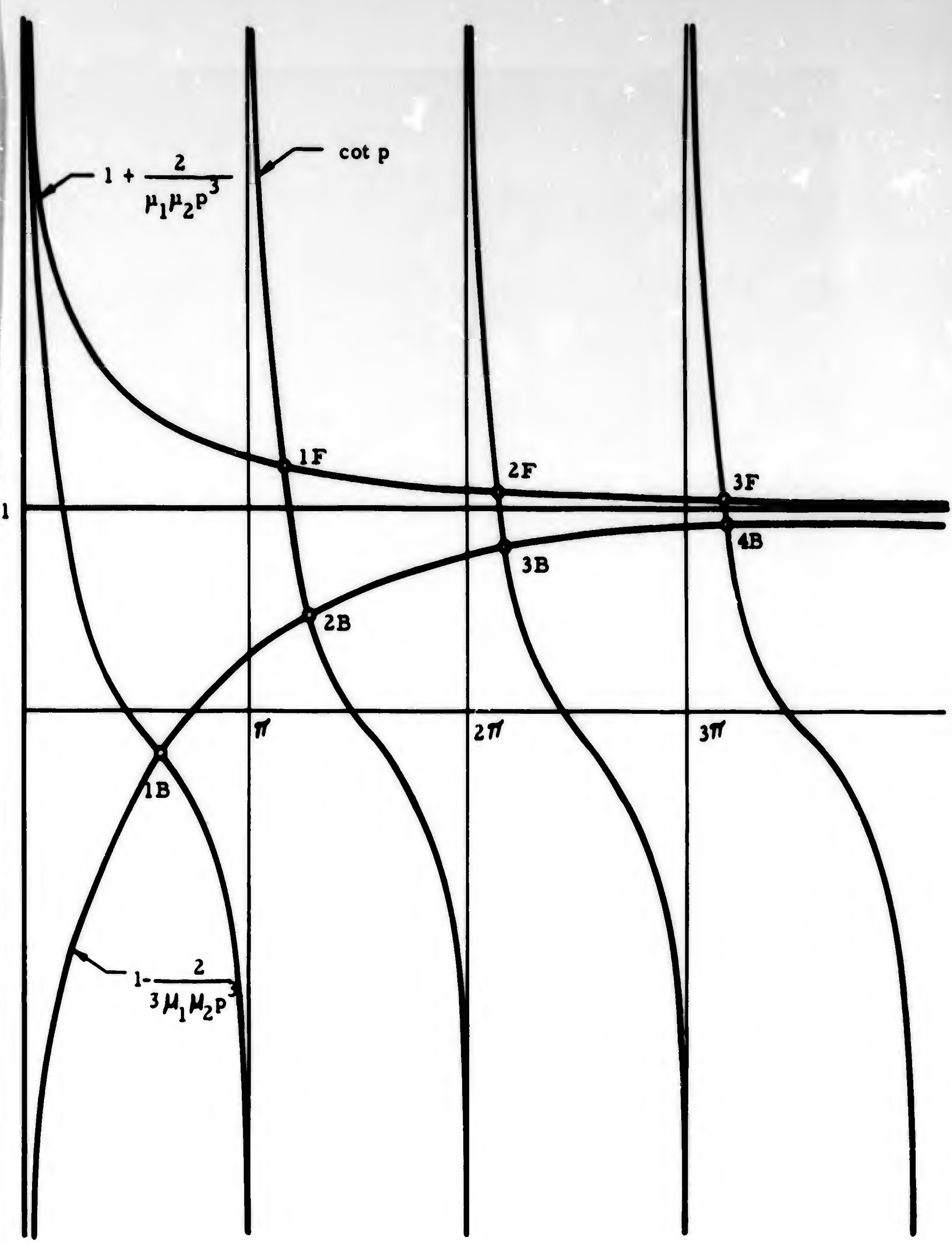

Figure 4 SOLUTION OF FREQUENCY EQUATIONS (3.27)

$$\mu_1 p \sin\ p/2\, C_5^L + (2\cosh p/2 + \mu_1 p \sinh p/2)\, C_7^L - 2\,\frac{\cosh p/2}{\cosh p}\, C_7^R = 0\ ,$$

$$2\mu_1\mu_2 p^3 \cos p/2\, C_1^L + 2\mu_1\mu_2 p^3 \cosh p/2\, C_3^L + (2\sin p/2 + \mu_1\mu_2 p^3 \cos p/2)\, C_5^L$$

$$+ \mu_1\mu_2 p^3 \cosh p/2\, C_7^L + 2\,\frac{\sin p/2}{\cos p}\, C_5^R = 0$$

$$\sin p/2\, C_1^L + \sinh p/2\, C_3^L + \frac{\sin p/2}{\cos p}\, C_1^R + \frac{\sinh p/2}{\cosh p}\, C_3^R = 0 \tag{3.28}$$

$$\cos p/2\, C_1^L + \cosh p/2\, C_3^L - \frac{\cos p/2}{\cos p}\, C_1^R - \frac{\cosh p/2}{\cosh p}\, C_3^R = 0$$

$$\sin p/2\, C_5^L + \sinh p/2\, C_7^L + \frac{\sin p/2}{\cos p}\, C_5^R + \frac{\sinh p/2}{\cosh p}\, C_7^R = 0$$

$$\cos p/2\, C_5^L + \cosh p/2\, C_7^L - \frac{\cos p/2}{\cos p}\, C_5^R - \frac{\cosh p/2}{\cosh p}\, C_7^R = 0$$

The symmetry of the system can be expressed as follows

$$\left.\begin{aligned} X_1^L(x) &= \pm X_1^R(1-x) \\ X_2^L(x) &= \pm X_2^R(1-x) \end{aligned}\right\} \tag{3.29}$$

where

+ odd modes

- even modes

using equations (3.13) and allowing $C_2^L = C_4^L = C_6^L = C_8^L = 0$ as previously noted.

The following relationships are obtained between the constants.

$$C_1^R = \mp \cos p\, C_1^L \qquad C_3^R = \mp \cosh p\, C_3^L$$

$$C_5^R = \mp \cos p\, C_5^L \qquad C_7^R = \mp \cosh p\, C_7^L$$

Inserting these relationships into the equations (3.28), the following new set of equations is obtained.

Let

$$G = \mu_1 p$$

$$H = \mu_1 \mu_2 p^3$$

$$(-\cos p/2 + G \sin p/2 \mp \cos p/2) C_1^L + (\cosh p/2 + C_7 \sinh p/2 \pm \cosh p/2) C_3^L = 0$$

$$(\sin p/2 + H \cos p/2 \mp \sin p/2)\, C_1^L + (-\sinh p/2 + H \cosh p/2 \pm \sinh p/2)\, C_3^L$$

$$+ 2\, H \cos p/2\, C_5^L + 2\, H \cosh p/2\, C_7^L = 0$$

(3.29)

$$(-\cos p/2 + G \sin p/2 \mp \cos p/2) C_5^L + (\cosh p/2 + C_7 \sinh p/2 \pm \cosh p/2) C_7^L = 0$$

$$2H \cos p/2\, C_1^L + 2H \cosh p/2\, C_3^L + (\sin p/2 + H \cos p/2 \mp \sin p/2)$$

$$+ (-\sinh p/2 + h \cosh p/2 \pm \sinh p/2)\, C_7^L = 0$$

$$(\sin p/2 \mp \sin p/2)\, C_1^L + (\sinh p/2 \mp \sinh p/2)\, C_3^L = 0$$

$$(\cos p/2 \pm \cos p/2)\, C_1^L + (\cosh p/2 \pm \cosh p/2)\, C_3^L = 0$$

$$(\sin p/2 \mp \sin p/2)\, C_5^L + (\sinh p/2 \mp \sinh p/2)\, C_7^L = 0$$

$$(\cos p/2 \pm \cos p/2)\, C_5^L + (\cosh p/2 \pm \cosh p/2)\, C_7^L = 0$$

Then for odd mode shapes

$$\tan p/2 = \tanh p/2 + \frac{4}{u_1 p} \tag{3.30}$$

for even mode shapes

$$\frac{4}{\mu_1 \mu_2 p^3} + \coth p/2 = \cot p/2$$

$$\tag{3.31}$$

$$\frac{-4}{2\mu_1 \mu_2 p^3} + \coth p/2 = \cot p/2$$

Equation (3.30) shows that the critical speeds of the odd modes depend only on the mass effect μ_1. The critical speeds for the even modes are governed by the frequency equations (3.31 a) and (b) which represent forward and backward whirl respectively. Figure 5 shows a rough plot of the roots for specific values of μ_1 and μ_2 and for $p/2 > \pi$.

In figure 5, the intersections of the dashed lines represent the roots of the odd modes and the intersections of the solid lines represent the roots of the even modes for $\xi = \frac{1}{2}$ and special values of μ_1 and μ_2. This figure shows the order in which the various critical speeds are

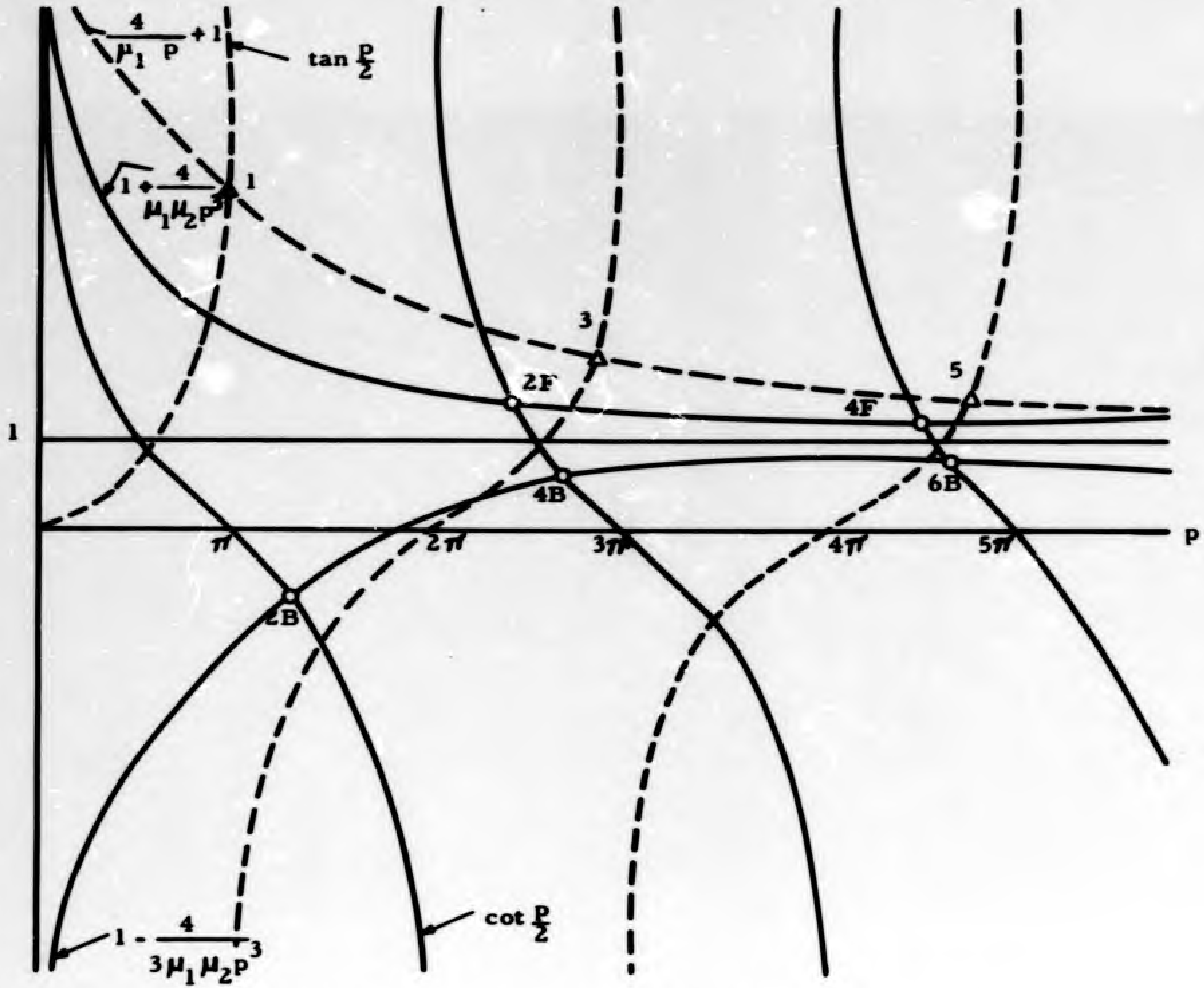

Figure 5 SOLUTION OF FREQUENCY EQUATIONS (3.30) AND (3.31)

encountered while increasing the angular velocity of the system. It also shows that three critical speeds of different order approach each other as the value of p, μ_1 and μ_2 increase. It can be seen from figure 5 that for large p

$$P_n^F = P_{n+1}^F = P_{n+2}^B \cong \frac{n\pi}{2} \tag{3.32}$$

where

$n = 5, 9, 13,$ etc.

P_n^F = nth mode forward whirl

P_{n+2}^B = n + 2th mode backward whirl

1. Solution of General Frequency Equation

The determinant of equations (3.21) on page 48 was evaluated for values of μ_2 varying between 0.01 and 0.2 and values of p varying between 0 and 16.0. This task was done with the aid of the IBM 7090 computer and was programmed in Fortran language. The flow diagram and nomenclature of the computer program are given in figure 6 on page 59.

The actual program is given on page 6[illegible]. Since the output from the computer program for the numerous values of p computed is voluminous, only a sample of it will be included in this report (pages 6[illegible] through 64). The remainder of the output is given in tabular form on pages 65 through 67 and in graphical form on pages 69, 71 and 72.

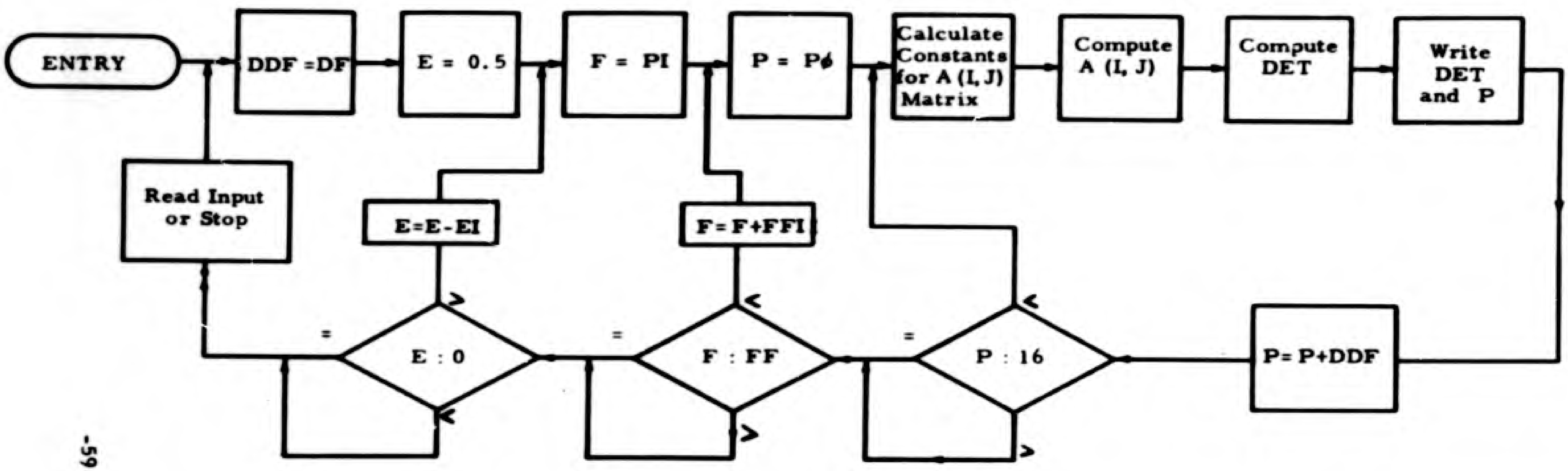

NOMENCLATURE

Pϕ = Initial value of Critical Speed (P)
DF = DDF = Increment of P
P = Critical Speed
F = μ_2 = Disk Effect
PI = Initial Value of Disk Effect
FF = Final Value of μ_2
FFI = Increment of μ_2

EI = Increment of Disk Location E
E = Disk Location
DET = Determinant
D = h/L
R = R_o/L
PC = $p\xi$
G = $\mu_1 p$
H = $\mu_1 \mu_2 p^3$

Figure 6 FLOW DIAGRAM

```
   23 READ INPUT TAPE 5,1,FF,FFI,EI,PI,DF,AC,PC,R,NF,D
    1 FORMAT(8F6.3,I2,F7.5)
      WRITE OUTPUT TAPE 6,3,FF,FFI,EI,PI,DF,AC,PO,R,NF,D
    3 FORMAT(74H1COMPUTATION OF CRITICAL SPEEDS FOR A SINGLE DISK ON A C
     1ONTINUOUS SHAFT  /////11H INPUT DATA//4H FF=E12.5,6H  FFI=E12.5,6H
     2  EI=E12.5,6H   PI=E12.6,6H   DF=E12.6/4H AC=E12.6,6H   PO=E12.6,
     36H     R=E12.6,6H   NF=I3,9X6H    C=E12.6////9X2H E,15X1HF,15X1HP,1
     44X3HDET/31H     DISK LOCATION      DISK SIZE,21X11HDETERMINANT///)
      DIMENSION A(8,8), B(8)
      DCF=DF
      F=.5
   25 F=FI
   22 P=PC
C     CALCULATE CONSTANTS FOR A(I,J) MATRIX
    8 U=4.*D*F/(R*R)
      PC=P*E
      TP=SINF(P)/COSF(P)
      SPC=EXPF(PC)
      CPC=.5*(SPC+1./SPC)
      SPC=.5*(SPC-1./SPC)
      TPC=SPC/CPC
      G=U*P
      H=U*F*P*P*P
      S=SINF(PC)
      C=COSF(PC)
      TA=TANHF(P)
C     GENERATE ELEMENTS FOR A(I,J) MATRIX
      DO 2 I=1,8
      DO 2 J=1,8
    2 A(I,J)=0.
      A(1,1)=-C+G*S
      A(1,2)=CPC+G*SPC
      A(1,5)=C+S*TP
      A(1,6)=-CPC+SPC*TA
      A(2,1)=S+H*C
      A(2,2)=-SPC+H*CPC
      A(2,3)=2.*H*C
      A(2,4)=2.*H*CPC
      A(2,5)=-S+C*TP
      A(2,6)=SPC-CPC*TA
      A(3,3)=A(1,1)
      A(3,4)=A(1,2)
      A(3,7)=A(1,5)
      A(3,8)=A(1,6)
      A(4,1)=A(2,3)
      A(4,2)=A(2,4)
      A(4,3)=A(2,1)
      A(4,4)=A(2,2)
      A(4,7)=A(2,5)
      A(4,8)=A(2,6)
      A(5,1)=S
      A(5,2)=SPC
      A(5,5)=A(2,5)
      A(5,6)=-A(2,6)
      A(6,1)=C
      A(6,2)=CPC
      A(6,5)=-A(1,5)
      A(6,6)=A(1,6)
      A(7,3)=S
      A(7,4)=SPC
      A(7,7)=A(2,5)
      A(7,8)=-A(2,6)
      A(8,3)=C
      A(8,4)=CPC
      A(8,7)=-A(1,5)
      A(8,8)=A(1,6)
C     DEFINITIONS BEFORE ENTRANCE TO LEQD
      I=8
      J=0
      IA=8
      IB=8
      CALL LEQD(A,B,I,J,IA,IB,DET)
      WRITE OUTPUT TAPE 6,4,E,F,P,DET
    4 FORMAT(4E16.5)
   11 P=P+DCF
      IF(P-16.) 8, 18, 18
   18 IF(F-FF) 21, 20, 20
   21 F=F+FFI
      GO TO 22
   20 IF(E) 23, 23, 24
   24 E=E-EI
      GO TO 25
      END(1,0,0,0,0,0,1,0,0,0,0,0,0,0,0)
```

COMPUTATION OF CRITICAL SPEEDS FOR A SINGLE DISK ON A CONTINUOUS SHAFT /

INPUT DATA

FF= 0.16000E-00 FFI= 0.30000E-01 EI= 0.25000E-00 PI=0.700000E-01 DF=0.200000E-01
AC=1.000000E-02 PO=0.300000E-01 R=0.500000E-01 NF= 5 D=0.138000E-01

E DISK LOCATION	F DISK SIZE	P	DET DETERMINANT
0.50000E 00	0.70000E-01	0.30000E-01	0.12960E-04
0.50000E 00	0.70000E-01	0.50000E-01	0.10000E-03
0.50000E 00	0.70000E-01	0.70000E-01	0.38416E-03
0.50000E 00	0.70000E-01	0.90000E-01	0.10498E-02
0.50000E 00	0.70000E-01	0.11000E-00	0.23426E-02
0.50000E 00	0.70000E-01	0.13000E-00	0.45701E-02
0.50000E 00	0.70000E-01	0.15000E-00	0.81009E-02
0.50000E 00	0.70000E-01	0.17000E-00	0.13366E-01
0.50000E 00	0.70000E-01	0.19000E-00	0.20858E-01
0.50000E 00	0.70000E-01	0.21000E-00	0.31131E-01
0.50000E 00	0.70000E-01	0.23000E-00	0.44803E-01
0.50000E 00	0.70000E-01	0.25000E-00	0.62556E-01
0.50000E 00	0.70000E-01	0.27000E-00	0.85134E-01
0.50000E 00	0.70000E-01	0.29000E-00	0.11335E-00
0.50000E 00	0.70000E-01	0.31000E-00	0.14808E-00
0.50000E 00	0.70000E-01	0.33000E-00	0.19026E-00
0.50000E 00	0.70000E-01	0.35000E-00	0.24092E-00
0.50000E 00	0.70000E-01	0.37000E-00	0.30115E-00
0.50000E 00	0.70000E-01	0.39000E-00	0.37211E-00
0.50000E 00	0.70000E-01	0.41000E-00	0.45506E-00
0.50000E 00	0.70000E-01	0.43000E-00	0.55131E 00
0.50000E 00	0.70000E-01	0.45000E-00	0.66230E 00
0.50000E 00	0.70000E-01	0.47000E-00	0.78954E 00
0.50000E 00	0.70000E-01	0.49000E-00	0.93466E 00
0.50000E 00	0.70000E-01	0.51000E 00	0.10994E 01
0.50000E 00	0.70000E-01	0.53000E 00	0.12856E 01
0.50000E 00	0.70000E-01	0.55000E 00	0.14953E 01
0.50000E 00	0.70000E-01	0.57000E 00	0.17306E 01
0.50000E 00	0.70000E-01	0.59000E 00	0.19939E 01
0.50000E 00	0.70000E-01	0.61000E 00	0.22876E 01
0.50000E 00	0.70000E-01	0.63000E 00	0.26144E 01
0.50000E 00	0.70000E-01	0.65000E 00	0.29772E 01
0.50000E 00	0.70000E-01	0.67000E 00	0.33794E 01
0.50000E 00	0.70000E-01	0.69000E 00	0.38243E 01
0.50000E 00	0.70000E-01	0.71000E 00	0.43157E 01
0.50000E 00	0.70000E-01	0.73000E 00	0.48579E 01
0.50000E 00	0.70000E-01	0.75000E 00	0.54556E 01
0.50000E 00	0.70000E-01	0.77000E 00	0.61137E 01
0.50000E 00	0.70000E-01	0.79000E 00	0.68382E 01
0.50000E 00	0.70000E-01	0.81000E 00	0.76352E 01
0.50000E 00	0.70000E-01	0.83000E 00	0.85120E 01
0.50000E 00	0.70000E-01	0.85000E 00	0.94766E 01
0.50000E 00	0.70000E-01	0.87000E 00	0.10538E 02
0.50000E 00	0.70000E-01	0.89000E 00	0.11707E 02
0.50000E 00	0.70000E-01	0.91000E 00	0.12994E 02
0.50000E 00	0.70000E-01	0.93000E 00	0.14414E 02
0.50000E 00	0.70000E-01	0.95000E 00	0.15982E 02
0.50000E 00	0.70000E-01	0.97000E 00	0.17715E 02
0.50000E 00	0.70000E-01	0.99000E 00	0.19638E 02
0.50000E 00	0.70000E-01	0.10100E 01	0.21768E 02
0.50000E 00	0.70000E-01	0.10300E 01	0.24139E 02
0.50000E 00	0.70000E-01	0.10500E 01	0.26785E 02
0.50000E 00	0.70000E-01	0.10700E 01	0.29748E 02
0.50000E 00	0.70000E-01	0.10900E 01	0.33071E 02
0.50000E 00	0.70000E-01	0.11100E 01	0.36820E 02
0.50000E 00	0.70000E-01	0.11300E 01	0.41066E 02
0.50000E 00	0.70000E-01	0.11500E 01	0.45897E 02
0.50000E 00	0.70000E-01	0.11700E 01	0.51427E 02
0.50000E 00	0.70000E-01	0.11900E 01	0.57797E 02
0.50000E 00	0.70000E-01	0.12100E 01	0.65186E 02
0.50000E 00	0.70000E-01	0.12300E 01	0.73827E 02
0.50000E 00	0.70000E-01	0.12500E 01	0.84026E 02
0.50000E 00	0.70000E-01	0.12700E 01	0.96191E 02
0.50000E 00	0.70000E-01	0.12900E 01	0.11087E 03
0.50000E 00	0.70000E-01	0.13100E 01	0.12885E 03
0.50000E 00	0.70000E-01	0.13300E 01	0.15120E 03
0.50000E 00	0.70000E-01	0.13500E 01	0.17953E 03
0.50000E 00	0.70000E-01	0.13700E 01	0.21627E 03

0.50000E 00	0.70000E-01	0.13900E 01	0.2651[illegible]E 03	
0.50000E 00	0.70000E-01	0.14100E 01	0.33257E 03	
0.50000E 00	0.70000E-01	0.14300E 01	0.42933E 03	
0.50000E 00	0.70000E-01	0.14500E 01	0.57598E 03	
0.50000E 00	0.70000E-01	0.14700E 01	0.81499E 03	
0.50000E 00	0.70000E-01	0.14900E 01	0.12466E 04	
0.50000E 00	0.70000E-01	0.15100E 01	0.21585E 04	
0.50000E 00	0.70000E-01	0.15300E 01	0.46874E 04	
0.50000E 00	0.70000E-01	0.15500E 01	0.17591E 05	
0.50000E 00	0.70000E-01	0.15700E 01	0.11660E 08	
0.50000E 00	0.70000E-01	0.15900E 01	0.19455E 05	
0.50000E 00	0.70000E-01	0.16100E 01	0.45127E 04	
0.50000E 00	0.70000E-01	0.16300E 01	0.19067E 04	
0.50000E 00	0.70000E-01	0.16500E 01	0.10231E 04	
0.50000E 00	0.70000E-01	0.16700E 01	0.62407E 03	
0.50000E 00	0.70000E-01	0.16900E 01	0.41203E 03	
0.50000E 00	0.70000E-01	0.17100E 01	0.28687E 03	
0.50000E 00	0.70000E-01	0.17300E 01	0.20733E 03	
0.50000E 00	0.70000E-01	0.17500E 01	0.15398E 03	
0.50000E 00	0.70000E-01	0.17700E 01	0.11668E 03	
0.50000E 00	0.70000E-01	0.17900E 01	0.89735E 02	
0.50000E 00	0.70000E-01	0.18100E 01	0.69768E 02	
0.50000E 00	0.70000E-01	0.18300E 01	0.54659E 02	
0.50000E 00	0.70000E-01	0.18500E 01	0.43034E 02	
0.50000E 00	0.70000E-01	0.18700E 01	0.33966E 02	
0.50000E 00	0.70000E-01	0.18900E 01	0.26818E 02	
0.50000E 00	0.70000E-01	0.19100E 01	0.21137E 02	
0.50000E 00	0.70000E-01	0.19300E 01	0.16593E 02	
0.50000E 00	0.70000E-01	0.19500E 01	0.12944E 02	
0.50000E 00	0.70000E-01	0.19700E 01	0.10010E 02	
0.50000E 00	0.70000E-01	0.19900E 01	0.76504E 01	
0.50000E 00	0.70000E-01	0.20100E 01	0.57581E 01	
0.50000E 00	0.70000E-01	0.20300E 01	0.42488E 01	
0.50000E 00	0.70000E-01	0.20500E 01	0.30553E 01	
0.50000E 00	0.70000E-01	0.20700E 01	0.21235E 01	
0.50000E 00	0.70000E-01	0.20900E 01	0.14094E 01	
0.50000E 00	0.70000E-01	0.21100E 01	0.87651E 00	
0.50000E 00	0.70000E-01	0.21300E 01	0.49436E-00	
0.50000E 00	0.70000E-01	0.21500E 01	0.23704E-00	
0.50000E 00	0.70000E-01	0.21700E 01	0.82250E-01	
0.50000E 00	0.70000E-01	0.21900E 01	0.10492E-01	
0.50000E 00	0.70000E-01	0.22100E 01	0.44173E-02	← 1F
0.50000E 00	0.70000E-01	0.22300E 01	0.48345E-01	
0.50000E 00	0.70000E-01	0.22500E 01	0.12784E-00	
0.50000E 00	0.70000E-01	0.22700E 01	0.22940E-00	
0.50000E 00	0.70000E-01	0.22900E 01	0.34013E-00	
0.50000E 00	0.70000E-01	0.23100E 01	0.44754E-00	
0.50000E 00	0.70000E-01	0.23300E 01	0.53934E 00	
0.50000E 00	0.70000E-01	0.23500E 01	0.60324E 00	
0.50000E 00	0.70000E-01	0.23700E 01	0.62679E 00	
0.50000E 00	0.70000E-01	0.23900E 01	0.59724E 00	
0.50000E 00	0.70000E-01	0.24100E 01	0.50139E 00	
0.50000E 00	0.70000E-01	0.24300E 01	0.32547E-00	
0.50000E 00	0.70000E-01	0.24500E 01	0.54999E-01	
0.50000E 00	0.70000E-01	0.24700E 01	-0.32535E-00	← 2B
0.50000E 00	0.70000E-01	0.24900E 01	-0.83185E 00	
0.50000E 00	0.70000E-01	0.25100E 01	-0.14819E 01	
0.50000E 00	0.70000E-01	0.25300E 01	-0.22941E 01	
0.50000E 00	0.70000E-01	0.25500E 01	-0.32884E 01	
0.50000E 00	0.70000E-01	0.25700E 01	-0.44863E 01	
0.50000E 00	0.70000E-01	0.25900E 01	-0.59109E 01	
0.50000E 00	0.70000E-01	0.26100E 01	-0.75874E 01	
0.50000E 00	0.70000E-01	0.26300E 01	-0.95426E 01	
0.50000E 00	0.70000E-01	0.26500E 01	-0.11806E 02	
0.50000E 00	0.70000E-01	0.26700E 01	-0.14409E 02	
0.50000E 00	0.70000E-01	0.26900E 01	-0.17385E 02	
0.50000E 00	0.70000E-01	0.27100E 01	-0.20773E 02	
0.50000E 00	0.70000E-01	0.27300E 01	-0.24612E 02	
0.50000E 00	0.70000E-01	0.27500E 01	-0.28945E 02	
0.50000E 00	0.70000E-01	0.27700E 01	-0.33821E 02	
0.50000E 00	0.70000E-01	0.27900E 01	-0.39289E 02	
0.50000E 00	0.70000E-01	0.28100E 01	-0.45407E 02	
0.50000E 00	0.70000E-01	0.28300E 01	-0.52233E 02	
0.50000E 00	0.70000E-01	0.28500E 01	-0.59834E 02	
0.50000E 00	0.70000E-01	0.28700E 01	-0.68281E 02	
0.50000E 00	0.70000E-01	0.28900E 01	-0.77651E 02	
0.50000E 00	0.70000E-01	0.29100E 01	-0.88028E 02	
0.50000E 00	0.70000E-01	0.29300E 01	-0.99503E 02	
0.50000E 00	0.70000E-01	0.29500E 01	-0.11218E 03	
0.50000E 00	0.70000E-01	0.29700E 01	-0.12615E 03	
0.50000E 00	0.70000E-01	0.29900E 01	-0.14155E 03	
0.50000E 00	0.70000E-01	0.30100E 01	-0.15850E 03	
0.50000E 00	0.70000E-01	0.30300E 01	-0.17713E 03	

0.50000E 00	0.70000E-01	0.30500E 01	-0.1976[illegible]E 03	
0.50000E 00	0.70000E-01	0.30700E 01	-0.22[illegible] 03	
0.50000E 00	0.70000E-01	0.30900E 01	-0.2[illegible]	
0.50000E 00	0.70000E-01	0.31100E 01	-0.271[illegible]	
0.50000E 00	0.70000E-01	0.31300E 01	-0.301[illegible]	
0.50000E 00	0.70000E-01	0.31500E 01	-0.333[illegible]	
0.50000E 00	0.70000E-01	0.31700E 01	-0.3[illegible]	
0.50000E 00	0.70000E-01	0.31900E 01	-0.4001[illegible]	
0.50000E 00	0.70000E-01	0.32100E 01	-0.4505[illegible]	
0.50000E 00	0.70000E-01	0.32300E 01	-0.4970[illegible]E 03	
0.50000E 00	0.70000E-01	0.32500E 01	-0.5477[illegible] 03	
0.50000E 00	0.70000E-01	0.68100E 01	-0.73002E 05	
0.50000E 00	0.70000E-01	0.68300E 01	-0.71810E 05	
0.50000E 00	0.70000E-01	0.68500E 01	-0.70621E 05	
0.50000E 00	0.70000E-01	0.68700E 01	-0.69410E 05	
0.50000E 00	0.70000E-01	0.68900E 01	-0.68203E 05	
0.50000E 00	0.70000E-01	0.69100E 01	-0.66982E 05	
0.50000E 00	0.70000E-01	0.69300E 01	-0.65746E 05	
0.50000E 00	0.70000E-01	0.69500E 01	-0.64509E 05	
0.50000E 00	0.70000E-01	0.69700E 01	-0.63252E 05	
0.50000E 00	0.70000E-01	0.69900E 01	-0.61980E 05	
0.50000E 00	0.70000E-01	0.70100E 01	-0.60711E 05	
0.50000E 00	0.70000E-01	0.70300E 01	-0.59431E 05	
0.50000E 00	0.70000E-01	0.70500E 01	-0.58136E 05	
0.50000E 00	0.70000E-01	0.70700E 01	-0.56827E 05	
0.50000E 00	0.70000E-01	0.70900E 01	-0.55511E 05	
0.50000E 00	0.70000E-01	0.71100E 01	-0.54182E 05	
0.50000E 00	0.70000E-01	0.71300E 01	-0.52844E 05	
0.50000E 00	0.70000E-01	0.71500E 01	-0.51494E 05	
0.50000E 00	0.70000E-01	0.71700E 01	-0.50139E 05	
0.50000E 00	0.70000E-01	0.71900E 01	-0.48765E 05	
0.50000E 00	0.70000E-01	0.72100E 01	-0.47385E 05	
0.50000E 00	0.70000E-01	0.72300E 01	-0.45997E 05	
0.50000E 00	0.70000E-01	0.72500E 01	-0.44595E 05	
0.50000E 00	0.70000E-01	0.72700E 01	-0.43186E 05	
0.50000E 00	0.70000E-01	0.72900E 01	-0.41767E 05	
0.50000E 00	0.70000E-01	0.73100E 01	-0.40340E 05	
0.50000E 00	0.70000E-01	0.73300E 01	-0.38903E 05	
0.50000E 00	0.70000E-01	0.73500E 01	-0.37457E 05	
0.50000E 00	0.70000E-01	0.73700E 01	-0.36004E 05	
0.50000E 00	0.70000E-01	0.73900E 01	-0.34547E 05	
0.50000E 00	0.70000E-01	0.74100E 01	-0.33079E 05	
0.50000E 00	0.70000E-01	0.74300E 01	-0.31605E 05	
0.50000E 00	0.70000E-01	0.74500E 01	-0.30121E 05	
0.50000E 00	0.70000E-01	0.74700E 01	-0.28634E 05	
0.50000E 00	0.70000E-01	0.74900E 01	-0.27139E 05	
0.50000E 00	0.70000E-01	0.75100E 01	-0.25637E 05	
0.50000E 00	0.70000E-01	0.75300E 01	-0.24122E 05	
0.50000E 00	0.70000E-01	0.75500E 01	-0.22601E 05	
0.50000E 00	0.70000E-01	0.75700E 01	-0.21073E 05	
0.50000E 00	0.70000E-01	0.75900E 01	-0.19522E 05	
0.50000E 00	0.70000E-01	0.76100E 01	-0.17956E 05	
0.50000E 00	0.70000E-01	0.76300E 01	-0.16366E 05	
0.50000E 00	0.70000E-01	0.76500E 01	-0.14732E 05	
0.50000E 00	0.70000E-01	0.76700E 01	-0.13043E 05	
0.50000E 00	0.70000E-01	0.76900E 01	-0.11279E 05	
0.50000E 00	0.70000E-01	0.77100E 01	-0.93822E 04	
0.50000E 00	0.70000E-01	0.77300E 01	-0.72738E 04	
0.50000E 00	0.70000E-01	0.77500E 01	-0.48001E 04	
0.50000E 00	0.70000E-01	0.77700E 01	-0.16361E 04	← 2F
0.50000E 00	0.70000E-01	0.77900E 01	0.30891E 04	
0.50000E 00	0.70000E-01	0.78100E 01	0.12213E 05	
0.50000E 00	0.70000E-01	0.78300E 01	0.42334E 05	
0.50000E 00	0.70000E-01	0.78500E 01	0.11074E 07	
0.50000E 00	0.70000E-01	0.78700E 01	0.23104E 05	
0.50000E 00	0.70000E-01	0.78900E 01	-0.64319E 04	← 4F
0.50000E 00	0.70000E-01	0.79100E 01	-0.73609E 04	
0.50000E 00	0.70000E-01	0.79300E 01	-0.63213E 04	
0.50000E 00	0.70000E-01	0.79500E 01	-0.51230E 04	
0.50000E 00	0.70000E-01	0.79700E 01	-0.40164E 04	
0.50000E 00	0.70000E-01	0.79900E 01	-0.30475E 04	
0.50000E 00	0.70000E-01	0.80100E 01	-0.22166E 04	
0.50000E 00	0.70000E-01	0.80300E 01	-0.15201E 04	
0.50000E 00	0.70000E-01	0.80900E 01	-0.95474E 03	
0.50000E 00	0.70000E-01	0.80700E 01	-0.51890E 03	
0.50000E 00	0.70000E-01	0.80900E 01	-0.21314E 03	
0.50000E 00	0.70000E-01	0.81100E 01	-0.40406E 02	
0.50000E 00	0.70000E-01	0.81300E 01	-0.39454E 01	← 3F
0.50000E 00	0.70000E-01	0.81500E 01	-0.10914E 03	
0.50000E 00	0.70000E-01	0.81700E 01	-0.36199E 03	
0.50000E 00	0.70000E-01	0.81900E 01	-0.76914E 03	
0.50000E 00	0.70000E-01	0.82100E 01	-0.13377E 04	

0.50000E 00	0.70000E-01	0.82300E 01	-0.20782E 04
0.50000E 00	0.70000E-01	0.82500E 01	-0.29983E 04
0.50000E 00	0.70000E-01	0.82700E 01	-0.41074E 04
0.50000E 00	0.70000E-01	0.82900E 01	-0.54176E 04
0.50000E 00	0.70000E-01	0.83100E 01	-0.69393E 04
0.50000E 00	0.70000E-01	0.83300E 01	-0.86822E 04
0.50000E 00	0.70000E-01	0.83500E 01	-0.10664E 05
0.50000E 00	0.70000E-01	0.83700E 01	-0.12894E 05
0.50000E 00	0.70000E-01	0.83900E 01	-0.15388E 05
0.50000E 00	0.70000E-01	0.84100E 01	-0.18157E 05
0.50000E 00	0.70000E-01	0.84300E 01	-0.21224E 05
0.50000E 00	0.70000E-01	0.84500E 01	-0.24603E 05
0.50000E 00	0.70000E-01	0.84700E 01	-0.28319E 05
0.50000E 00	0.70000E-01	0.84900E 01	-0.32368E 05
0.50000E 00	0.70000E-01	0.85100E 01	-0.36788E 05
0.50000E 00	0.70000E-01	0.85300E 01	-0.41598E 05
0.50000E 00	0.70000E-01	0.85500E 01	-0.46815E 05
0.50000E 00	0.70000E-01	0.85700E 01	-0.52467E 05
0.50000E 00	0.70000E-01	0.85900E 01	-0.58580E 05
0.50000E 00	0.70000E-01	0.86100E 01	-0.65139E 05
0.50000E 00	0.70000E-01	0.86300E 01	-0.72234E 05
0.50000E 00	0.70000E-01	0.86500E 01	-0.79872E 05
0.50000E 00	0.70000E-01	0.86700E 01	-0.88073E 05
0.50000E 00	0.70000E-01	0.86900E 01	-0.96869E 05
0.50000E 00	0.70000E-01	0.87100E 01	-0.10630E 06
0.50000E 00	0.70000E-01	0.87300E 01	-0.11640E 06
0.50000E 00	0.70000E-01	0.87500E 01	-0.12719E 06
0.50000E 00	0.70000E-01	0.87700E 01	-0.13874E 06
0.50000E 00	0.70000E-01	0.87900E 01	-0.15107E 06
0.50000E 00	0.70000E-01	0.88100E 01	-0.16422E 06
0.50000E 00	0.70000E-01	0.88300E 01	-0.17823E 06
0.50000E 00	0.70000E-01	0.88500E 01	-0.19316E 06
0.50000E 00	0.70000E-01	0.88700E 01	-0.20908E 06
0.50000E 00	0.70000E-01	0.88900E 01	-0.22605E 06
0.50000E 00	0.70000E-01	0.89100E 01	-0.24410E 06
0.50000E 00	0.70000E-01	0.89300E 01	-0.26329E 06
0.50000E 00	0.70000E-01	0.89500E 01	-0.28369E 06
0.50000E 00	0.70000E-01	0.89700E 01	-0.30536E 06
0.50000E 00	0.70000E-01	0.89900E 01	-0.32842E 06
0.50000E 00	0.70000E-01	0.90100E 01	-0.35284E 06
0.50000E 00	0.70000E-01	0.90300E 01	-0.37868E 06
0.50000E 00	0.70000E-01	0.90500E 01	-0.40624E 06
0.50000E 00	0.70000E-01	0.90700E 01	-0.43548E 06
0.50000E 00	0.70000E-01	0.90900E 01	-0.46649E 06
0.50000E 00	0.70000E-01	0.91100E 01	-0.49938E 06
0.50000E 00	0.70000E-01	0.91300E 01	-0.53425E 06
0.50000E 00	0.70000E-01	0.91500E 01	-0.57121E 06

Table 2 Data Obtained From the Frequency Equation (3.21) for $\xi = 0$

F=.01	F=.02	F=.03	F=.04	F=.05	F=.07	F=.1	F=.13	F=.16	F=.19
3.04	2.76	2.46	2.20	2.00	1.72	1.44	1.28	1.14	1.06
3.18	3.28	3.42	3.56	3.66	3.78	3.86	3.88	3.90	3.90
5.44	4.52	4.20	4.08	4.02	3.98	3.96	3.94	3.94	3.94
6.52	6.82	6.94	7.00	7.02	7.04	7.06	7.06	7.06	7.07
7.56	7.18	7.12	7.10	7.08	7.08	7.08	7.08	7.08	7.07
9.90	10.12	10.16	10.18	10.20	10.20	10.20	10.20	10.20	10.20
10.36	10.24	10.22	10.22	10.22	10.22	10.22	10.22	10.22	10.22
10.18	13.30	13.34	13.34	13.34	13.34	13.34	13.35	13.35	13.35
13.42	13.36	13.36	13.36	13.36	13.36	13.36	13.35	13.35	13.35

Table 3 Data Obtained From the Frequency Equation (3.21) for $\xi = .25$

F=.01	F=.02	F=.03	F=.04	F=.05	F=.07	F=.1	F=.13	F=.16	F=.19
2.94	2.74	2.54	2.36	2.20	1.96	1.70	1.50	1.38	1.26
3.00	2.90	2.80	2.76	2.72	2.66	2.58	2.52	2.44	2.38
5.79	5.24	4.52	4.08	3.78	3.42	3.08	2.88	2.72	2.62
5.79	5.58	5.48	5.42	5.38	5.34	5.32	5.30	5.31	5.28
7.34	5.86	5.60	5.52	5.48	5.40	5.36	5.32	5.31	5.30
9.40	9.50	9.52	9.51	9.50	9.49	9.48	9.46	9.46	9.45
9.98	9.70	9.60	9.56	9.54	9.52	9.48	9.48	9.46	9.45
13.48	13.64	13.68	13.68	13.68	13.67	13.65	13.64	13.63	13.63
13.90	13.78	13.72	13.70	13.69	13.67	13.65	13.64	13.63	13.63
		15.96	15.92	15.90	15.84	15.80	15.78	15.77	15.77
			15.96	15.92	15.86	15.82	15.80	15.77	15.77

Table 4 Data Obtained From the Frequency Equation (3.21) for $\xi = .5$

F=.01	F=.02	F=.03	F=.04	F=.05	F=.07	F=.1	F=.13	F=.16	F=.19
2.87	2.68	2.54	2.43	2.34	2.21	2.06	1.80	1.62	1.5
2.87	2.68	2.54	2.43	2.34	2.21	2.06	1.94	1.85	1.79
5.54	4.40	3.68	3.22	2.90	2.46	2.06	1.64	1.85	1.79
6.56	7.12	7.48	7.62	7.70	7.78	7.82	7.84	7.84	7.84
8.79	8.16	8.00	7.94	7.90	7.88	7.86	7.86	7.86	7.86
8.79	8.52	8.37	8.27	8.21	8.13	8.05	8.01	7.99	7.97
9.04	8.52	8.37	8.27	8.21	8.13	8.05	8.01	7.99	7.97
13.62	13.98	14.06	14.10	14.12	14.12	14.13	14.13		
14.36	14.20	14.16	14.16	14.14	14.14	14.13	14.13		
14.86	14.6	14.47	14.41	14.36	14.31	14.25	14.23	14.21	14.20
14.86	14.6	14.47	14.41	14.36	14.31	14.25	14.23	14.21	14.20

Discussion of Results

The critical speeds of a system consisting of a continuous shaft carrying a single disk, mounted on fixed short bearings are shown in graphical form on pages 69, 71, and 72 for a range of values of the disk size. Each of three graphs shows the critical speeds for a disk mounted at a specific location on the shaft.

The values of the critical speeds for zero radius and mass disks on a plain shaft are shown as $n\pi$. This result was obtained because the gyroscopic effects dominate except at very small disk sizes. Therefore these results are in slight error for very small disk sizes.

In calculating the critical speeds, the "disk effect" $\left(\frac{R_D}{2L}\right)^2$ was varied from 0 to .20 and usually the first four ordered modes were considered.

In general it can be said that the so called "mass effect" (ratio of mass of the disk to mass of the shaft) lowers the critical speeds of the system as the mass of the disk is increased. The gyroscopic effects on the system tend to effectively stiffen or soften the spring of the system and thus depending upon the speed of the shaft rotation the gyroscopic effects will either increase or decrease the critical speeds of the system. This results in a backward and a forward whirl at the same order mode when gyroscopic effects are in effect.

Figure 7 represents the critical speeds of a system with the disk located at the bearing which means that there will be no "mass effect" on the critical speeds but only gyroscopic and rotatory inertia effects. This case then has two critical speeds (one of backward whirl and one of forward whirl) at each order mode shape and as the "disk effect" and

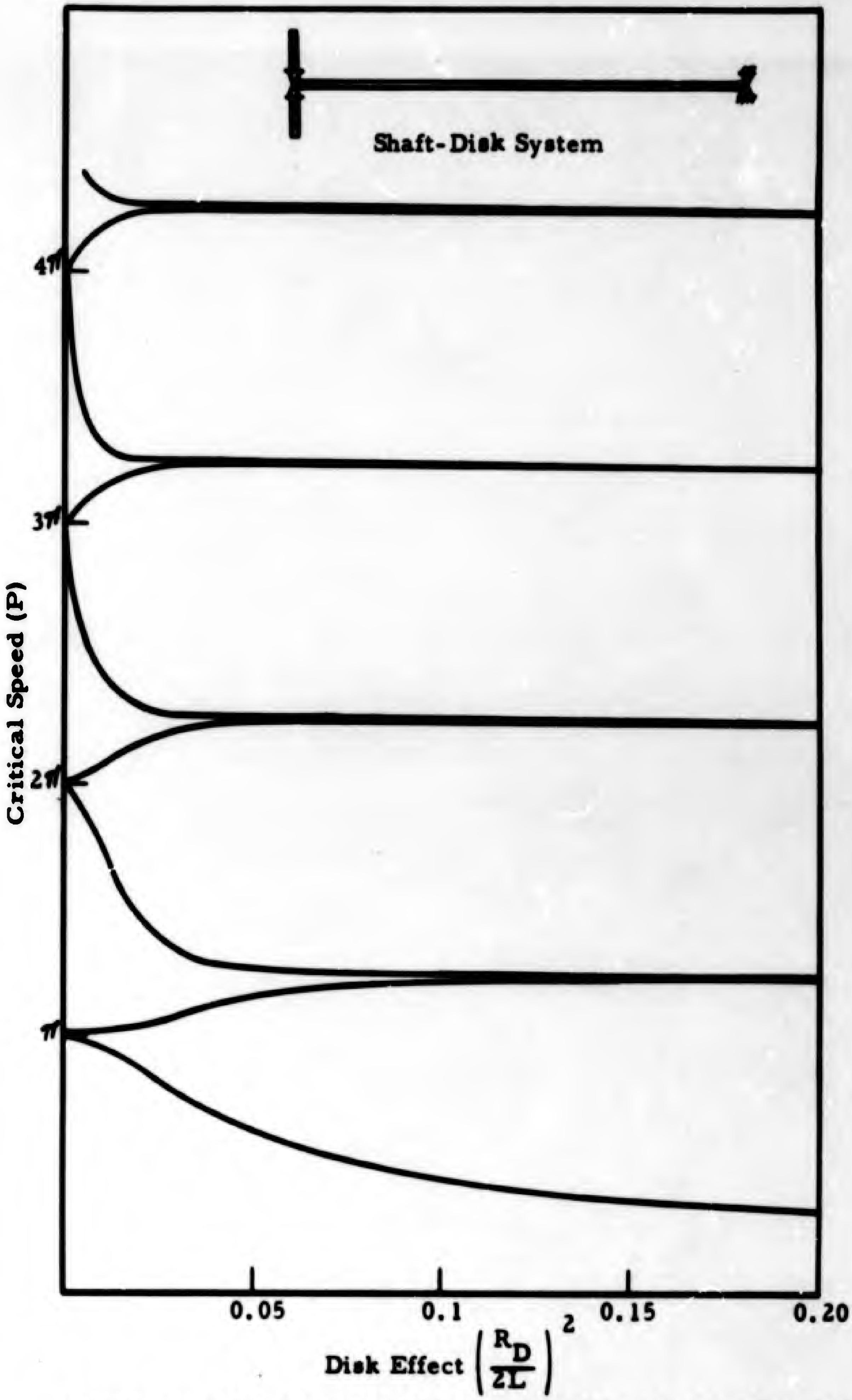

Figure 7 THE VARIATION OF CRITICAL SPEEDS OF A DISK MOUNTED ON A CONTINUOUS SHAFT DUE TO GYROSCOPIC AND ROTATORY INERTIA EFFECTS

critical speed are increased, p^B_{n+1} approaches p^F_n and both approach a value of $\frac{n\pi}{4}$ where n = 5, 9, 13 etc. This result is shown graphically on page 69 and was obtained mathematically from equations (3.27) on page 52.

Figure 8 shows the variation of critical speeds with "disk effect" for a system with the disk mounted at the quarter point along the shaft. Note that the critical speeds of the first and second order modes are in general decreased by the "mass effect" as well as showing two criticals for each order mode which incicates that gyroscopic effects are also in action here. The third order critical speeds show less "mass effect" and fourth order critical speeds show virtually none because of the proximity of the disk to a modal point. However, the gyroscopic effect is strong in these cases.

Figure 9 shows the variation of critical speeds with "disk effect" for a system with the disk mounted in the center of the shaft. Two types of critical speeds are obtained here. Only one critical speed is obtained for the odd order modes while two critical speeds are obtained for the even order modes. This occurs because of the symmetry of the system. The critical speeds obtained from the odd order modes are in general decreased as a result of increasing the size of the disk. This result was shown in analytical form as equation (3.30) which only depends on μ_1 the "mass effect". The critical speeds for the even mode shapes show no "mass effect" but have gyroscopic effects as shown by figure 9 and equations (3.31). Finally, as p, μ_1, and μ_2 are increased, both figure 9 and equations (3.30) and (3.31) show that

$$p^F_n = P^F_{n+1} = P^B_{n+2} \quad \frac{n\pi}{2} \quad \text{where } n = 5, 9, 13 \text{ etc.}$$

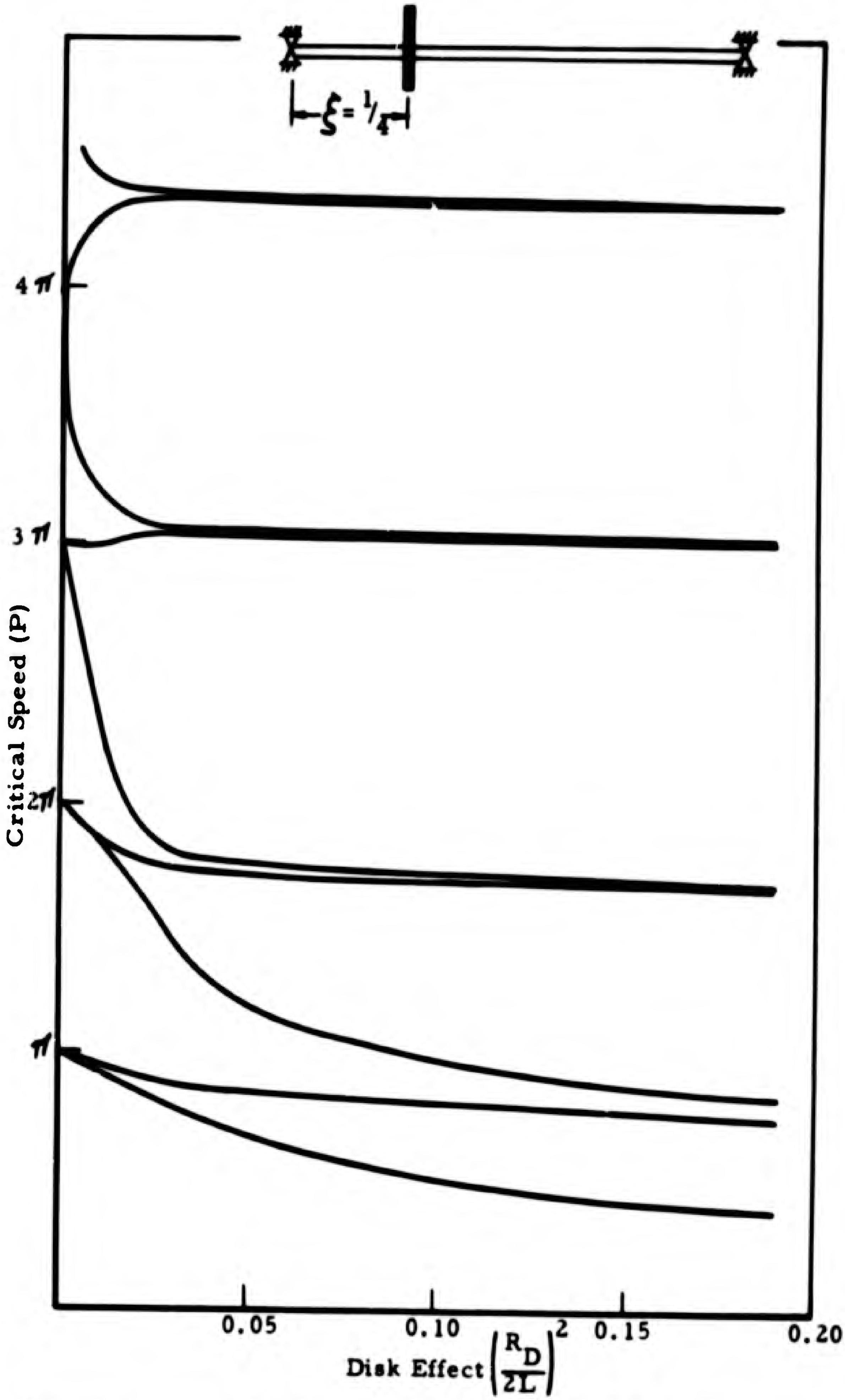

Figure 8 THE VARIATION OF CRITICAL SPEEDS OF A DISK MOUNTED ON A CONTINUOUS SHAFT DUE TO GYROSCOPIC AND ROTATORY INERTIA EFFECTS

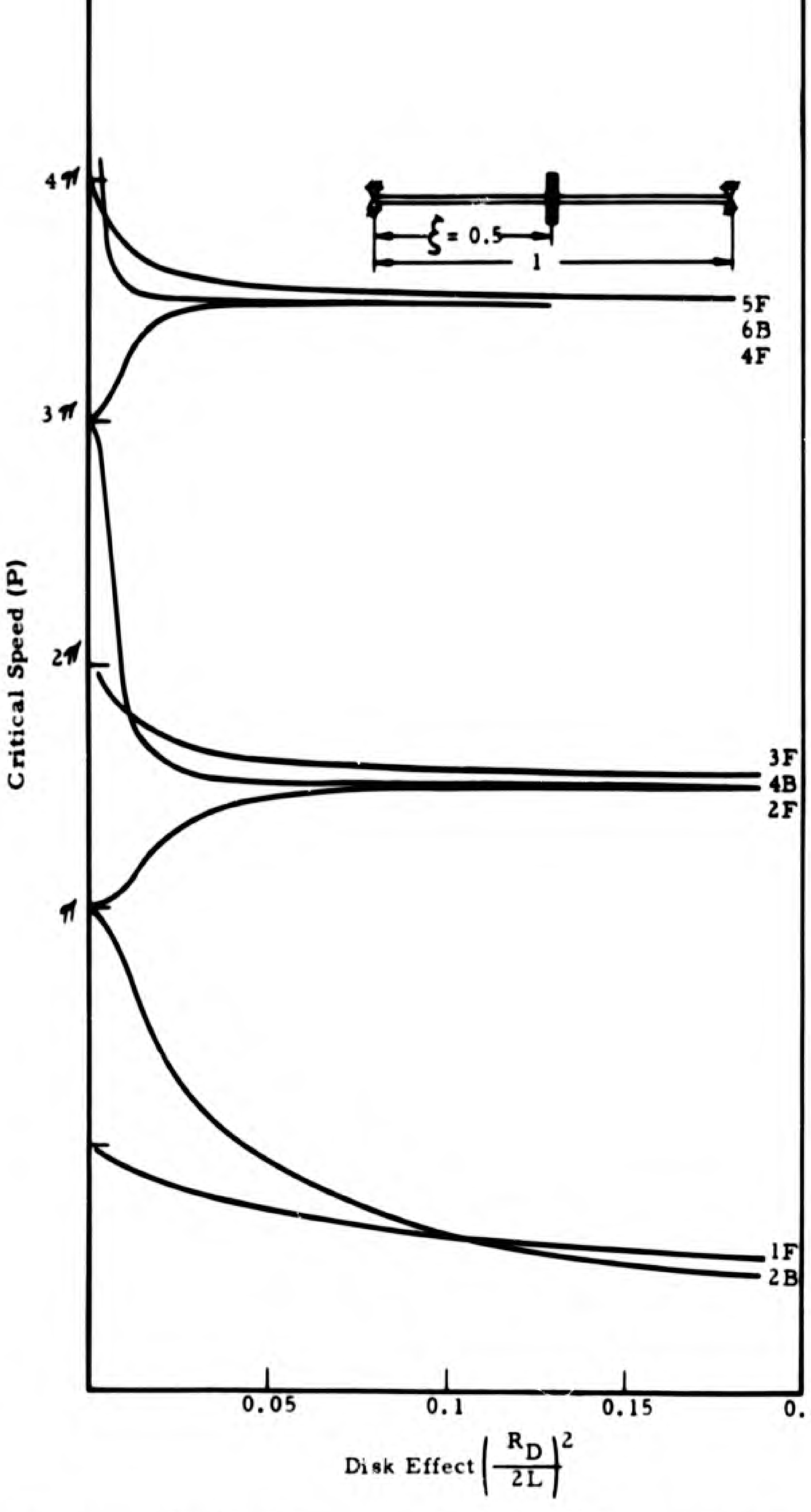

Figure 9 THE VARIATION OF CRITICAL SPEEDS OF A DISK MOUNTED ON A CONTINUOUS SHAFT DUE TO GYROSCOPIC AND ROTATORY INERTIA EFFECTS

IV. EXPERIMENTATION;CONCLUSIONS

The test fixture, figure 10, which was developed for this continuing series has undergone continuous modification directed toward elimination of spurious responses, reduction in experimental error, and incorporation of new features which permit the investigation of additional phenomena. Operation at high speeds has also shown the necessity of incorporating additional features which permit safe operation at such speeds.

The text fixtures can be considered as consisting of four major subelements or subassemblies:

1. The supporting structure, figure 10
2. The drive system, figure 16
3. The rotor and end bearing fixtures, figures 20, 23, 25, 26
4. The response indicators and instrumentation, figure 11.

The supporting structure which was developed under Contract No. NObs–86805 was modified only with regard to operational safety. This base structure consists of a welded box beam 11-1/2 inches wide by 19-/12 inches deep, with four stiffening baffles, all constructed of 3/4 inch mild steel plate. This rugged beam is supported on 8 inch steel pipe pedestals which raise the rotor support assemblies to a convenient height. Two very stiff A-frames are bolted to the beam for mounting the end-bearing assemblies. These end frames were modified to accommodate new end bearing fixtures, as described later.

Large shaft excursions in critical speed ranges have previously caused the shaft to disengage itself from the bearings. This endangers operational personnel and damages expensive test equipment. The steel protective cage which was previously used as a safety device was undesirable since it makes operation inconvenient and while protecting the experimentalists, does little to protect the test equipment. A simple, versatile device was developed to avoid these difficulties. Drawings of this device are printed in Appendix C and it can be seen in figures 10 and 15; it consists of a stiff frame which is supported on a rail mounted to the base; thus, the frame can easily be positioned along the length of the shaft. The frame carries three rollers, adjustable laterally (horizontally and vertically). In operation, these rollers are spaced around the rest position of the shaft with a clearance which ranges from zero to 1/2 inch, depending on the experiment to be performed. Should the shaft attempt to attain larger displacements, the rollers restrain it. The fixture can be used to safely accelerate the rotating system through a critical speed since the roller can be engaged while the system is in operation. The fixture has been found to operate quite satisfactorily.

The drive section is mounted on a stiff, cross-braced system which is separate from the main rotor base. Isolation between the drive and the rotor is increased by means of isolation pads and flexible connections between the drive and the rotor. The drive system, figure 16, consists of a heavy D. C. motor which is coupled to a flywheel whose polar moment of inertia is 59.64 in-lb-sec^2. The polar moment of inertia of the basic 3/4 inch shaft is only 0.0011 in-lb-sec^2, while the hub and disk used in some of the experiments have a polar moment of inertia of 1.20 in.-lb-sec^2, thus the flywheel tends to insure that shaft vibration has little effect on its rotational speed. The basic goals in the drive system design were those of high attainable speed, stable motor speed, and "stiffness" of the drive system, to insure that load variations have little effect on rotational speed. These goals were approached through several avenues. A constant voltage transformer feeds a semiconductor D.C. power supply through two variable transformers, connected to give vernier voltage adjustment. Thus, line fluctuations have little effect on D.C. output voltage and the relatively low output impedance of the D.C. supply yields a "stiff" input to the motor. The motor, itself, was increased in capacity to the present one horsepower 6000 RPM unit which drives the flywheel through a compliant timing belt drive with a two-to-one speed step-up. Both the power capacity of the motor and the compliance of the drive tend to filter out speed fluctuations.

Since the bearings are not fixed, it was necessary to have a flexible connection between the flywheel and the rotor proper. This connection is composed of two hooke joints, figure 17, connected back-to-back to yield a constant-speed configuration.

The 50 inch long rotor, figure 20, was carefully turned to a nominal 3/4 inch diameter (measured as 0.749 inches). A disk, figure 24, of 14 inch diameter and thickness of 0.433 inches was attached to the rotor for some of the experimental work. The attachment is executed by means of a collet-type hub, which permits placement of the disk at any point along the length of the rotor. The shaft ends are carried in bearing blocks, figure 23, each of which may carry a single ball bearing assembly, or two such assemblies. The single assembly reproduces "pinned ends," while the double assembly restrains the end rotation.

The bearing blocks are carried in the "A" frames by means of tension springs, figure 25. Several sets of these springs are available with differing moduli. Spring hangers, figure 26, with varying hole spacing can be attached to the bearing blocks, thus the ratio of lateral elastic restraint to angular elastic restraint can be adjusted.

Bearing response was sensed by C. R. L. accelerometers on the bearing blocks and measured with a Ballantine Model 300 vacuum tube voltmeter and a calibrated Tektronix Model 535 Oscilloscope. A tachometer was used for rough speed measurement. The speed was measured and checked by means of the calibrated sweep of an oscilloscope, together with a Tektronix type 183B rotational analyzer. A Hewlett-Packard electronic counter was also used. Additional output measurements were afforded by an IRD type 600 response indicator and a General Motors Portable Pulse Synchronized Unbalance Indicator (PSUI). A Krohn-Hite variable bandpass filter was used to eliminate spurious signals.

The experimental work was performed as a check on the validity of the analyses which were reported in previous chapters. Significant effort was also devoted to an attempt to observe the theoretically predicted gravity critical speeds in circular shafts. This last attempt proved to be fruitless, although additional data which confirmed the analyses of Contract NObs—78753 and of Contract NObs—86805 was obtained.

The curves included in Appendix E of the final report for Contract NObs—86805 were used to calculate the natural frequencies of the pinned-pinned rotor, without the disk, mounted as shown in figure 10. The preceding analysis included the effect of the bearing mass and support stiffness on the natural frequencies of the system. These analytical results from Contract NObs—86805 are compared to the experimental and analytical results obtained during the program in Table 5.

The physical characteristics of the experimental fixture are:

Diameter of Rotor: 0.75 inches

Length of Rotor: 50.1875 inches

Weight of support bearing: 2.25 lb

Stiffness of support springs:

$k = 3.168 \times 10^6$ lb/in.

("Rigid supports"), 100 lb/in., 150 lb/in.

Diameter of Disk: 14.0 inches

Weight of Disk: 18.44 lb

Thickness of Disk: 0.433 inches

Material of Disk and Rotor: steel

Figure 29 shows the amplitude of displacement (mils) of the bearing support plotted against speed of rotation of the plain rotor. The IRD Vibration analyzer was used in conjunction with the rotational analyzer to obtain this record. A sample of the data is given in figure 28 which indicates 0.05 mils displacement at 1400 RPM. The apparent straight line is a series of angular reference marks and a complete revolution is indicated by the small marks at the top of the photograph. This record gives the speed of rotation of the shaft as well as an indication of the history of the whirl of the shaft during each revolution.

Figures 30, 31, and 32 show displacement amplitude-speed curves for the rotor with a disk mounted at various locations. This data was obtained by using the method previously described.

Tables 5 and 6 show comparison of experimental and analytical results for the plain rotor and various disk-shaft combinations respectively.

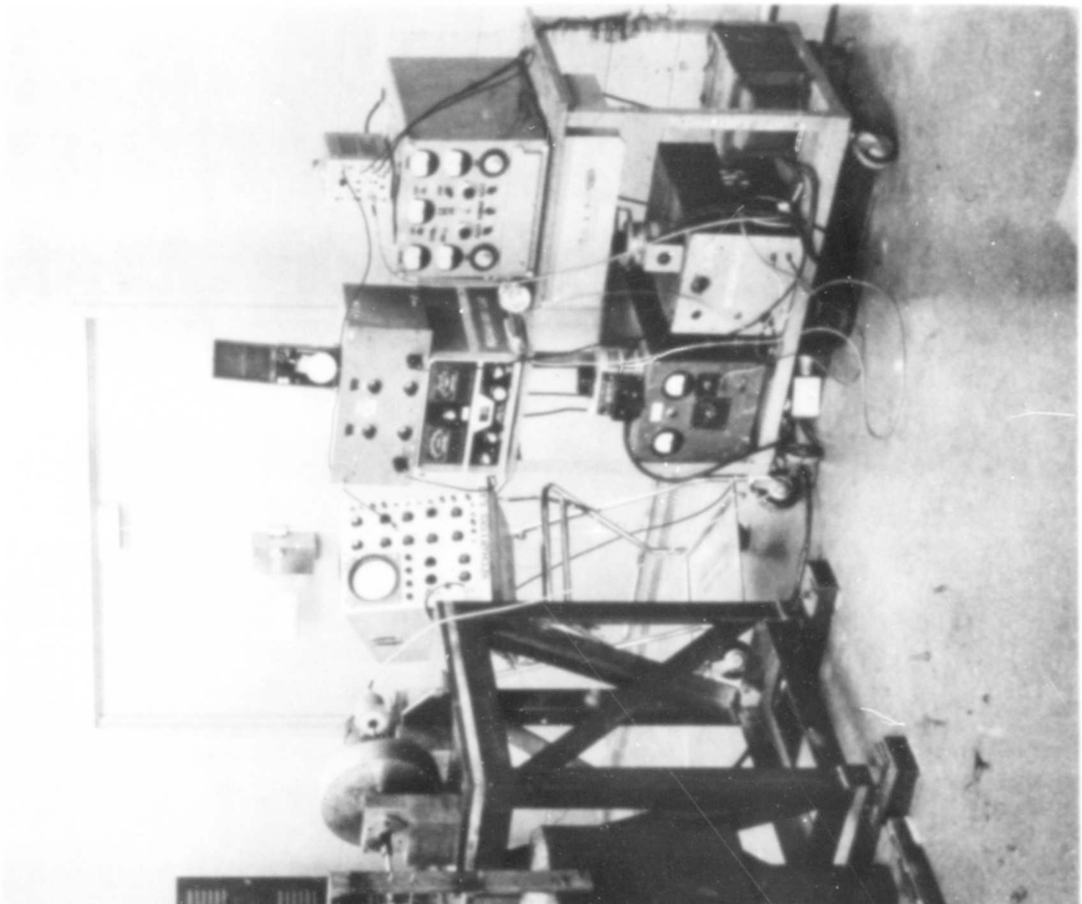

Fig. 10 EXPERIMENTAL FIXTURE ARRANGEMENT

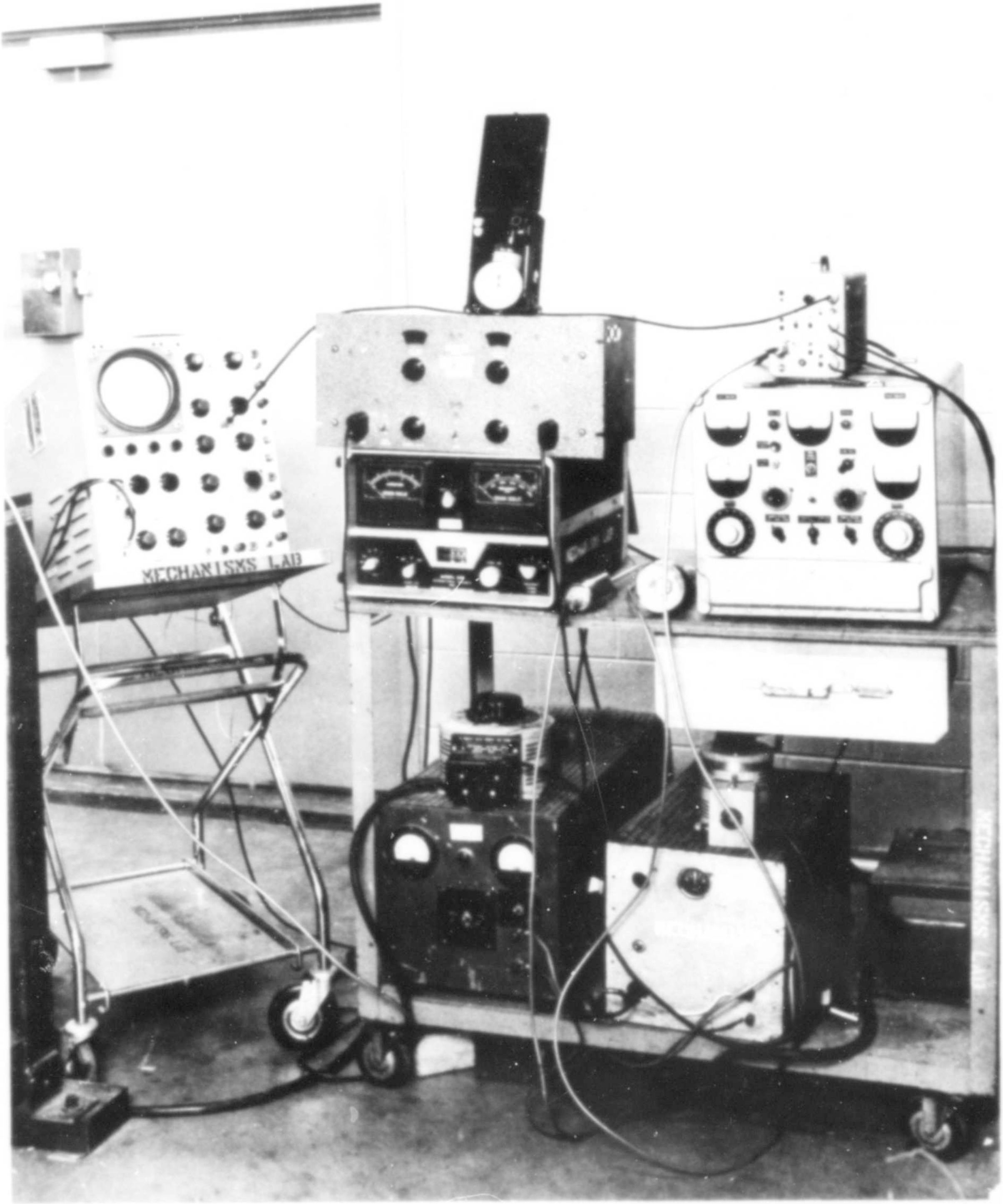

Fig. 11 INSTRUMENTATION

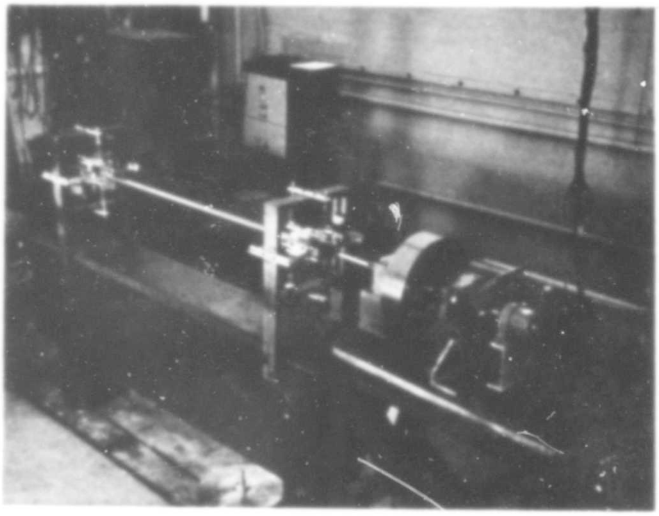

Fig. 12 EXPERIMENTAL FIXTURE WITH ELASTICALLY CONSTRAINED ENDS

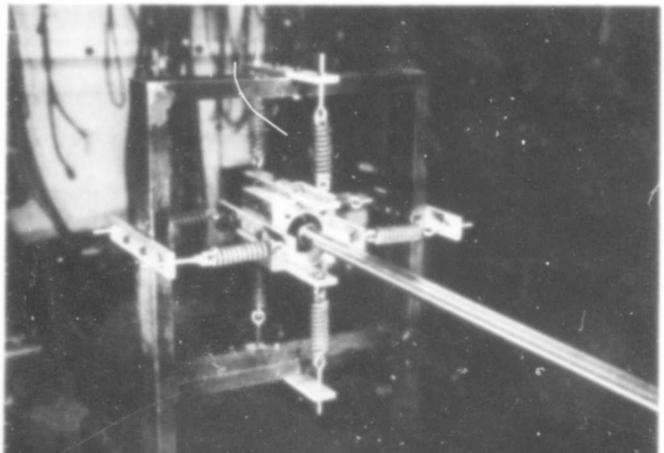

Fig. 13 ELASTICALLY CONSTRAINED END

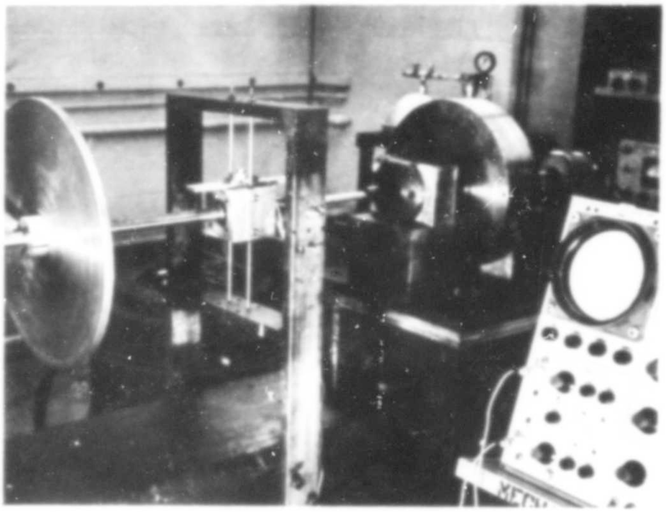

Fig. 14 DISK ATTACHED TO ROTOR WITHOUT SAFETY DEVICE

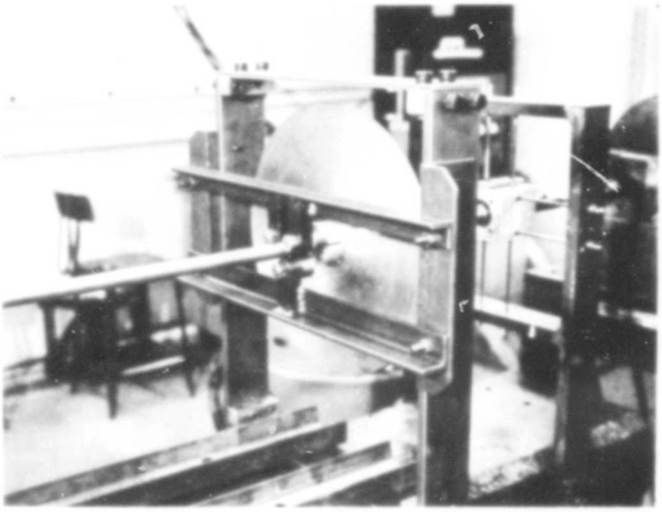

Fig. 15 DISK ATTACHED TO ROTOR WITH SAFETY DEVICE IN "LOCKED IN" POSITION

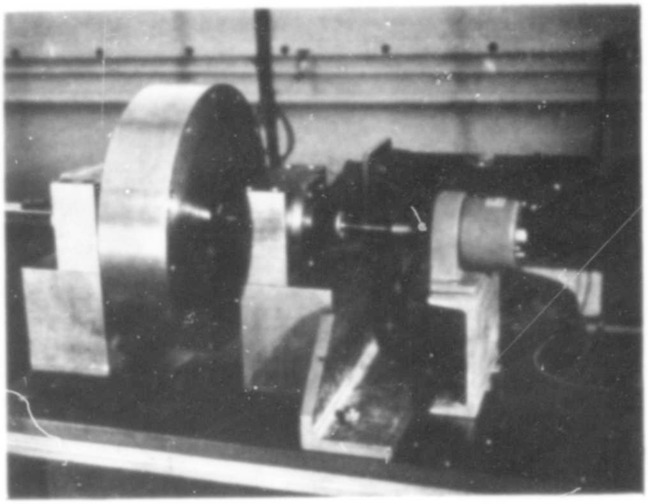

Fig. 16 THE DRIVE SYSTEM

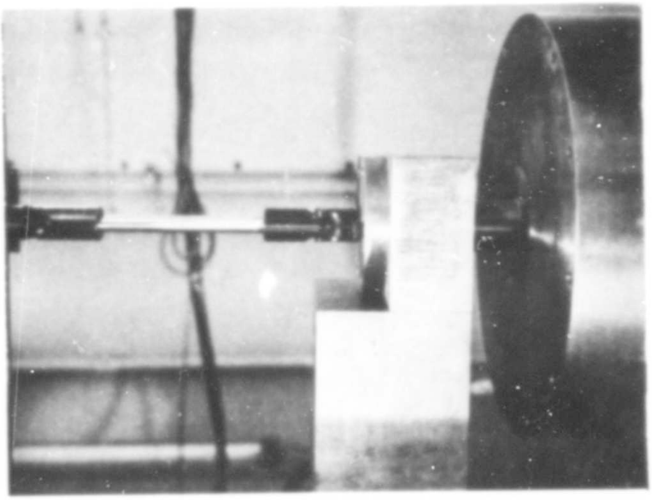

Fig. 17 FLEXIBLE CONNECTION AND FLYWHEEL

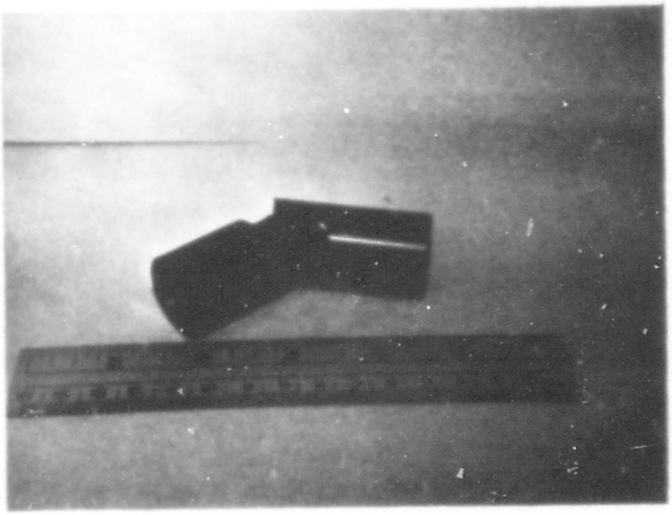

Fig. 18 HOOKE JOINT

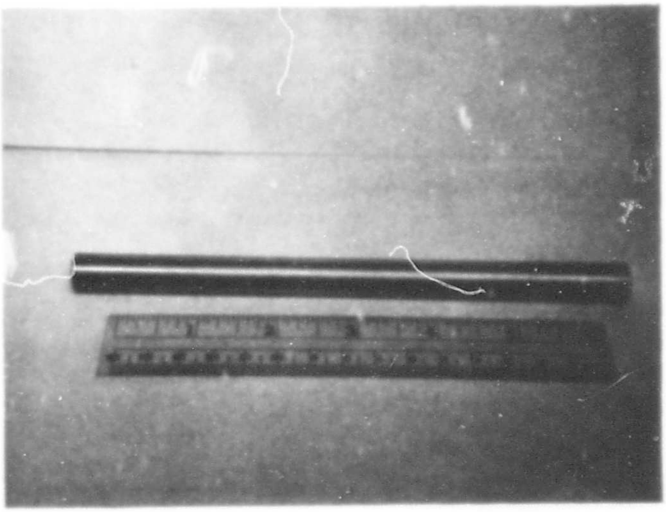

Fig. 19 SHAFT SEGMENT

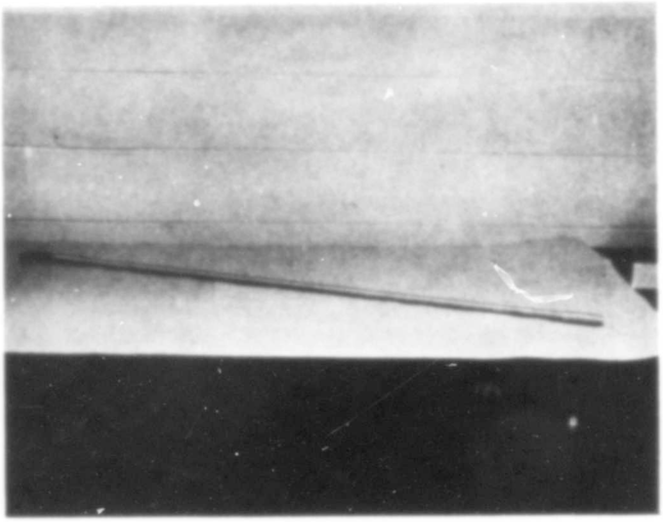

Fig. 20 ROTOR

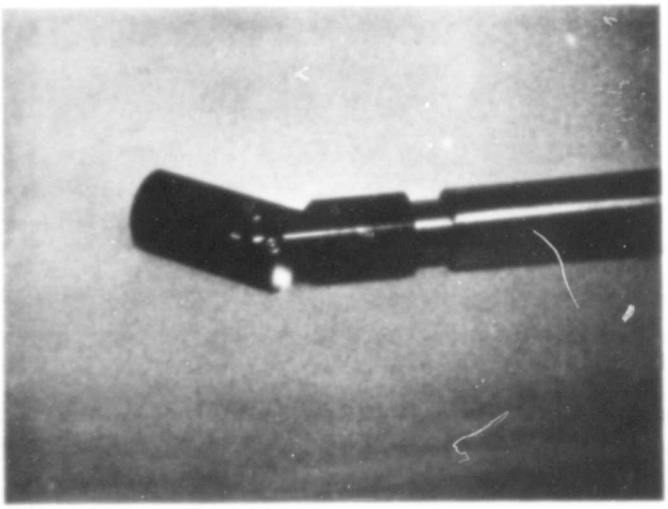

Fig. 21 HOOKE JOINT MOUNTED ON ROTOR

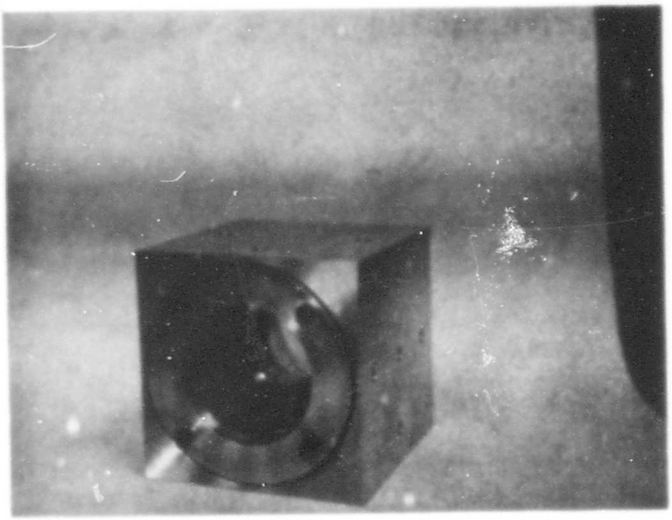

Fig. 22 BEARING BLOCK

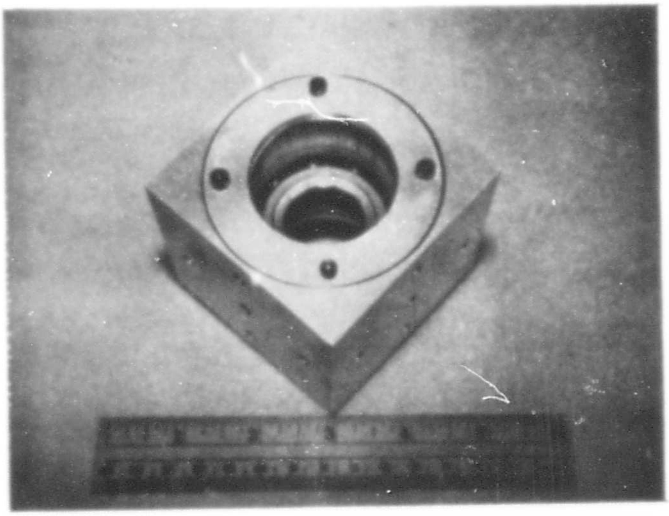

Fig. 23 BEARING BLOCK

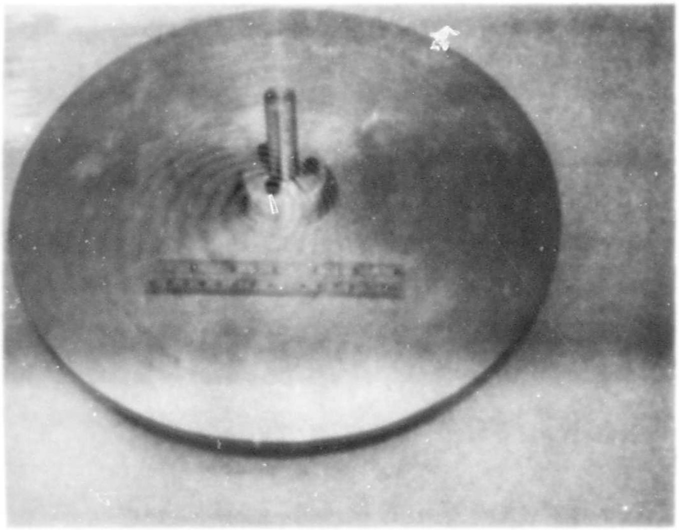

Fig. 24 DISK

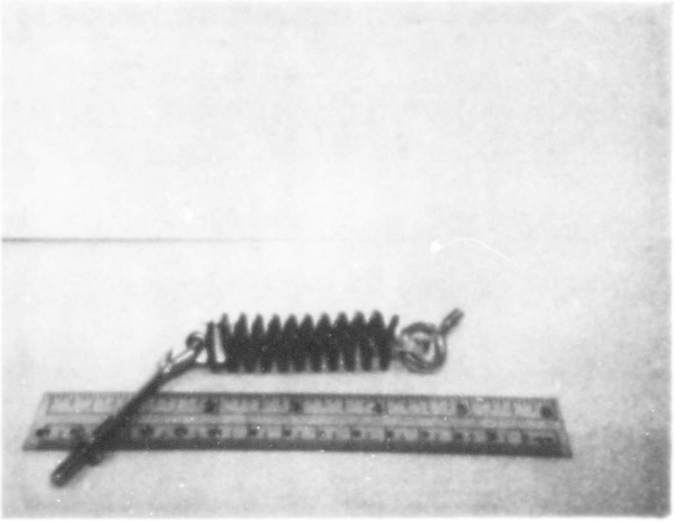

Fig. 25 TENSION SPRING AND MOUNTING FIXTURES

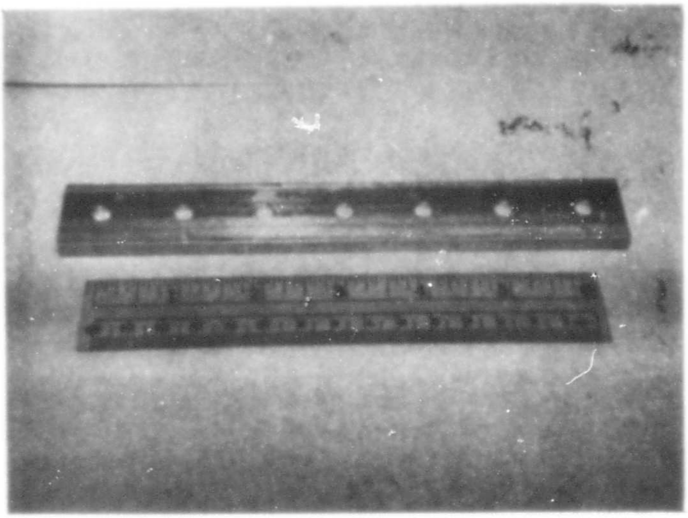

Fig. 26 SPRING HANGER

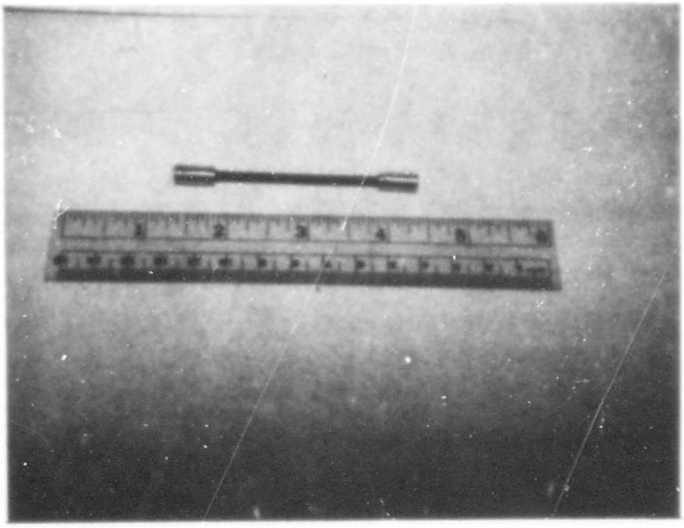

Fig. 27 ROTAN PICK UP COUPLING DEVICE

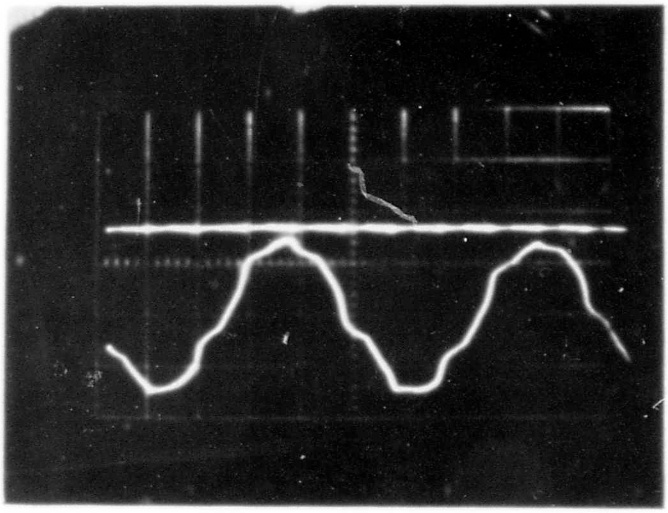

Fig. 28 OSCILLOSCOPE RECORD OF BEARING SUPPORT DISPLACEMENT

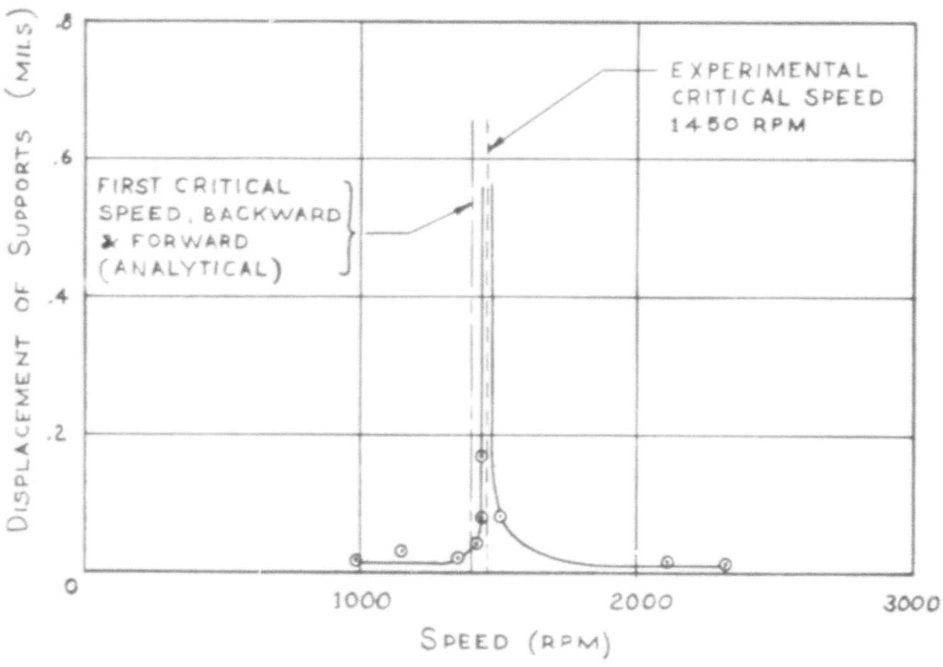

Fig. 29 BEARING SUPPORT DISPLACEMENT AMPLITUDE OF PLAIN ROTOR

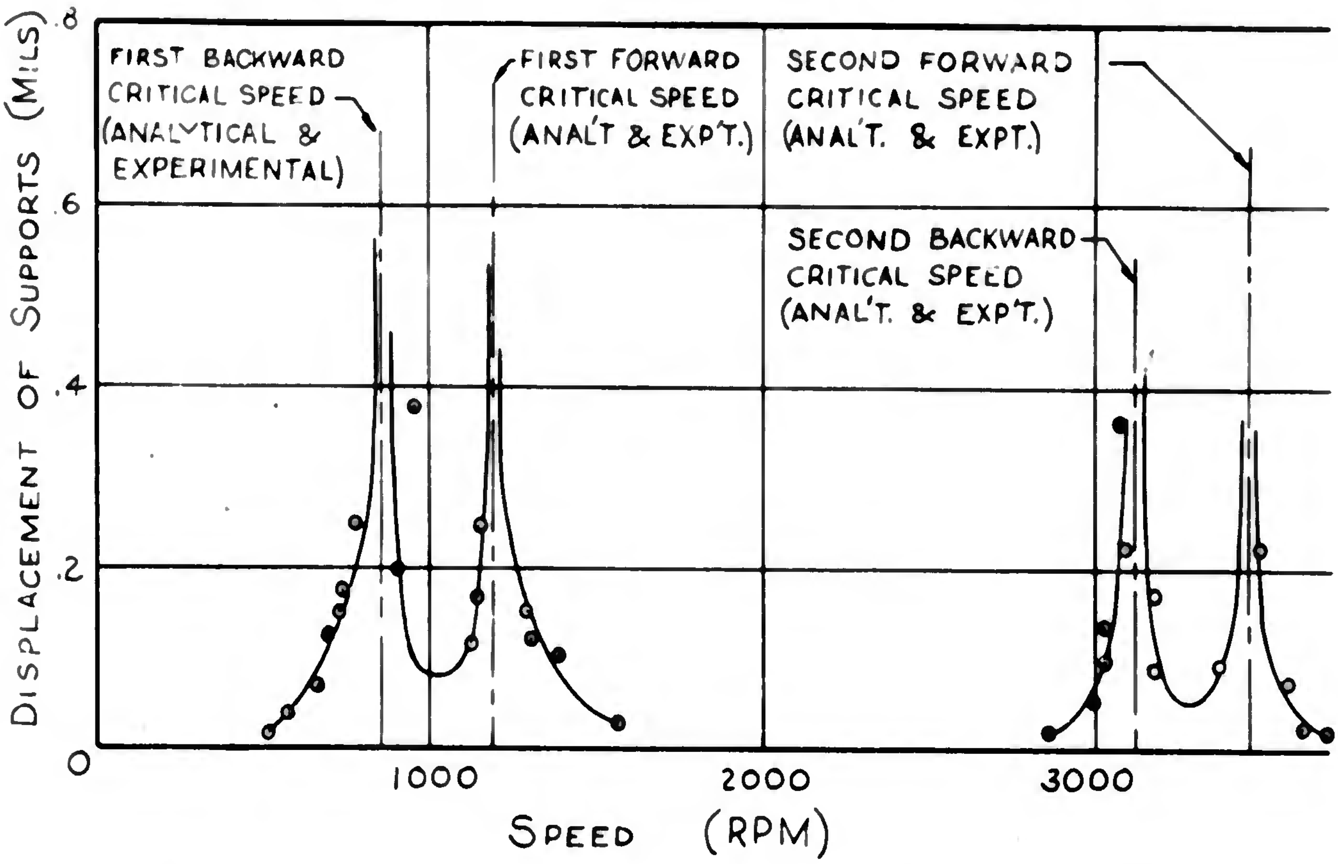

Fig. 30 BEARING SUPPORT DISPLACEMENT AMPLITUDE OF ROTOR-DISK (ζ = 0. 1) SYSTEM

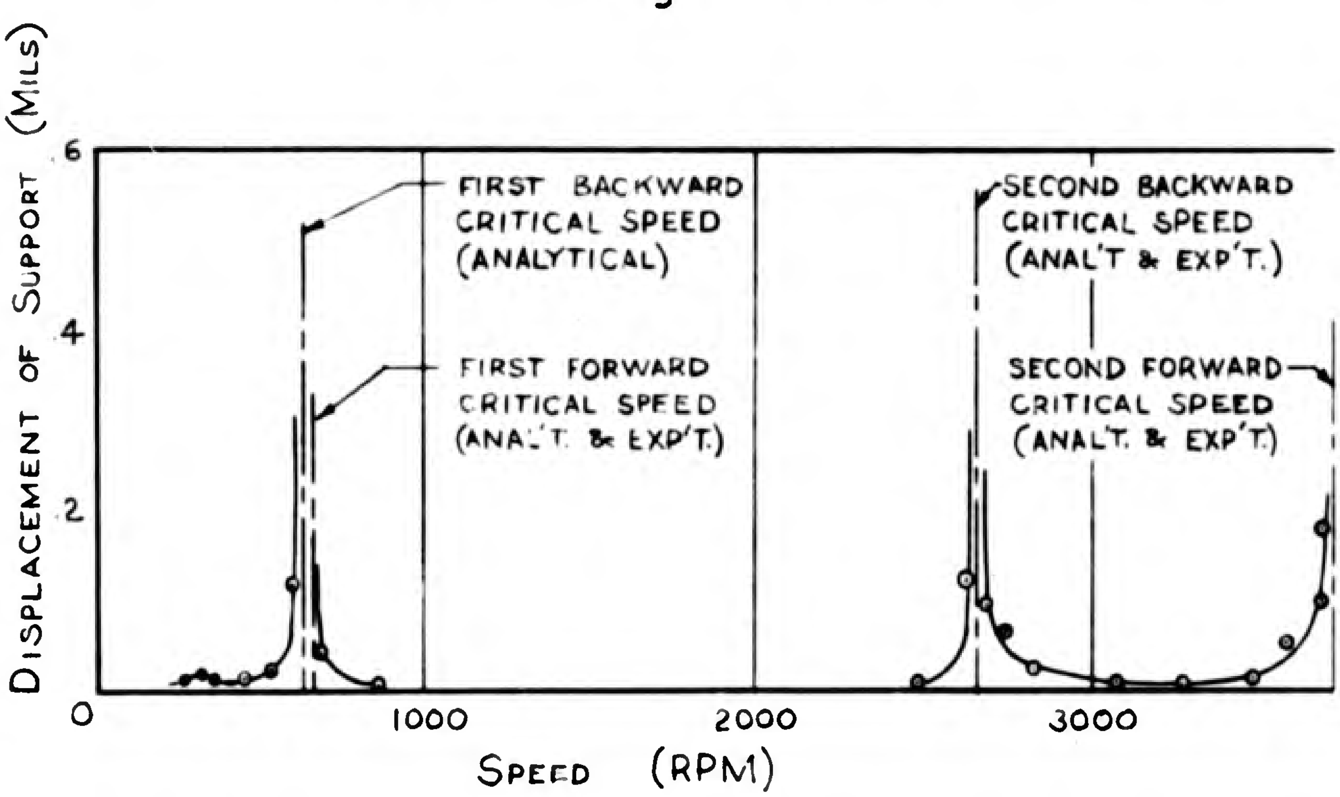

Fig. 31 BEARING SUPPORT DISPLACEMENT AMPLITUDE OF ROTOR-DISK (ζ = 0. 25) SYSTEM

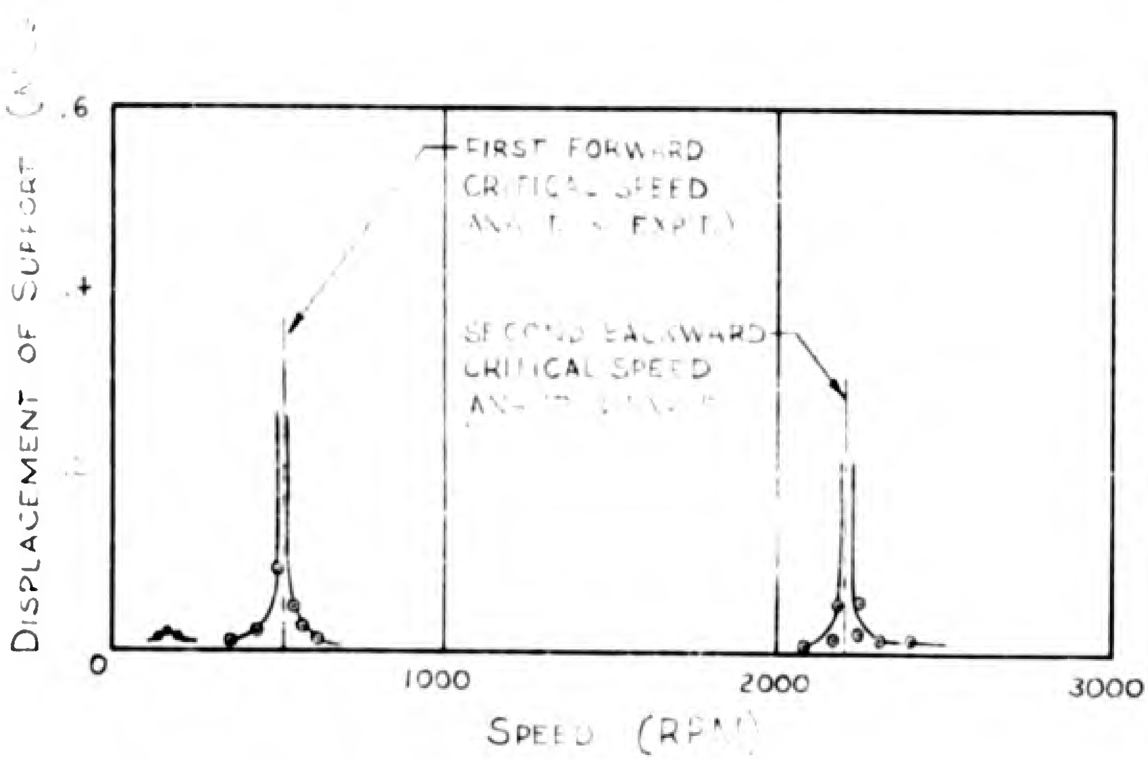

Fig. 32 BEARING SUPPORT DISPLACEMENT AMPLITUDE OF ROTOR-DISK (ζ = 0 50) SYSTEM

Table 5

CRITICAL SPEEDS FOR THE PLAIN ROTOR

Critical Speed	NObs–86805 Analytical	NObs–88607 Analytical	NObs–88607 Experimental
1	1335 RPM	1399 B 1400 F	1450 F
2	4885 RPM	5593 B 5600 F	*

*Maximum Speed Attained - 4600 RPM

Table 6

CRITICAL SPEEDS OF THE ROTOR-DISK SYSTEM

Disk Location	Critical Speed	Analytical	Experimental
0. 1	1-B	859	860
0. 1	1-F	1195	1190
0. 1	2-B	3110	3100
0. 1	2-F	3464	3450
0. 1	3-B	5779	*
0. 1	3-F	8773	*
0. 25	1B	640	
0. 25	1F	675	675
0. 25	2B	2650	2650
0. 25	2F	3721	3720
0. 25	3B	4389	*
0. 25	3F	12, 493	*
0. 5	--	---	---
0. 5	1F	524	524
0. 5	2B	2203	2200
0. 5	2F	7692	*
0. 5	--	---	---
0. 5	3F	9110	*

*Maximum Speed Attained 3800 RPM

The results of the experimental program are summarized and compared with analytical results of this contract and Contract No. NObs—86805 in Tables 5 and 6. Specific displacement amplitude-speed curves for the plain rotor and the disk-rotor system are included as figures 29 through 32, respectively.

In general, the results of the analytical analyses were verified experimentally except at speeds where the drive system could not supply the necessary power. The critical speeds of the plain rotor are shown in Table 5 as reported by three different methods. The analysis of Contract No. NObs—86805 included the effects of bearing mass and support stiffness but neither rotatory inertia nor gyroscopic effects. The analysis of the rotor in this program assumed rigid supports ($k = 3.168 \times 10^5$ lb/in.) but included gyroscopic and rotatory inertia effects. In general, the results of Contract No. NObs—86805 are lower than the results given in this program because of the flexible supports and omission of rotatory inertia and gyroscopic effects. The analytical results for the first critical speeds (forward whirl) are lower than the experimental results because of the omission of transverse shear effects. The effect of transverse shear tends to raise the first critical speed, forward whirl, as much at 2 to 4 per cent. Therefore, good correspondence was obtained between experimental and analytical results but only the first critical, forward whirl, could be obtained experimentally as shown in figure 29. While the rotor ran very smooth at speeds other than critical speeds, the IRD transducer was mounted on the bearing supports and picked up some background noise caused by the ball bearings. This accounts for the small displacement of the support at speeds other than critical speeds.

The experimental results for the various combinations of the disk-rotor system agree with the analytical results derived in a previous section of this report. The experimental results for the disk located at the one-tenth point are shown in Table 6 and figure 30. The first critical speed, backward whirl, was nonviolent compared to the first critical speed, forward whirl. The experimental results obtained for the disk located at the quarter point are given in Table 6 and specifically in figure 31. The first criticals, forward and backward whirl, could not be separated and manifest themselves as a wide resonance band but the second criticals were observed independently. The second critical speed, backward whirl, was difficult to detect while the second critical, forward whirl, was violent. The experimental results obtained for the disk located at the midpoint of the rotor are given in Table 6 and more specifically in figure 32. Experimental results obtained in this case were in close agreement with the previously derived analytical results.

Gravity critical speeds were obtained at 260 RPM when the disk was located at the midpoint and 325 RPM when the disk was located at the quarter point. These experimental results agreed with the analytical results of Contract No. NObs—86805 which predicted gravity critical speeds for a round shaft at one-half the natural frequencies of the system.

The experimental fixture was well balanced and ran relatively smooth at speeds other than criticals, and in general, the critical speeds were easy to detect. It was difficult to obtain data close to some of the more violent critical speeds.

The drive system provides a source of constant speed, however, the power output was found to be insufficient to attain the maximum rotational speeds. Rotational speeds up to 3800 RPM were obtained with the disk on the rotor and 4600 RPM without the disk on the rotor.

APPENDIX A

EXTENDED EQUATIONS OF MOTION

APPENDIX A

EXTENDED EQUATIONS OF MOTION

Equations of motion for rotating shafts have been derived many times. Some of the more general derivations have appeared in earlier IITRI reports to BuShips*, while others are available in the open literature. Of necessity, all of the resultant systems of equations reflect simplifying and particularizing assumptions related to a specific investigation; none of these systems is sufficiently complete to apply to the investigations of the current project. It was, consequently, necessary to derive a new set of governing equations.

The equations derived on the following pages are not intended to characterize all of the phenomena of rotor dynamics. For example, no attempt has been made to include the effects of applied torque or axial thrust. A system of equations which included all possible effects would probably be intractable. The equations do include such effects as rotary inertia and gyroscopic forces, which strongly affect the motion in many cases. The equations of motion are also restricted to cross sections of equal inertial moment, to correspond with the scope of the present project.

---

* See, for example, the Final Reports on Contracts NObs-72244, NObs-78753, and NObs-86805.

We consider a rotor of circular cross section and arbitrary cross sectional variation. The rotor is supported in lubricated, massive bearings on flexible damped supports. Material damping in the shaft and external damping, such as air damping, are assumed small in comparison with the support damping. We introduce, at the centroid of each section, axes $OX_1X_2X_3$ which have fixed space orientation. Axis OX_3 coincides with the undeflected axis of centroids, which is assumed to coincide with the bearing centerline. Plane cross sections of the rotor which are initially perpendicular to the centroidal axis (OX_3) are assumed to remain plane and perpendicular to the deflected centerline. Introduce axes $O'Y_1Y_2Y_3$ whose orientation is fixed in the shaft. Thus, $O'Y_1Y_2Y_3$ initially coincides with $OX_1X_2X_3$ and rotates with the shaft. Axis $O'Y_3$ is tangent to the deformed centroidal axis.

The coordinates of the elastic axis of the shaft at section Σ are, in coordinates $OX_1X_2X_3$, respectively U_1, U_2, U_3. The coordinates of the elastic axis of the shaft at section Σ are, in coordinates $OY_1Y_2Y_3$, respectively V_1, V_2, V_3. The elastic axis is assumed inextensible, thus $U_3 = V_3$.

The coordinates of the line of mass centers of the shaft in the $OX_1X_2X_3$ axis system are U_1^c, U_2^c, U_3^c. Figures A-1 and A-2 illustrate some of these concepts.

The assumption that plane sections remain plane implies neglect of the effect of transverse shear on the rotor deflections. It has been

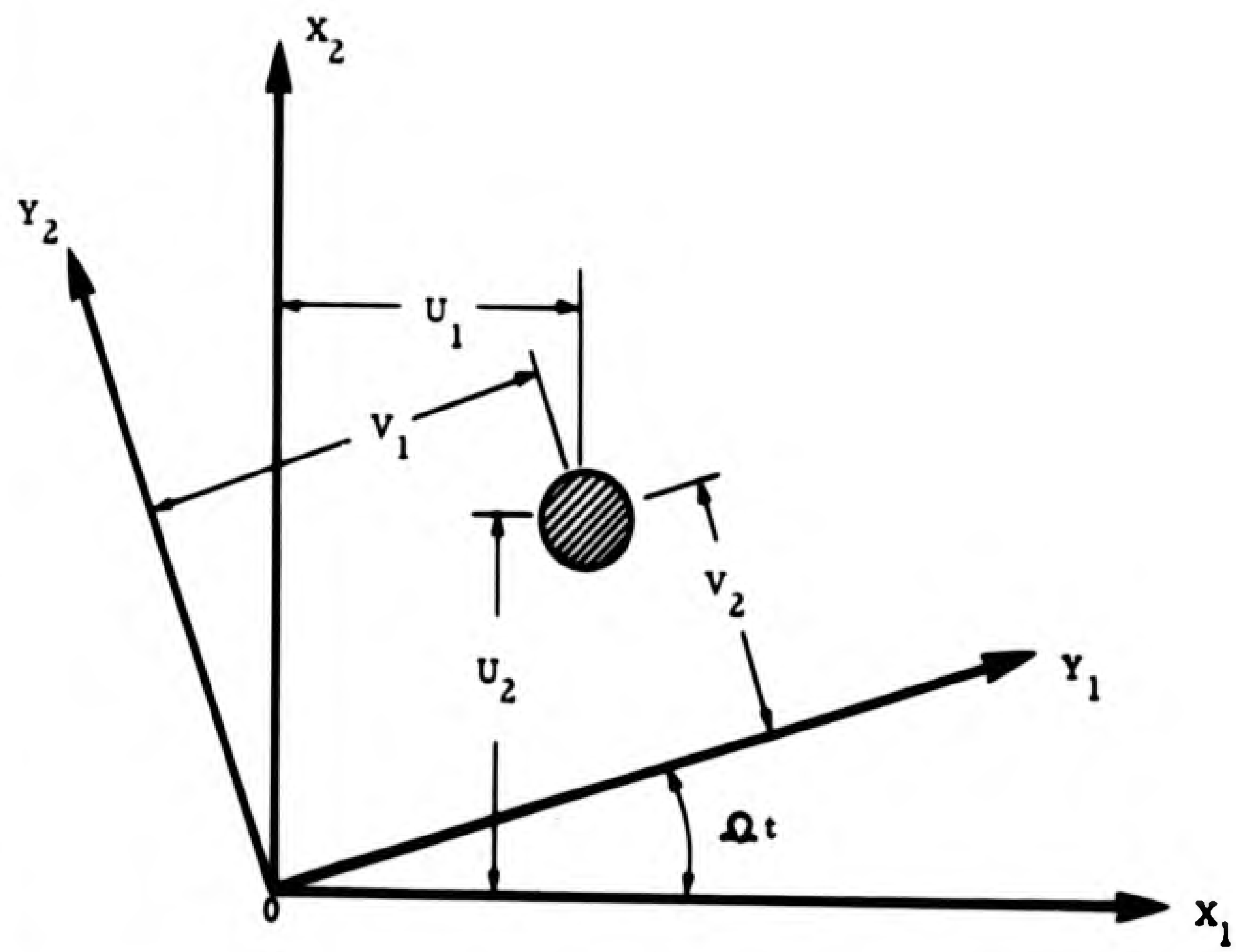

Figure A-1 FIXED AND ROTATING COORDINATE SYSTEM

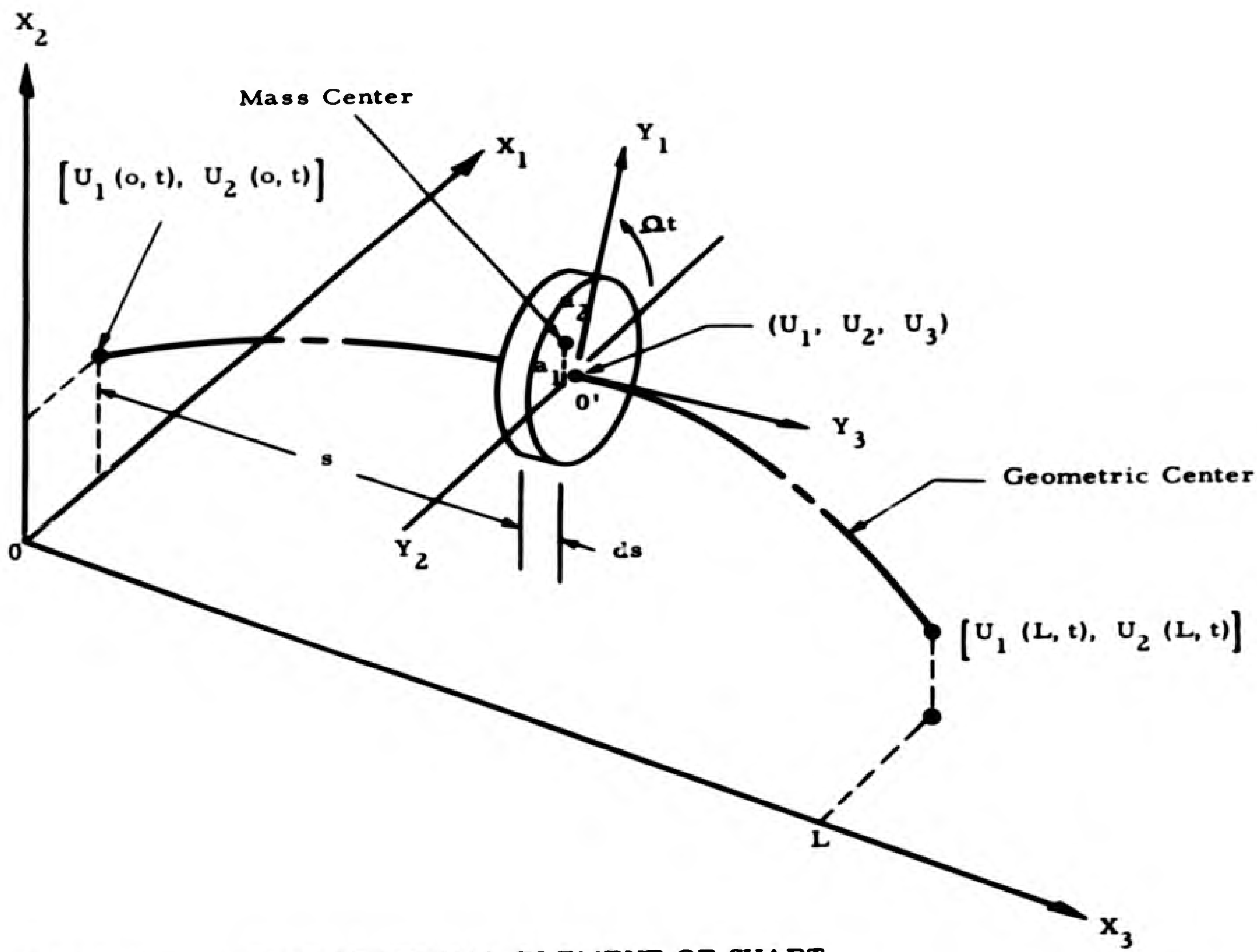

Figure A-2 CROSS SECTIONAL ELEMENT OF SHAFT demonstrated that this effect is small* for high aspect ratio. The section at a generic point x can be taken from its initial position to its final position through the following unique sequence of transformations shown in Figure A-3.**

1. A positive (clockwise rotation ϕ, about the axis OX_3, this carries OX_1 to OX_1' and OX_2 to OX'_2.

2. A positive rotation θ about the axis OX_2; this carried OX_3 to OY_3 and OX'_1 to OX''_1.

3. A positive rotation ψ about OY_3; this carries OX''_1 to OY_1 and OX'_2 to OY_2. This is the required final position.

The relationship between the axes (direction cosines is shown in the scheme of Table A-1.

	X_3	X_1	X_2
Y_3	$\cos\theta$	$\cos\phi\sin\theta$	$\sin\phi\sin\theta$
Y_1	$-\sin\theta\cos$	$\cos\phi\cos\theta\cos\psi-\sin\phi\sin\psi$	$\sin\phi\cos\theta\cos\psi+\cos\phi\sin\psi$
Y_2	$\sin\theta\sin\psi$	$-\cos\phi\cos\theta\sin\psi-\sin\phi\cos\psi$	$-\sin\phi\cos\theta\sin\psi+\cos\phi\cos\psi$

Table A-1 Direction cosines of coordinate axes

---

* Sutherland, J. G. and L. E. Goodman: "Vibrations of Prismatic Bars Including Rotatory Inertia and Shear Corrections", Department of Civil Engineering, University of Illinois, Urbana, Illinois, April 15, 1951.

** These "Eulerian angles" are discussed in all intermediate and advanced texts on rigid body mechanics. The notation here is that of E. T. Whittaker, "A Treatise on the Analytical Dynamics of Particles and Rigid Bodies", Dover Publications, New York.

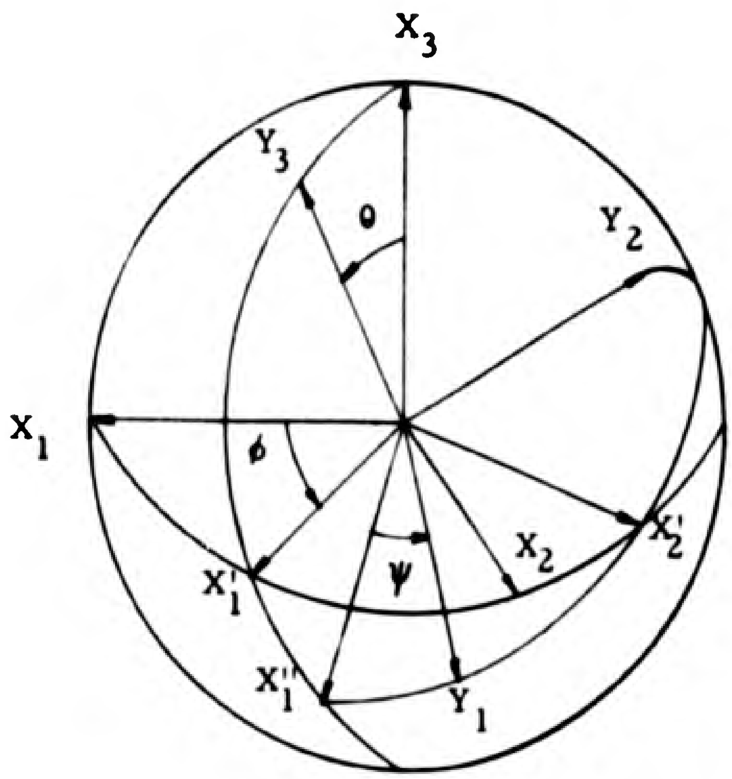

Fig. A-3 Eulerian Angles Characterizing Shaft Rotations

Rotational velocities in the two axis systems can also be recorded.

$$\left.\begin{aligned}
\omega_{X_3} &= \frac{\partial \phi}{\partial t} + \cos\theta \frac{\partial \psi}{\partial t} \\
\omega_{X_1} &= \cos\phi \sin\theta \frac{\partial \psi}{\partial t} - \sin\phi \frac{\partial \theta}{\partial t} \\
\omega_{X_2} &= \sin\phi \sin\theta \frac{\partial \psi}{\partial t} + \cos\phi \frac{\partial \theta}{\partial t}
\end{aligned}\right\} \qquad (1)$$

$$\left.\begin{aligned}
\omega_{Y_3} &= \cos\theta \frac{\partial \phi}{\partial t} + \frac{\partial \psi}{\partial t} \\
\omega_{Y_1} &= \sin\psi \frac{\partial \theta}{\partial t} - \sin\theta \cos\psi \frac{\partial \phi}{\partial t} \\
\omega_{Y_2} &= \cos\psi \frac{\partial \theta}{\partial t} + \sin\theta \sin\psi \frac{\partial \phi}{\partial t}
\end{aligned}\right\} \qquad (2)$$

A third set of axes, of interest because of their simplifying effect on the equations, is $OX''_1X'_2Y_3$. The rotational velocity of $OY_1Y_2Y_3$ has the following form when resolved in this system.

$$\left.\begin{aligned}
\omega_{X''_1} &= -\sin\theta \frac{\partial \phi}{\partial t} \\
\omega_{X'_2} &= \frac{\partial \theta}{\partial t} \\
\omega_{Y_3} &= \cos\theta \frac{\partial \phi}{\partial t} + \frac{\partial \psi}{\partial t}
\end{aligned}\right\} \qquad (3)$$

The curvature in the plane perpendicular to OX''_1 is

$$k_1 = -\sin\theta \frac{\partial \phi}{\partial s} \tag{4}$$

The curvature in the plane perpendicular to OX'_2 is

$$k_2 = \frac{\partial \theta}{\partial s} \tag{5}$$

The position of the shaft centerline in fixed space is given by $U_1(s, t)$, $U_2(s, t)$, $U_3(s, t)$, where, by Table A-1

$$\left.\begin{aligned} \frac{\partial U_1}{\partial s} &= \sin\theta \cos\phi \\ \frac{\partial U_2}{\partial s} &= \sin\theta \sin\phi \\ \frac{\partial U_3}{\partial s} &= \cos\theta \end{aligned}\right\} \tag{6}$$

The geometric specifications are completed by prescribing the rotor configuration. The rotor has length L and is supported in bearings at $s = 0$ and $s = L$. The cross section and material may vary along the length but the shaft is homogeneous in any cross section. The mass per unit volume is $\rho(s)$ and the cross sectional area is $A(s)$. The diametral moment of inertia of the cross sectional area about axes perpendicular to Y_3 is $I(s)$. The corresponding flexural rigidity is $E(s)\, I(s) = S(s)$, where $E(s)$ is the (variable) Young's modulus.

We can obtain the conservative equations of motion from energy considerations and append dissipative terms later. The kinetic energy of the system is given by equation (7)

$$
\begin{aligned}
T = \frac{1}{2} \int_0^L A\rho \left[\left(\frac{\partial U_1^c}{\partial t}\right)^2 + \left(\frac{\partial U_2^c}{\partial t}\right)^2 + \left(\frac{\partial U_3^c}{\partial t}\right)^2 \right] ds \\
+ \frac{1}{2} \int_0^L \rho I \left[\omega_{X''_1}^2 + \omega_{X'_2}^2 + 2\,\omega_{Y_3}^2 \right] ds \\
+ \frac{1}{2} m_1 L^2 \int_0^L A\rho ds \left[\left(\frac{d\xi_1}{dt}\right)^2 + \left(\frac{d\xi_2}{dt}\right)^2 \right] \\
+ \frac{1}{2} m_2 L^2 \int_0^L A\rho ds \left[\left(\frac{d\eta_1}{dt}\right)^2 + \left(\frac{d\eta_2}{dt}\right)^2 \right]
\end{aligned}
\tag{7}
$$

where $I = \frac{AR^2}{4}$.

Here we have introduced the bearing blocks, which have mass $m_1 \int_0^L A\rho ds$ at $s = 0$ and $m_2 \int_0^L A\rho ds$ at $s = L$. The bearings are separated from the shaft by an oil film, thus the motion of a block may differ from that of a "coincident point" of the rotor. The position of m_1 in the X_1 and X_2 directions is given by $L\xi_1$ and $L\xi_2$, while $L\eta_1$ and $L\eta_2$ have similar roles for m_2. Figure A-4 illustrates the bearing configuration. Introduce the following definition and conclusion:

$$
\begin{aligned}
\tau &= \phi + \psi \\
\omega_{Y_3} &= \frac{\partial \tau}{\partial t} + (\cos \theta - 1) \frac{\partial \phi}{\partial t}
\end{aligned}
\tag{8}
$$

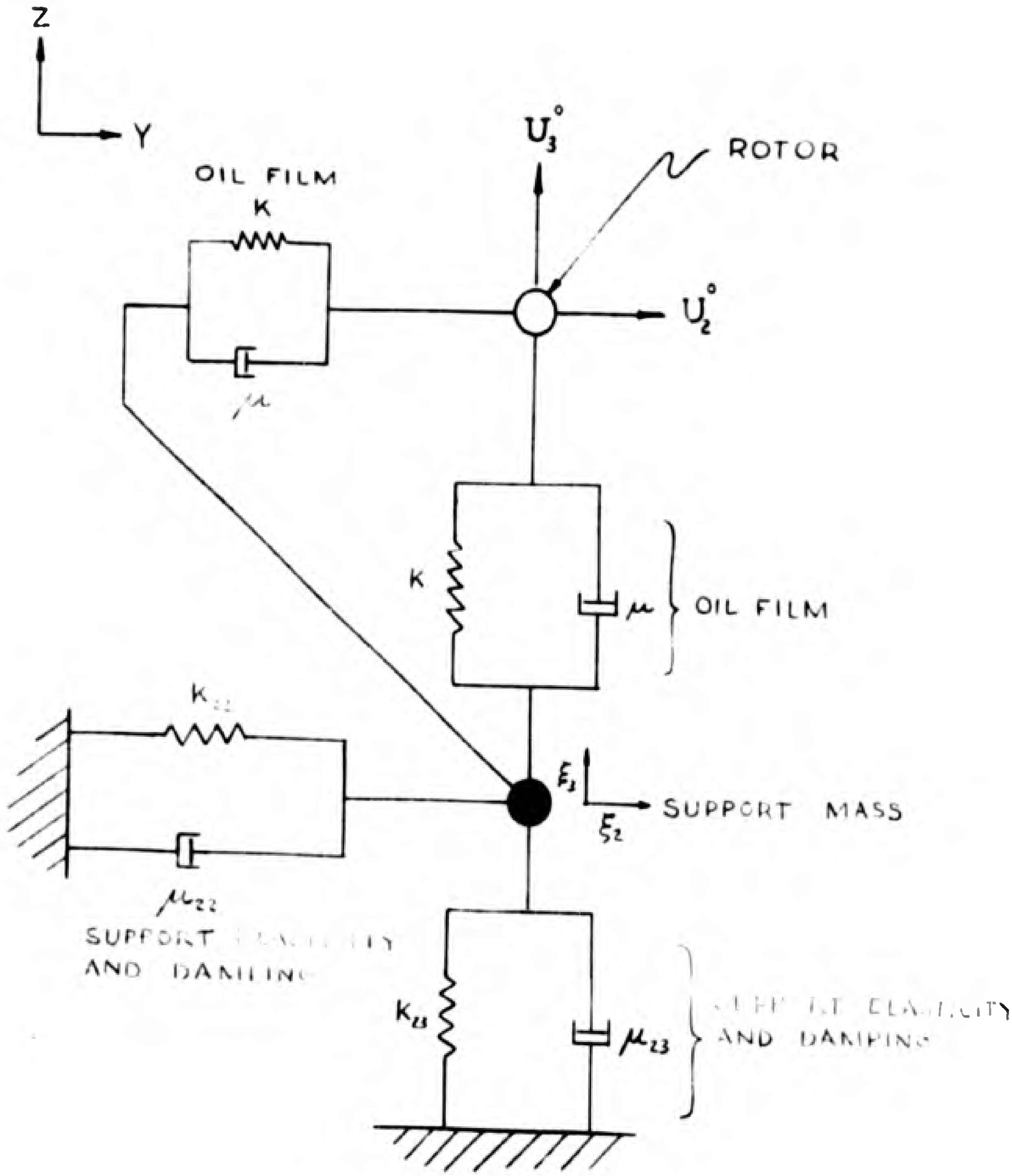

Figure A-4 Schematic of End Support System

Equations (8) are exact, but we can interpret τ as the angle of rotation about Y_3 for small displacements. We also note that (3) and (6) imply

$$\omega_{X''_1}^2 + \omega_{X'_2}^2 = \left(\frac{\partial \theta}{\partial t}\right)^2 + \sin^2 \theta \left(\frac{\partial \phi}{\partial t}\right)^2$$

$$= \left(\frac{\partial^2 U_1}{\partial s \partial t}\right)^2 + \left(\frac{\partial^2 U_2}{\partial s \partial t}\right)^2 + \left(\frac{\partial^2 U_3}{\partial s \partial t}\right)^2 \qquad (9)$$

$$\frac{\partial^2 U_1}{\partial s \partial t} \frac{\partial U_2}{\partial s} - \frac{\partial^2 U_2}{\partial s \partial t} \frac{\partial U_1}{\partial s} = -\frac{\partial \phi}{\partial t} \sin^2 \theta$$

The functions U_1^c and U_2^c are the position of the center of gravity in the cross section. Since τ is (approximately) the angle the section rotates about Y_3, we define the position of the c.g. in the section to be $La_1(s)$, $La_2(s)$ and observe that

$$U_1^c = U_1 + (a_1 \cos \tau - a_2 \sin \tau) L$$

$$U_2^c = U_2 + (a_1 \sin \tau + a_2 \cos \tau) L \qquad (10)$$

$$U_3^c = U_3$$

Hence,

$$\frac{\partial U_1^{\,c}}{\partial t} = \frac{\partial U_1}{\partial t} - \frac{\partial \tau}{\partial t}\left[a_1 \sin\tau + a_2 \cos\tau\right] L$$

$$\frac{\partial U_2^{\,c}}{\partial t} = \frac{\partial U_2}{\partial t} + \frac{\partial \tau}{\partial t}\left[a_1 \cos\tau - a_2 \sin\tau\right] L \qquad (11)$$

The kinetic energy thus has the form,

$$T = \frac{1}{2}\int_0^L A\rho\left\{\left(\frac{\partial U_1}{\partial t}\right)^2 + \left(\frac{\partial U_2}{\partial t}\right)^2 + \left(\frac{\partial \tau}{\partial t}\right)^2 (a_1^{\,2} + a_2^{\,2}) L^2\right.$$

$$+ \left(\frac{\partial U_3}{\partial t}\right)^2 + 2\frac{\partial \tau}{\partial t}\left[a_1\left(\cos\tau\,\frac{\partial U_2}{\partial t} - \sin\tau\,\frac{\partial U_1}{\partial t}\right)\right.$$

$$\left. - a_2\left(\sin\tau\,\frac{\partial U_2}{\partial t} + \cos\tau\,\frac{\partial U_1}{\partial t}\right)\right] L \qquad (12)$$

$$+ L^2\frac{r^2}{4}\left[2\left(\frac{\partial \tau}{\partial t}\right)^2 + \left(\frac{\partial^2 U_1}{\partial s\partial t}\right)^2 + \left(\frac{\partial^2 U_2}{\partial s\partial t}\right)^2 + \left(\frac{\partial^2 U_3}{\partial s\partial t}\right)^2\right]$$

$$+ m_1 L^2\left[\left(\frac{d\xi_1}{dt}\right)^2 + \left(\frac{d\xi_2}{dt}\right)^2\right] + m_2 L^2\left[\left(\frac{d\eta_1}{dt}\right)^2 + \left(\frac{d\eta_2}{dt}\right)^2\right]$$

$$\left. + \frac{L^2 r^2}{2}\left[2(\cos\theta - 1)\frac{\partial \phi}{\partial t}\frac{\partial \tau}{\partial t} + (\cos - 1)^2\left(\frac{\partial \phi}{\partial t}\right)^2\right]\right\} ds$$

where Lr is the radius of the shaft.

The potential energy, U can also be written directly.

$$U = \frac{1}{2} \int_0^L \left\{ S \left[k_1^{\,2} + k_2^{\,2} \right] + 2 A \rho g U_2 \right\} ds$$

$$+ \frac{1}{2} \int_0^L A \rho L^2 \Omega^2 \left\{ \left[K_{11} \xi_1^{\,2} + K_{12} \xi_2^{\,2} + K_{21} \eta_1^{\,2} + K_{22} \eta_2^{\,2} \right. \right.$$

$$+ K \left\{ \left[\frac{U_1(o,t)}{L} - \xi_1 \right]^2 + \left[\frac{U_2(o,t)}{L} - \xi_2 \right]^2 \right. \qquad (13)$$

$$\left. \left. + \left[\frac{U_1(L,t)}{L} - \eta_1 \right]^2 + \left[\frac{U_2(L,t)}{L} - \eta_2 \right]^2 \right\} \right\} ds$$

where Ω is a constant to be defined with dimensions of frequency

K = Equivalent non-dimensional lubricant spring constant

K_{11} = Non-dimensional support spring constant in U_1 direction at $s = 0$

K_{12} = Non-dimensional support spring constant in U_2 direction at $s = 0$

K_{21} = Non-dimensional support spring constant in U_1 direction at $s = L$

K_{22} = Non-dimensional support spring constant in U_2 direction at $s = L$

g = Gravitational acceleration.

Figure A-4 is a bearing schematic.

By (4), (5), and (6)

$$k_1^2 + k_2^2 = \left(\frac{\partial \theta}{\partial s}\right)^2 + \sin^2 \theta \left(\frac{\partial \phi}{\partial s}\right)^2$$

$$= \left(\frac{\partial^2 U_1}{\partial s^2}\right)^2 + \left(\frac{\partial^2 U_2}{\partial s^2}\right)^2 + \left(\frac{\partial^2 U_3}{\partial s^2}\right)^2 \tag{14}$$

Hamilton's principle states that the action is stationary. Thus, we have

$$\delta \int_0^{t_0} (T-U)\, dt = 0 \tag{16}$$

Observe that, to this point, only one possible approximation has been made; that of (10) which positions the mass center line. Otherwise the energies derived are applicable for large deformations of a torsionally stiff circular shaft. At this point, we observe that, since the deformations of physical shafts are small, U_3 is independent of time to a high order and, indeed, approximately, $U_3 = s$. Thus, we apply the constraints

$$\frac{\partial U_3}{\partial t} = 0$$

$$\frac{\partial^2 U_3}{\partial s^2} = 0 \tag{17}$$

It is convenient to introduce nondimensional parameters wherever possible. We thus define

$$s = Lx$$

$$U_1(s) = Lu_1(x) \tag{18}$$

$$U_2(s) = Lu_2(x)$$

The parameter τ is a variable. We fix it through the (previously implied) demand that it be independent of s (or x) and that its rate be constant. Thus

$$\tau = \Omega t \tag{19}$$

and τ becomes the second independent variable. We also note that, if the angle θ is small, (8) and (9) permit ω_{Y_3} to be written in terms of τ and U_1, U_2. The final observation that U_1 and U_2 are small leads to (A-20).

$$\frac{2(T-U)}{L^3\,\Omega^2} = \int_0^1 A\rho \left\{ \left[\left(\frac{\partial u_1}{\partial \tau}\right)^2 + \left(\frac{\partial u_2}{\partial \tau}\right)^2 + (a_1^{\,2} + a_2^{\,2}) \right.\right.$$

$$+ 2 \left[a_1 \left(\cos\tau \frac{\partial u_2}{\partial \tau} - \sin\tau \frac{\partial u_1}{\partial \tau}\right) - a_2 \left(\sin\tau \frac{\partial u_2}{\partial \tau} + \cos\tau \frac{\partial u_1}{\partial \tau}\right) \right]$$

$$- \frac{S}{L^4 A\rho\Omega^2} \left[\left(\frac{\partial^2 u_1}{\partial x^2}\right)^2 + \left(\frac{\partial^2 u_2}{\partial x^2}\right)^2 \right] - 2 \frac{g}{L\Omega^2} u_2$$

$$- (K_{11}\xi_1^{\,2} + K_{12}\xi_2^{\,2} + K_{21}\eta_1^{\,2} + K_{22}\eta_2^{\,2}) \qquad (20)$$

$$- K \left\{ \left[u_1(0,\tau) - \xi_1\right]^2 + \left[u_2(0,\tau) - \xi_2\right]^2 + \left[u_1(1,\tau) - \eta_1\right]^2 + \left[u_2(1,\tau) - \eta_2\right]^2 \right\}$$

$$+ \frac{r^2}{4} \left\{ \left(\frac{\partial^2 u_1}{\partial x \partial \tau}\right)^2 + \left(\frac{\partial^2 u_2}{\partial x \partial \tau}\right)^2 + 2 + 2 \frac{\partial^2 u_1}{\partial x \partial \tau} \frac{\partial u_2}{\partial x} - 2 \frac{\partial^2 u_2}{\partial x \partial \tau} \frac{\partial u_1}{\partial x} \right\}$$

$$\left.+ m_1 \left[\left(\frac{d\xi_1}{d\tau}\right)^2 + \left(\frac{d\xi_2}{d\tau}\right)^2 \right] + m_2 \left[\left(\frac{d\eta_1}{d\tau}\right)^2 + \left(\frac{d\eta_2}{d\tau}\right)^2 \right] \right\} dx$$

We now examine variations with respect to $u_1, u_2, \xi_1, \xi_2, \eta_n$, and η_2. The variation with respect to u_1 yields

$$- \frac{\partial^2 u_1}{\partial \tau^2} + a_1 \cos\tau - a_2 \sin\tau - \frac{1}{\rho A L^4 \Omega^2} \frac{\partial^2}{\partial x^2} \left(S \frac{\partial^2 u_1}{\partial x^2}\right)$$

$$+ \frac{1}{4\rho A} \frac{\partial}{\partial x} \left\{ r^2 A\rho \left[\frac{\partial^3 u_1}{\partial x \partial \tau^2} + 2 \frac{\partial^2 u_2}{\partial x \partial \tau} \right] \right\} = 0 \qquad (a)$$

on $x = 0$ $\quad u_1$ is prescribed or

$$\frac{1}{ML^4 \Omega^2} \frac{\partial}{\partial x} \left(S \frac{\partial^2 u_1}{\partial x^2} \right) - \frac{r^2 m_o}{4} \frac{\partial^2}{\partial x \partial \tau} \left[\frac{\partial u_1}{\partial \tau} + 2 u_2 \right]$$

(b)

$$+ K \left[u_1 - \xi_1 \right] = 0$$

on $x = 0$ $\quad \frac{\partial u_1}{\partial x}$ is prescribed or

$$\frac{\partial^2 u_1}{\partial x^2} = 0 \qquad \text{(c)}$$

on $x = 1$ $\quad u_1$ is prescribed or

(21)

$$\frac{1}{ML^4 \Omega^2} \frac{\partial}{\partial x} \left(S \frac{\partial^2 u_1}{\partial x^2} \right) - \frac{r^2 m_1}{4} \frac{\partial^2}{\partial x \partial \tau} \left[\frac{\partial u_1}{\partial \tau} + 2 u_2 \right]$$

(d)

$$- K \left[u_1 - \eta_1 \right] = 0$$

on $x = 1$ $\quad \frac{\partial u_1}{\partial x}$ is prescribed or

$$\frac{\partial^2 u_1}{\partial x^2} = 0 \qquad \text{(e)}$$

where:

$$m_1 = \frac{(\rho A)}{M} \qquad x = 1$$

$$m_o = \frac{(\rho A)}{M} \qquad x = 0$$

and $$M = \int_o^1 \rho A \, dx$$

The variation with respect to u_2 yields

$$-\frac{\partial^2 u_2}{\partial \tau^2} + a_1 \sin \tau + a_2 \cos \tau - \frac{g}{L\Omega^2} - \frac{1}{\rho A L^4 \Omega^2} \frac{\partial^2}{\partial x^2}\left(S \frac{\partial^2 u_2}{\partial x^2}\right)$$

$$+ \frac{1}{4 A\rho} \frac{\partial}{\partial x}\left[\rho A r^2 \left\{\frac{\partial^3 u_2}{\partial x \partial \tau^2} - 2 \frac{\partial^2 u_1}{\partial x \partial \tau}\right\}\right] = 0 \qquad \text{(a)}$$

on $x = 0$ u_2 is prescribed or

$$\frac{1}{ML^4\Omega^2} \frac{\partial}{\partial x} \left(S \frac{\partial^2 u_2}{\partial x^2}\right) + \frac{m_o r^2}{4} 2\left[\frac{\partial^2 u_1}{\partial x \partial \tau} - \frac{\partial^3 u_2}{\partial x \partial \tau^2}\right] + K\left[u_2 - \xi_2\right] = 0 \qquad \text{(b)}$$

on $x = 0$ $\frac{\partial u_2}{\partial x}$ is prescribed or

$$\frac{\partial^2 u_2}{\partial x^2} = 0 \qquad \text{(c)}$$

on $x = 1$ u_2 is prescribed or

(22)

$$\frac{1}{ML^4\Omega^2}\frac{\partial}{\partial x}\left(S\frac{\partial^2 u_2}{\partial x^2}\right) - \frac{m_1 r^2}{4}\left(\frac{\partial^3 u_2}{\partial x \partial \tau^2} - 2\frac{\partial^2 u_1}{\partial x \partial \tau}\right) - K(u_2 - \eta_2) = 0$$

(d)

on $x = 1$ $\frac{\partial u_2}{\partial x}$ is prescribed or

$$\frac{\partial^2 u_2}{\partial x^2} = 0 \qquad (e)$$

The variation with respect to ξ_1 yields

$$m_1 \frac{d^2 \xi_1}{d\tau^2} - K(u_1(o, \tau) - \xi_1) + K_{11}\xi_1 = 0 \qquad (23)$$

The variation with respect to ξ_2 yields

$$m_1 \frac{d^2 \xi_2}{d\tau^2} + K(\xi_2 - u_2(o, \tau)) + K_{12}\xi_2 = 0 \qquad (24)$$

The variation with respect to η_1 yields

$$m_2 \frac{d^2 \eta_1}{d\tau^2} - K(u_1 11, \tau) - \eta_1) + K_{21}\eta_1 = 0 \qquad (25)$$

The variation with respect to η_2 yields

$$m_2 \frac{d^2 \eta_2}{d \tau^2} - K \left(u_2 (1, \tau) - \eta_2 \right) + K_{22} \eta_2 = 0 \tag{26}$$

Equations (21) and (22) are coupled through gyroscopic terms. The mechanism through which these terms arise makes it clear that they are a result of the influence of the shaft deformation on the local axis of rotation.

The end conditions and differential equations for ξ_1, ξ_2, η_1, and η_2 are easily altered to reflect lubrication and support damping. The latter equations follow:

$$m_1 \frac{d^2 \xi_1}{d \tau^2} + (K + K_{11}) \, \xi_1 + (\mu + \mu_{11}) \frac{d\xi_1}{d\tau} = K \, u_1 (o, \tau) + \mu \frac{\partial}{\partial \tau} u_1 (o, \tau)$$

$$m_1 \frac{d^2 \xi_1}{d \tau^2} + (K + K_{12}) \, \xi_2 + (\mu + \mu_{12}) \frac{d\xi_2}{d\tau} = K \, u_2 (o, \tau) + \mu \frac{\partial}{\partial \tau} u_2 (o, \tau) \tag{27}$$

$$m_2 \frac{d^2\eta_1}{d\tau^2} + (K + K_{21})\,\eta_1 + (\mu + \mu_{21}) \frac{d\eta_1}{d\tau}$$

$$= K u_1 (1, \tau) + \mu \frac{\partial}{\partial \tau} u_1 (1, \tau)$$

(27)

$$m_2 \frac{d^2\eta_2}{d\tau^2} + (K + K_{22})\,\eta_2 + (\mu + u_{22}) \frac{d\eta_2}{d\tau}$$

$$= K u_2 (1, \tau) + \mu \frac{\partial u_2}{\partial \tau} (1, \tau)$$

Similarly, the only end conditions affected by the damping ((21 b, d), (22 b, d)) have the following form:

on $x = 0$ u_1 is prescribed or

$$\frac{1}{ML^4 \Omega^2} \frac{\partial}{\partial x} (S \frac{\partial^2 u_1}{\partial x^2}) - \frac{m_o r^2}{4} (\frac{\partial^3 u_1}{\partial x \partial \tau^2} + 2 \frac{\partial^2 u_2}{\partial x \partial \tau}$$

(a) (28)

$$+ K (u_1 - \xi_1) + \mu (\frac{\partial u_1}{\partial \tau} - \frac{d\xi_1}{d\tau}) = 0$$

on $x = 1$ u_1 is prescribed or

$$\frac{1}{ML^4\Omega^2}\frac{\partial}{\partial x}\left(S\frac{\partial^2 u_1}{\partial x^2}\right) - \frac{m_1 r^2}{4}\left(\frac{\partial^3 u_1}{\partial x \partial \tau^2} + 2\frac{\partial^2 u_2}{\partial x \partial \tau}\right)$$

(b)

$$- K(u_1 - \eta_1) - \mu\left(\frac{\partial u_1}{\partial \tau} - \frac{d\eta_1}{d\tau}\right) = 0$$

on $x = 0$ u_2 is prescribed or

$$\frac{1}{ML^4\Omega^2}\frac{\partial}{\partial x}\left(S\frac{\partial^2 u_2}{\partial x^2}\right) - \frac{m_o r^2}{4}\left(\frac{\partial^3 u_2}{\partial x \partial \tau^2} + 2\frac{\partial^2 u_1}{\partial x \partial \tau}\right) \quad (28)$$

(c)

$$+ K(u_2 - \xi_2) + \mu\left(\frac{\partial u_2}{\partial \tau} - \frac{d\xi_2}{d\tau}\right) = 0$$

on $x = 1$ u_2 is prescribed or

$$\frac{1}{ML^4\Omega^2}\frac{\partial}{\partial x}\left(S\frac{\partial^2 u_2}{\partial x^2}\right) - \frac{m_1 r^2}{4}\left(\frac{\partial^3 u_2}{\partial x \partial \tau^2} - 2\frac{\partial^2 u_1}{\partial x \partial \tau}\right)$$

(d)

$$- K(u_2 - \eta_2) + \mu\left(\frac{\partial u_2}{\partial \tau} - \frac{d\eta_2}{d\tau}\right) = 0$$

APPENDIX B

A CRITICAL SURVEY OF THE JASPER APPROACH

APPENDIX B

A CRITICAL SURVEY OF THE JASPER APPROACH

1. INTRODUCTION

This appendix is an extract of three reports by N. H. Jasper[1, 2, 3] on a procedure for determining the natural whirling frequencies of shaft-disk systems. The analysis presented here takes into account the considerations of rotary inertia, gyroscopic precession of the disk, and flexibility of shaft supports, as well as lumped and distributed masses.

The basis of this analysis is the assumption that vibrations exist in two orthogonal directions normal to the longitudinal shaft axis and that these vibrational modes are decoupled. In Section 5, it is shown that the assumption of decoupled vibratory modes is a direct result of ignoring, as second order effects, the gyroscopic terms associated with the shaft. With neglect of the gyroscopic moment of the shaft, the governing differential equations become decoupled linear differential equations with constant coefficients. Following these assumptions, the principle of superposition is employed,

---

1/ Jasper, N. H., "A Theoretical Approach to the Problem of Critical Whirling Speeds of Shaft-Disk Systems", David Taylor Model Basin Report 827, December 1954.

2/ Jasper, N, H., "A Design Approach to the Problem of Critical Whirling Speeds of Shaft-Disk Systems", David Taylor Basin Report 890, December 1954.

3/ Jasper, N. H., "Determination of Influence Coefficients as Applied to Calculation of Critical Whirling Speeds of Propeller-Shaft Systems", David Taylor Model Basin Report 1050, May 1957.

i.e., the deflections caused by individual loads may be added to obtain the total shaft deflection when the loads are applied jointly. These individual deflections are evaluated at their load source and the resulting displacements, both transverse and rotational, are denoted as influence coefficients. For example, a concentrated transverse force on a shaft will result in a unique deflection and slope at the point of the applied force. Accordingly, the influence coefficient δ^P is defined as the static deflection due to a concentrated force, and the influence coefficient θ^P is defined as the static slope of the shaft due to a concentrated force. Similarly, δ^M and θ^M are defined, at the point of the applied load, as the static displacement and slope due to a concentrated moment.

The inertial and gyroscopic loads resulting from a rotating disk can now be defined and represented as concentrated forces and moments, and then by employing the method of influence coefficients, their affect upon the system can be determined directly. For example, if the magnitude of the loads are multiplied by their respective influence coefficients, the sum of these products will then yield:

(a) The deflection equation when the δ coefficients are used.

(b) The slope equation when the θ coefficients are used.

2. DETERMINATION OF INERTIAL AND GYROSCOPIC LOADS

To determine the shaft loads resulting from a rotating disk, consider the case of a shaft specimen with a uniform angular velocity ω about its longitudinal axis and carrying a rigid disk at some point along its span. The procedure will be to consider the case in which the time variations of the existing moments, which are physically necessary to maintain whirling motion, are known multiples of the shaft speed, and to assume the shaft is massless and that gravity effects may be neglected.

The nomenclature and directions used in this development are given in Fig. B-1. In this notation; the triad X, Y, X is a set of axes fixed in space and x, y, z is a set of axes parallel to X, Y, Z and moving with the center of mass of an element of the shaft. The moving coordinate system is also used as coordinates of the center of gravity of the shaft element on the disk under consideration. The shaft disk system is illustrated in Fig. B-2. The bearing restraints and location of the disk on the shaft are arbitrary. It is assumed that the disk has symmetry about the y, and z axes. The disk has mass m_o, a diametral mass moment of inertia, τ_d, and a polar moment of inertia τ. The y and z axes are assumed to be oriented to coincide with the directions of maximum and minimum rigidity of the shaft supports, these directions are assumed the same for all supports.

To obtain the moment resulting from the rotating disk, it is assumed that the disk possesses an angular velocity component in three orthogonal directions not necessarily colinear with the (x, y, z) axes. From Fig. 1, it is seen the angular velocity vector is

$$\overline{\omega} = (\omega_1 , \quad \dot{\alpha}' , \dot{\beta}')$$

where,

ω = angular velocity component along the polar inertial axis of the disk

$\dot{\alpha}^1, \dot{\beta}^1$ = angular velocity component along the diametral inertial axis of the disk, respectively.

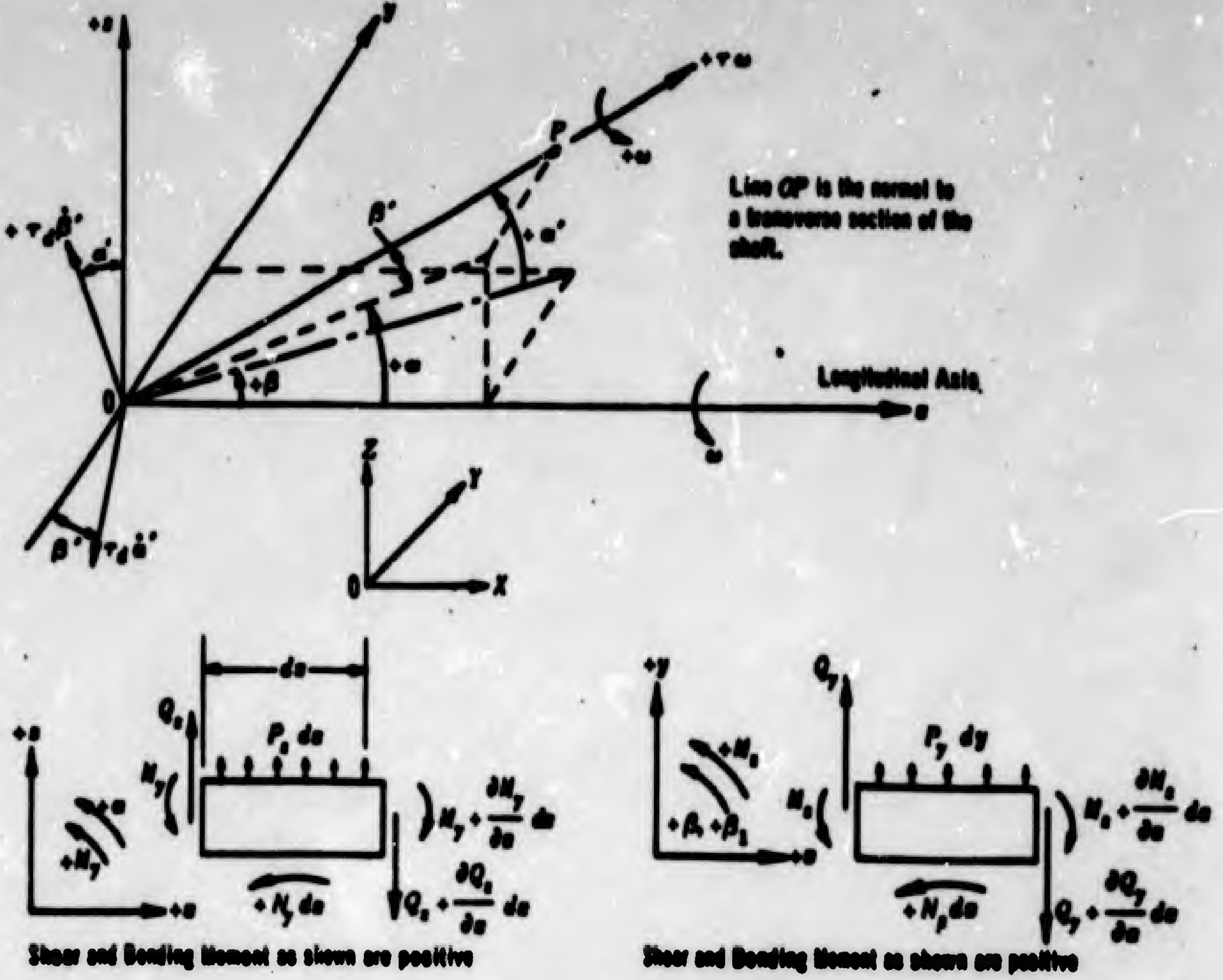

α' Angle between the line OP and the xy-plane.

β' Angle between the line OP and the xz-plane.

Positive shear is a positive force acting on the shaft to the right of a section.

The directions of axes ox, oy, and oz are fixed in space; the origin, Point 0, is moving with the center of gravity of the shaft element.

Figure B-1 Spinning and Whirling Shaft Element

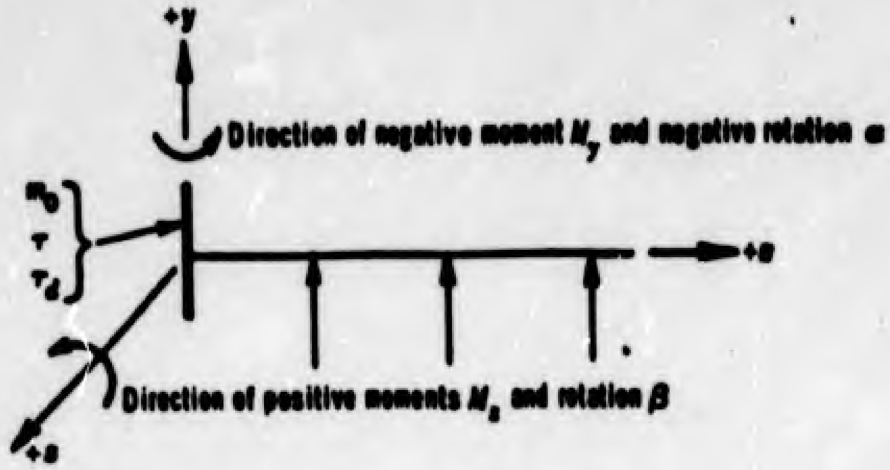

The sign of the influence coefficients must be chosen in accordance with the above sign convention.

The disk and shaft supports may be located anywhere along the shaft.

The disk is assumed to be thin at its point of attachment to the shaft.

Figure B-2 Schematic Diagram of Single Shaft-Disk System

In vector notation, the angular momentum of the disk is

$$\underline{L} = \begin{bmatrix} \tau & 0 & 0 \\ 0 & \tau_d & 0 \\ 0 & 0 & \tau_d \end{bmatrix} \begin{bmatrix} \omega \\ \dot{\alpha}' \\ \dot{\beta}' \end{bmatrix} \qquad (1)$$

Projecting the components of the L vector along the ox, oy, and oz axis (see Fig.B-1) results in

$$\tau\omega \cos\alpha' \cos\beta - \tau_d \dot{\beta}' (\cos\beta)(\sin\alpha') + \tau_d \dot{\alpha}' (\cos\alpha)(\sin\beta') = L_x$$

$$-\tau\omega (\cos\alpha') \sin\beta + \tau_d \dot{\alpha}' (\cos\beta') + \tau_d \beta'(\sin\alpha')(\sin\beta) = L_y$$

$$\tau\omega (\sin\alpha') + \tau_d \dot{\beta}' (\cos\alpha') + \tau_d \dot{\alpha}' (\sin\beta')(\sin\alpha) = L_x$$

where,

L_x = angular momentum per unit length about axis ox

L_y = angular momentum per unit length about axis oy

L_z = angular momentum per unit length about axis oz

In obtaining these expressions for the components of angular momentum, a salient point to observe is the sign convention as illustrated in Figure B-1. The angular momentum components directed in the positive direction of the ox and oz axis are taken as positive, whereas angular momentum components directed along the positive oy axis are taken as negative. This sign convention is used to maintain conformity with the sign convention used for a bending movement as illustrated in Figure B-1.

For small angles, $\cos \xi = 1$, $\sin \xi = \xi$, $\alpha' = \alpha$ and $\beta' = \beta$. Therefore

$$\begin{aligned} L_x &= \tau\omega - \tau_d \dot{\beta} \alpha + \tau_d \dot{\alpha} \beta \\ L_y &= -\tau\omega \beta + \tau_d \dot{\alpha} + \tau_d \dot{\beta} \alpha \beta \\ L_z &= \tau\omega \alpha + \tau_d \dot{\beta} + \tau_d \dot{\alpha} \beta \alpha \end{aligned} \qquad (2)$$

Neglecting products of small angles and their derivatives as higher order terms, the components of angular momentum are

$$
\begin{aligned}
L_x &= \tau\omega \\
L_y &= -\tau\omega\beta + \tau_d\dot{\alpha} \\
L_z &= \tau\omega\alpha + \tau_d\dot{\beta}
\end{aligned}
\qquad (3)
$$

Notice that the time rate of change of angular momentum about an axis fixed in the center of gravity is equal to the moment about that axis. Therefore, the gyroscopic moments are

$$
\begin{aligned}
M_x^m &= \frac{d}{dt} L_x = 0 \\
M_y^m &= \frac{d}{dt} L_y = -\tau\omega\dot{\beta} + \tau_d\ddot{\alpha} \\
M_z^m &= \frac{d}{dt} L_z = \tau\omega\dot{\alpha} + \tau_d\ddot{\beta}
\end{aligned}
\qquad (4)
$$

where,

M_x^m, M_y^m, and M_z^m are the moments about the x, y, and z axis, respectively. The result, $M_x^m = 0$, agrees with the assumption that the shaft is spinning with a uniform angular velocity.

In the x y plane, the forces and moments acting on the disk are F_y and M_z^m respectively, i.e.,

$$
\begin{aligned}
F_y &= M_o\ddot{y} \\
M_z^m &= \tau\omega\dot{\alpha} + \tau_d\ddot{\beta}
\end{aligned}
\qquad (5)
$$

The forces and moments acting on the shaft are then equal to but opposite in direction to those acting on the disk. Thus,

$$\begin{aligned} \text{Force on shaft} &= -M_o\ddot{y} \\ \text{Moment on shaft} &= -(\tau\omega\dot{\alpha} + \tau_d\ddot{\beta}) \end{aligned} \tag{6}$$

Consider the shaft is spinning in the positive direction (from y toward z) and whirling about the x-axis in an elliptical path. Then at the location of the disk

$$\begin{aligned} \alpha &= \alpha_o \sin \Omega t \qquad & \beta &= \beta_o \cos \Omega t \\ y &= y_o \cos \Omega t \qquad & z &= z_o \sin \Omega t \end{aligned} \tag{7}$$

where

α_o, β_o, y_o, and z_o are constants

Ω = angular whirling velocity of the normal to the shaft section about the stationary position of the longitudinal axis of the shaft.

Let

$$\tau/\tau_d = k$$

$$\frac{\omega}{\Omega} = h$$

$$\frac{\alpha_o}{\beta_o} = s$$

under the conditions assumed here, h is known. A positive h represents a whirl in the positive direction, assuming ω always is positive.

Then

$$-F_y = M_o \Omega^2 y$$

$$-M_z^m = -(khs-1)\ \tau_d \Omega^2 \beta \qquad (8)$$

3. DETERMINATION OF FREQUENCY EQUATIONS

The linear and angular deflections of the disk in the xy plane are determined by multiplying the above loads by their respective influence coefficients, i.e.,

$$y = M_o y \Omega^2 \delta^P - (khs-1)\ \tau_d \Omega^2 \beta\ \delta^M$$

$$\beta = M_o y \Omega^2 \theta^P - (khs-1)\ \tau_d \Omega^2\ \beta\ \theta^M \qquad (9)$$

By collecting coefficients of y and β, two homogeneous equations result, i.e.,

$$(m_o y \Omega^2 \delta^P - 1) y - \left[(khs-1)\tau_d \Omega^2\ \delta^M\right] B = 0 \qquad (10)$$

$$m_o \Omega^2 \theta^P y - \left[(khs-1)\ \ \tau_d \Omega^2 \theta^M + 1\right] B = 0 \qquad (11)$$

y and β can have values other than zero, only if the determinant of their coefficients is equal to zero. The result of this determinant vanishing is a frequency equation with Ω replaced by Ω_N.

$$\Omega^4_N \left[m_o \tau_d (khs-1) (\delta^M \theta^P - \delta^P \theta^M) - \Omega^2_N \left[m_o \delta^P - \theta^M \tau_d (khs-1) \right] + 1 = 0 \right.$$

or

$$\Omega^2_N = \frac{m_o (\delta^P + \theta^M G) \pm \sqrt{(m_o \delta^P + \theta^M G)^2 - 4 m_o G (\delta^P \theta^M - \delta^M \theta^P)}}{2 m_o G (\delta^P \theta^M - \delta^M \theta^P)} \tag{13}$$

where

$$G = (1 - khs) \tau_d$$

The frequencies Ω_N are always real. This statement is verified by noting that

$$\delta^M = \theta^P \tag{14}$$

which is a direct result of Maxwell's theorem.[4]

Another necessary condition required for real Ω_N is

$$\delta^P \theta^M - \delta^M \theta^P \geq 0 \tag{15}$$

This inequality is obtained as follows:

Construct a vector with one component as y and the other as β, e.g., $\underline{y} = \binom{y}{\beta}$. Then from equation 9, it is seen that

$$\underline{y} = A \underline{y} \tag{16}$$

---

[4] Any elasticity book.

where

$$
A = \begin{bmatrix} m_o \Omega^2 \delta^P & -(khs-1)\, \tau_d \Omega^2 \delta^M \\ m_o \Omega^2 \theta^P & -(khs-1)\, \tau_d \Omega^2 \theta^M \end{bmatrix} \tag{17}
$$

It is immediately seen that the scalar product

$$\langle y , Ay \rangle = \| y \|$$

and the scalar product

$$\langle Ay , y \rangle = \| y \|$$

where $\| y \|$ = modulus of the vector $\underline{y}$

Therefore,

$$\langle y , Ay \rangle = \langle Ay , y \rangle$$

Or in other words, the matrix A is a self adjoint matrix. The eigenvalues of a self adjoint matrix are real [5/]. Therefore,

$$
\begin{vmatrix} m_o \Omega^2 \delta^P - \lambda & -(khs-1)\, \tau_d \Omega^2 \delta^M \\ m_o \Omega^2 \theta^P & -(khs-1)\, \tau_d \Omega^2 \theta^M - \lambda \end{vmatrix} = 0 \tag{19}
$$

where λ are the eigenvalues.

5/ Friedman, B., Principles and Techniques of Applied Mathematics, J. Wiley and Son, Inc., 1962.

Solving this determinental equation results in

$$\lambda^2 - \lambda \left[\Omega^2 (m_o \delta^P + G\theta^M)\right] + m_o \Omega^4 G \left[\delta^P \theta^M - \delta^M \theta^P\right] = 0$$

$$\lambda_{1,2} = \frac{\Omega}{2}^2 \left[(m_o \delta^P + G\theta^M) \pm \sqrt{(m_o \delta^P - G\theta^M)^2 + 4 m_o G \delta^M \theta^P}\right] \quad (20)$$

Now consider the following cases:

For Ω real, a real λ demands that the quantity

$$(m_o \delta^P - G\theta^M)^2 + 4 m_o G \delta^M \theta^P \geq 0$$

For imaginary Ω, a real λ requires the bracketed quality of equation (20) to be the complex conjugate of Ω^2. This is impossible because of equation (13). Therefore Ω is not imaginary and from equation (13) the relationship which ensures that Ω is real for both positive and negative G is

$$\delta^P \theta^M - \delta^M \theta^P \geq 0$$

It is significant to note that for negative G there will be only one physically real natural whirling frequency, whereas for positive G there will always be two positive values of Ω^2 corresponding to two natural whirling frequencies. This is evident when the equation for G is considered, e.g.,

$$G = (1 - khs)\ \tau_d$$

For $G > 0$, h can either be positive or negative. For $G < 0$, h can only be negative.

A similar procedure is employed in the X-Z plane to obtain

$$\Omega_N = \frac{(m_o \; {}_*^{P} - G_* \theta^{M}) \pm \sqrt{(m_o \; {}_*^{P} + G_* \theta_*^{M})^2 - 4 m_o G_* (\; {}_* \theta_*^{M} - \; {}_*^{M} \theta_*^{P}}}{2 m_o G_* (\delta_*^{P} \theta_*^{M} - \delta_*^{M} \theta_*^{P})}$$

(21)

where $G_* = (1 - \frac{kh}{s}) \tau_d$ and the star subscript is used to designate the constants applicable to the x-z plane from those in the x-y plane.

4. CALCULATION OF Ω_N

Equations (13) and (21) both express Ω_N in terms of h, which is assumed known, and s, which in general is unknown. A value of s may be determined by trial such that equations (13) and (21) give the same value of Ω_N; this value is then one of the natural frequencies of whirl and the corresponding critical value of ω is $\omega = h\Omega_N$.

The procedure for calculating Ω_N covers both the symmetrical case (s = 1) and the unsymmetrical case ($s \neq 1$). In the symmetrical case, the amplitudes of motion must be the same in both the xy and xz plane. Therefore $s = 1$ and $\delta^P = \delta_*^P$, $\delta^M = \delta_*^M$, $\theta^P = \theta_*^P$, and $\theta^M = \theta_*^M$. Thus equations (13) and (21) are identical and the values for Ω_N are the natural whirling frequencies for a given h. For each value of h, equation (13) will give either one or two natural frequencies of whirling vibration. A forward whirl is denoted by a positive h, and a counter-whirl is denoted by a negative h.

For the unsymmetrical case ($s \neq 1$), the center of the shaft moves in an elliptical path and both equations (13) and (21) are necessary to solve for Ω_N. It is possible to obtain the solution by a trial and error approximation.

Equation (13) and (21) must give the same value of Ω_N for a chosen h, if the proper value of s is used. Therefore, a value of s may be assumed and substituted into equations (13) and (21). The values for Ω_N^2 are then obtained. By plotting the difference between the calculated frequencies versus the assumed s, the resulting curve will indicate the direction of the assumptions on s. The correct values of s and Ω_N are obtained when the difference is zero.

For the unsymmetrical case, a direct mathematical approach is to substitute the quantities U and U_* into equations (13) and (21),

$$\Omega_N^4 m_o \tau_d (khs-1)\, U - \Omega_N^2 \left[m_o \delta' - \theta^m \tau_d (khs-1) \right] + 1 = 0$$

$$\Omega_N^4 m_o \tau_d \left(\frac{kh}{s} - 1\right) U_* - \Omega_2^N \left[m_o \delta_*^P - \theta_*^M \tau_d \left(\frac{kh}{s} - 1\right) \right] + 1 = 0 \tag{22}$$

where

$$U = \delta^M \theta^P - \delta^P \theta^M$$

$$U_* = \delta_*^M \theta_*^P - \delta_*^P \theta_*^M$$

Rearranging terms

$$\left[\Omega_N^4 m_o \tau_d U + \Omega_N^2 \theta^M \tau_d \right] khs = \Omega_N^4 m_o \tau_d U + \Omega_N^2 (m_o \delta^P + \theta^M \tau_d) + 1$$

$$\left[\Omega_N^4 m_o \tau_d U_* + \Omega_N^2 \theta_*^M \tau_d \right] kh = \left[\Omega_N^4 m_o \tau_d U_* + \Omega_N^2 (m_o \delta_*^P + \theta_*^M \tau_d) + 1 \right] S$$

Multiplying, cancelling s, and collecting terms gives a fourth-degree frequency equation in Ω_N^2 which is independent of s and in which the coefficients of Ω_N are constants for any given spin to whirl ratio h.

$$\Omega_N^8 \left[m_o^2 \tau_d^2 U U_*(k^2h^2-1) \right] + \Omega_6 \left[(\theta_*^M V + \theta^M U_*) m_o \tau_d^2 k^2 h^2 - \right.$$

$$\left. \left\{ U_* (m_o \delta^P + \theta^M \tau_d) + U (m_o \delta_*^P + \theta^M \tau_d) \right\} m_o \tau_d \right] + \Omega_N^4 \left[m_o \tau_d (U + U_* \right.$$

$$\left. - \theta_*^M \delta^P - \theta^M \delta_*^P) + k^2 h^2 - \tau_d^2 \theta^M \theta_*^M - \theta^M \theta_*^M \tau_d^2 - m_o \delta_*^P \delta^P \right]$$

$$+ \Omega_N^2 \left[m_o \delta^P + \theta^M \tau_d + m_o \delta_*^P + \theta_*^M \tau_d \right] + 1 = 0 \qquad (23)$$

This equation may be solved for Ω_N for any given h by a number of numerical methods.

If the substitution $h = \frac{\omega}{\Omega_N}$ is made in equation (23), it becomes an equation for the determination of the natural whirling frequencies in terms of the spin velocity and the constants of the system, e.g.,

$$EK\Omega_N^8 + \left[EH + FK - AC \right] \Omega_N^6 + \left[FH - K - E - BC + AD \right] \Omega_N^4$$

$$+ \left[BD - F - H \right] \Omega_N^2 + 1 = 0 \qquad (24)$$

where

$$A = m_o \tau_d k \omega U \qquad B = \tau_d k \omega \theta^M \qquad E = m_o \tau_d U$$

$$C = -m_o \tau_d k \omega U \qquad D = -\tau_d k \omega \theta^M \qquad K = m_o \tau_d U_*$$

$$F = \theta^M \tau_d + m_o \delta^P$$

$$H = \theta_*^M \tau_d + m_o \delta_*^P$$

This equation is a fourth degree equation in Ω_N^2 and may be solved by numerical methods. It applies to shafts with symmetrical as well as unsymmetrical bearing supports. With α_o and β_o taken as positive, the sign of Ω_N is determined by the differential equations of motion so that there are, in general, just four natural frequencies for each value of ω.

In order to solve equations (13), (21), or (24), it is necessary to obtain the translational and rotary displacements due to a concentrated force and a concentrated moment. In other words, obtain the force and moment influence coefficients. This can be done by employing beam theory to evaluate these displacements. The conjungate beam method [6/] or the method of singularity functions [7/] are but a few of the techniques that may be used. Reliance upon the above references or deflection equations given in handbooks will yield the desired results. To evaluate these influence coefficients, one basic point remains: after using the equations of beam theory, the equations will still be indeterminate since rotary and translational freedom of the bearing mountings are to be considered here. It is finally necessary to apply the equations of equilibrium to each flexible support, i.e., the displacement at the support due to external loads is equal to the reaction at the support divided by the appropriate spring constant.

5. ENGINEERING APPROXIMATIONS

The two values of Ω_N, which are obtained from equations (13), (21), or (24), give the two lowest modes of vibration corresponding to a given h. Obviously, the lowest frequency is obtained when the negative sign is used in front of the radical in equations (13) and (21). Similarly, the highest of the two frequencies is obtained when the plus sign is used. When using

6/ loc. cit., p.

7/ Scopelite, Thomas M., "The Singularity Functions of Uniform Beams", M.S. Thesis, Illinois Institute of Technology, 1964.

the negative in front of the radical, the difference of the first few significant figures might be negligible. Therefore, when the minus sign is used, multiply both the numerator and the denominator by the conjugate of the numerator. The equation for the lowest mode frequency of vibration takes the form

$$\Omega_{N_1}^{2} = \frac{2}{(m_o\delta^P + \theta^M G) + \sqrt{(m_o\delta^P + \theta^M G)^2 - 4m_o G(\delta^P\theta^M - \delta^M\theta^P)}} \tag{25}$$

if G is taken as zero, then

$$\Omega_{N_1} = \sqrt{\frac{1}{\delta^P m_o}} \tag{26}$$

Letting $G = 0$ is equivalent to the assumption that the disk acts as if it were a point mass system, i.e., $\tau_d = 0$. This assumption gives an underestimate of the first order forward whirl. For the most important case of the first order forward whirl ($h = 1$), G will become zero if $k = 1$. Since for any real disk, k is larger than 1; therefore G will actually be negative for this first order whirl resulting in a higher computed natural frequency (Eq. 25) than would be obtained from equations (26) where $G = 0$. Thus, if G is set equal to zero, an underestimate is obtained, which is on the side of safety.

The critical frequency is influenced by the mass of the shaft. This influence can be estimated by adding to the disk an effective mass, m_{es}. This effective mass is defined by the following

$$\frac{1}{(m_o + m_{es})\ \delta^P} = \frac{g}{\delta'_{static}} \tag{27}$$

where δ'_{static} is the static deflection at the center of the disk due to the weight $g(m + m_{es})$ applied at the center of the propeller. Therefore, the first natural frequency becomes

$$\Omega_{N_1} = \sqrt{\frac{1}{(m_o + m_{es})\,\delta^P}} = \sqrt{\frac{g}{\delta'_{static}}} \tag{28}$$

when $G = 0$.

The effective mass of the shaft can also be considered to be equivalent to a mass located at the center of the disk, which will have a maximum kinetic energy equal to the maximum kinetic energy of the shaft when it is vibrating in the particular mode under consideration. Jasper has determined that estimates of m_{es}, determined by the use of the lowest mode shapes found for several propeller-shaft systems, have fallen within the

$$0.10\ m_s < m_{es} < 0.40\ m_s \tag{29}$$

for the lowest mode of vibration and where m_s = mass of the shaft.

In order to make the frequency equations (13), (21), and (24) more manageable, further simplifying assumptions as to the nature of the parameter G can be made. These assumptions will make available to the designer a method for making rough estimates of the critical whirling speeds while at the same time illustrating the manner in which the various physical parameters of the system affect the critical speeds. If it is assumed the radial stiffnesses are identical at all bearing supports, i.e., $s = \frac{\alpha_o}{\beta_o} = 1$, and if the disk is thin, i.e., $k = \frac{\tau}{\tau_d} = 2$, then one may think of G as an effective inertia with

$$G = (1 - 2h)\,\tau_d$$

where h is the ratio of shaft speed to whirling speed. Accordingly,

$$\begin{aligned}
G &= -\tau_d && \text{for the important first order forward whirl } (h = 1) \\
G &= 3\tau_d && \text{for the first order counter whirl } (h = -1) \\
G &= (1+\tfrac{2}{n})\,\tau_d && \text{for the nth order counter whirl } (h = -\tfrac{1}{n}) \\
G &= (1-\tfrac{2}{n})\,\tau_d && \text{for the nth order forward whirl } (h = \tfrac{1}{n}).
\end{aligned} \qquad (30)$$

For the first two of the above equations (30) can be used in equation (25) to estimate first order whirl speeds, whereas the last two equations of (30) must be used in equations (13) and (21) or (24) to obtain the critical whirling speeds of order n.

6. DIFFERENTIAL EQUATIONS FOR A WHIRLING SHAFT

(a) Differential Equations of Motion

To obtain the differential equations of motion of a whirling shaft, apply the principles of mechanics to an element of the shaft vibrating in transverse plane (see Fig.B-1). From Fig.B-1 a positive bending movement and a positive shear force are defined as a positive moment and force acting on the portion of the beam to the right of the section. Then by summing forces and moments in the x z plane

$$\frac{\partial Q_z}{\partial x} - P_z + m\ddot{z} = 0$$

$$-Q_z + N_y - \frac{\partial M_y}{\partial x} - M_y^{m} = 0$$

where

$$M_y^{m} = -\tau\,\omega\,\dot{\beta} + \tau_d\,\ddot{a} \qquad \text{(see equation 4)}$$

and also

$$\frac{\partial z}{\partial x} = a + \epsilon x_z$$

where

ϵx_z = the component of slope of the neutral axis due to shear.

From beam theory and the sign convection adopted here

$$M_y = -\frac{1}{EI}\frac{\partial a}{\partial x}$$

$$Q_z = -KAG\left[\frac{\partial z}{\partial x} - a\right]$$

where

EI = bending stiffness of the shaft

K = shear coefficient

A = shaft cross-sectional area

G = modulous of elasticity in shear

Substituting these equations into the equilibrium relationships results in

$$KAG\left[\frac{\partial^2 z}{\partial x^2} - \frac{\partial \alpha}{\partial x}\right] + P_z - m\ddot{z} = 0$$

$$KAG\left[\frac{\partial z}{\partial x} - \alpha\right] + N_y + EI\frac{\partial^2 \alpha}{\partial x^2} + \tau\omega\dot{\beta} - \tau_d\dot{\alpha} = 0 \qquad (31)$$

By applying a similar procedure to an element in the xy plane and using the relationships

$$M_z = -\frac{1}{EI}\frac{\partial \beta}{\partial x} \qquad M_z^m = \tau\omega\dot{\alpha} + \tau_d\ddot{\beta}$$

$$Q_y = -KAG\,\epsilon_{xy} \qquad \epsilon_{xy} = \frac{\partial y}{\partial x} - \beta$$

the following equations are obtained:

$$KAG\left[\frac{\partial^2 y}{\partial x^2} - \frac{\partial \beta}{\partial x}\right] + P_y - m\ddot{y} = 0$$

$$EI\frac{\partial^2 \beta}{\partial x^2} + KAG\left[\frac{\partial y}{\partial x} - \beta\right] + N_z - \tau\omega\dot{\alpha} - \tau_d\ddot{\beta} = 0 \qquad (32)$$

(b) An analytical Solution to the Differential Equations of a Whirling Shaft-Disk System with Gyroscopic Effects of the Shaft Neglected

Equations (31) and (32) represent the equations of motion in the variables x, y, z, α, β, their derivatives, and time. These equations are not readily solvable for the general case. However, by ignoring the gyroscopic effects of the shaft, a highly reasonable description of the problem results. This modified model includes the mass of the shaft, mass of the disk, gyroscopic effects of the disk, and the effect of shear deformation. By excluding the gyroscopic moment of the shaft, the field equations in the x-z plane are

$$\frac{\partial Q_2}{\partial x} = P_z - m\Omega^2 z$$

$$\frac{\partial M_y}{\partial x} = -Q_z + N_y \qquad (33)$$

$$\frac{\partial z}{\partial x} = \alpha - fQ_z$$

$$\frac{\partial \alpha}{\partial x} = -EIM_y$$

where f = KAG and it is assumed that

$$z = z(x) \sin \Omega t$$

$$\alpha = \alpha(x) \sin \Omega t$$

By successive differentiation and substitution of the above field equations, a fourth order differential equation results:

$$\frac{\partial^4 z}{\partial x^4} - fm\Omega^2 \frac{\partial^2 z}{\partial x^2} + \frac{m\Omega^2}{EI} z = \frac{P_z}{EI} - f\frac{\partial^2 P_z}{\partial x^2} - \frac{1}{EI}\frac{\partial N_y}{\partial x} \quad (34)$$

Similarly, for the x-y plane

$$\frac{\partial Q_y}{\partial x} = P_y - m\Omega^2 y$$

$$\frac{\partial M_z}{\partial x} = - Q_y + N_z$$

$$\frac{\partial y}{\partial x} = B - fQ_y$$

$$\frac{\partial \beta}{\partial x} = - EIM_z$$

and

$$\frac{\partial^4 y}{\partial x^4} - fm\Omega^2 \frac{\partial^2 y}{\partial x^2} + \frac{m\Omega^2}{EI} y = \frac{P_y}{EI} - f\frac{\partial^2 P_y}{\partial x^2} - \frac{1}{EI}\frac{\partial N_z}{\partial x} \quad (35)$$

$$y = y(x) \cos \Omega t$$

$$\beta = \beta(x) \cos \Omega t$$

The problem as stated by equations (31) and (36) has now been reduced to two decoupled fourth order linear differential equations with constant coefficients. Therefore, under the assumptions considered here, the principle of superposition is valid, since any linear combination of fundamental solutions to a linear differential equation is still a solution of the governing equation. The characteristic polynomial to equations (34) and (35) is

$$m^4 - 4r^2 (u^2-1) m + 4r^4 = 0 \tag{36}$$

where

$$4r^4 = \frac{m\Omega^2}{EI}$$

$$4r^2 (u^2-1) = fm\Omega^2$$

and its four roots are

$$\pm r_1 = \pm r (u + \sqrt{u^2-2})$$

$$\pm r_2 = \pm r (u - \sqrt{u^2-2})$$

These roots are distinct as long as $t^2 \neq 2$; this will be assumed to be the case. A set of fundamental solutions to (34) and (35) is

$$\left\{ e^{r_1 x}, e^{r_2 x}, e^{-r_1 x}, e^{-r_2 x} \right\}$$

Therefore the solutions to the homogeneous equations of (34) and (35) are

$$y = \left\{ A_1 e^{r_1 x} + A_2 e^{-r_1 x} + A_3 e^{r_2 x} + A_4 e^{-r_2 x} \right\} \cos \Omega t$$

$$z = \left\{ B_1 e^{r_1 x} + B_2 e^{-r_1 x} + B_3 e^{r_2 x} + B_4 e^{-r_2 x} \right\} \sin \Omega t \qquad (37)$$

where A_i and B_i are constants to be evaluated from the boundary conditions or some other prescribed condition within the span of the structure $(i = i, 2, 3, 4)$.

All that remains analytically is to satisfy the discontinuity conditions that arise from a jump in the respective derivatives of y and z due to discontinuous applied and reactive loads such as P_y, P_z, N_y, N_z, the forces and moments resulting from the rotating disk, and the reactive forces and moments due to the supports. It has been shown,[8] that for linear systems, a function can be associated with each type of loading condition. This function represents a particular solution to (34) or (35) resulting from a discontinuity condition imposed on the deflection or its derivatives. For $1 \leq t^2 < 2$, the following four particular solutions are of significant importance:

$$Cc + \frac{u^2 - 1}{ug} Sc \sim \text{particular solution for a unit jump in deflection} = \langle s \rangle^{-4} \qquad (38)$$

$$\frac{1}{2\,rug}\left[uCs + gSc\right] \sim \text{particular solution for a unit jump in the section slope - } \alpha \text{ or } \beta = \langle s \rangle^{-3}$$

[8] loc. cit., p.

$- \frac{2r^2}{kug}$ Ss $\sim$ particular solution for a concentrated unit moment = $<s>^2$

$\frac{r}{kug}\left[u(3-2u^2)\,Cs + g(1-2u^2)Sc\right]$ $\sim$ particular solution for a unit concentrated force = $<s>^{-1}$

where:

$C = \cosh r\,u\,(x-a)$ $\qquad S = \sinh r\,u\,(x-a)$

$c = \cos r\,g\,(x-a)$ $\qquad s = \sin r\,g\,(x-a)$

$ig = \sqrt{t^2-2}\,, \; g>0$

$i = \sqrt{-1}$

a = point of application of the applied r reactive load.

By substituting any of the equations of (38) into (34) or (35), it can be verified that equations (38) are in fact particular solutions. Employing the notation

$$<f(x-a)> = \begin{cases} 0 & x<a \\ f(x-a) & x>a \end{cases}$$

and (39)

$$\frac{d^n}{dx^n} <f(x-a)> = \begin{cases} 0 & x<a \\ \frac{d^n}{dx^n} f(x-a) & x>a \end{cases}$$

the complete deflection equation for both vibrational modes can be written down immediately. For example, consider the following shaft-disk system:

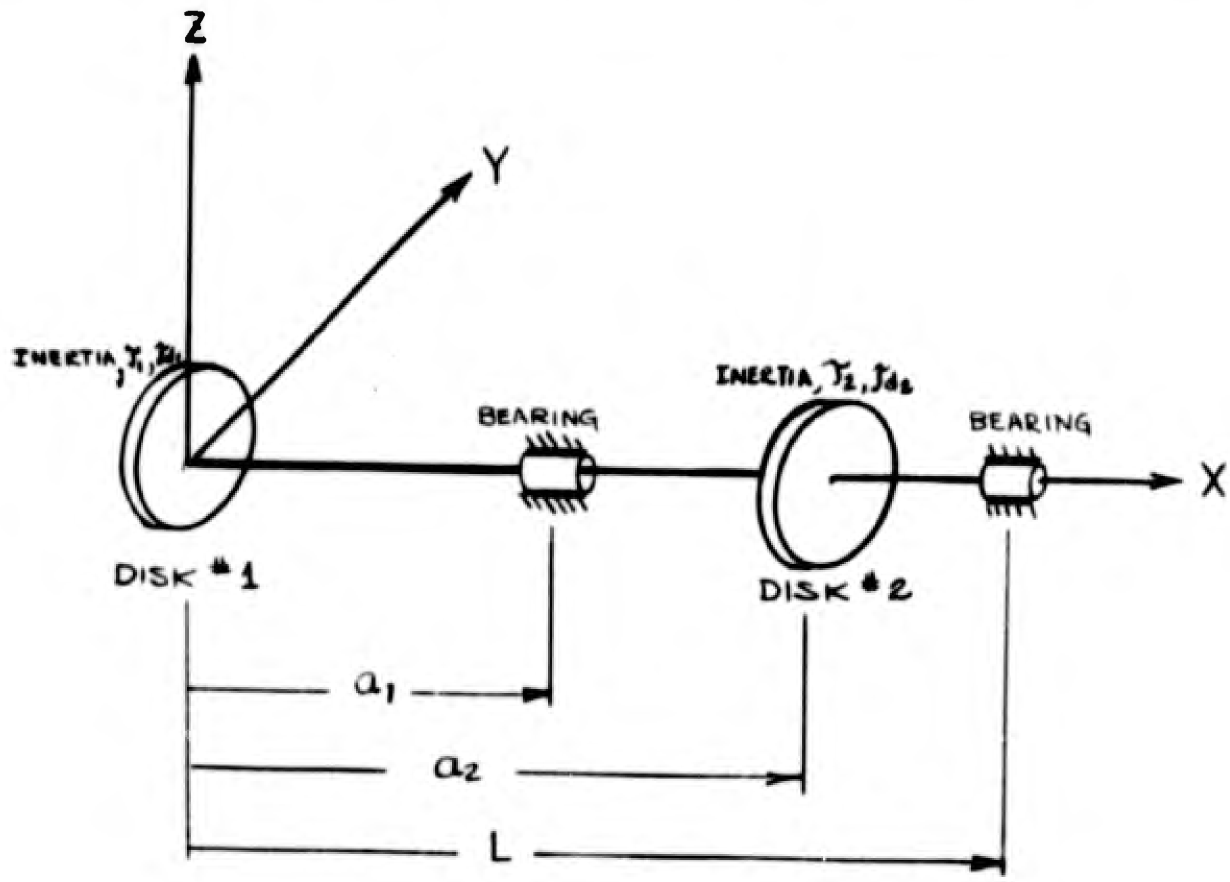

In the xy plane, disk No. 1 supplies to the shaft, at the point $x = 0$, the moment

$$\tau_1 \omega \underline{\dot{\alpha}} + \tau_{d_1} \omega \underline{\ddot{\beta}}$$

where

$$\underline{\dot{a}} = \frac{d}{dt} \left\{ a\,(o) \sin \Omega\, t \right\} = a\,(o)\, \Omega \cos \Omega\, t = \frac{a\,(o)}{\beta\,(o)}\, \underline{\dot{\beta}}$$

$$\underline{\ddot{\beta}} = \frac{d^2}{dt^2} \left\{ \beta\,(o) \cos \Omega\, t \right\} = -\Omega^2\, \beta\,(o) \cos \Omega\, t = -\Omega^2 \underline{\beta}$$

and the force

$$-m\Omega^2 y(o)$$

Disk No. 2 supplies to the shaft the moment

$$\tau_2 \omega \dot{\underline{\underline{\alpha}}} + \tau_{d_2} \omega \dot{\underline{\underline{\beta}}}$$

where

$$\ddot{\underline{\underline{\beta}}} = -\beta(a_2)\Omega^2 \cos \Omega t = -\underline{\underline{\beta}}\Omega^2$$

$$\dot{\underline{\underline{\alpha}}} = \frac{\alpha(a_2)}{\beta(a_2)} \underline{\underline{\beta}}$$

and the force,

$$-m\Omega^2 y(a_2)$$

Letting

k_{yi} = y direction linear spring constant at $x = a_i$

k_{zi} = z direction linear spring constant at $x = a_i$

R_{yi} = y direction rotary spring constant at $x = a_i$

R_{zi} = z direction rotary spring constant at $x = a_i$

and using the particular solutions of (38) and the notation of (39), the xy plane deflection can be written immediately as

$$y = \left[y(o) < s >^{-4} + \beta(o) < s >^{-3} - (\tau_1 \omega \underline{\dot{a}} - \tau_{d_1} \omega \underline{\ddot{\beta}}) < s >^{-2} - m\Omega^2 y(o) < s >^{-1} \right]_{a=o} + k_{y_1} y(a_1) < s >^{-1} \Big|_{a=a_1} + R_{y_1} \beta(a_1) < s >^{-2} \Big|_{a=a_1}$$

$$+ \left[-(\tau_2 \omega \underline{\underline{\dot{a}}} - \tau_{d_2} \omega \underline{\underline{\ddot{\beta}}}) < s >^{-2} - m\Omega^2 y(a_2) < s >^{-1} \right]_{a=a_2}$$

A similar equation can be written for the displacement in the x z plane. The above equation, when solved to satisfy the boundary conditions, will result in a transcendental equation involving $\Omega_N^{\ 2}$. The solution to this transcendental equation must then be identical to the result obtained for the x z plane.

APPENDIX C

DRAWINGS OF TEST FIXTURE

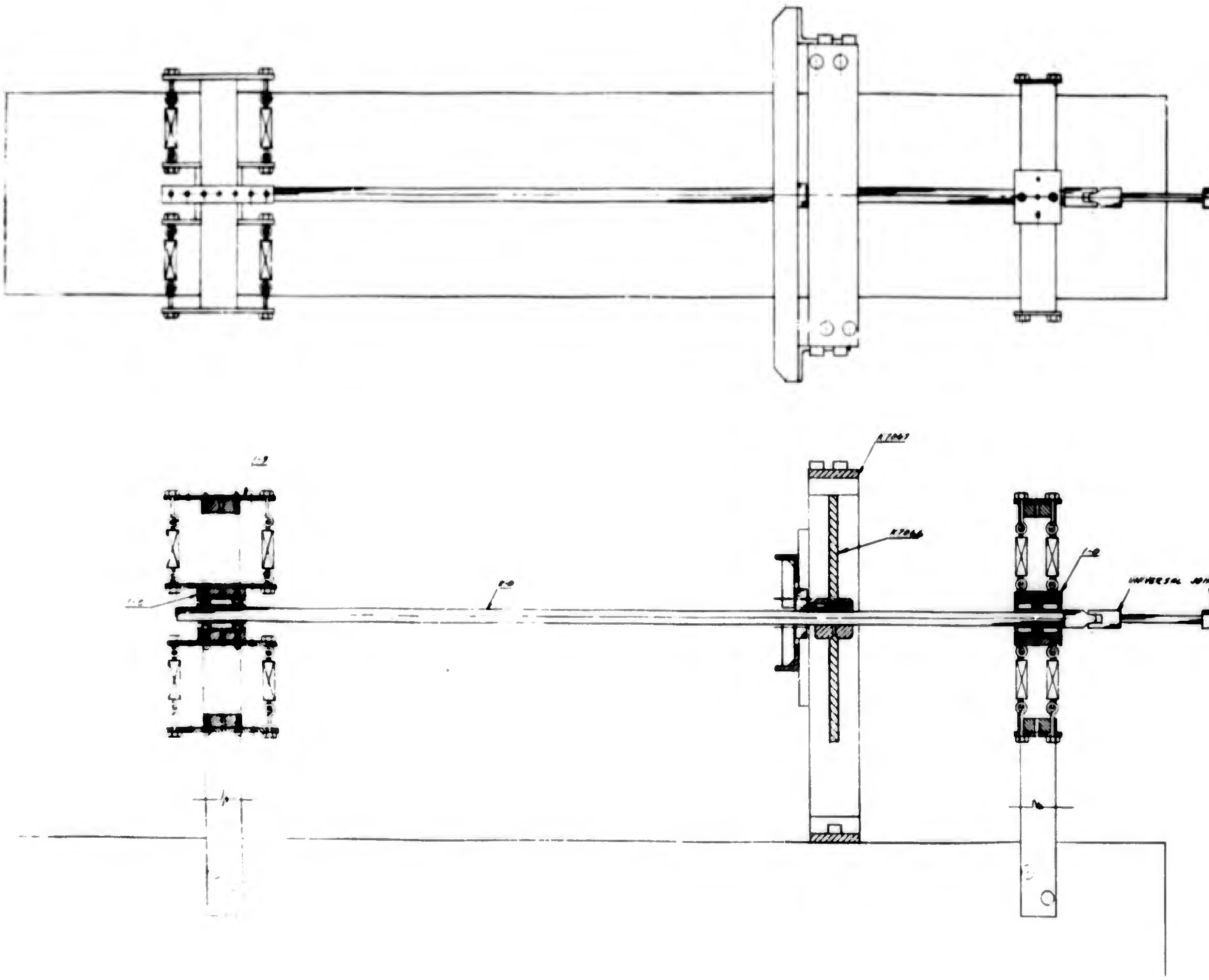
UNIVERSAL

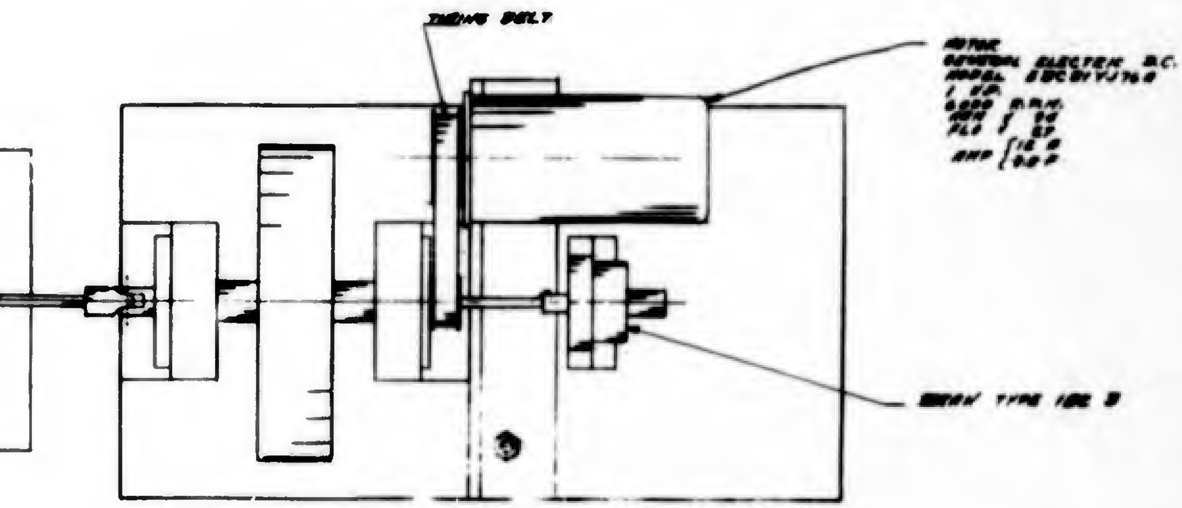

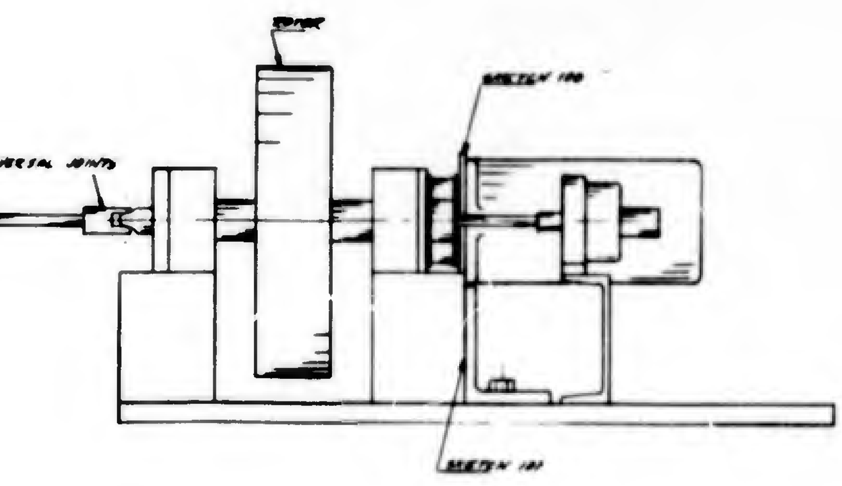

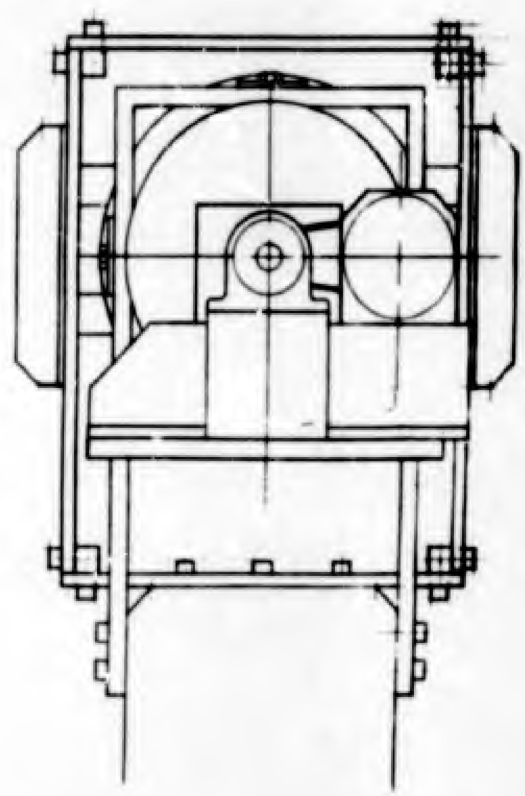

EXPERIMENTAL FIXTURE ARRANGEMENT
IITRI PROJECT K6056

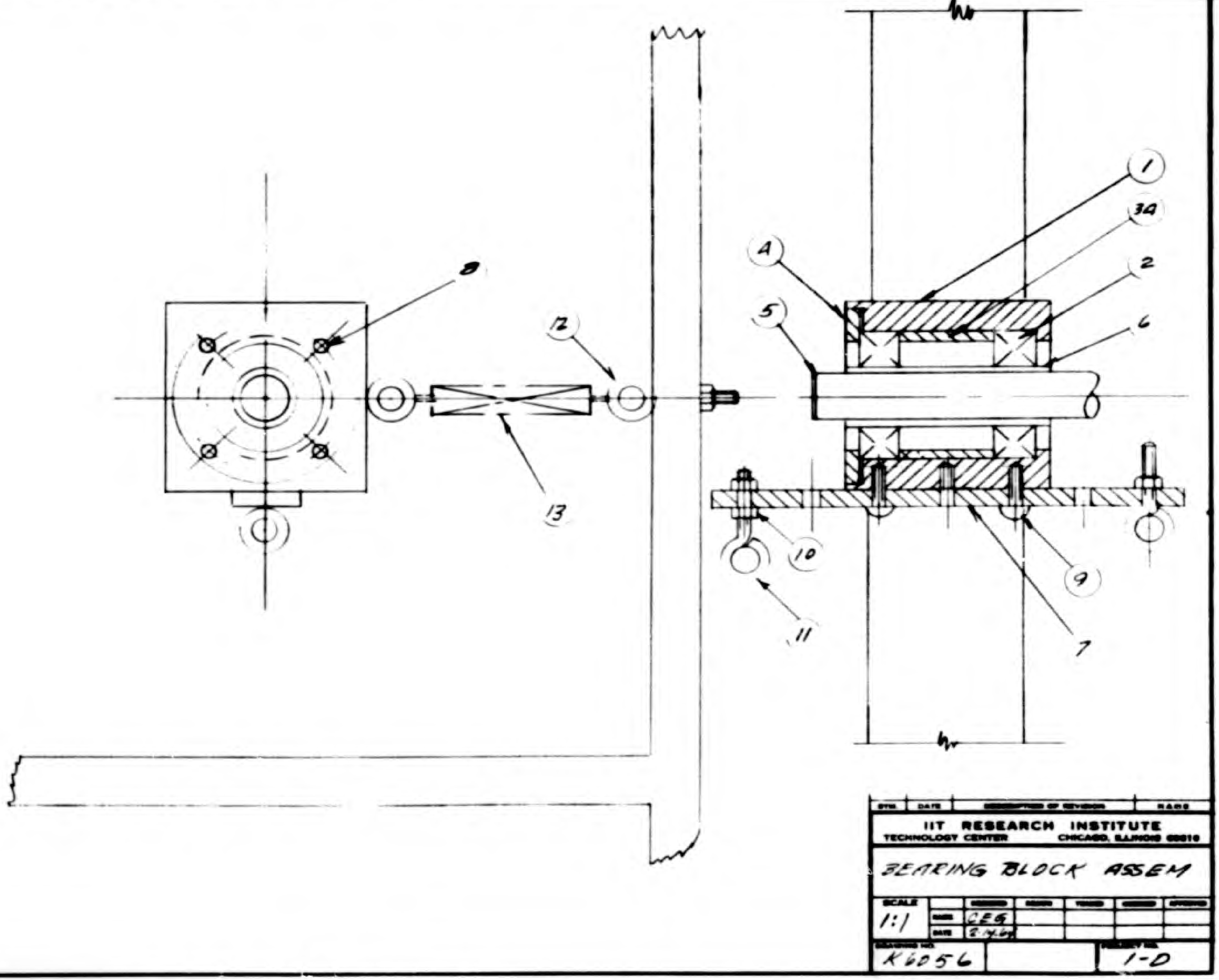

1
3A
A
2
5
6
8
12
13
10
9
11
7
IIT RESEARCH INSTITUTE
TECHNOLOGY CENTER
CHICAGO, ILLINOIS 60616
BEARING BLOCK ASSEM
SCALE
1:1
CEG
DRAWING NO.
K6056
1-D

BILL OF MATERIALS FOR	PROJECT NO.	DRAWING NO.	BY	REVISIONS	SHEET NO
BEARING BLOCK ASSY.	K 6056	1-0	RE DATE 9/18/64		OF

SIZE	DESCRIPTION	DWG NO	NO. REQ.	SPECIFICATIONS	CAT NO OR GRADE	NOTES
C	BEARING BLOCK ASSY	1-0	2			
B	BEARING BLOCK	1-1	2			
	BEARING		4			
A	BEARING SPACER "A"	1-3A	2			
A	BEARING SPACER "B"	1-3B	4			
A	BEARING BLOCK CAP	1-4	2			
B	SHAFT ASSEM	2-0	1			
A	SHAFT SLEEVE	1-6	2			
A	SPRING MOUNT	1-9	16			
	#6-40 SOCKET HD. CAP SCREWS		8			
	#10-24 SOCKET HD. CAP SCREWS		16			
	#10-24 NUT		16			
	EYE BOLT 1" LG.		16			
	EYE BOLT 2" LG.		16			
	SPRING		8			

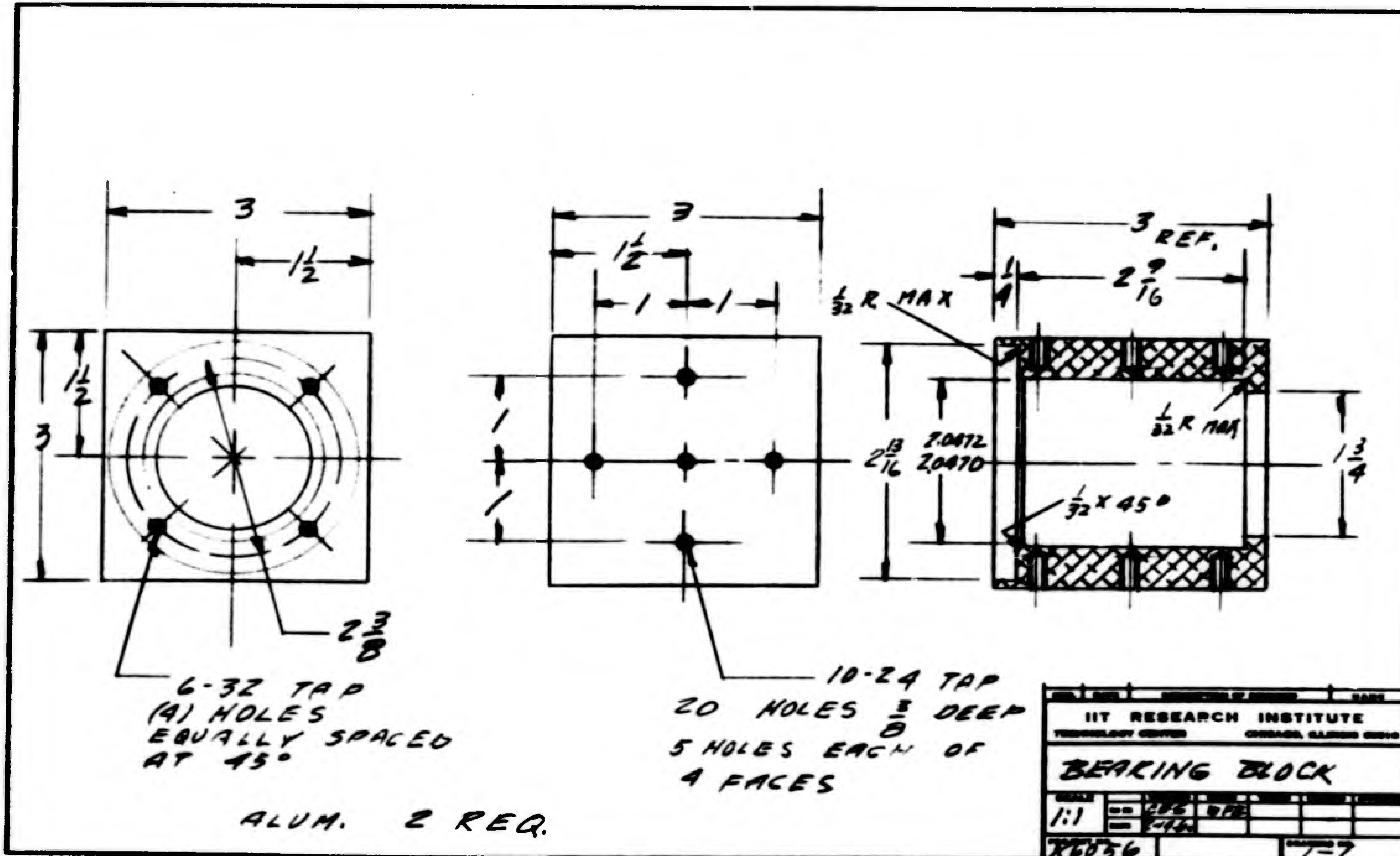

3
1/2
3
1/2
2 3/8
6-32 TAP
(4) HOLES
EQUALLY SPACED
AT 45°
ALUM. 2 REQ.
3
1/2
1
1
1
1
10-24 TAP
20 HOLES 3/8 DEEP
5 HOLES EACH OF
4 FACES
3 REF.
1/4
2 9/16
1/32 R MAX
2 13/16
2.0472
2.0470
1/32 R MAX
1/32 X 45°
1 3/4
IIT RESEARCH INSTITUTE
BEARING BLOCK
1:1
7-7

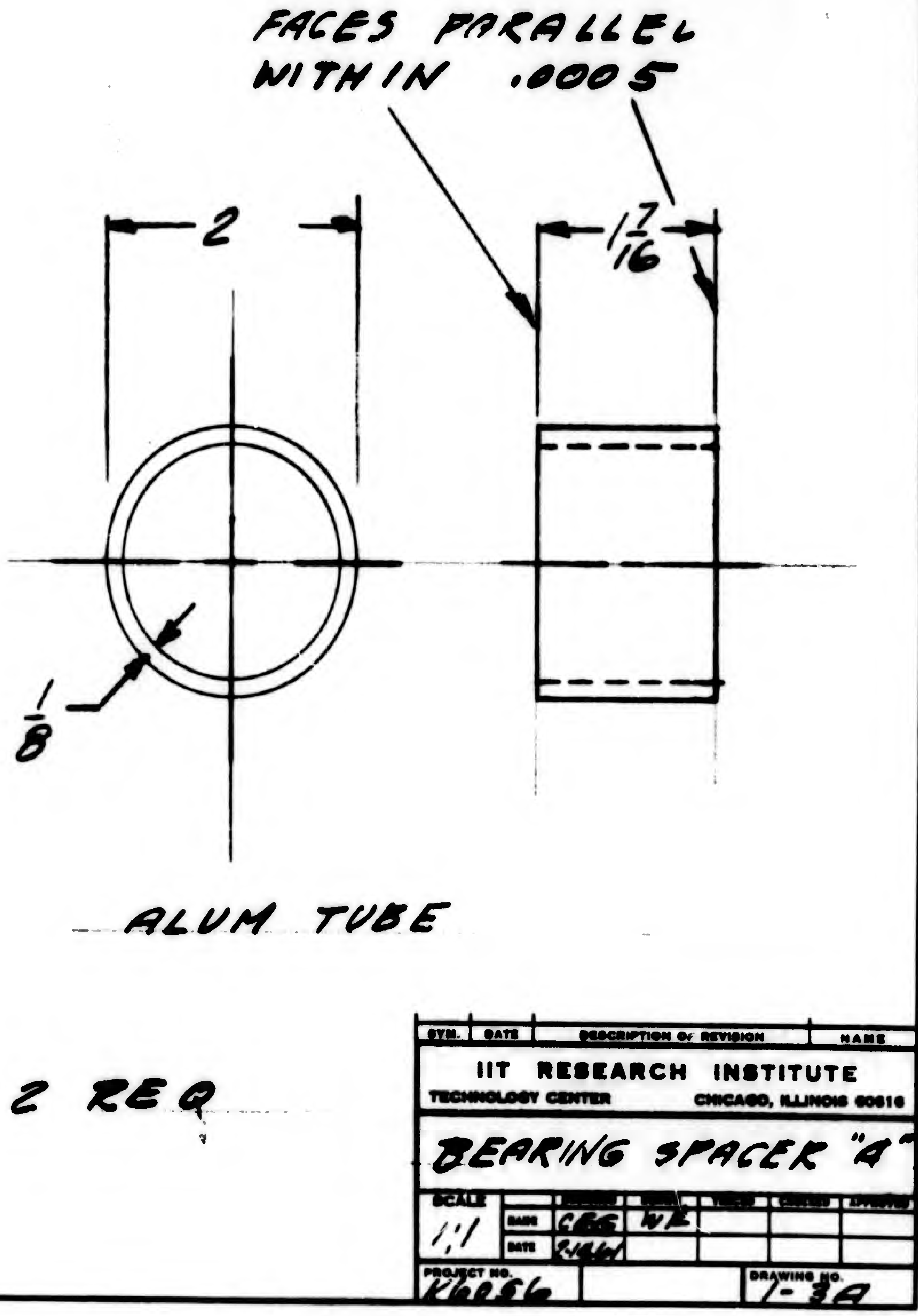
FACES PARALLEL
WITHIN .0005
2
1 7/16
1/8
ALUM TUBE
2 REQ
SYM.
DATE
DESCRIPTION OF REVISION
NAME
IIT RESEARCH INSTITUTE
TECHNOLOGY CENTER
CHICAGO, ILLINOIS 60616
BEARING SPACER "A"
SCALE
1:1
PROJECT NO.
DRAWING NO.
1-3A

FACES PARALLEL
WITHIN .0005

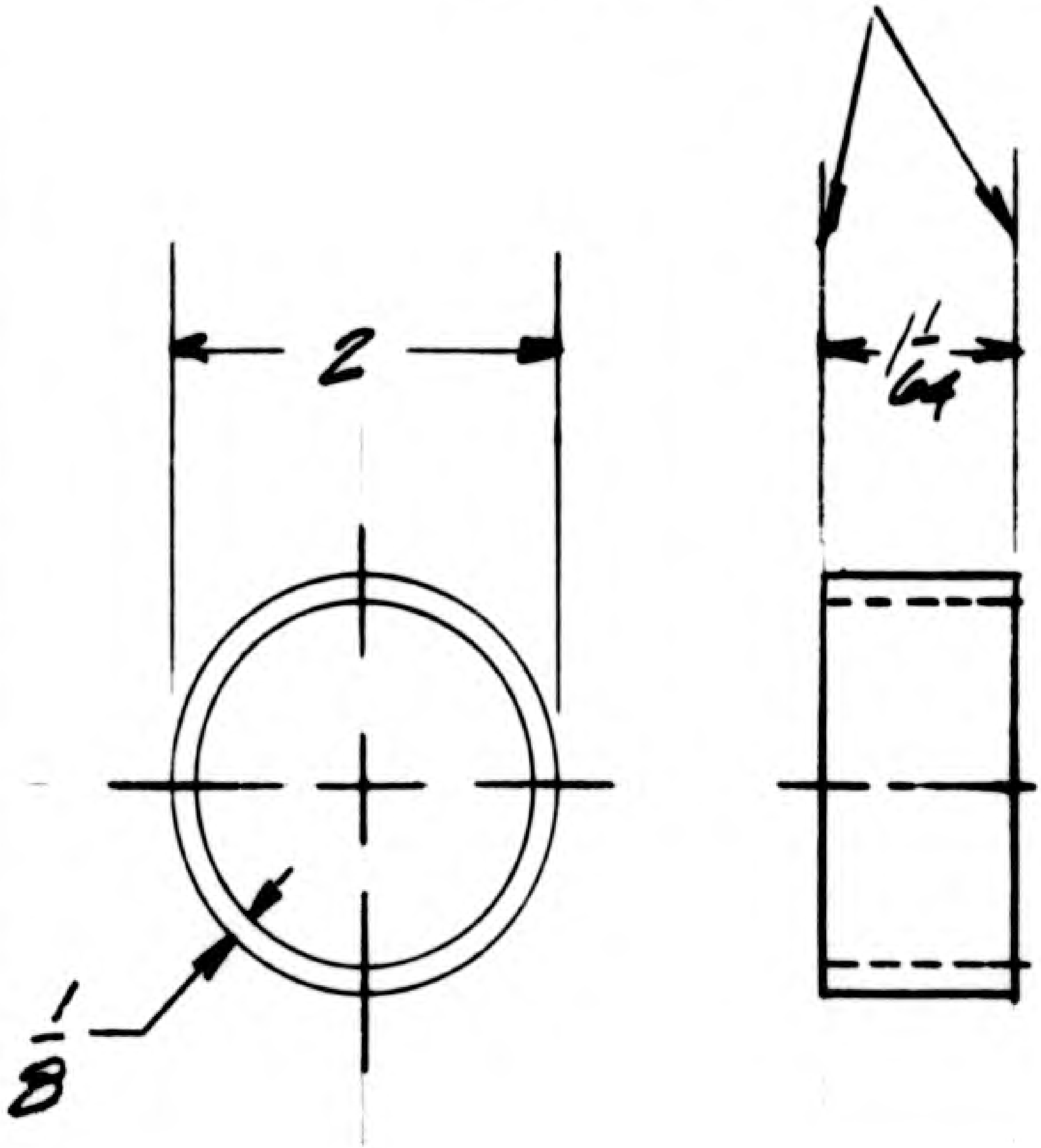

ALUM TUBE

4 REQ

SYM.	DATE	DESCRIPTION OF REVISION	NAME

IIT RESEARCH INSTITUTE
TECHNOLOGY CENTER CHICAGO, ILLINOIS 60616

BEARING SPACER "B"

SCALE		DESIGNED	DRAWN	TRACED	CHECKED	APPROVED
1:1	NAME	CEG	[illegible]			
	DATE	7-19-6[illegible]				

PROJECT NO.		DRAWING NO.
K6056		1-3B

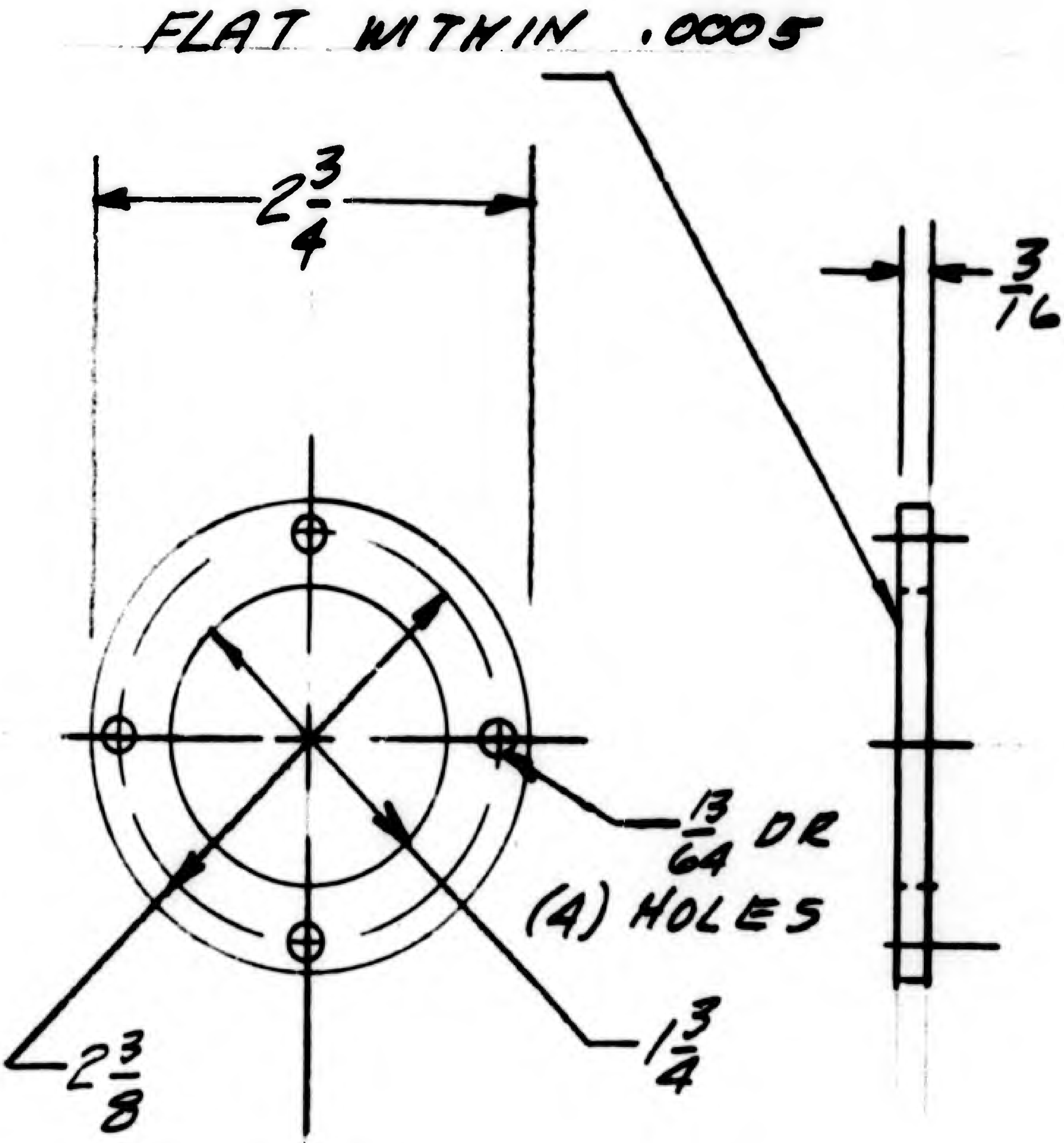

ALUMINUM

2 REQ

SYM.	DATE	DESCRIPTION OF REVISION	NAME

IIT RESEARCH INSTITUTE

TECHNOLOGY CENTER CHICAGO, ILLINOIS 60616

BEARING BLOCK CAP

SCALE						
1:1	NAME	CEG	WR			
	DATE	[illegible]				

PROJECT NO.		DRAWING NO.
K6056		1-4

CLASS 5 FIT WITH BEARING
REF ITEM (2) COMMERCIAL
AFTER ASSEM.

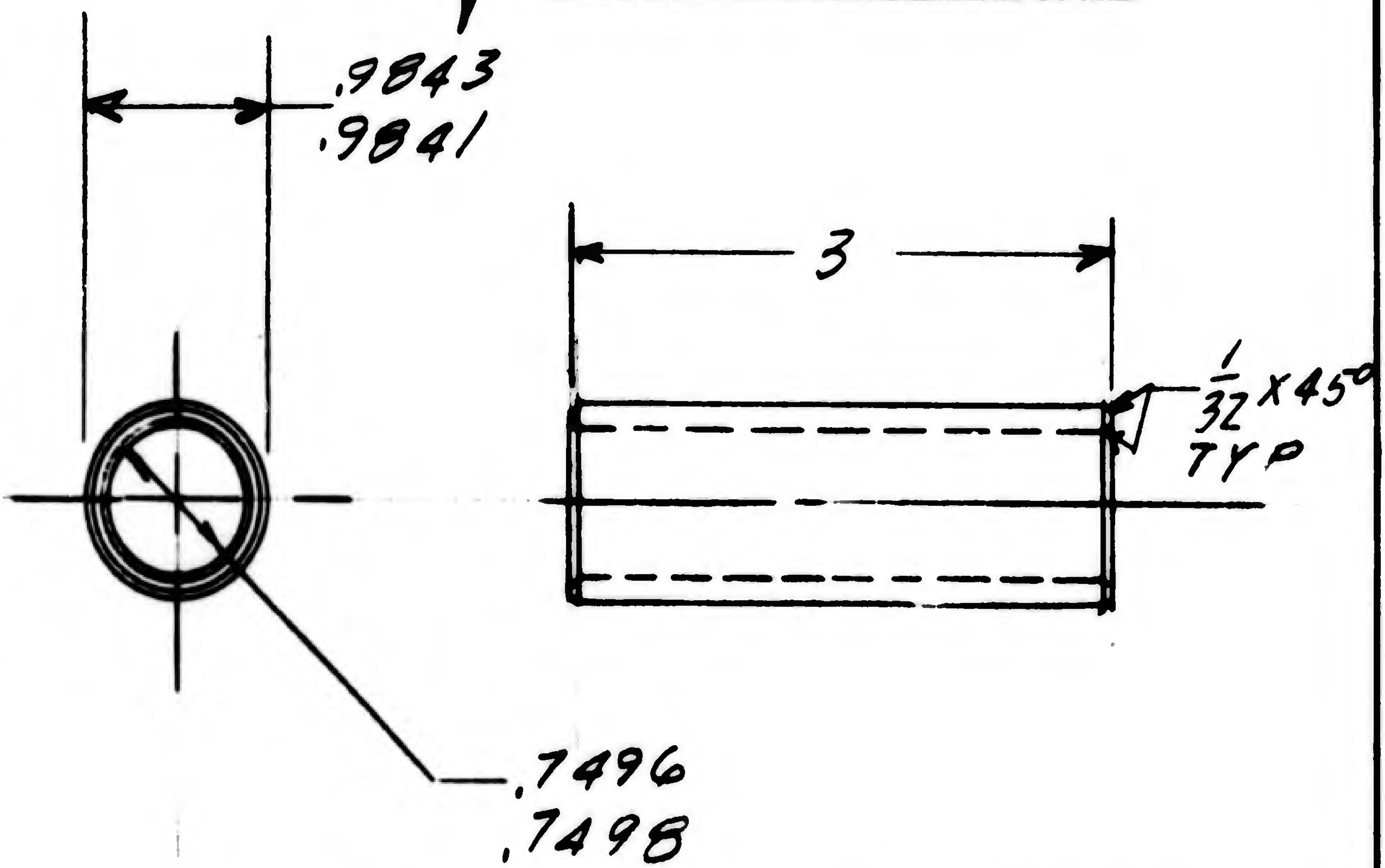

CLASS 6 FIT WITH SHAFT O.D.
REF. DWG. K6056-2-0

NOTE: GRIND O.D.
AFTER ASSEM
WITH SHAFT

2 REQ.

STEEL

SYM.	DATE	DESCRIPTION OF REVISION	NAME

IIT RESEARCH INSTITUTE
TECHNOLOGY CENTER — CHICAGO, ILLINOIS 60616

SHAFT SLEEVE

SCALE		DESIGNED	DRAWN	TRACED	CHECKED	APPROVED
1:1	NAME	CEG	WR			
	DATE	7-14-64				

PROJECT NO. K6056 — DRAWING NO. 1-6

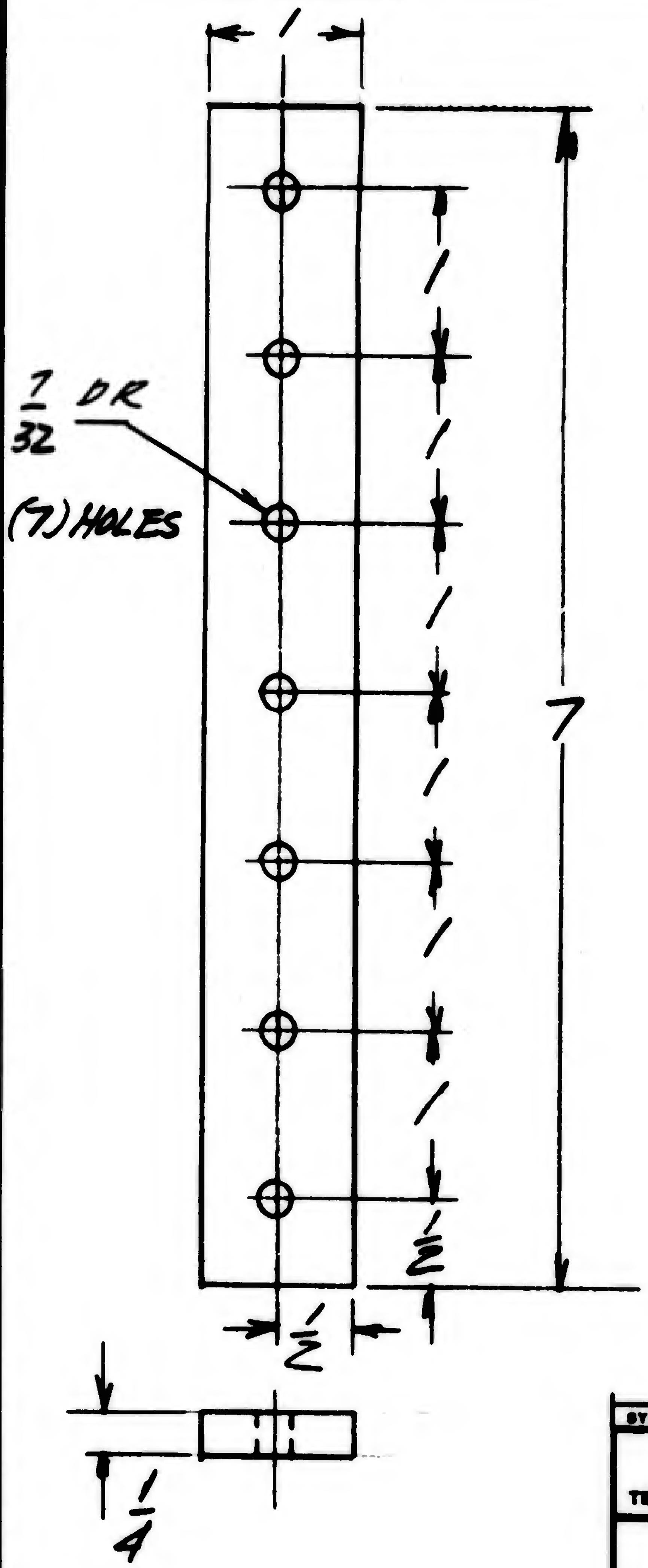

ALUMINUM

16 REQ.

SYM.	DATE	DESCRIPTION OF REVISION	NAME

IIT RESEARCH INSTITUTE

TECHNOLOGY CENTER — CHICAGO, ILLINOIS 60616

SPRING MOUNT

SCALE		DESIGNED	DRAWN	TRACED	CHECKED	APPROVED
1:1	NAME	CEG	WR			
	DATE	[illegible]				

PROJECT NO.		DRAWING NO.
K6056		1-9

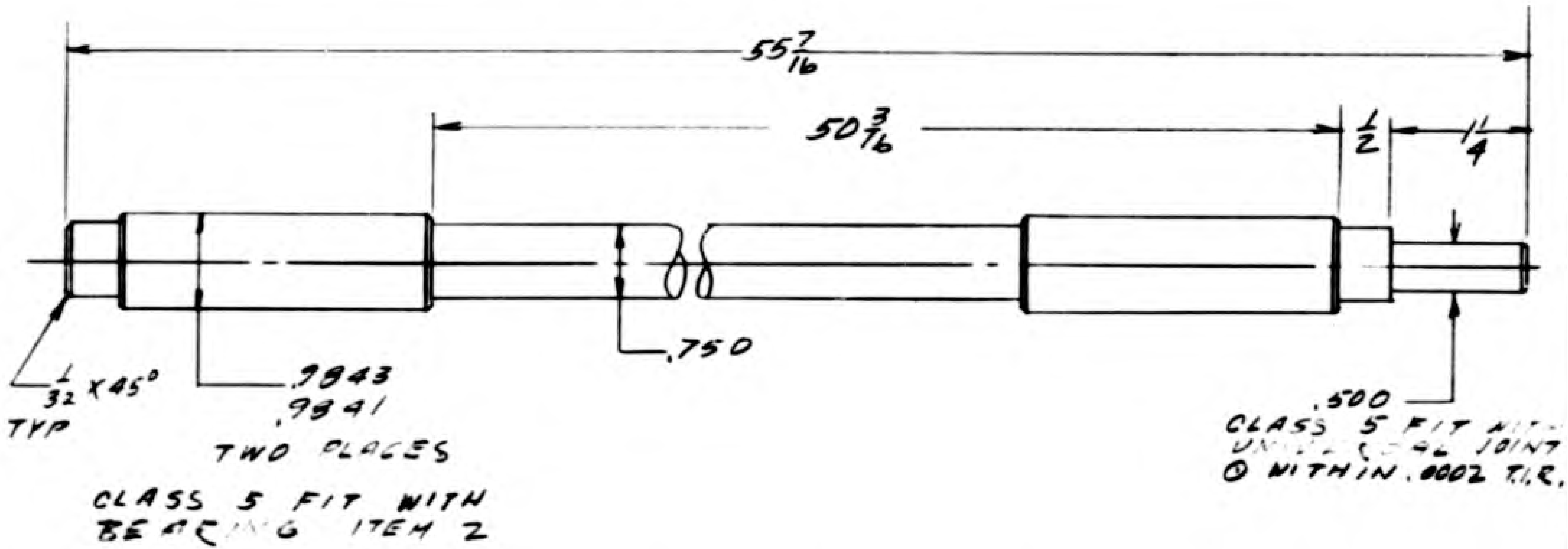

NOTE- SHAFT MUST BE STRAIGHTEN
WITHIN .0002 T.I.R. OVER LENGTH

ONE REQ.

SYM.	DATE	DESCRIPTION OF REVISION	NAME
IIT RESEARCH INSTITUTE TECHNOLOGY CENTER CHICAGO, ILLINOIS 60616			
SHAFT ASSEM			
SCALE 1:1	NAME CEG	DATE 2-14-??	
PROJECT NO. K6056		DRAWING NO. 2-0	

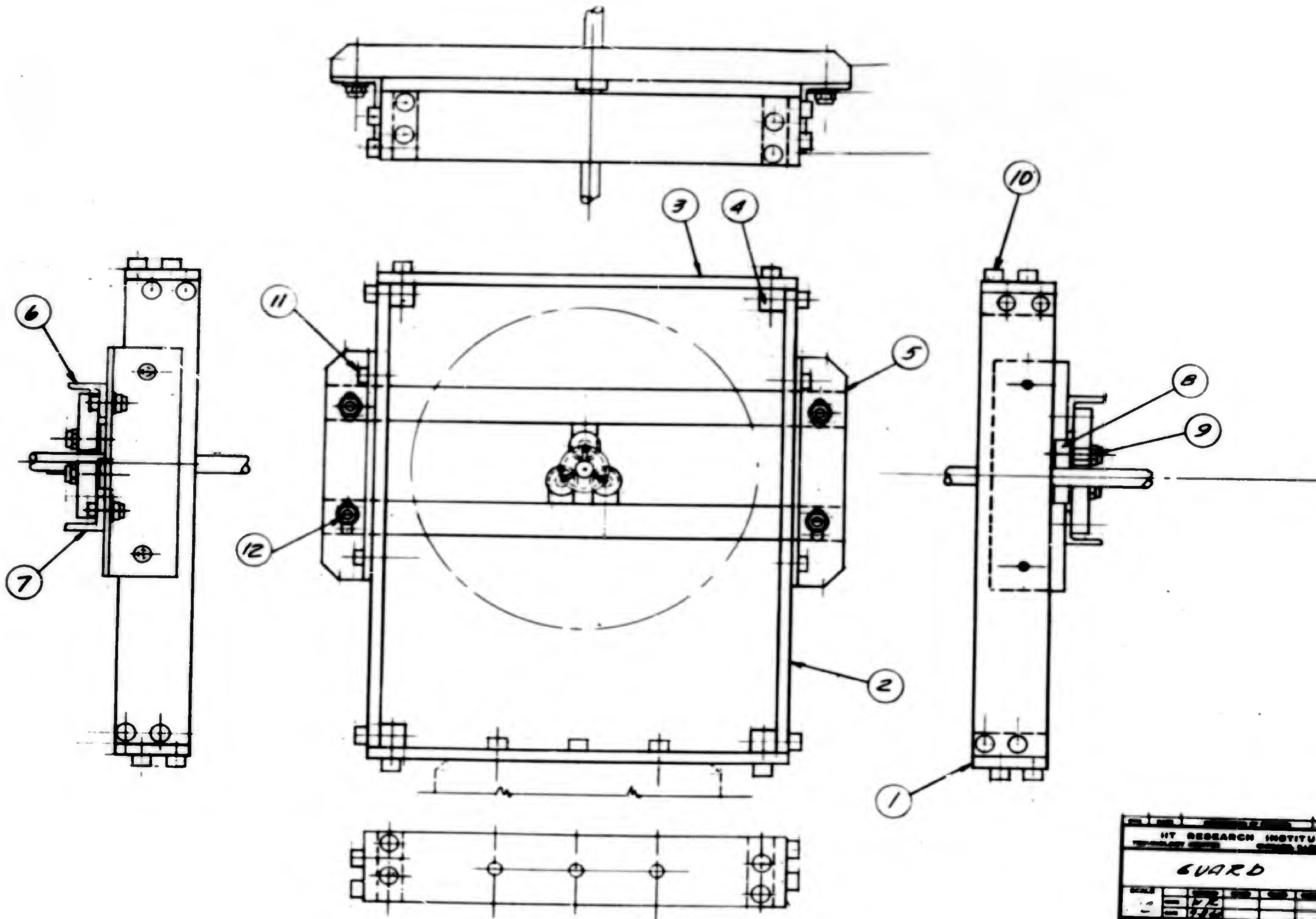

IIT RESEARCH INSTITUTE

GUARD

A 6056

K 7067

ARMOUR RESEARCH FOUNDATION CHICAGO ILLINOIS

BILL OF MATERIALS FOR	PROJECT NO	DRAWING NO	BY	REVISIONS	SHEET NO
GUARD	K6056	K7067	WK DATE 9-8-64		OF

SIZE	DESCRIPTION	DWG NO	NO REQ	SPECIFICATIONS	CAT NO OR GRADE	NOTES
D	GUARD	K7067				
B	BAR	-1	1			
B	BAR	-2	2			
B	BAR	-3	1			
B	BLOCK	-4	4			
B	ANGLE	-5	2			
B	ANGLE	-6	1			
B	ANGLE	-7	1			
A	ROLLER	-8	3			
A	NUT	-9	3			
A	SCR	-10	19			
A	SCR	-11	4			
A	SCR	-12	4			

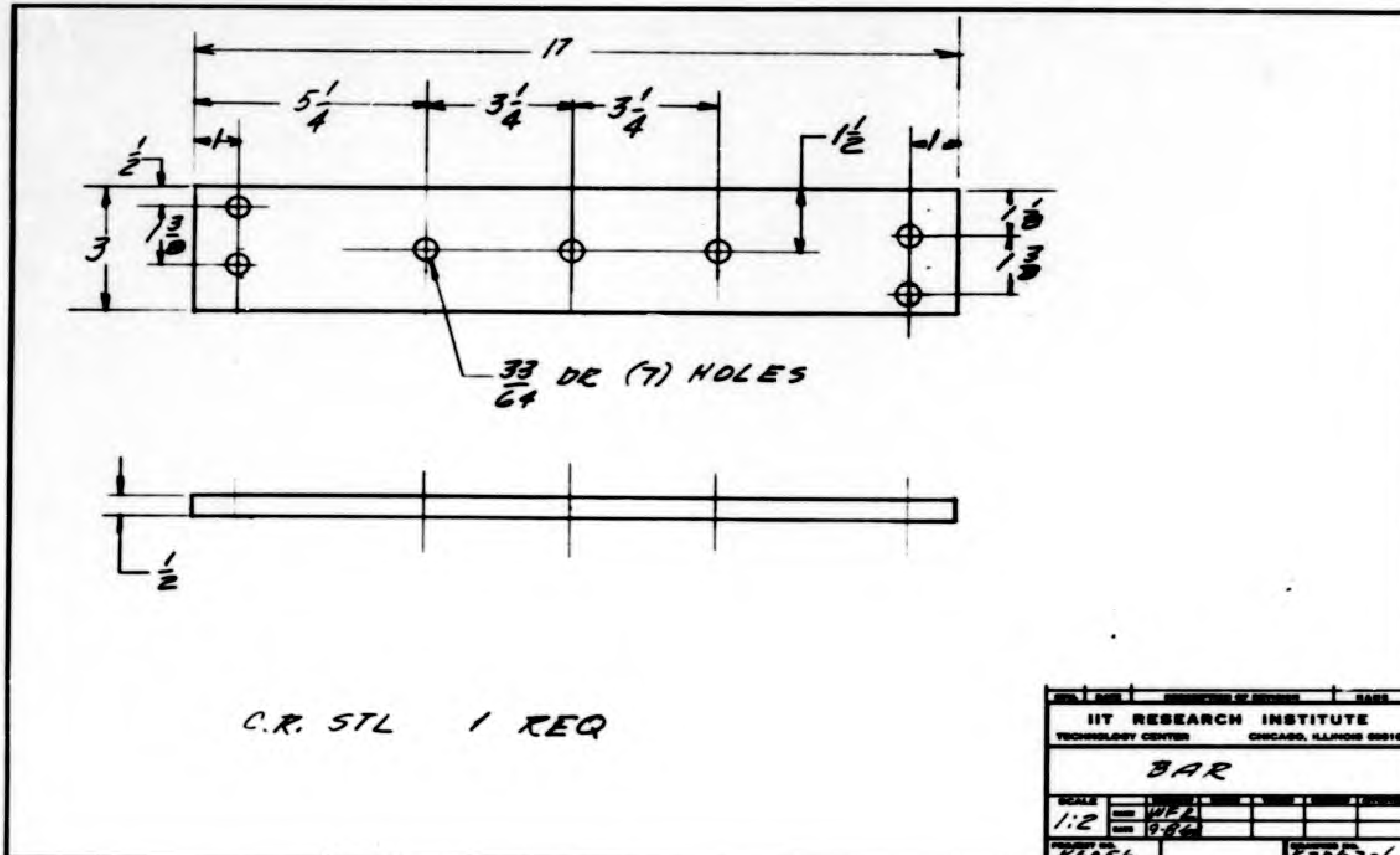

17
5 1/4
3 1/4
3 1/4
1
1 1/2
1
1/2
3
1 3/8
1 1/8
1 3/8
33/64 DR (7) HOLES
1/2
C.R. STL 1 REQ
IIT RESEARCH INSTITUTE
TECHNOLOGY CENTER
CHICAGO, ILLINOIS
BAR
SCALE
1:2
WFZ
9-86
K6056
K7067-1

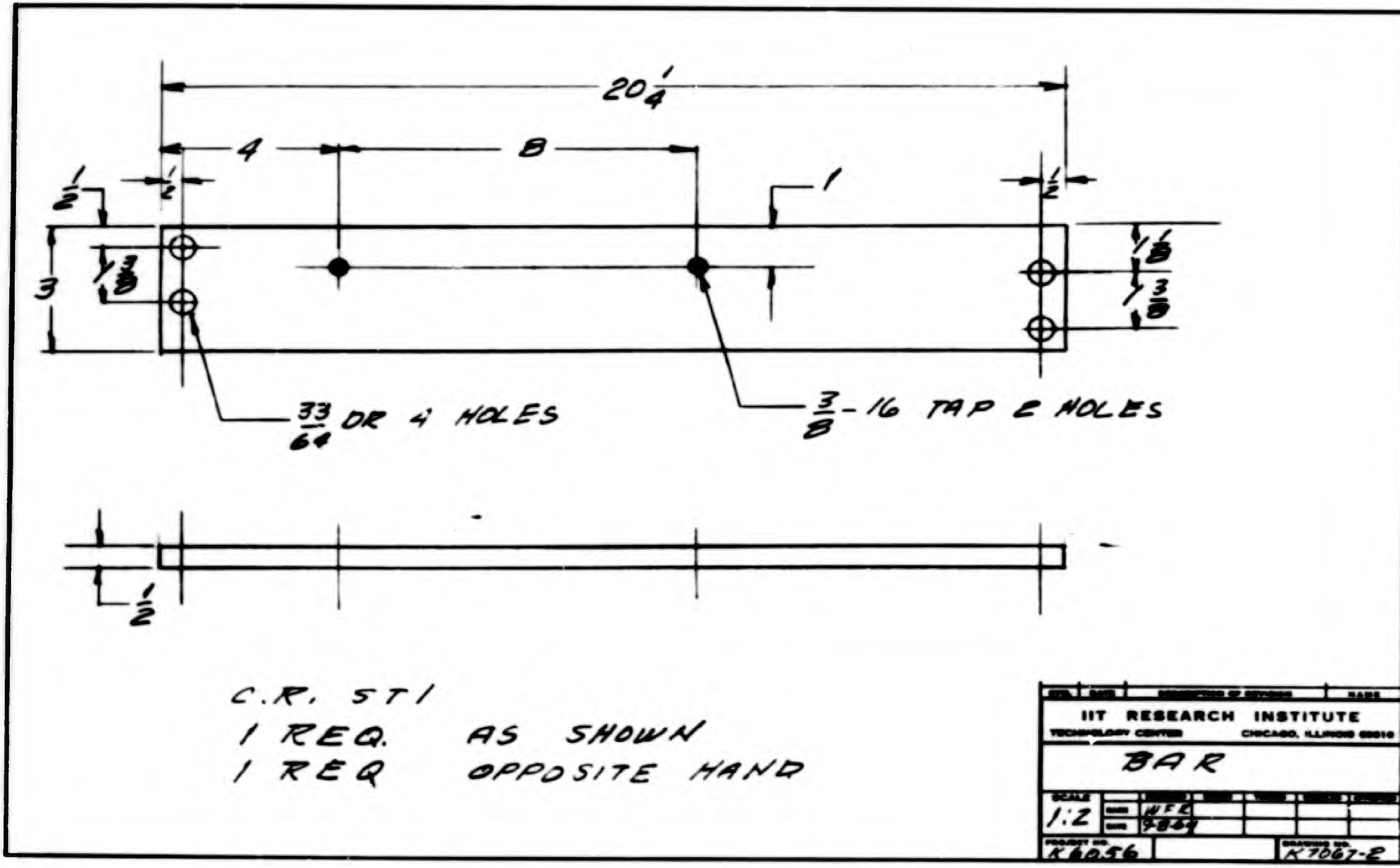
20 1/4
4
8
1/2
1/2
1
1/2
3
1 3/8
1 1/8
1 3/8
33/64 DR 4 HOLES
3/8-16 TAP 2 HOLES
1/2
C.R. STl
1 REQ. AS SHOWN
1 REQ OPPOSITE HAND
IIT RESEARCH INSTITUTE
TECHNOLOGY CENTER
CHICAGO, ILLINOIS 60616
BAR
SCALE
1:2
WFE
7864
PROJECT NO.
K6056
DRAWING NO.
K7067-2

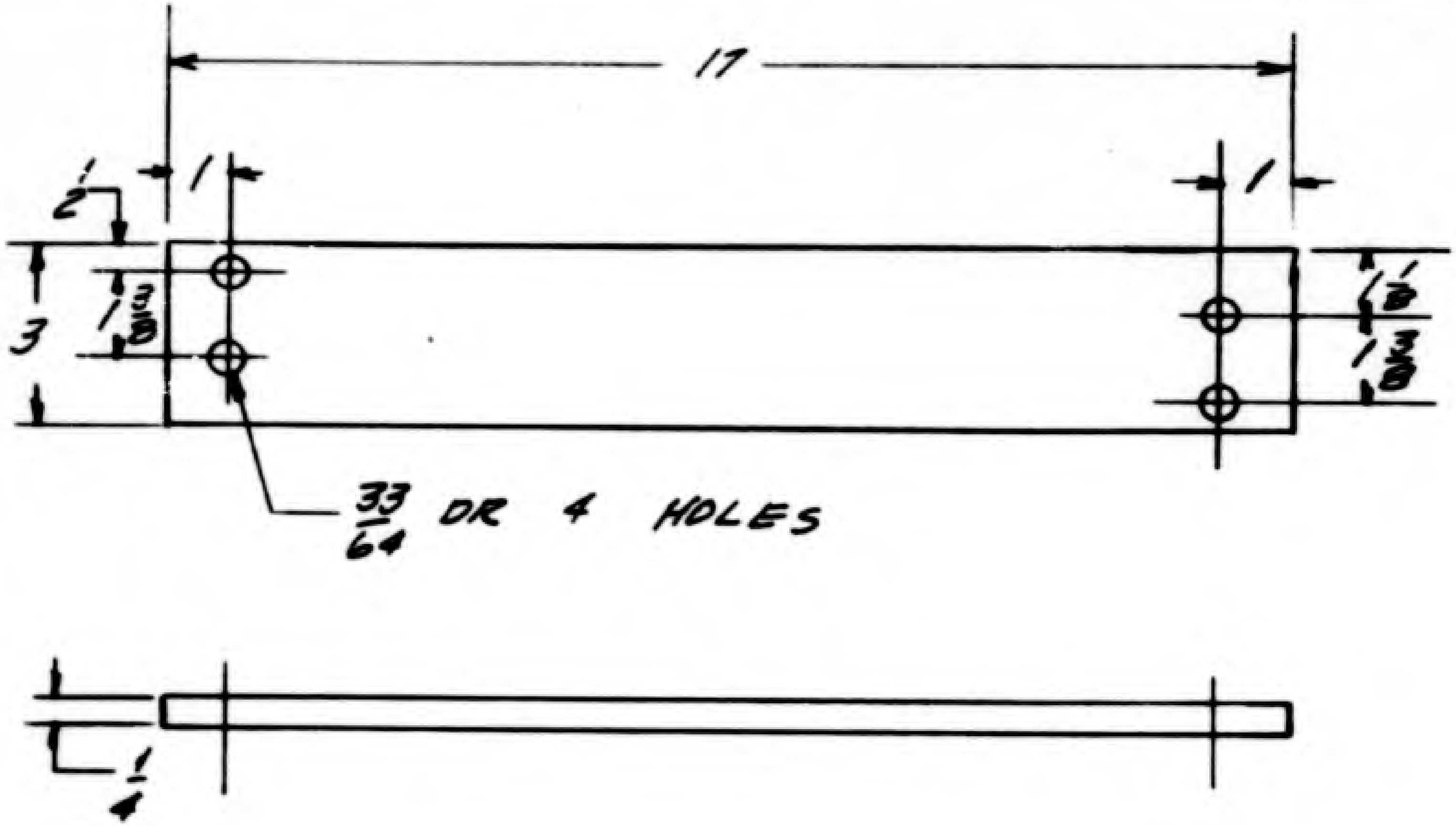

C.R. STL. 1 REQ

IIT RESEARCH INSTITUTE

BAR

SCALE 1:2

K6056

K7267-3

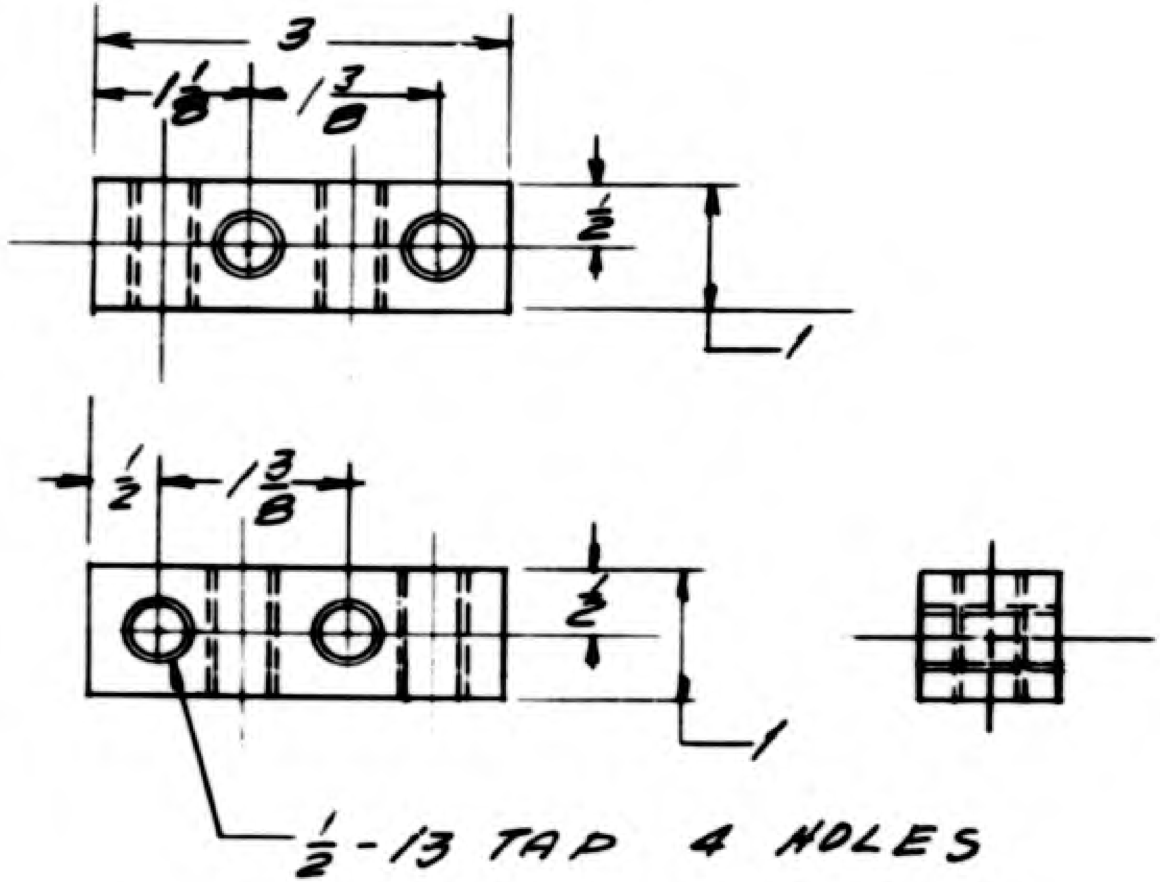

C.R. STL
4 REQ

IIT RESEARCH INSTITUTE
TECHNOLOGY CENTER CHICAGO, ILLINOIS 60616

BLOCK

SCALE	1:1
	WFR
	3-64
PROJECT NO.	K6066
DRAWING NO.	K7067-4

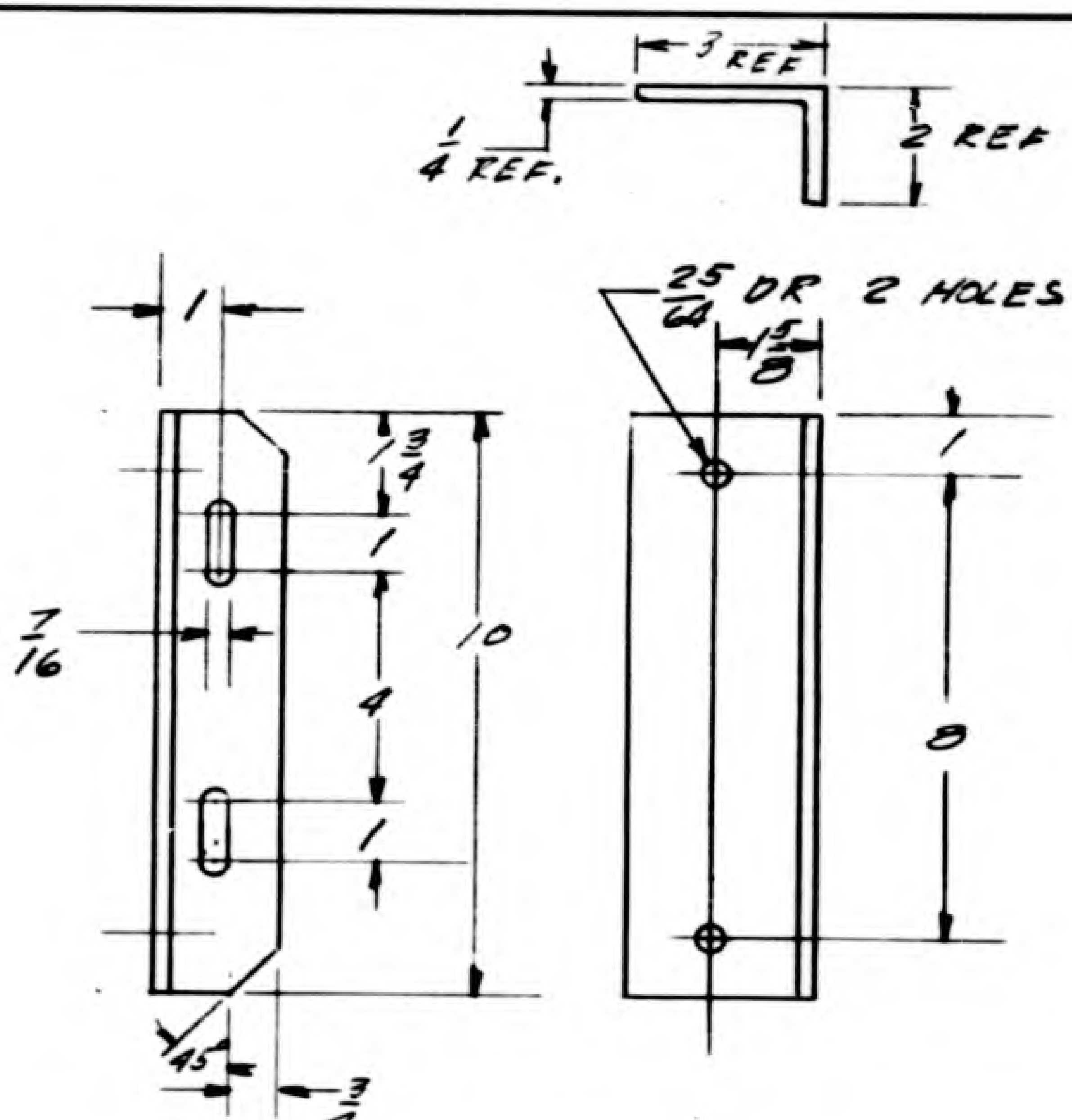

3X2X1/4 ANGLE
1 REQ. AS SHOWN
1 REQ. OPP. HAND

IIT RESEARCH INSTITUTE
TECHNOLOGY CENTER CHICAGO, ILLINOIS 60616

ANGLE

SCALE 1:2
WRK
3-26-64
K-6056
K7067-5

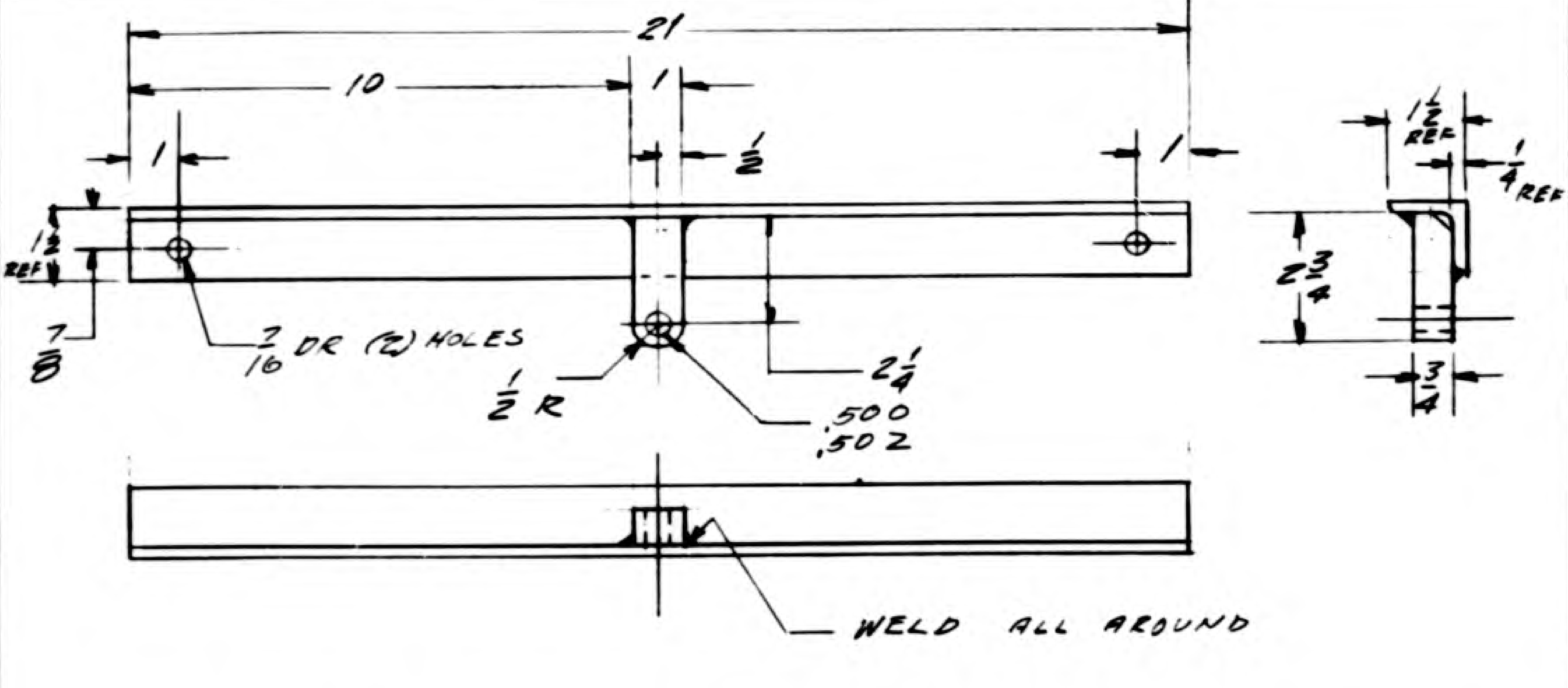

1 1/2 X 1 1/2 X 1/4 ANGLE   3/4 X 1 X 2 3/4 STL

1 REQ

IIT RESEARCH INSTITUTE

TECHNOLOGY CENTER   CHICAGO, ILLINOIS 60616

ANGLE

SCALE 1:2	WEP	
PROJECT NO. K6056		DRAWING NO. K7062-6

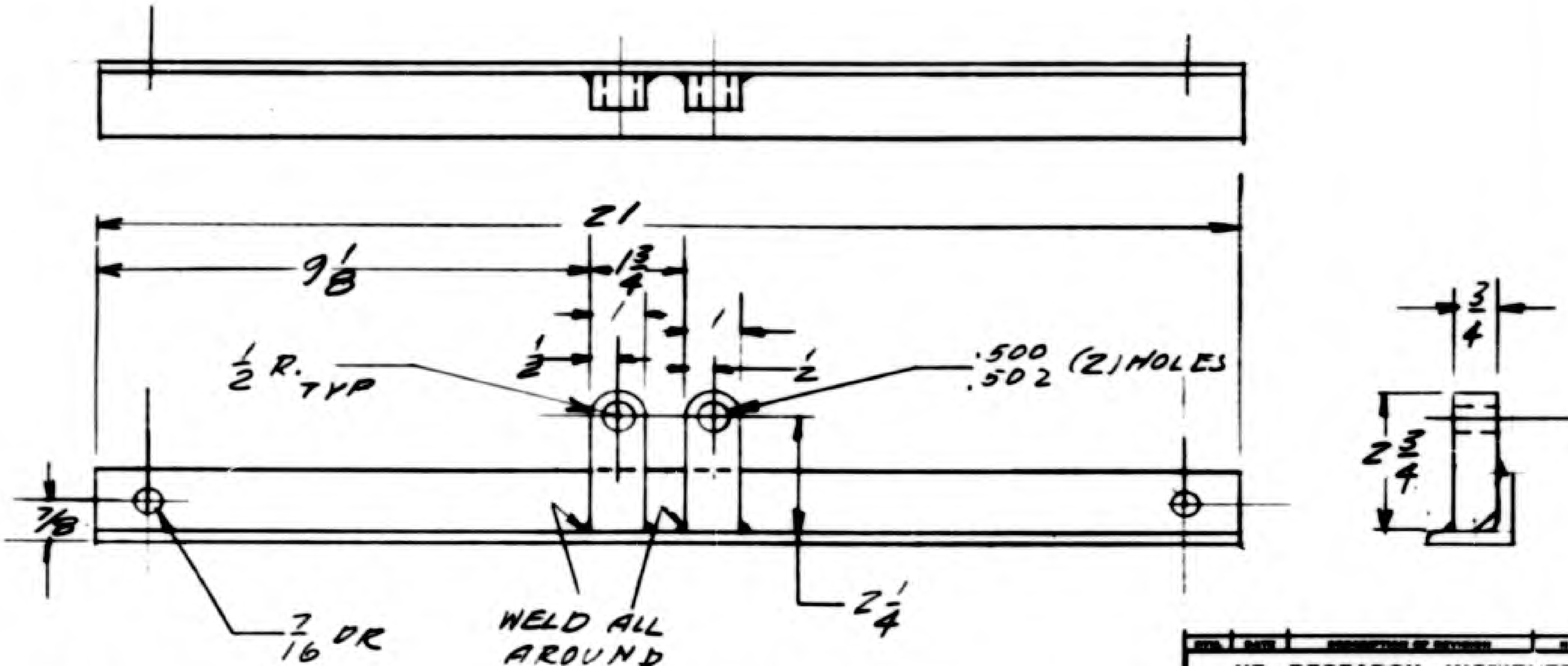

2

$1\frac{1}{4} \times 1\frac{1}{4} \times \frac{1}{4}$ ANGLE $\frac{3}{4} \times 1 \times 2\frac{3}{4}$ (2) PIECES

1 ASSEM REQ

IIT RESEARCH INSTITUTE
TECHNOLOGY CENTER   CHICAGO, ILLINOIS 60616

ANGLE

SCALE 1:2

CAM ROLLER

TORRINGTON # CR-20

1.250 Ø X $\frac{3}{4}$ ROLLER

$\frac{1}{2}$ Ø X $1\frac{1}{4}$ STUD

3 REQ

SYM.	DATE	DESCRIPTION OF REVISION	NAME

IIT RESEARCH INSTITUTE

TECHNOLOGY CENTER CHICAGO, ILLINOIS 60616

ROLLER

SCALE		DESIGNED	DRAWN	TRACED	CHECKED	APPROVED
	NAME	WR				
	DATE	9-8-64				

PROJECT NO. K6056

DRAWING NO. K7067-8

HEX STL NUT

$\frac{1}{2}$ - 20 N.F.

3 REQ

SYM.	DATE	DESCRIPTION OF REVISION	NAME

IIT RESEARCH INSTITUTE

TECHNOLOGY CENTER CHICAGO, ILLINOIS 60616

NUT

SCALE		DESIGNED	DRAWN	TRACED	CHECKED	APPROVED
	NAME					
	DATE					

PROJECT NO. K6056

DRAWING NO. K7067-9

SOC. HD CAP SCR

$\frac{1}{2}$ - 13 X 1$\frac{1}{2}$ LG

19 REQ

SYM.	DATE	DESCRIPTION OF REVISION	NAME

IIT RESEARCH INSTITUTE

TECHNOLOGY CENTER CHICAGO, ILLINOIS 60616

SCR

SCALE		DESIGNED	DRAWN	TRACED	CHECKED	APPROVED
	NAME					
	DATE					

PROJECT NO. K6056

DRAWING NO. K7067-10

SOC HD. CAP SCR

$\frac{3}{8}$ -16 X $\frac{3}{4}$

4 REQ

SYM.	DATE	DESCRIPTION OF REVISION	NAME

IIT RESEARCH INSTITUTE

TECHNOLOGY CENTER CHICAGO, ILLINOIS 60616

SCR

SCALE		[illegible]	[illegible]	[illegible]	[illegible]	[illegible]
	NAME					
	DATE					

PROJECT NO. K6056

DRAWING NO. K7067-11

SOC. HD. CAP SCR

WITH HEX NUTS

AND WASHERS

$\frac{3}{8}$-16 X $1\frac{1}{2}$

4 REQ

SYM.	DATE	DESCRIPTION OF REVISION	NAME

IIT RESEARCH INSTITUTE
TECHNOLOGY CENTER CHICAGO, ILLINOIS 60616

SCR

SCALE		DESIGNED	DRAWN	TRACED	CHECKED	APPROVED
	NAME					
	DATE					

PROJECT NO. K6056

DRAWING NO. K7067-17

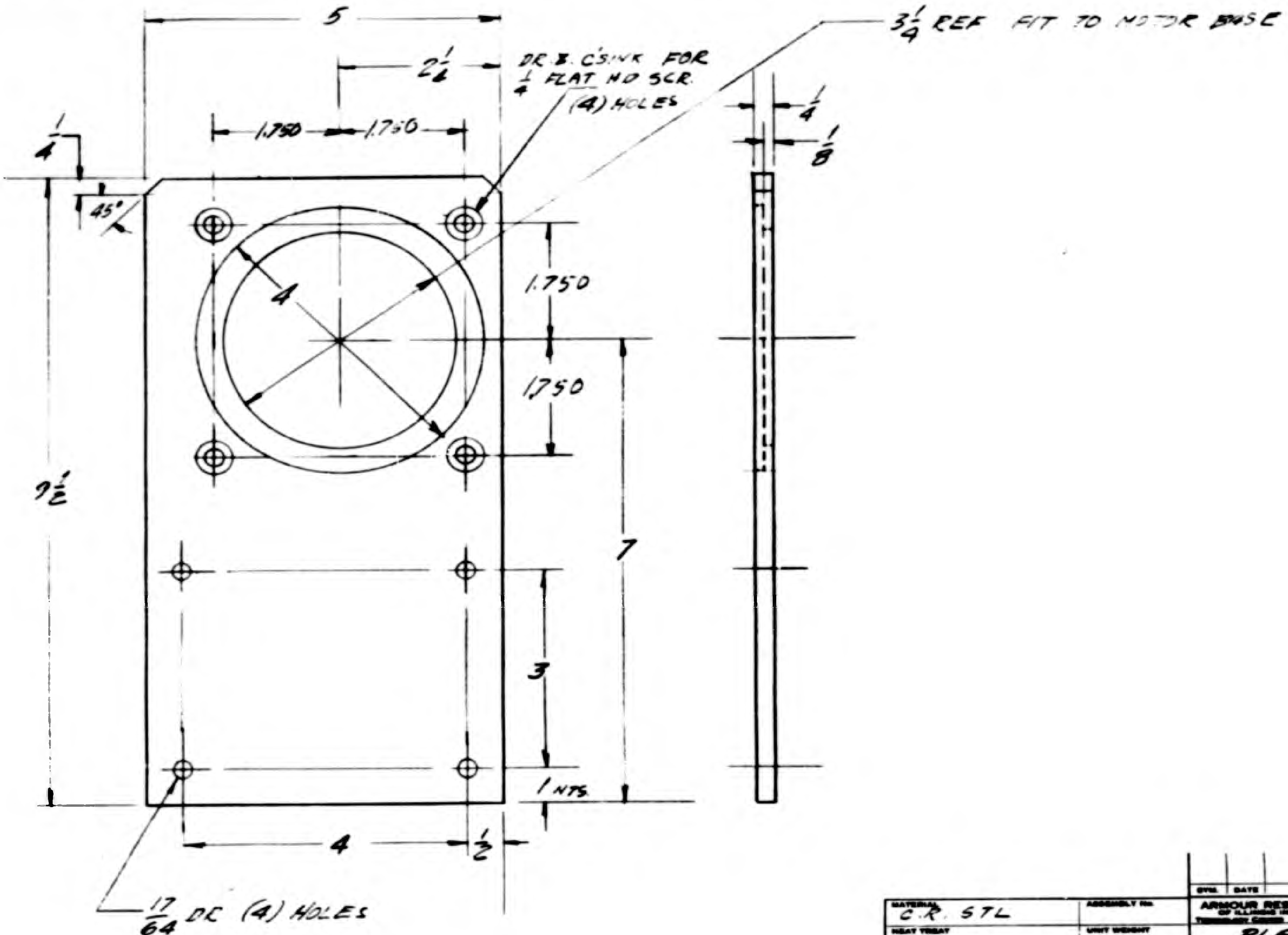

MATERIAL C.R. STL	ASSEMBLY No.	ARMOUR RESEARCH FOUNDATION OF ILLINOIS INSTITUTE OF TECHNOLOGY	
HEAT TREAT	UNIT WEIGHT	PLATE	
TOLERANCES UNLESS OTHERWISE SPECIFIED		NAME W.F.R.	
FRACTIONS ± 1/64	DECIMALS ± .005	DATE 4-22-64	
ANGULAR ± 1°		PROJECT No. K6056	DRAWING No. SKETCH 100
SCALE 1:1			

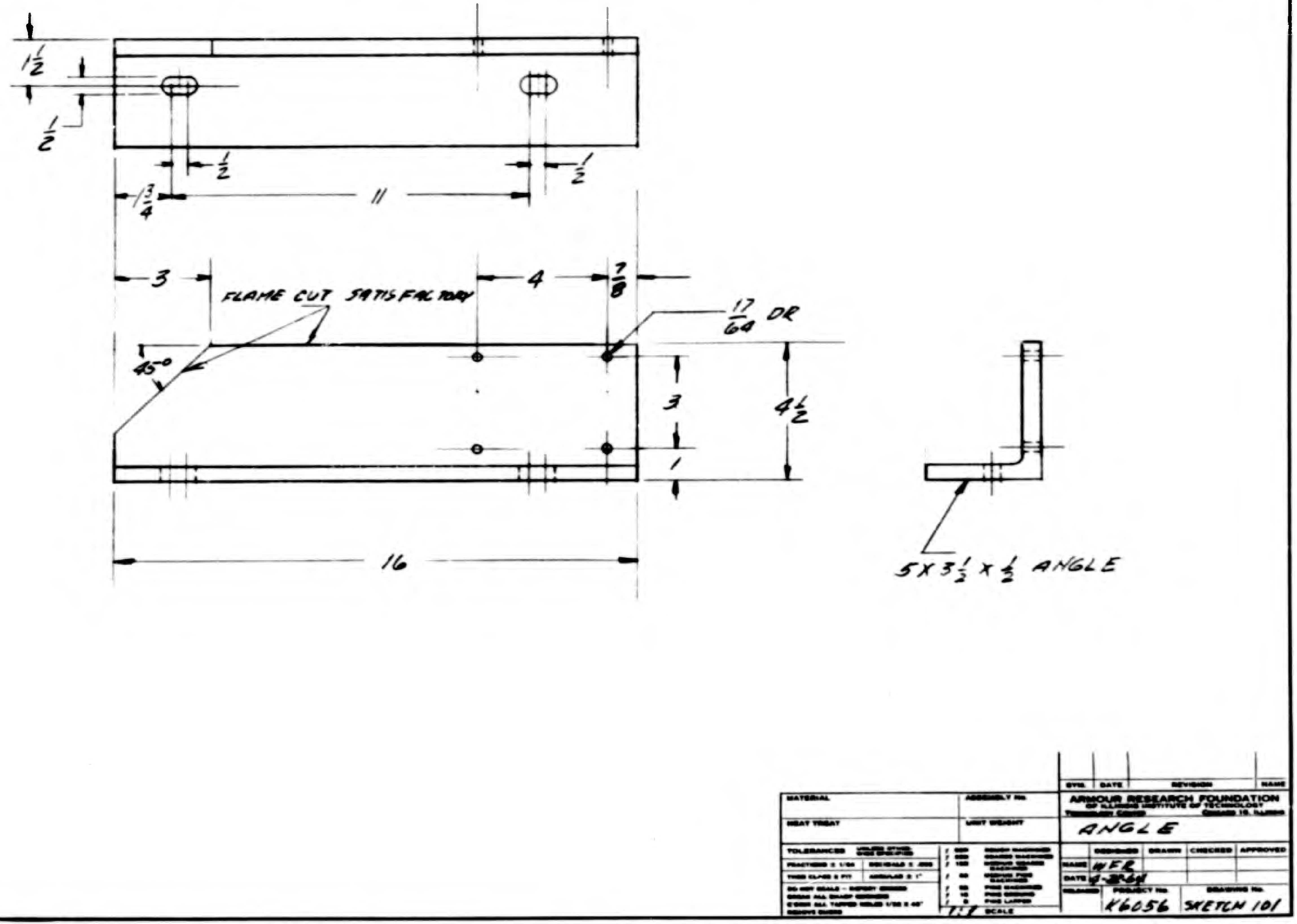
1 1/2
1/2
1/2
1/2
1 3/4
11
3
4
7/8
FLAME CUT SATISFACTORY
17/64 DR
45°
3
4 1/2
1
16
5 X 3 1/2 X 1/2 ANGLE
MATERIAL
HEAT TREAT
TOLERANCES
ASSEMBLY No.
UNIT WEIGHT
SYM. DATE REVISION NAME
ARMOUR RESEARCH FOUNDATION
OF ILLINOIS INSTITUTE OF TECHNOLOGY
ANGLE
DESIGNED DRAWN CHECKED APPROVED
NAME WFR
DATE
PROJECT No. K6056
DRAWING No. SKETCH 101
1:1 SCALE

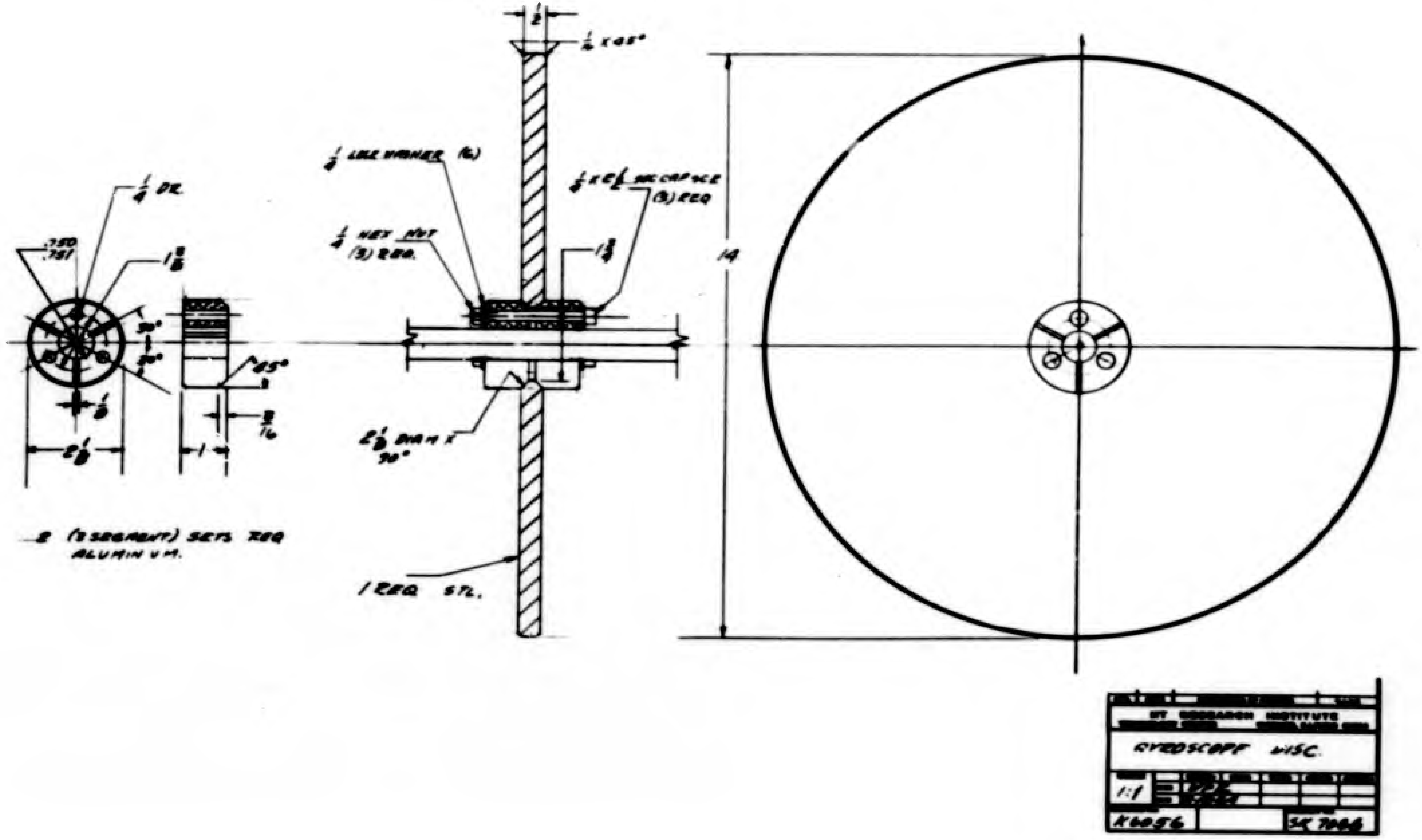

1/4 DR.
.750
.751
1 3/8
30°
30°
1/8
2 1/8
1
45°
3/16
2 (3 SEGMENT) SETS REQ
ALUMINUM.
1/2
1/4 x 45°
1/4 LOCK WASHER (6)
1/4 HEX NUT
(3) REQ.
1/4 x 2 1/4 SOC CAP SCR
(3) REQ
1 3/4
2 1/8 DIAM x 90°
1 REQ STL.
14
MT. WOODARD INSTITUTE
GYROSCOPE DISC.
1:1
K6056
SK 7066

APPENDIX D

DESCRIPTION OF COMPUTER PROGRAM FOR ANALYSIS OF COMPLEX SHAFTING SYSTEMS

APPENDIX D

DESCRIPTION OF COMPUTER PROGRAM FOR ANALYSIS OF COMPLEX SHAFTING SYSTEMS

GENERAL DESCRIPTION

This program computes natural frequencies, normal mode shapes and forced vibration data for lateral vibration of a hollow stepped shaft supported on bearings having both torsional and linear stiffness. The shaft may carry lumped masses and/or lumped inertias. A typical shaft is shown in figure D-1.

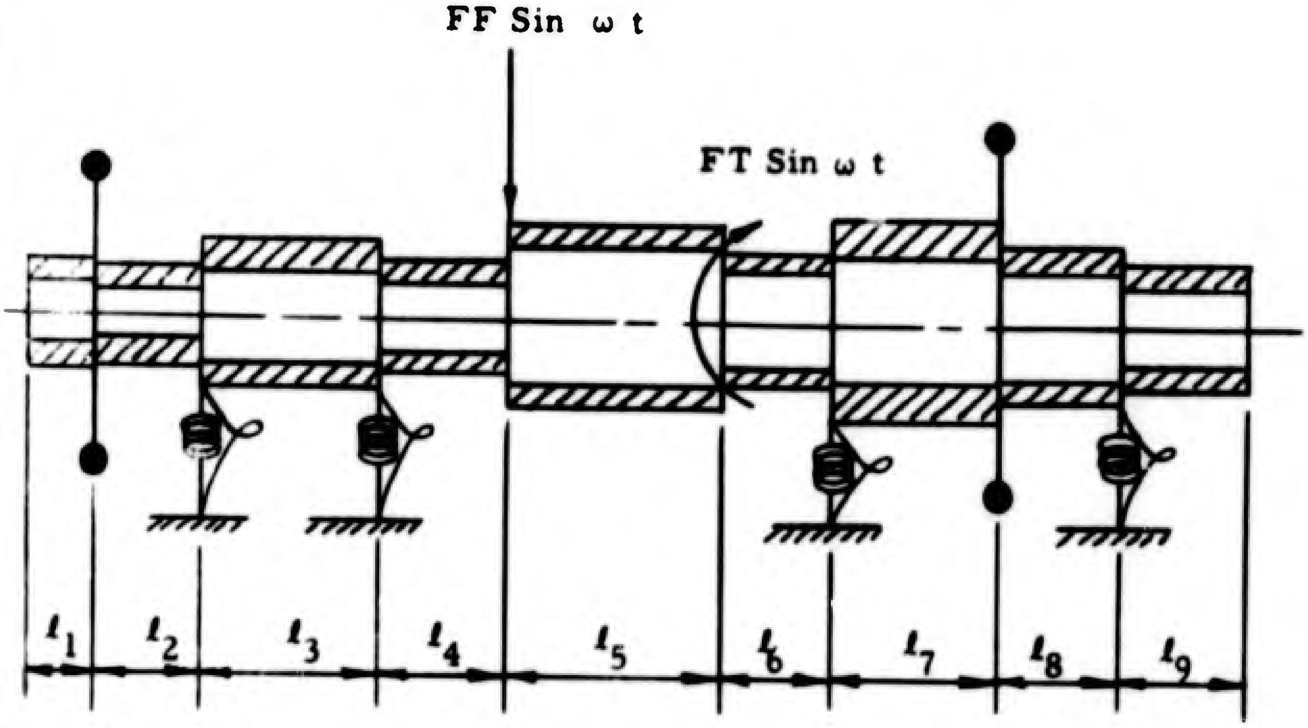

Figure D-1 TYPICAL SHAFT

The shaft is broken into sections by placing a cut at each change in cross section, each linear or torsional spring, each lumped mass or lumped inertia and each force or moment input. The sections are then numbered consecutively from 1 to NS. The following input-output options are available.

	Input	Output
(1)	Description of shaft	Natural frequencies
(2)	Description of shaft	Natural frequencies Normal mode shapes
(3)	Description of shaft Description of forcing function	Natural frequencies Forced vibration data
(4)	Description of shaft Description of forcing function	Natural frequencies Normal mode shapes Forced vibration data
(5)	Description shaft Description of forcing function Natural frequencies Normal mode shapes	Forced vibration

The equations necessary for the computational scheme to be used were developed in the Supplement to Report #1 for IITRI Research Project K6056. They are reproduced here with some changes in nomenclature.

$$P^4(i) = \lambda^2_n A(i) \gamma(i) / \left[E(i) I(i) g\right]$$

$$C_1(i) = \left\{SO(i) / P(i) + VO(i) / \left[E(i) I(i) P^3(i)\right]\right\} /2$$

$$C_2(i) = \left\{YO(i) + TO(i) / \left[E(i) I(i) P^2(i)\right]\right\} /2$$

$$C_3(i) = \left\{SO(i) / P(i) - VO(i) / \left[E(i) I(i) P^3(i)\right]\right\} /2$$

$$C_4(i) = \left\{YO(i) - TO(i) / \left[E(i) I(i) P^2(i)\right]\right\} /2$$

$$YL(i) = C_1(i) \sin\left[P(i) L(i)\right] + C_2(i) \cos\left[P(i) L(i)\right] + C_3(i) \sinh\left[P(i) L(i)\right] + C_4(i) \cosh\left[P(i) L(i)\right]$$

$$SL(i) = P(i) \Big\{ C_1(i) \cos\left[P(i)\, L(i)\right] - C_2(i) \sin\left|P(i)\, L(i)\right| + C_3(i) \cosh\left[P(i)\, L(i)\right] + C_4(i) \sinh\left[P(i)\, L(i)\right] \Big\}$$

$$TL(i) = \left[E(i)\, I(i)\, P^2(i)\right] \Big\{ C_1(i) \sin\left[P(i)\, L(i)\right] + C_2(i) \cos\left[P(i)\, L(i)\right] - C_3(i) \sinh\left[P(i)\, L(i)\right] - C_4(i) \cosh\left[P(i)\, L(i)\right] \Big\}$$

$$VL(i) = \left[E(i)\, I(i)\, P^3(i)\right] \Big\{ C_1(i) \cos\left[P(i)\, L(i)\right] - C_2(i) \sin\left[P(i)\, L(i)\right] - C_3(i) \cosh\left[P(i)\, L(i)\right] - C_4 \sinh\left[P(i)\, L(i)\right] \Big\}$$

$$YO(i+1) = YL(i)$$

$$SO(i+1) = SL(i)$$

$$TO(i+1) = TL(i) - \phi(i)\, SL(i) + J(i)\, \lambda_n^2\, SL(i)$$

$$VO(i+1) = VL(i) + K(i)\, YL(i) - M(i)\, \lambda_n^2\, YL(i)$$

$$\Delta = \begin{vmatrix} \dfrac{\overline{TL}(NS)}{\alpha} & \dfrac{TL'(NS)}{\beta} \\[2ex] \dfrac{\overline{VL}(NS)}{\alpha} & \dfrac{VL'(NS)}{\beta} \end{vmatrix}$$

$$SO(1) = YO(1)\left[\overline{TL}(NS)\,\beta\,/TL'(NS)\,\alpha\right]$$

$$Z_n = \sum_{i=1}^{NS}\left\{\frac{\pi\,\gamma\,(i)}{4g}\int_0^{L_i}(D_i^2 - d_i^2)\,Y_n^2(i)\,d\,X_i + M(i)\,YL^2(i) + J(i)\,SL^2(i)\right\}$$

$$G_n = \frac{1}{Z_n}\sum_{i=1}^{NS}\left\{\frac{YL(i)\;FF(i)}{\left\{\left[\lambda_n^2 - FFF^2(i)\right]^2 + \left[2C_n\,FFF(i)\right]^2\right\}^{1/2}}\right.$$

$$\left. + \frac{SL(i)\;FT(i)}{\left\{\left[\lambda_n^2 - FFT^2(i)\right]^2 + \left[2C_n\,FFT(i)\right]^2\right\}^{1/2}}\right\}$$

$$YFO(i) = \sum_{n=1}^{NF} YO(i)\,G_n$$

$$TFO(i) = \sum_{n=1}^{NF} TO(i)\,G_n$$

$$VFO(i) = \sum_{n=1}^{NF} VO(i)\,G_n$$

$$YFL(i) = \sum_{n=1}^{NF} YL(i)\,G_n$$

$$TFL(i) = \sum_{n=1}^{NF} TL(i)\,G_n$$

$$VFL(i) = \sum_{n=1}^{NF} VL(i)\,G_n$$

The nomenclature used here is

λ_n	=	natural frequency of shaft
L(i)	=	length of section i
A(i)	=	cross-sectional area of section i
γ(i)	=	weight density of section i
E(i)	=	modulus of elasticity for section i
I(i)	=	area moment of inertia about a diameter of section i
g	=	acceleration due to gravity
D(i)	=	outer diameter of section i
d(i)	=	inner diameter of section i

C_1(i), C_2(i), C_3(i), C_4(i)	constants in equations for deflection of section i
YL(i), SL(i), TL(i), VL(i)	deflection, slope, moment and shear at end of section i toward section i + 1
YO(i), SO(i), TO(i), VO(i)	deflection, slope, moment and shear at beginning of section i
Y_n(i)	modal deflection of section i
σ (i)	torsional spring constant between section i and section i + 1
K(i)	linear spring constant between section i and section i + 1
J(i)	lumped inertia between section i and section i + 1
M(i)	lumped mass between section i and section i + 1
Δ	determinant (Δ = 0 at all natural frequencies)

$\overline{TL}$ (NS), $\overline{VL}$ (NS)	values of moment and shear at end of shaft for slope, moment, and shear equal to zero and deflection equal to α at beginning of shaft.
TL'(NS), VL'(NS)	values of moment and shear at end of shaft for deflection, moment and shear equal to zero and slope equal to β at beginning of shaft.
C_n	modal damping factor
Z_n	normalizing factor
G_n	modal forcing function
FF (i)	force applied at section i
FFF (i)	frequency of force applied at section i
FT (i)	moment applied at section i
FFT (i)	frequency of moment applied at section i
YFO (i)	forced displacement at beginning of section i
TFO (i)	forced moment at beginning of section i
VFO (i)	forced shear at beginning of section i
YFL (i)	forced displacement at end of section i
TFL (i)	forced moment at end of section i
VFL (i)	forced shear at end of section i
NF	number of frequencies

A flow diagram defining a procedure whereby the above equations can be used to analyze a complex shaft is given in figure D-2. A FORTRAN program for the IBM 7090 Digital Computer which carries out this procedure follows at the end of this report. The output for a sample problem, see figure D-3, is also listed. The output of the program is self-explanatory. The input has the following format.

CARD 1 (all run types)

Column 1	*
Column 2-6	blank
Column 7-10	DATA
Column 11-80	blank

CARD 2 (all run types)

Columns 1-4	shaft identification number — Format (I4)
Columns 5-6	run type - Format (I2)
Columns 7-80	blank

CARD 3 (run types 1, 2, 3, and 4)

Columns 1-3	number of shaft sections-Format (I3)
Columns 4-6	number of frequencies desired-Format (I3)
Columns 7-16	required accuracy of frequencies Format (F10.0)
Columns 17-26	approximation to first natural frequency Format (F 10.0)
Columns 27-36	frequency increment-Format (F10.0)
Columns 37-80	blank

CARD 3 (run type 5)

Columns 1-3	number of shaft sections-Format (I3)
Columns 4-6	number of frequencies-Format (I3)

Cards 4, 5, ----,(NS + 3) all have the same format (NS is the total number of shaft sections). Each card describes one shaft section. The cards must be arranged in the same order as the shaft sections (card 4 describes section 1, card 5 describes section 2, etc.).

ID = IDENTIFICATION
K = RUN TYPE

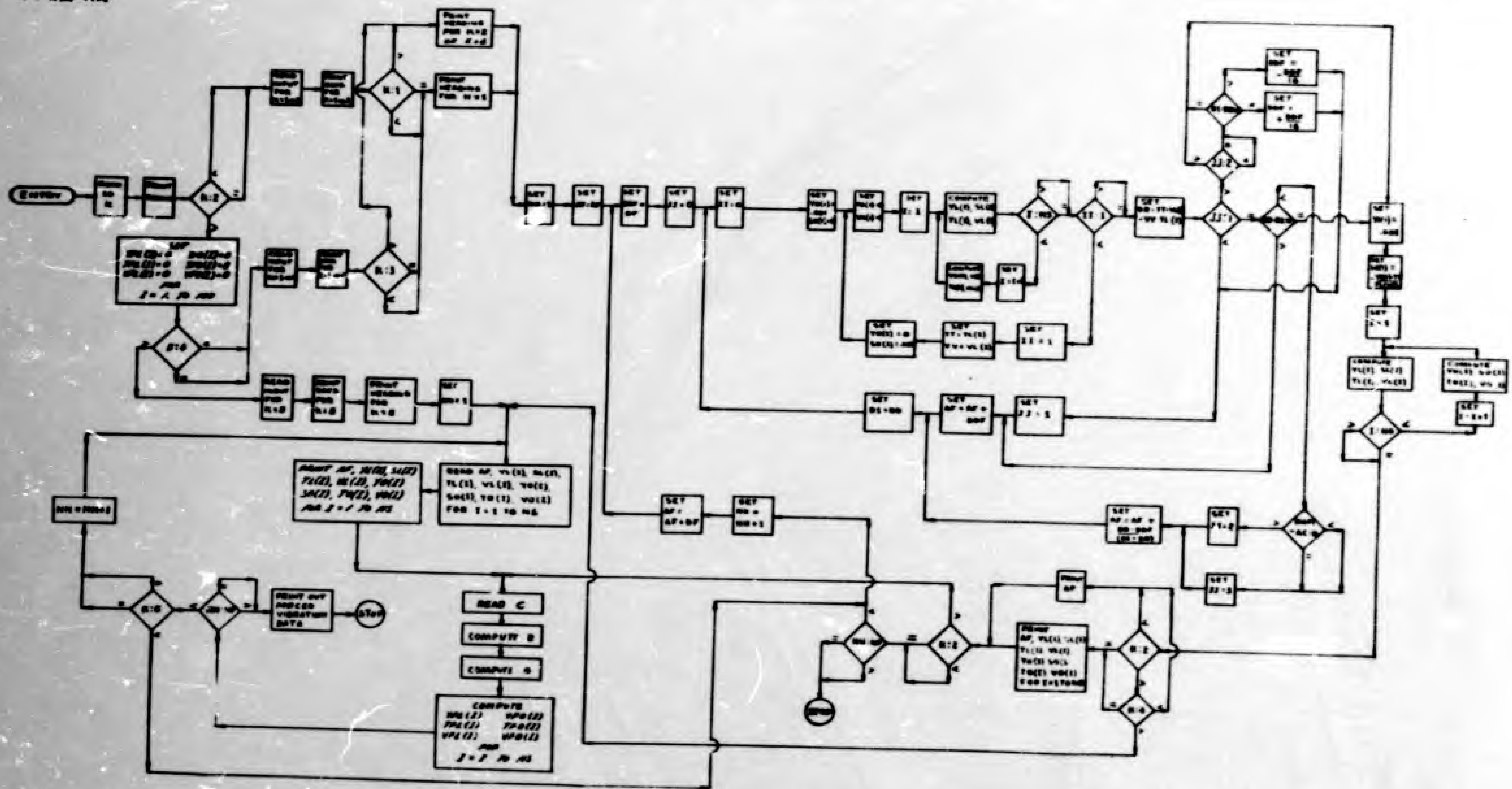

Figure D-2

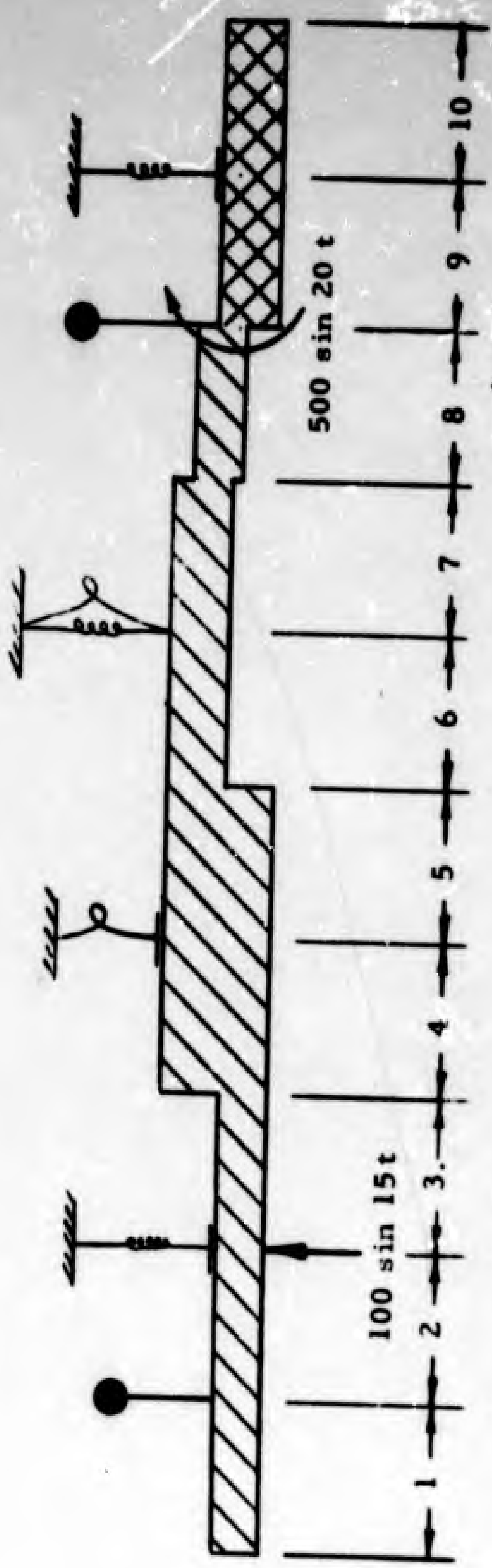

Figure D-3 SAMPLE SHAFT

CARD 4, 5, etc. (run types 1, 2, 3, and 4)

Columns 1-8	section length	Format (F 8.0)
9-16	section outer diameter	Format (F 8.0)
17-24	section inner diameter	Format (F 8.0)
25-32	section weight density	Format (F 8.0)
33-40	section modulus of elasticity	Format (F 8.0)
41-48	section lumped mass	Format (F 8.0)
49-56	section lumped inertia	Format (F 8.0)
57-64	section linear spring	Format (F 8.0)
65-72	section torsional spring	Format (F 8.0)
73-80	blank	

CARDS 4, 5, etc. (run type 5)

Columns 1-8	section length	Format (F 8.0)
9-16	section outer diameter	Format (F 8.0)
17-24	section inner diameter	Format (F 8.0)
25-32	section weight density	Format (F 8.0)
33-40	section modulus of elasticity	Format (F 8.0)
41-48	section lumped mass	Format (F 8.0)
49-56	section lumped inertia	Format (F 8.0)
57-80	blank	

This concludes the input for run types 1 and 2. Run types 3 and 4 have the following additional data.

Additional Cards 1, 2, - - - NS (Run types 3 and 4)

Columns 1-10	force input at section i	Format (F 10.0)
Columns 11-20	frequency of force input at section i	Format (F 10.0)
Columns 21-30	moment input at section i	Format (F 10.0)
Columns 31-40	frequency of moment input at section i	Format (F 10.0)
Columns 41-80	blank	

Additional Cards 1, 2, - - - (run type 5)

Columns 1-10	force input at section i	Format (F 10.0)
Columns 11-20	frequency of force input at section i	Format (F 10.0)
Columns 21-30	moment input at section i	Format (F 10.0)
Columns 31-40	frequency of moment at section i	Format (F 10.0)
Columns 41-80	blank	

Additional Card NS + 1 (run type 5)

Columns 1-13	natural frequency	Format (E 13.6)
Columns 14-80	blank	

Additional Cards* NS + 2, NS + 4, - - - 3 NS (run type 5)

Columns 1-13	modal deflection at beginning of section i	Format (E13.6)
Columns 14-26	modal slope at beginning of section i	Format (E13.6)
Columns 27-39	modal moment at begin- of section i	Format (E13.6)
Columns 40-52	modal shear at beginning of section i	Format (E13.6)
Columns 53-80	blank	

* Note alternate cards

Additional Cards* NS + 3, NS + 5, - - -, 3 NS + 1 (run type 5)

Columns 1-13	modal deflection at end of section i	Format (E 13.6)
Columns 14-26	modal slope at end of section i	Format (E 13.6)
Columns 27-39	modal moment at end of section i	Format (E 13.6)
Columns 40-52	modal shear at end of section i	Format (E 13.6)
Columns 53-80	blank	

Additional Card 3NS + 6 (run type 5)

Columns	modal damping factor	Format (F 10.0)
Columns	blank	

Cards describing additional natural frequencies, mode shapes and damping factors follow with the same format as for the first mode. These cards conclude the input for run type 5.

* Note alternate Cards

The format (I4, F 10.0, E13.6, etc.) specifies the form in which the data must be punched. The specification Iw requires that the data be an integer containing at most w digits. The specification Fw.0 requires that the data be punched with a decimal point or with the decimal point assumed to be in the column immediately to the right of the space saved for the data. The specification E 13.6 is satisfied if the data is written in the form ± 0.123456 E ± 12. The E ± 12 specifies the power of 10 by which ± 0.123456 is multiplied.

The approximation to the first natural frequency for card 3 must be below the actual first natural frequency. The frequency increment must be less than the interval between any two natural frequencies of the shaft. However, since computing time is very dependent on the magnitude of these quantities they should be kept as large as possible.

Table D-1

SAMPLE PROBLEM DATA

Section	Length (in.)	Outer Diameter (in.)	Inner Diameter (in.)	Weight Density (lb/in^3)	Modulus of Elasticity (lb/in^2)	Lumped Mass (lb-sec^2/in)	Lumped Inertia (lb-sec^2-in)	Compression Spring (lb/in)	Torsion Spring (in. lb/radian)
1	10	4	2	.283	$29.5 \cdot 10^6$	0.8	360	0	0
2	20	4	2	.283	$29.5 \cdot 10^6$	0	0	$2.0 \cdot 10^6$	0
3	40	4	2	.283	$29.5 \cdot 10^6$	0	0	0	0
4	40	6	2	.283	$29.5 \cdot 10^6$	0	0	0	$5.0 \cdot 10^4$
5	30	6	2	.283	$29.5 \cdot 10^6$	0	0	0	0
6	40	6	4	.283	$29.5 \cdot 10^6$	0	0	$1.5 \cdot 10^6$	$4.0 \cdot 10^4$
7	10	6	4	.283	$29.5 \cdot 10^6$	0	0	0	0
8	20	5	3	.283	$29.5 \cdot 10^6$	3.5	700	0	0
9	10	4	2	.098	$10.6 \cdot 10^6$	0	0	$3.0 \cdot 10^5$	0
10	10	4	2	.098	$10.6 \cdot 10^6$	0	0	0	0

$$\left[\lambda_1\right] > 10 \text{ rad/sec}$$

$$\left[\lambda_n - \lambda_{n-1}\right] > 10 \text{ rad/sec}$$

```
*SHAFT ANALYSIS   K06056    P55HAIN E        131REPORT  (10)

*     XEQ
*     LABEL

COMP2 SHAFT ANALYSIS                                                       4/21/64        PAGE 1

      0DIMENSION SLL(20),SOD(20),SID(20),SWD(20),SEE(20),SLM(20),SLI(20),
      1SLS(20),STS(20),E(20),FR(20),Y0(20),S0(20),T0(20),V0(20),VL(20),S
      2L(20),TL(20),VL(20),YFU(20),TFO(20),VFO(20),YFL(20),TFL(20),VFL(20
      3),FF(20),FFF(20),FT(20),FFT(20)
    1 READ INPUT TAPE 5,50,ID,K
   50 FORMAT (I4,I2)
      WRITE OUTPUT TAPE 6,51,ID,K
   510FORMAT (17HIANALYSIS OF COMPLEX SHAFTING SYSTEMS////29H SHAFT IDEN
      1TIFICATION NUMBER I4//10H RUN TYPE I2)
      IF (K-2) 2,2,41
    20READ INPUT TAPE 5,52,NS,NF,AC,AF,DF,(SLL(I),SOD(I),SID(I),SWD(I),S
      1EE(I),SLM(I),SLI(I),SLS(I),STS(I),I=1,NS)
   52 FORMAT (2I3,3F10.0/(9F8.0))
      DO 53 I=1,NS
      0E(I)=SEE(I)*(.049087385)*(SOD(I)*SOD(I)*SID(I)*SID(I))*(SOD(I)+SI
      1D(I))*(SOD(I)-SID(I))
   530FR(I)=1.041443906*SWD(I)/(SEE(I)*(SOD(I)*SOD(I)+SID(I)*SID(I)))**
      1.25
      WRITE OUTPUT TAPE 6,54,NS,NF,AC,AF,DF
   540FORMAT (/26H THE SHAFT IS COMPOSED OF I3,13H SECTIONS.I4,73H NATUR
      1AL FREQUENCIES WILL BE COMPUTED WITHIN AN ACCURACY OF PLUS OR MINU
      2S/E14.6,67H . IT WAS ESTIMATED THAT THE FIRST NATURAL FREQUENCY WA
      3S GREATER THANE14.6,19H RADIANS PER SECOND/56H AND THAT NO TWO NAT
      4URAL FREQUENCIES WILL BE CLOSER THANE14.6,20H RADIANS PER SECOND.)
      0WRITE OUTPUT TAPE 6,55,(SLL(I),SOD(I),SID(I),SWD(I),SEE(I),SLM(I),
      1SLI(I),SLS(I),STS(I),I=1,NS)
   550FORMAT (/1H ,10X5HOUTER,8X5HINNER,7X6HWEIGHT,5X10HMODULUS OF,5X6HL
      1UMPED,7X6HLUMPED,7X6HLINEAR,6X9HTORSIONAL/1H ,4X6HLENGTH,6X8HDIAME
      2TER,5X8HDIAMETER,6X7HDENSITY,4X10HELASTICITY,6X4HMASS,8X7HINERTIA,
      36X6HSPRING,7X6HSPRING/1H ,5X5H(IN.),8X5H(IN.),8X5H(IN.),6X9H(LB/IN
      4.3),4X7H(LB/IN.2),2X13H(LB SEC2/IN.),14H (LB SEC2 IN.),9H (LB/IN.)
      5,17H  (IN. LB/RADIAN)/(9E13.4))
      IF (K-1) 3,3,40
    3 WRITE OUTPUT TAPE 6,56
   56 FORMAT (///42H NATURAL FREQUENCIES IN RADIANS PER SECOND/)
    4 NN=1
      AF=AF
    5 DCF=DF
      JJ=0
    6 II=0
      Y0(1)=.001
      S0(1)=0.
    7 T0(1)=0.
      V0(1)=0.
      I=1
    8 P=FR(I)*SQRTF(AF)
      EIP2=E(I)*P*P
      EIP3=EIP2*P
      C1 (S0(I)/P*V0(I)/EIP3)/2.
      C2=(Y0(I)+T0(I)/EIP2)/2.
      C3=(S0(I)/P-V0(I)/EIP3)/2.
      C4=(Y0(I)-T0(I)/EIP2)/2.
      CIN=SINF(P*SLL(I))
      SOS=COSF(P*SLL(I))
      SINH=EXPF(P*SLL(I))
```

```
      COSH=(SINH+1./SINH)/2.
      SINH=(SINH-1./SINH)/2.
      VL(I)=C1*CIN+C2*SOS+C3*SINH+C4*COSH
      SL(I)=P*(C1*SOS-C2*CIN+C3*COSH+C4*SINH)
      TL(I)=EIP2*(C1*CIN+C2*SOS-C3*SINH-C4*COSH)
      VL(I)=EIP3*(C1*SOS-C2*CIN-C3*COSH-C4*SINH)
      IF (I-NS) 9,10,10
    9 I=I+1
      VO(I)=VL(I-1)
      SO(I)=SL(I-1)
      TO(I)=TL(I-1)-STS(I-1)*SL(I-1)+SL(I-1)*SL(I-1)*AF*AF
      VO(I)=VL(I-1)+SLS(I-1)*VL(I-1)-SLM(I-1)*VL(I-1)*AF*AF
      GO TO 8
   10 IF (II-1) 11,12,12
   11 II=1
      TT=TL(NS)
      VV=VL(NS)
      VO(1)=0.
      SO(1)=.001
      GO TO 7
   12 DD=TT*VL(NS)-VV*TL(NS)
      IF (JJ-1) 13,16,21
   13 JJ=1
   14 AF=AF+DDF
   15 D1=DD
      GO TO 6
   16 IF (DD*D1) 17,25,14
   17 IF (DDF*DDF-AC*AC) 20,20,18
   18 JJ=2
   19 AF=AF+(DD*DDF)/(D1-DD)
      GO TO 15
   20 JJ=3
      GO TO 19
   21 IF (JJ-2) 22,22,25
   22 IF (DD*D1)23,25,24
   23 DDF=DDF/16.
      GO TO 13
   24 DDF=(-DDF)/16.
      GO TO 13
   25 VO(1)=.001
      SO(1)=(-VO(1)*TT)/TL(NS)
      I=1
   26 P=FA(I)*SQRTF(AF)
      EIP2=FI(I)*P*P
      EIP3=EIP2*P
      C1=(SO(I)/P+VO(I)/EIP3)/2.
      C2=(VO(I)+TO(I)/EIP2)/2.
      C3=(SO(I)/P-VO(I)/EIP3)/2.
      C4=(VO(I)-TO(I)/EIP2)/2.
      CIN=SINF(P*SLL(I))
      SOS=COSF(P*SLL(I))
      SINH=EXPF(P*SLL(I))
      COSH=(SINH+1./SINH)/2.
      SINH=(SINH-1./SINH)/2.
      VL(I)=C1*CIN+C2*SOS+C3*SINH+C4*COSH
      SL(I)=P*(C1*SOS-C2*CIN+C3*COSH+C4*SINH)
```

```
      TL(I)=EIP2*(C1*CIN+C2*SOS-C3*SINH-C4*COSH)
      VL(I)=EIP3*(C1*SOS-C2*CIN-C3*COSH-C4*SINH)
      IF (I-NS) 27,28,28
   27 I=I+1
      VO(I)=VL(I-1)
      SO(I)=SL(I-1)
      TO(I)=TL(I-1)-STS(I-1)*SL(I-1)+SLI(I-1)*SL(I-1)*AF*AP
      VO(I)=VL(I-1)+SLS(I-1)*VL(I-1)-SLM(I-1)*VL(I-1)*AF*AP
      GO TO 26
   28 IF (K-2) 29,33,34
   29 WRITE OUTPUT TAPE 6,57,AF
   57 FORMAT (E20.6)
   30 IF (K-2) 31,31,36
   31 IF (NN-NF) 32,1,1
   32 NN=NN+1
      AF=AF+DF
      GO TO 9
   33OWRITE OUTPUT TAPE 6,58,AF,(I,VO(I),SO(I),TO(I),VO(I),VL(I),SL(I),T
     1L(I),VL(I),I=1,NS)
   58 FORMAT (//F15.6//(I4,E18.5,7E14.6))
      GO TO 30
   34 IF (K-4) 29,33,35
   35OREAD INPUT TAPE 5,59,AF,(VO(I),SO(I),TO(I),VO(I),VL(I),SL(I),VL(I)
     1,VL(I),I=1,NS)
   59 FORMAT (E13.6/(4E13.6))
      OWRITE OUTPUT TAPE 6,58,AF,(I,VO(I),SO(I),TO(I),VO(I),VL(I),SL(I),T
     1L(I),VL(I),I=1,NS)
   36 READ INPUT TAPE 5,72,C
      Z=0.
      DO 60 I=1,NS
      P=FR(I)*SQRTF(AF)
      EIP2=EI(I)*P*P
      EIP3=EIP2*P
      PL=P*SLL(I)
      C1=(SO(I)/P+VO(I)/EIP3)/2.
      C2=(VO(I)+TO(I)/EIP2)/2.
      C3=(SO(I)/P-VO(I)/EIP3)/2.
      C4=(VO(I)-TO(I)/EIP2)/2.
      CIN=SINF(PL)
      SOS=COSF(PL)
      SINH=EXPF(PL)
      COSH=(SINH+1./SINH)/2.
      SINH=(SINH-1./SINH)/2.
   60Z=Z+.0201347103*SWD(I)*(SOD(I)+SID(I))*(SOD(I)-SID(I))*(C1*C1*(PL-C
     1IN*SOS)/2.+C2*C2*(PL+CIN*SOS)/2.+C3*C3*(SINH*COSH-PL)/2.+C4*C4*(SI
     2NH*COSH+PL)/2.+C1*C2*CIN*CIN+C1*C3*(COSH*CIN-SINH*SOS)+C1*C4*(SINH
     3*CIN-COSH*SOS+1.)+C2*C3*(COSH*SOS+SINH*CIN-1.)+C2*C4*(COSH*CIN+SIN
     4H*SOS)+C3*C4*SINH*SINH)/P+SLM(I)*VL(I)*VL(I)+SLI(I)*SL(I)*SL(I)
      GZ=0.
      DO 61 I=1,NS
   61GZ=GZ+FF(I)*VL(I)/SQRTF((AF*AF-FFF(I)*FFF(I))*(AF*AF-FFF(I)*FFF(I
     1))+4.*C*C*FFF(I)*FFF(I))+FT(I)*SL(I)/SQRTF((AF*AF-FFT(I)*FFT(I))*(A
     2F*AF-FFT(I)*FFT(I))+4.*C*C*FFT(I)*FFT(I))
      DO 62 I=1,NS
      VFO(I)=VFO(I)+VO(I)*GZ/Z
      TFO(I)=TFO(I)+TO(I)*FI(I)*GZ/Z
```

```
      VFO(I)=VFO(I)+VO(I)*EI(I)*GZ/2
      VFL(I)=VFL(I)+VL(I)*GZ/2
      TFL(I)=TFL(I)+TL(I)*EI(I)*GZ/2
   62 VFL(I)=VFL(I)+VL(I)*F(I)*GZ/2
      IF (NN-NF) 37,39,39
   37 IF (K-5) 32,38,38
   38 NN=NN+1
      GO TO 35
   39OWRITE OUTPUT TAPE 6,63,(I,YFO(I),TFO(I),VFO(I),YFL(I),TFL(I),VFL(I
     1),I=1,NS)
   630FORMAT (18H1FORCED VIBRATIONS////80H          DISPLACEMENT      MOM
     1ENT          SHEAR       DISPLACEMENT      MOMENT           SHEAR/89H SEC
     2TION  AT BEGINNING  AT BEGINNING  AT BEGINNING      AT END          A
     3T END          AT END//(I5,E18.6,5E14.6))
      GO TO 1
   40 WRITE OUTPUT TAPE 6,64
   640FORMAT (///18H NATURAL FREQUENCY/17H (RADIANS/SECOND)//11H MODE SH
     1APE/116H              DISPLACEMENT       SLOPE              MOMENT         SHE
     2AR        DISPLACEMENT       SLOPE            MOMENT          SHEAR/117H SE
     3CTION  AT BEGINNING  AT BEGINNING  AT BEGINNING  AT BEGINNING
     4AT END          AT END           AT END           AT END)
      GO TO 4
   41 DO 65 I=1,20
      YFO(I)=0.
      TFO(I)=0.
      VFO(I)=0.
      YFL(I)=0.
      TFL(I)=0.
   65 VFL(I)=0.
      IF (K-4) 42,42,43
   420READ INPUT TAPE 5,52,NS,NF,AC,AF,DF,(SLL(I),SOD(I),SID(I),SWD(I),S
     1EE(I),SLM(I),SLI(I),SLS(I),STS(I),I=1,NS)
      READ INPUT TAPE 5,66,(FF(I),FFF(I),FT(I),FFT(I),I=1,NS)
   66 FORMAT (4F19.3)
      DO 67 I=1,NS
     OEI(I)=SEE(I)*(.0490873851*(SOD(I)*SOD(I)+SID(I)*SID(I))*(SOD(I)+SI
     1D(I))*(SOD(I)-SID(I))
   670F(I)=1.041443936*SWD(I)/(SEE(I)*(SOD(I)*SOD(I)+SID(I)*SID(I)))**
     1.25
      WRITE OUTPUT TAPE 6,54,NS,NF,AC,AF,DF
     OWRITE OUTPUT TAPE 6,55,(SLL(I),SOD(I),SID(I),SWD(I),SEE(I),SLM(I),
     1SLI(I),SLS(I),STS(I),I=1,NS)
      WRITE OUTPUT TAPE 6,68,(FF(I),FFF(I),FT(I),FFT(I),I=1,NS)
   680FORMAT (/64H          FORCE            FREQUENCY              MOMENT
     1 FREQUENCY/64H               (LB)            (RAD/SEC)             (IN.LB)
     2    (RAD/SEC)/(F16.6,E15.6,E20.6,E15.6))
      IF (K-3) 1,1,40
   430READ INPUT TAPE 5,69,NS,NF,(SLL(I),SOD(I),SID(I),SWD(I),SEE(I),SLM
     1(I),SLI(I),I=1,NS)
   69 FORMAT (2I3/(7F9.0))
      READ INPUT TAPE 5,66,(FF(I),FFF(I),FT(I),FFT(I),I=1,NS)
      DO 70 I=1,NS
     OEI(I)=SEE(I)*(.0490873851*(SOD(I)*SOD(I)+SID(I)*SID(I))*(SOD(I)+SI
     1D(I))*(SOD(I)-SID(I))
   700F(I)=1.041443936*SWD(I)/(SEE(I)*(SOD(I)*SOD(I)+SID(I)*SID(I)))**
     1.25
```

```
   0WRITE OUTPUT TAPE 6,71,NS,NF,(SLL(I),SOD(I),SID(I),SWD(I),SEE(I),S
   1LM(I),SL(I),I=1,NS)
 71 FORMAT (/26H THE SHAFT IS COMPOSED OF I3,10H SECTIONS.I4,57H MODES
   1 WILL BE USED IN THE FORCED VIBRATION CALCULATIONS.//1H ,108X9HOUTE
   2R,9X5HINNER,7X6HWEIGHT,5X10HMODULUS OF,5X6HLUMPED,7X6HLUMPED/1H ,4
   3X6HLENGTH,6X8HDIAMETER,5X8HDIAMETER,4X7HDENSITY,4X10HELASTICITY,6X
   44HMASS,8X7HINERTIA/1H ,5X5H(IN.),8X5H(IN.),8X5H(IN.),6X9H(LB/IN.3)
   5,6X9H(LB/IN.2),7X13H(LB SEC2/IN.),14H (LB SEC2 IN.)/(7F13.4))
    WRITE OUTPUT TAPE 6,60,(FF(I),FFF(I),FT(I),FFT(I),I=1,NS)
    WRITE OUTPUT TAPE 6,64
    NN=1
    GO TO 39
 72 FORMAT (F10.0)
    END(1,0,0,0,0,0,1,0,0,0,0,0,0,0,0)
```

STORAGE NOT USED BY PROGRAM

DEC	OCT	DEC	OCT
2571	05013	32561	77461

STORAGE LOCATIONS FOR VARIABLES APPEARING IN DIMENSION AND EQUIVALENCE STATEMENTS

	DEC	OCT		DEC	OCT		DEC	OCT		DEC	OCT		DEC	OCT
FI	2390	04526	FFP	2050	04002	FF	2070	04026	FFT	2010	03732	FR	2370	04502
FT	2030	03756	SO	2330	04432	SEE	2490	04672	SID	2530	04742	SLI	2450	04622
SLL	2570	05012	SLM	2470	04646	SL	2250	04312	SLS	2430	04576	SOO	2550	04766
SIS	2410	04552	SWO	2510	04716	TO	2310	04406	TFO	2170	04172	TFL	2110	04076
TL	2230	04266	VO	2290	04362	VFO	2150	04146	VFL	2090	04052	VL	2210	04242
VO	2350	04456	VFO	2190	04216	VFL	2130	04122	VL	2270	04336			

STORAGE LOCATIONS FOR VARIABLES NOT APPEARING IN COMMON, DIMENSION, OR EQUIVALENCE STATEMENT

	DEC	OCT		DEC	OCT		DEC	OCT		DEC	OCT		DEC	OCT
AC	1990	03706	AF	1989	03705	C1	1988	03704	C2	1987	03703	C3	1986	03702
C4	1985	03701	CIN	1984	03700	COSH	1983	03677	C	1982	03676	D1	1981	03675
DUF	1980	03674	DD	1979	03673	DF	1978	03672	EIP2	1977	03671	EIP3	1976	03670
G2	1975	03667	ID	1974	03666	II	1973	03665	I	1972	03664	JJ	1971	03663
K	1970	03662	NF	1969	03661	NN	1968	03660	NS	1967	03657	PL	1966	03656
P	1965	03655	SINH	1964	03654	SOS	1963	03653	TT	1962	03652	VV	1961	03651
Z	1960	03650												

SYMBOLS AND LOCATIONS FOR SOURCE PROGRAM FORMAT STATEMENTS

	EFN	LOC		EFN	LOC		EFN	LOC		EFN	LOC		EFN	LOC
811I	50	03610	811J	51	03606	811K	52	03565	811M	54	03561	811N	55	03473
811O	56	03377	811P	57	03366	811Q	58	03364	811R	59	03357	811V	63	03354
8120	64	03305	8122	66	03221	8124	68	03217	8125	69	03163	8127	71	03160
8128	72	03057												

LOCATIONS FOR OTHER SYMBOLS NOT APPEARING IN SOURCE PROGRAM

	DEC	OCT		DEC	OCT		DEC	OCT		DEC	OCT		DEC	OCT
1)	1929	03611	2)	1559	03027	3)	1566	03036	4)	32767	77777	6)	1576	03050
C1G0	1958	03646	C1G2	1959	03647	D110H	404	00624	D120C	197	00305	D1214	696	01270
D1401	15	00017	EIF	364	00554	EIM	403	00623	EIP	435	00663	EIS	469	00725
E115	701	01275	E117	713	01311	E118	756	01364	E1113	684	01254			

LOCATIONS OF NAMES IN TRANSFER VECTOR

	DEC	OCT		DEC	OCT		DEC	OCT		DEC	OCT		DEC	OCT
COS	8	00010	EXP	9	00011	EXP(3	5	00005	SIN	7	00007	SQRT	6	00006
(FIL)	4	00004	(FPT)	0	00000	(RTN)	2	00002	(STH)	3	00003	(TSH)	1	00001

ENTRY POINTS TO SUBROUTINES NOT OUTPUT FROM LIBRARY

COS EXP EXP(3 SIN SQRT (FIL) (FPT) (RTN) (STH) (TSH)

EXTERNAL FORMULA NUMBERS WITH CORRESPONDING INTERNAL FORMULA NUMBERS AND OCTAL LOCATIONS

EFN	IFN	LOC	EFN	IFN	LOC	EFN	IFN	LOC	EFN	IFN	LOC	EFN	IFN	LOC
1	19	00023	2	24	00054	53	32	00156	3	41	00267	4	42	00275
5	44	00301	6	46	00306	7	49	00314	8	52	00323	9	69	00555
10	75	00617	11	76	00625	12	82	00640	13	84	00653	14	85	00655
15	86	00660	16	88	00664	17	89	00670	18	90	00701	19	91	00703
20	93	00716	21	95	00721	22	96	00726	23	97	00732	24	99	00736
25	101	00742	26	104	00754	27	121	01205	28	127	01250	29	128	01255
30	130	01271	31	131	01276	32	132	01302	33	135	01312	34	142	01357
35	143	01365	36	155	01470	60	172	01627	61	175	02035	62	182	02165
37	184	02201	38	185	02206	39	187	02212	40	193	02251	41	195	02260
65	201	02273	42	203	02303	67	216	02432	43	230	02571	70	243	02706

ENTRY POINTS TO SUBROUTINES REQUESTED FROM LIBRARY,
(FPT) (TSHM) (RTN) (STHM) (FIL) EXP(3 SQRT SIN COS EXP

PREPROCESSING TIME = 000.96 MIN.

EXECUTION

ANALYSIS OF COMPLEX SHAFTING SYSTEMS

SHAFT IDENTIFICATION NUMBER 1

RUN TYPE 1

THE SHAFT IS COMPOSED OF 10 SECTIONS. 2 NATURAL FREQUENCIES WILL BE COMPUTED WITHIN AN ACCURACY OF PLUS OR MINUS 1.000000E-03 . IT WAS ESTIMATED THAT THE FIRST NATURAL FREQUENCY WAS GREATER THAN 0.100000E 02 RADIANS PER SECOND AND THAT NO TWO NATURAL FREQUENCIES WILL BE CLOSER THAN 0.100000E 02 RADIANS PER SECOND.

LENGTH (IN.)	OUTER DIAMETER (IN.)	INNER DIAMETER (IN.)	WEIGHT DENSITY (LB/IN.3)	MODULUS OF ELASTICITY (LB/IN.2)	LUMPED MASS (LB SEC2/IN.)	LUMPED INERTIA (LB SEC2 IN.)	LINEAR SPRING (LB/IN.)	TORSIONAL SPRING (IN. LB/RADIAN)
0.1000E 02	0.4000E 01	0.2000E 01	0.2830E-00	0.2950E 08	0.0000E 00	0.3600E 03	-0.	-0.
0.2000E 02	0.4000E 01	0.2000E 01	0.2830E-00	0.2950E 08	-0.	-0.	0.2000E 06	-0.
0.4000E 02	0.4000E 01	0.2000E 01	0.2830E-00	0.2950E 08	-0.	-0.	-0.	-0.
0.6000E 02	0.6000E 01	0.2000E 01	0.2830E-00	0.2950E 08	-0.	-0.	-0.	0.5000E 05
0.3000E 02	0.6000E 01	0.2000E 01	0.2830E-00	0.2950E 08	-0.	-0.	-0.	-0.
0.4000E 02	0.6000E 01	0.4000E 01	0.2830E-00	0.2950E 08	-0.	-0.	0.1500E 06	0.6000E 05
0.1000E 02	0.6000E 01	0.4000E 01	0.2830E-00	0.2950E 08	-0.	-0.	-0.	-0.
0.2000E 02	0.5000E 01	0.3000E 01	0.2830E-00	0.2950E 08	0.3500E 01	0.7000E 03	-0.	-0.
0.1000E 02	0.4000E 01	0.2000E 01	0.9800E-01	0.1060E 08	-0.	-0.	0.3000E 06	-0.
0.1000E 02	0.4000E 01	0.2000E 01	0.9800E-01	0.1060E 08	-0.	-0.	-0.	-0.

NATURAL FREQUENCIES IN RADIANS PER SECOND
0.918640E 02
0.175710E 03

ANALYSIS OF COMPLEX SHAFTING SYSTEMS

SHAFT IDENTIFICATION NUMBER 1

RUN TYPE 2

THE SHAFT IS COMPOSED OF 10 SECTIONS. 2 NATURAL FREQUENCIES WILL BE COMPUTED WITHIN AN ACCURACY OF PLUS OR MINUS 1.000000E-03 . IT WAS ESTIMATED THAT THE FIRST NATURAL FREQUENCY WAS GREATER THAN 0.100000E 02 RADIANS PER SECOND AND THAT NO TWO NATURAL FREQUENCIES WILL BE CLOSER THAN 0.100000E 02 RADIANS PER SECOND.

LENGTH (IN.)	OUTER DIAMETER (IN.)	INNER DIAMETER (IN.)	WEIGHT DENSITY (LB/IN.3)	MODULUS OF ELASTICITY (LB/IN.2)	LUMPED MASS (LB SEC2/IN.)	LUMPED INERTIA (LB SEC2 IN.)	LINEAR SPRING (LB/IN.)	TORSIONAL SPRING (IN. LB/RADIAN)
0.1000E 02	0.4000E 01	0.2000E 01	0.2830E-00	0.2950E 08	0.8000E 00	0.3600E 03	-0.	-0.
0.2000E 02	0.4000E 01	0.2000E 01	0.2830E-00	0.2950E 08	-0.	-0.	0.2000E 06	-0.
0.4000E 02	0.4000E 01	0.2000E 01	0.2830E-00	0.2950E 08	-0.	-0.	-0.	-0.
0.4000E 02	0.4000E 01	0.2000E 01	0.2830E-00	0.2950E 08	-0.	-0.	-0.	0.5000E 05
0.1200E 02	0.6000E 01	0.2000E 01	0.2830E-00	0.2950E 08	-0.	-0.	-0.	-0.
0.4000E 02	0.6000E 01	0.4000E 01	0.2830E-00	0.2950E 08	-0.	-0.	0.1500E 06	0.4000E 05
0.1000E 02	0.6000E 01	0.4000E 01	0.2830E-00	0.2950E 08	-0.	-0.	-0.	-0.
0.2000E 02	0.5000E 01	0.3000E 01	0.2830E-00	0.2950E 08	0.3500E 01	0.7000E 03	-0.	-0.
0.1000E 02	0.4000E 01	0.2000E 01	0.9800E-01	0.1060E 08	-0.	-0.	0.3000E 06	-0.
0.1000E 02	0.4000E 01	0.2000E 01	0.9800E-01	0.1060E 08	-0.	-0.	-0.	-0.

NATURAL FREQUENCY
(RADIANS/SECOND)

MODE SHAPE

SECTION	DISPLACEMENT AT BEGINNING	SLOPE AT BEGINNING	MOMENT AT BEGINNING	SHEAR AT BEGINNING	DISPLACEMENT AT END	SLOPE AT END	MOMENT AT END	SHEAR AT END
0.218640E 02								
1	1.000000E-01	-0.353496E-04	0.	0.	0.646569E-01	-0.353241E-04	-0.257166E 01	-0.479987E-00
2	0.646567E-01	-0.353241E-04	0.109888E 03	-0.484510E 01	0.224834E-04	-0.261094E-04	-0.211172E 03	-0.521728E 01
3	0.224834E-04	-0.261094E-04	-0.211172E 03	-0.720603E 00	-0.514979E-01	-0.415510E-06	-0.229252E 03	0.538756E-01
4	-0.514977E-01	-0.415510E-06	-0.229252E 03	0.538756E-01	-0.437542E-01	0.405281E-05	-0.164364E 03	0.310927E 01
5	-0.437542E-01	0.405281E-05	-0.164567E 03	0.310927E 01	-0.284716E-01	0.580917E-05	-0.437200E 02	0.481430E 01
6	-0.284716E-01	0.580917E-05	-0.437200E 02	0.481430E 01	-0.647528E-04	0.426274E-05	0.164735E 03	0.567354E 01
7	-0.647528E-04	0.426274E-05	0.164565E 03	-0.423914E 01	-0.271214E-04	0.331017E-05	0.122421E 03	-0.419547E 01
8	-0.271214E-04	0.331017E-05	0.122421E 03	-0.419547E 01	0.150917E-04	0.126548E-05	0.386598E 02	-0.419142E 01
9	0.150917E-04	0.126548E-05	0.461354E 02	-0.463718E 01	0.154645E-04	-0.571815E-06	-0.251398E-00	-0.464057E 01
10	0.154645E-04	-0.571815E-06	-0.253398E-00	-0.122792E-02	0.985939E-05	-0.550653E-06	-0.279381E-00	-0.377985E-02
0.175718E 03								
1	1.000000E-01	-0.346954E-04	0.	0.	0.653284E-01	-0.346020E-04	-0.943257E 01	-0.176323E 01
2	0.653284E-01	-0.346020E-04	0.395054E 01	-0.179332E 02	0.258855E-01	-0.120950E-05	-0.772000E 03	-0.196008E 02
3	0.258865E-01	-0.120950E-05	-0.772000E 03	0.321641E 02	0.102261E-02	0.160648E-04	0.439217E 03	0.271776E 02
4	0.102261E-02	0.160648E-04	0.439217E 03	0.271776E 02	0.115638E-02	-0.135446E-05	0.983871E 03	-0.124075E 01
5	0.115638E-02	-0.135446E-05	0.983939E 03	-0.124075E 01	0.109368E-02	-0.151516E-04	0.612853E 03	-0.227425E 02
6	0.109368E-02	-0.151516E-04	0.612853E 03	-0.227425E 02	0.347209E-01	-0.170355E-04	-0.550083E 03	-0.330861E 02
7	0.347229E-01	-0.170355E-04	-0.553632E 03	0.189952E 02	0.192691E-01	-0.140725E-04	-0.354662E 03	0.180442E 02
8	0.192691E-01	-0.140725E-04	-0.354662E 03	0.180442E 02	0.289151E-04	-0.958678E-05	-0.826606E-01	0.176209E 02

9	-0.287151E-04	-0.958678E-05	-0.207288E 01	0.207457E 02	-0.694855E-04	-0.129849E-05	0.353247E-00	0.207072E 02
10	-0.694855E-04	-0.129849E-05	0.353247E-00	-0.584864E-01	-0.825515E-04	-0.131053E-05	0.410931E-01	-0.233606E-02

ANALYSIS OF COMPLEX SHAFTING SYSTEMS

SHAFT IDENTIFICATION NUMBER 1

RUN TYPE 3

THE SHAFT IS COMPOSED OF 10 SECTIONS. 2 NATURAL FREQUENCIES WILL BE COMPUTED WITHIN AN ACCURACY OF PLUS OR MINUS 1.000000E-03 . IT WAS ESTIMATED THAT THE FIRST NATURAL FREQUENCY WAS GREATER THAN 0.100000E 02 RADIANS PER SECOND AND THAT NO TWO NATURAL FREQUENCIES WILL BE CLOSER THAN 0.100000E 02 RADIANS PER SECOND.

LENGTH (IN.)	OUTER DIAMETER (IN.)	INNER DIAMETER (IN.)	WEIGHT DENSITY (LB/IN.3)	MODULUS OF ELASTICITY (LB/IN.2)	LUMPED MASS (LB SEC2/IN.)	LUMPED INERTIA (LB SEC2 IN.)	LINEAR SPRING (LB/IN.)	TORSIONAL SPRING (IN. LB/RADIAN)
0.1000E 02	0.4000E 01	0.2000E 01	0.2830E-00	0.2950E 08	0.0000E 00	0.3600E 03	-0.	-0.
0.2000E 02	0.4000E 01	0.2000E 01	0.2830E-00	0.2950E 08	-0.	-0.	0.2000E 06	-0.
0.4000E 02	0.4000E 01	0.2000E 01	0.2830E-00	0.2950E 08	-0.	-0.	-0.	-0.
0.4000E 02	0.6000E 01	0.2000E 01	0.2830E-00	0.2950E 08	-0.	-0.	-0.	0.5000E 05
0.3000E 02	0.6000E 01	0.2000E 01	0.2830E-00	0.2950E 08	-0.	-0.	-0.	-0.
0.4000E 02	0.6000E 01	0.4000E 01	0.2830E-00	0.2950E 08	-0.	-0.	0.1500E 06	0.4000E 05
0.1000E 02	0.6000E 01	0.4000E 01	0.2830E-00	0.2950E 08	-0.	-0.	-0.	-0.
0.2000E 02	0.5000E 01	0.3000E 01	0.2830E-00	0.2950E 08	0.3500E 01	0.7000E 03	-0.	-0.
0.1000E 02	0.4000E 01	0.2000E 01	0.9800E-01	0.1060E 08	-0.	-0.	0.3000E 06	-0.
0.1300E 02	0.4000E 01	0.2000E 01	0.9800E-01	0.1060E 08	-0.	-0.	-0.	-0.

FORCE (LB)	FREQUENCY (RAD/SEC)	MOMENT (IN.LB)	FREQUENCY (RAD/SEC)
-0.	-0.	-0.	-0.
0.100000E 03	0.150000E 02	-0.	-0.
-0.	-0.	-0.	-0.
-0.	-0.	-0.	-0.
-0.	-0.	-0.	-0.
-0.	-0.	-0.	-0.
-0.	-0.	0.500000E 03	0.200000E 02
-0.	-0.	-0.	-0.
-0.	-0.	-0.	-0.

NATURAL FREQUENCIES IN RADIANS PER SECOND
0.918640E 02
0.175718E 03

FORCED VIBRATIONS

SECTION	DISPLACEMENT AT BEGINNING	MOMENT AT BEGINNING	SHEAR AT BEGINNING	DISPLACEMENT AT END	MOMENT AT END	SHEAR AT END
1	0.104749E-03	0.	0.	0.677263E-04	-0.157071E 09	-0.293413E 08
2	0.677063E-04	-0.662843E 10	-0.297120E 09	0.864537E-05	-0.120894E 11	-0.323020E 09
3	0.864537E-05	-0.120894E 11	0.277092E 09	-0.130273E-04	-0.216362E 10	0.252000E 09
4	-0.130273E-04	-0.115393E 11	0.134031E 10	0.190516E-05	0.247230E 11	0.309126E 09
5	0.190516E-05	0.246979E 11	0.309126E 09	0.605619E-05	0.238672E 11	-0.424402E 09
6	0.605619E-05	0.193921E 11	-0.344092E 09	0.417977E-05	-0.225060E 10	-0.681037E 09
7	0.417977E-05	-0.225143E 10	0.262374E 09	0.300840E-05	0.192823E 09	0.229429E 09
8	0.300940E-05	0.100861E 09	0.120007E 09	0.409795E-06	0.237793E 10	0.111303E 09
9	0.409795E-06	-0.238657E 09	0.236913E 08	-0.643683E-06	-0.129874E 07	0.237959E 08
10	-0.640683E-06	-0.129874E 07	-0.206312E 06	-0.147705E-05	-0.258959E 07	-0.446407E 05

ANALYSIS OF COMPLEX SHAFTING SYSTEMS

SHAFT IDENTIFICATION NUMBER 1

RUN TYPE 4

THE SHAFT IS COMPOSED OF 10 SECTIONS. 2 NATURAL FREQUENCIES WILL BE COMPUTED WITHIN AN ACCURACY OF PLUS OR MINUS 1.000000E-03 . IT WAS ESTIMATED THAT THE FIRST NATURAL FREQUENCY WAS GREATER THAN 0.100000E 02 RADIANS PER SECOND AND THAT NO TWO NATURAL FREQUENCIES WILL BE CLOSER THAN 0.100000E 02 RADIANS PER SECOND.

LENGTH (IN.)	OUTER DIAMETER (IN.)	INNER DIAMETER (IN.)	WEIGHT DENSITY (LB/IN.3)	MODULUS OF ELASTICITY (LB/IN.2)	LUMPED MASS (LB SEC2/IN.)	LUMPED INERTIA (LB SEC2 IN.)	LINEAR SPRING (LB/IN.)	TORSIONAL SPRING (IN. LB/RADIAN)
0.1000E 02	0.4000E 01	0.2000E 01	0.2830E-00	0.2950E 08	0.0000E 00	0.3600E 03	-0.	-0.
0.2000E 02	0.4000E 01	0.2000E 01	0.2830E-00	0.2950E 08	-0.	-0.	0.2000E 06	-0.
0.4000E 02	0.4000E 01	0.2000E 01	0.2830E-00	0.2950E 08	-0.	-0.	-0.	-0.
0.4000E 02	0.6000E 01	0.2000E 01	0.2830E-00	0.2950E 08	-0.	-0.	-0.	0.5000E 05
0.3000E 02	0.6000E 01	0.2000E 01	0.2830E-00	0.2950E 08	-0.	-0.	-0.	-0.
0.4000E 02	0.6000E 01	0.4000E 01	0.2830E-00	0.2950E 08	-0.	-0.	0.1500E 06	0.4000E 05
0.1000E 02	0.6000E 01	0.4000E 01	0.2830E-00	0.2950E 08	-0.	-0.	-0.	-0.
0.2000E 02	0.5000E 01	0.3000E 01	0.2830E-00	0.2950E 08	0.3500E 01	0.7000E 03	-0.	-0.
0.1000E 02	0.4000E 01	0.2000E 01	0.9800E-01	0.1060E 08	-0.	-0.	0.3000E 06	-0.
0.1000E 02	0.4000E 01	0.2000E 01	0.9800E-01	0.1060E 08	-0.	-0.	-0.	-0.

FORCE (LB)	FREQUENCY (RAD/SEC)	MOMENT (IN.LB)	FREQUENCY (RAD/SEC)
-0.	-0.	-0.	-0.
0.100000E 03	0.150000E 02	-0.	-0.
-0.	-0.	-0.	-0.
-0.	-0.	-0.	-0.
-0.	-0.	-0.	-0.
-0.	-0.	-0.	-0.
-0.	-0.	-0.	-0.
-0.	-0.	0.500000E 03	0.200000E 02
-0.	-0.	-0.	-0.
-0.	-0.	-0.	-0.

NATURAL FREQUENCY
(RADIANS/SECOND)

MODE SHAPE

SECTION	DISPLACEMENT AT BEGINNING	SLOPE AT BEGINNING	MOMENT AT BEGINNING	SHEAR AT BEGINNING	DISPLACEMENT AT END	SLOPE AT END	MOMENT AT END	SHEAR AT END
0.918640E 02								
1	1.000000E-03	-0.353496E-04	0.	0.	0.646569E-03	-0.353241E-04	-0.257166E 01	-0.479987E-00
2	0.646569E-03	-0.353241E-04	-0.109888E 03	-0.484510E 01	0.224834E-04	-0.261054E-04	-0.211172E 03	-0.521728E 01
3	0.224834E-04	-0.261054E-04	-0.211172E 03	-0.720603E 00	-0.514979E-03	-0.415518E-06	-0.229252E 03	0.538756E-01
4	-0.514979E-03	-0.415518E-06	-0.229252E 03	0.538756E-01	-0.437542E-03	0.405281E-05	-0.164364E 03	0.310927E 01
5	-0.437542E-03	0.405281E-05	-0.164567E 03	0.310927E 01	-0.284716E-03	0.580917E-05	-0.439200E 02	0.481430E 01
6	-0.284716E-03	0.580917E-05	-0.439200E 02	0.481430E 01	-0.647528E-04	0.426274E-05	0.164735E 03	0.547359E 01
7	-0.647528E-04	0.426274E-05	0.164565E 03	-0.423934E 01	-0.271214E-04	0.331017E-05	0.122421E 03	-0.419547E 01
8	-0.271214E-04	0.331017E-05	0.122421E 03	-0.419547E 01	0.150917E-04	0.126548E-05	0.386590E 02	-0.419142E 01
9	0.150917E-04	0.126548E-05	0.461354E 02	-0.463718E 01	0.154645E-04	-0.571815E-06	-0.253398E-00	-0.464057E 01

10	0.154645E-04	-0.571815E-06	-0.251398E-00	-0.122792E-02	0.985039E-05	-0.550653E-06	-0.279301E-00	-0.377965E-02

0.175718E 03

1	1.000000E-03	-0.346956E-04	0.	0.	0.653284E-03	-0.346020E-04	-0.943297E 01	-0.176323E 01
2	0.653284E-03	-0.346020E-04	-0.394054E 03	-0.179002E 02	0.250065E-03	-0.120950E-05	-0.772000E 03	-0.196000E 02
3	0.250065E-03	-0.120950E-05	-0.772000E 03	0.371441E 02	0.102261E-02	0.160648E-04	0.439217E 03	0.271776E 02
4	0.102261E-02	0.160648E-04	0.439217E 03	0.271776E 02	0.135638E-02	-0.135446E-05	0.903071E 03	-0.124079E 01
5	0.135638E-02	-0.135446E-05	0.903939E 03	-0.124079E 01	0.109360E-02	-0.151516E-04	0.612893E 03	-0.227429E 02
6	0.109360E-02	-0.151516E-04	0.612893E 03	-0.227429E 02	0.347209E-03	-0.170355E-04	-0.940803E 03	-0.330061E 02
7	0.347209E-03	-0.170355E-04	-0.539402E 03	0.109992E 02	0.192691E-03	-0.140725E-04	-0.354662E 03	0.180442E 02
8	0.192691E-03	-0.140725E-04	-0.354662E 03	0.180442E 02	-0.209151E-04	-0.950670E-05	-0.826600E-01	0.176209E 02
9	-0.209151E-04	-0.950670E-05	-0.207200E 03	0.207457E 02	-0.694055E-04	-0.129049E-05	0.353247E-00	0.207072E 02
10	-0.694055E-04	-0.129049E-05	0.353247E-00	-0.584848E-01	-0.825519E-04	-0.131093E-05	0.410931E-01	-0.233606E-02

FORCED VIBRATIONS

SECTION	DISPLACEMENT AT BEGINNING	MOMENT AT BEGINNING	SHEAR AT BEGINNING	DISPLACEMENT AT END	MOMENT AT END	SHEAR AT END
1	0.104749E-01	0.	0.	0.679063E-04	-0.157071E 09	-0.293413E 08
2	0.679063E-04	-0.662843E 10	-0.297120E 09	0.864537E-05	-0.128094E 11	-0.323020E 09
3	0.864537E-05	-0.128094E 11	0.277092E 09	-0.130273E-04	-0.216362E 10	0.252000E 09
4	-0.130273E-04	-0.115393E 11	0.134831E 10	0.190516E-05	0.247230E 11	0.309126E 09
5	0.190516E-05	0.246970E 11	0.309126E 09	0.605619E-05	0.238672E 11	-0.424402E 09
6	0.605619E-05	0.193921E 11	-0.344092E 09	0.417977E-05	-0.225060E 10	-0.601037E 09
7	0.417977E-05	-0.225143E 10	0.262374E 09	0.300840E-05	0.192023E 09	0.279425E 09
8	0.300840E-05	0.100861E 09	0.120007E 09	0.409795E-06	0.237793E 10	0.111303E 09
9	0.409795E-06	-0.230657E 09	0.236513E 08	-0.640603E-06	-0.129874E 07	0.237999E 08
10	-0.640603E-06	-0.129874E 07	-0.206332E 06	-0.142705E-05	-0.250959E 07	-0.446487E 05

ANALYSIS OF COMPLEX SHAFTING SYSTEMS

SHAFT IDENTIFICATION NUMBER 1

RUN TYPE 5

THE SHAFT IS COMPOSED OF 10 SECTIONS. 2 MODES WILL BE USED IN THE FORCED VIBRATION CALCULATIONS.

LENGTH (IN.)	OUTER DIAMETER (IN.)	INNER DIAMETER (IN.)	WEIGHT DENSITY (LB/IN.3)	MODULUS OF ELASTICITY (LB/IN.2)	LUMPED MASS (LB SEC2/IN.)	LUMPED INERTIA (LB SEC2 IN.)
0.1000E 02	0.4000E 01	0.2000E 01	0.2830E-00	0.2950E 08	0.0000E 00	0.3600E 03
0.2000E 02	0.4000E 01	0.2000E 01	0.2830E-00	0.2950E 08	-0.	-0.
0.4000E 02	0.4000E 01	0.2000E 01	0.2830E-00	0.2950E 08	-0.	-0.
0.4000E 02	0.6000E 01	0.2000E 01	0.2830E-00	0.2950E 08	-0.	-0.
0.3000E 02	0.6000E 01	0.2000E 01	0.2830E-00	0.2950E 08	-0.	-0.
0.4000E 02	0.6000E 01	0.4000E 01	0.2830E-00	0.2950E 08	-0.	-0.
0.1000E 02	0.6000E 01	0.4000E 01	0.2830E-00	0.2950E 08	-0.	-0.
0.2000E 02	0.5000E 01	0.3000E 01	0.2830E-00	0.2950E 08	0.3900E 01	0.7000E 03
0.1000E 02	0.4000E 01	0.2000E 01	0.9800E-01	0.1060E 08	-0.	-0.
0.1000E 02	0.4000E 01	0.2000E 01	0.9800E-01	0.1060E 08	-0.	-0.

FORCE (LB)	FREQUENCY (RAD/SEC)	MOMENT (IN.LB)	FREQUENCY (RAD/SEC)
0.	-0.	-0.	-0.
0.100000E 01	0.150000E 02	-0.	-0.
-0.	-0.	-0.	-0.
-0.	-0.	-0.	-0.
-0.	-0.	-0.	-0.
-0.	-0.	-0.	-0.
-0.	-0.	-0.	-0.
-0.	-0.	0.500000E 01	0.200000E 02
-0.	-0.	-0.	-0.
-0.	-0.	-0.	-0.

NATURAL FREQUENCY
(RADIANS/SECOND)

MODE SHAPE

0.918640E 02

SECTION	DISPLACEMENT AT BEGINNING	SLOPE AT BEGINNING	MOMENT AT BEGINNING	SHEAR AT BEGINNING	DISPLACEMENT AT END	SLOPE AT END	MOMENT AT END	SHEAR AT END
1	1.000000E-03	-0.353496E-04	0.	0.	0.646569E-03	-0.353241E-04	-0.257166E 01	-0.479987E-00
2	0.646569E-03	-0.353241E-04	-0.109888E 03	-0.484510E 01	0.224834E-04	-0.261054E-04	-0.211172E 03	-0.521172E 01
3	0.224834E-04	-0.261054E-04	-0.211172E 03	-0.720603E 00	-0.514979E-03	-0.415518E-06	-0.229252E 03	0.538756E-01
4	-0.514979E-03	-0.415518E-06	-0.229252E 03	0.538756E-01	-0.437542E-03	0.405281E-05	-0.164364E 03	0.310927E 01
5	-0.437542E-03	0.405281E-05	-0.164567E 03	0.310927E 01	-0.284716E-03	0.580917E-05	-0.439200E 02	0.481410E 01
6	-0.284716E-03	0.580917E-05	-0.439200E 02	0.481410E 01	-0.647528E-04	0.426274E-05	0.164735E 03	0.547339E 01
7	-0.647528E-04	0.426274E-05	0.164565E 03	-0.423934E 01	-0.271214E-04	0.331017E-05	0.122421E 03	-0.419547E 01
8	-0.271214E-04	0.331017E-05	0.122421E 03	-0.419547E 01	0.150917E-04	0.126548E-05	0.386598E 02	-0.419142E 01
9	0.150917E-04	0.126548E-05	0.461354E 02	-0.446171E 01	0.154645E-04	-0.571815E-06	-0.253398E-00	-0.466057E 01
10	0.154645E-34	-0.571815E-36	-0.253398E-00	-0.122792E-02	0.985039E-05	-0.550653E-06	-0.277381E-00	-0.377985E-02

0.175718E 03

1	1.000000E-03	-0.346754E-04	0.	0.	0.653284E-03	-0.346020E-04	-0.943257E 01	-0.176323E 01
2	0.653284E-03	-0.346020E-04	-0.374054E 01	-0.179002E 02	0.258865E-03	-0.120950E-05	-0.772000E 03	-0.190088E 02
3	0.258865E-03	-0.120950E-05	-0.772000E 03	0.371441E 02	0.102261E-02	0.160648E-04	0.419217E 03	0.271776E 02
4	0.102261E-02	0.160648E-04	0.419217E 03	0.271776E 02	0.135638E-02	-0.135446E-05	0.983071E 03	-0.124075E 01
5	0.135638E-02	-0.135446E-05	0.783939E 03	-0.124075E 01	0.109368E-02	-0.155516E-04	0.612853E 03	-0.227425E 02
6	0.109368E-02	-0.151516E-04	0.612853E 03	-0.227425E 02	0.347209E-03	-0.170355E-04	-0.540083E 03	-0.330961E 02
7	0.347209E-03	-0.170355E-04	-0.539402E 03	0.189952E 02	0.192691E-03	-0.140725E-04	-0.354662E 03	0.180447E 02
8	0.192691E-03	-0.140725E-04	-0.354662E 03	0.180447E 02	-0.289151E-04	-0.958670E-05	-0.826606E-01	0.176209E 02
9	-0.289151E-04	-0.958678E-05	-0.207288E 01	0.207457E 02	-0.694855E-04	-0.129849E-05	0.353247E-00	0.207872E 02
10	-0.694855E-04	-0.129849E-05	0.153247E-00	-0.584848E-01	-0.825515E-04	-0.131053E-05	0.410931E-01	-0.233606E-02

FORCED VIBRATIONS

SECTION	DISPLACEMENT AT BEGINNING	MOMENT AT BEGINNING	SHEAR AT BEGINNING	DISPLACEMENT AT END	MOMENT AT END	SHEAR AT END
1	0.104749E-03	0.	0.	0.679062E-03	-0.157071E 09	-0.293413E 08
2	0.679062E-04	-0.662842E 10	-0.297119E 09	0.864536E-05	-0.128893E 11	-0.323027E 09
3	0.864536E-05	-0.128893E 11	0.277891E 09	-0.130275E-04	-0.216364E 10	0.252807E 09
4	-0.130275E-04	-0.115394E 11	0.134839E 10	0.190513E-05	0.747229E 11	0.389126E 09
5	0.190513E-05	0.246960E 11	0.389126E 09	0.685613E-05	0.238671E 11	-0.424475E 09
6	0.685613E-05	0.193920E 11	-0.344886E 07	0.417973E-05	-0.225063E 10	-0.681829E 09
7	0.417973E-05	-0.225134E 10	0.262371E 09	0.300839E-05	0.192839E 09	0.229421E 09
8	0.300839E-05	0.100869E 09	0.120009E 09	0.409797E-06	0.237793E 10	0.111381E 09
9	0.409797E-06	-0.239654E 09	0.236909E 08	-0.640674E-06	-0.129874E 07	0.237957E 08
10	-0.640674E-06	-0.129874E 07	-0.206331E 06	-0.142705E-05	-0.258959E 07	-0.446486E 05

646 LINES OUTPUT THIS JOB.

K06056 M55HANN E 131KFORT 04/21/66 00001.26 MIN.

IITRI

IIT Research Institute
10 West 35 Street, Chicago, Illinois 60616
312/225-9600

Mod

608168

February 9, 1965

Address: Cameron Station
Alexandria, Virginia 22314

Subject: "Dynamics of Flexible Rotors"(U)
Contract No. NObs-88607
IITRI Project No. K6056

Gentlemen:

Enclosed please find 10 copies of an errata sheet for the above mentioned final report.

Should you have any additional questions regarding same, please do not hesitate to call upon us.

Very truly yours,

Ronald L. Eshleman

R. L. Eshleman
Assistant Research
Engineer

APPROVED:

W. E. Reynolds

W. E. Reynolds
Manager, Machine Design

CW

ERRATA SHEET
FINAL REPORT IITRI PROJECT K6056
DYNAMICS OF FLEXIBLE ROTORS

Page 4	Line 11	"disk mass"
Page 8	Equation (2.3)	"$= a_1 \cos \tau - a_2 \sin \tau$"
Page 9	After Equation (2.7)	"Explicity in Terms of ν"
Page 12	Equations (2.15) Lower Left Hand Element	$\alpha_1^2 e^{\alpha_1}$
Page 12	Equation (2.18)	$(V_1 + iV_2) e^{i\tau}$
Page 14	Insert Shear Correction Sheet	
Page 18	Line 4 and Equations (2.37)	Replace ν by V
Page 19	Equations (2.38) and (2.39)	Replace ν by V
Page 33	Line 3	$R_D = Lr_D$
Page 39	Equation (3.5)	Replace $\frac{\partial^4 u_2}{\partial x^4}$ by $\frac{\partial^2 u_2}{\partial x^2}$
Page 53	Figure 4	1F = 1st Mode, Forward Whirl 2B = 2nd Mode, Backward Whirl
Page 57	Figure 5	F = Forward Whirl B = Backward Whirl
Page 70	Line 8	"Indicates"
Page 70	Line 11	"Nodal Point"
Page A-5	Table A-1 1st Column, 2nd Row	"$\sin \theta \cos \psi$"
Page A-12	Last Row	"$(\cos \theta - 1)^2$"

Shear Correction

Equations 2.25 (a) & 2.25(b) on Page 14 can be corrected for shear deformation. The whirl frequencies of a plain rotor in pin-ended, solid supports are:

$$P_+ = \frac{n^2\pi^2}{\sqrt{1 - \frac{r^2n^2\pi^2}{4}}} \qquad P_- = \frac{n^2\pi^2}{\sqrt{1 + \frac{3r^2n^2\pi^2}{4}}}$$

where n = 0, 1, 2, ...

The shear correction term (approximately) is $\frac{4}{k'G}$

Then:

$$P_+ = \frac{n^2\pi^2}{\sqrt{1 - \frac{r^2n^2\pi^2}{4}\left(1 + \frac{E}{k'G}\right)}}$$

$$P_- = \frac{n^2\pi^2}{\sqrt{1 + \frac{3r^2\pi^2n^2}{4}\left(1 + \frac{E}{k'G}\right)}}$$

Example:

For a circular shaft $k' = \frac{10}{9}$

or $\frac{E}{k'G} = 2.4$

		Copies
1.	Boston Naval Shipyard Boston 29, Massachusetts Attn: Design Division	1
2.	Charleston Naval Shipyard Charleston, South Carolina Attn: Design Division	1
3.	Puget Sound Naval Shipyard Bremerton, Washington Attn: Design Division	1
4.	New York Naval Shipyard Brooklyn 1, New York Attn: Design Division	1
5.	Long Beach Naval Shipyard Long Beach 2, California Attn: Design Division	1
6.	Pearl Harbor Naval Shipyard FPO San Francisco, California Attn: Design Division	1
7.	Philadelphia Naval Shipyard Broad and Government Avenues Philadelphia 12, Pennsylvania Attn: Design Division	1
8.	Portsmouth Naval Shipyard Portsmouth, New Hampshire Attn: Design Division	1
9.	Norfolk Naval Shipyard Portsmouth, Virginia Attn: Design Division	1
10.	San Francisco Naval Shipyard San Francisco 24, California Attn: Design Division	
11.	Mare Island Naval Shipyard Vallejo, California Attn: Design Division	1
12.	David Taylor Model Basin Department of the Navy Washington 7, D. C. Attn: Library	2
13.	David Taylor Model Basin Department of the Navy Washington 7, D. C. Attn: Code 760	2

		Copies
14.	David Taylor Model Basin Department of the Navy Washington, D. C. Attn: Code 761	2
15.	Philadelphia Naval Shipyard Broad and Government Avenues Philadelphia 12, Pennsylvania Attn: Naval Boiler and Turbine Laboratory	2
16.	New York Naval Shipyard Brooklyn 1, New York Attn: Applied Science Laboratory	2
17.	Cameron Station Alexandria, Virginia 22314 Attn: Defense Documentation Center	10
18.	University of Houston Cullen Boulevard Houston 4, Texas Attn: Dr. D. Muster	1
19.	General Dynamics Corporation Groton, Connecticut Attn: Electric Boat Division	1
20.	Newport News Shipbuilding and Dry Dock Company 4100 Washington Avenue Newport News, Virginia	1
21.	Bureau of Ships Department of the Navy Washington 25, D. C. Attn: Code 345	5
	2108	2
	436	1
	641	2
	644A	2
	645	2
	6495	1
	660E	2
22.	Mr. F. F. Vane Section Head U.S. Navy, Bureau of Ships Code 345 Washington 25, D. C.	5
23.	Mr. A. Paladino U.S. Navy, Bureau of Ships Code 345 Washington 25, D. C.	5

AD 608168

ERRATA SHEET
FINAL REPORT IITRI PROJECT K6056
DYNAMICS OF FLEXIBLE ROTORS

Page 4	Line 11	"disk mass"
Page 8	Equation (2.3)	"$= a_1 \cos \tau - a_2 \sin \tau$"
Page 9	After Equation (2.7)	"Explicity in Terms of ν"
Page 12	Equations (2.15) Lower Left Hand Element	$\alpha_1^2 e^{\alpha_1}$
Page 12	Equation (2.18)	$(V_1 + iV_2)\, e^{i\tau}$
Page 14	Insert Shear Correction Sheet	
Page 18	Line 4 and Equations (2.37)	Replace ν by V
Page 19	Equations (2.38) and (2.39)	Replace ν by V
Page 33	Line 3	$R_D = Lr_D$
Page 39	Equation (3.5)	Replace $\frac{\partial^4 u_2}{\partial x^4}$ by $\frac{\partial^2 u_2}{\partial x^2}$
Page 53	Figure 4	1F = 1st Mode, Forward Whirl 2B = 2nd Mode, Backward Whirl
Page 57	Figure 5	F = Forward Whirl B = Backward Whirl
Page 70	Line 8	"Indicates"
Page 70	Line 11	"Nodal Point"
Page A-5	Table A-1 1st Column, 2nd Row	"Sin θ cos ψ"
Page A-12	Last Row	"$(\cos \theta - 1)^2$"

Shear Correction

Equations 2.25 (a) & 2.25(b) on Page 14 can be corrected for shear deformation. The whirl frequencies of a plain rotor in pin-ended, solid supports are:

$$P_+ = \frac{n^2\pi^2}{\sqrt{1 - \frac{r^2n^2\pi^2}{4}}} \qquad P_- = \frac{n^2\pi^2}{\sqrt{1 + \frac{3r^2n^2\pi^2}{4}}}$$

where n = 0, 1, 2, ...

The shear correction term (approximately) is $\frac{4}{k'G}$

Then:

$$P_+ = \frac{n^2\pi^2}{\sqrt{1 - \frac{r^2n^2\pi^2}{4}\left(1 + \frac{E}{k'G}\right)}}$$

$$P_- = \frac{n^2\pi^2}{\sqrt{1 + \frac{3r^2\pi^2n^2}{4}\left(1 + \frac{E}{k'G}\right)}}$$

Example:

For a circular shaft $k' = \frac{10}{9}$

or $\frac{E}{k'G} = 2.4$